

Volume 2 Issue 7

July 2011



ISSN 2156-5570(Online)

ISSN 2158-107X(Print)



www.ijacsa.thesai.org



INTERNATIONAL JOURNAL OF
ADVANCED COMPUTER SCIENCE AND APPLICATIONS



A Publication of
The Science and Information Organization



IJACSA Editorial

From the Desk of Managing Editor...

It is a pleasure to present our readers with the July 2011 Issue of International Journal of Advanced Computer Science and Applications (IJACSA).

IJACSA is one of the most prominent publications in the field, delivering up-to-date and authoritative coverage of advanced computer science and applications.

The Journal aims to publish the highest quality material, both informative and scientific, on all aspects of Computer Science research. It includes articles related to research findings, technical evaluations, and reviews. In addition it provides a forum for the exchange of information on all aspects.

The Associate Editor Board consists of senior level researchers and/or practitioners, who constantly advise the Co-Editors-in-Chief with respect to the content of and direction to be pursued by the Journal. They may also from time to time be called upon to review manuscripts but that is not their primary role.

Some of the papers have an introductory character, some of them access highly desired extensions for a particular method, and some of them even introduce completely new approaches to computer science research in a very efficient manner. This diversity was strongly desired and should contribute to evoke a picture of this field at large. As a consequence only 29% of the received articles have been finally accepted for publication.

The scope of the journal is fairly broad, although more defined than that of some other journals. Our focus is squarely on experimental research, rather than on work that is largely descriptive.

By having in mind such future issues, we hope to establish a regular outlet for contributions and new findings in the field of Computer science and applications. Therefore, IJACSA in general, could serve as a reliable resource for everybody loosely or tightly attached to this field of science.

And if only a single young researcher is inspired by this issue to contribute in the future to solve some of the problems sketched here or contribute to exiting methodologies and research work, the effort of all the contributors will be rewarded. In that sense we would like to thank all the authors and reviewers that contributed to this issue for their efforts and their collaboration in this project.

We hope to continue exploring the always diverse and often astonishing fields in Advanced Computer Science and Applications.

Thank You for Sharing Wisdom!

Managing Editor

IJACSA

Volume 2 Issue 7, July 2011

editorijacsa@thesai.org

ISSN 2156-5570 (Online)

ISSN 2158-107X (Print)

©2011 The Science and Information (SAI) Organization

Editorial Board

Dr. Kohei Arai – Editor-in-Chief

Saga University

Domains of Research: Human-Computer Interaction, Networking, Information Retrievals, Optimization Theory, Modeling and Simulation, Satellite Remote Sensing, Computer Vision, Decision Making Methodology

Dr. Ka Lok Man

Xi'an Jiaotong-Liverpool University (XJTLU)

Domain of Research: Computer Science and Microelectronics

Dr. Sasan Adibi

Research In Motion (RIM)

Domain of Research: Security of wireless systems, Quality of Service

Dr. Zuqing Zuh

University of Science and Technology of China

Domains of Research : Optical Communication Systems, Optical network architecture and design, Next generation Internet, Signal processing, Broadband access network, such as cable access (DOCSIS) networks, passive optical networks (PON), fiber to the home (FTTH), Energy-efficient network and green technologies

Dr. Sikha Bagui

University of West Florida

Domain of Research: Database, database modeling, ER diagrams, XML data, web databases, data mining, association rule mining, data preprocessing

Dr. T. V. Prasad

Lingaya's University

Domain of Research: Bioinformatics, Natural Language Processing, Image Processing, Robotics, Knowledge Representation

Dr. Mohd Helmy Abd Wahab

Universiti Tun Hussein Onn Malaysia

Domain of Research: Data Mining, Database, Web-based Application, Mobile Computing

IJACSA Reviewer Board

- **A Kathirvel**
Karpaga Vinayaka College of Engineering and Technology, India
- **Abbas Karimi**
I.A.U_Arak Branch (Faculty Member) & Universiti Putra Malaysia
- **Dr. Abdul Wahid**
Gautam Buddha University, India
- **Abdul Khader Jilani Saudagar**
Al-Imam Muhammad Ibn Saud Islamic University
- **Abdur Rashid Khan**
Gomal University
- **Dr. Ahmed Nabih Zaki Rashed**
Menoufia University, Egypt
- **Ahmed Sabah AL-Jumaili**
Ahlia University
- **Md. Akbar Hossain**
Aalborg University, Denmark and AIT, Greeceas
- **Albert Alexander**
Kongu Engineering College,India
- **Prof. Alcinia Zita Sampaio**
Technical University of Lisbon
- **Amit Verma**
Rayat & Bahra Engineering College, India
- **Ammar Mohammed Ammar**
Department of Computer Science, University of Koblenz-Landau
- **Arash Habibi Lashakri**
University Technology Malaysia (UTM), Malaysia
- **Asoke Nath**
St. Xaviers College, India
- **B R SARATH KUMAR**
Lenora College of Engineering, India
- **Binod Kumar**
Lakshmi Narayan College of Technology, India
- **Bremananth Ramachandran**
School of EEE, Nanyang Technological University
- **Dr.C.Suresh Gnana Dhas**
Park College of Engineering and Technology, India
- **Mr. Chakresh kumar**

Manav Rachna International University, India

- **Chandra Mouli P.V.S.S.R**
VIT University, India
- **Chandrashekhar Meshram**
Shri Shankaracharya Engineering College, India
- **Constantin POPESCU**
Department of Mathematics and Computer Science, University of Oradea
- **Prof. D. S. R. Murthy**
SNIST, India.
- **Deepak Garg**
Thapar University.
- **Prof. Dhananjay R.Kalbande**
Sardar Patel Institute of Technology, India
- **Dhirendra Mishra**
SVKM's NMIMS University, India
- **Divya Prakash Shrivastava**
EL JABAL AL GARBI UNIVERSITY, ZAWIA
- **Dragana Becejski-Vujaklija**
University of Belgrade, Faculty of organizational sciences
- **Fokrul Alom Mazarbhuiya**
King Khalid University
- **G. Sreedhar**
Rashtriya Sanskrit University
- **Ghalem Belalem**
University of Oran (Es Senia)
- **Hanumanthappa.J**
University of Mangalore, India
- **Dr. Himanshu Aggarwal**
Punjabi University, India
- **Huda K. AL-Jobori**
Ahlia University
- **Dr. Jamaiah Haji Yahaya**
Northern University of Malaysia (UUM), Malaysia
- **Jasvir Singh**
Communication Signal Processing Research Lab
- **Jatinderkumar R. Saini**
S.P.College of Engineering, Gujarat
- **Prof. Joe-Sam Chou**
Nanhua University, Taiwan
- **Dr. Juan Josè Martínez Castillo**

Yacambu University, Venezuela

- **Dr. Jui-Pin Yang**
Shih Chien University, Taiwan
- **Dr. K.PRASADH**
Mets School of Engineering, India
- **Ka Lok Man**
Xi'an Jiaotong-Liverpool University (XJTLU)
- **Dr. Kamal Shah**
St. Francis Institute of Technology, India
- **Kodge B. G.**
S. V. College, India
- **Kohei Arai**
Saga University
- **Kunal Patel**
Ingenuity Systems, USA
- **Lai Khin Wee**
Technischen Universität Ilmenau, Germany
- **Latha Parthiban**
SSN College of Engineering, Kalavakkam
- **Mr. Lijian Sun**
Chinese Academy of Surveying and Mapping, China
- **Long Chen**
Qualcomm Incorporated
- **M.V.Raghavendra**
Swathi Institute of Technology & Sciences, India.
- **Madjid Khalilian**
Islamic Azad University
- **Mahesh Chandra**
B.I.T, India
- **Mahmoud M. A. Abd Ellatif**
Mansoura University
- **Manpreet Singh Manna**
SLIET University, Govt. of India
- **Marcellin Julius NKENLIFACK**
University of Dschang
- **Md. Masud Rana**
Khunla University of Engineering & Technology, Bangladesh
- **Md. Zia Ur Rahman**
Narasaraopeta Engg. College, Narasaraopeta
- **Messaouda AZZOUZI**
Ziane AChour University of Djelfa

- **Dr. Michael Watts**
University of Adelaide, Australia
- **Miroslav Baca**
University of Zagreb, Faculty of organization and informatics / Center for biomet
- **Mohamed Ali Mahjoub**
Preparatory Institute of Engineer of Monastir
- **Mohammad Talib**
University of Botswana, Gaborone
- **Mohammed Ali Hussain**
Sri Sai Madhavi Institute of Science & Technology
- **Mohd Helmy Abd Wahab**
Universiti Tun Hussein Onn Malaysia
- **Mohd Nazri Ismail**
University of Kuala Lumpur (UniKL)
- **Mueen Uddin**
Universiti Teknologi Malaysia UTM
- **Dr. Murugesan N**
Government Arts College (Autonomous), India
- **Nitin S. Choubey**
Mukesh Patel School of Technology Management & Eng
- **Dr. Nitin Surajkishor**
NMIMS, India
- **Paresh V Virparia**
Sardar Patel University
- **Dr. Poonam Garg**
Institute of Management Technology, Ghaziabad
- **Raj Gaurang Tiwari**
AZAD Institute of Engineering and Technology
- **Rajesh Kumar**
National University of Singapore
- **Rajesh K Shukla**
Sagar Institute of Research & Technology- Excellence, India
- **Dr. Rajiv Dharaskar**
GH Raisonni College of Engineering, India
- **Prof. Rakesh. L**
Vijetha Institute of Technology, India
- **Prof. Rashid Sheikh**
Acropolis Institute of Technology and Research, India
- **Ravi Prakash**
University of Mumbai
- **Rongrong Ji**

Columbia University

- **Dr. Ruchika Malhotra**
Delhi Technological University, India
- **Dr.Sagarmay Deb**
University Lecturer, Central Queensland University, Australia
- **Saleh Ali K. AlOmari**
Universiti Sains Malaysia
- **Dr. Sana'a Wafa Al-Sayegh**
University College of Applied Sciences UCAS-Palestine
- **Santosh Kumar**
Graphic Era University, India
- **Sasan Adibi**
Research In Motion (RIM)
- **Saurabh Pal**
VBS Purvanchal University, Jaunpur
- **Seyed Hamidreza Mohades Kasaei**
University of Isfahan
- **Shahanawaj Ahamad**
The University of Al-Kharj
- **Shaidah Jusoh**
University of West Florida
- **Sikha Bagui**
Zarqa University
- **Dr. Smita Rajpal**
ITM University
- **Suhas J Manangi**
Microsoft
- **SUKUMAR SENTHILKUMAR**
Universiti Sains Malaysia
- **Sunil Taneja**
Smt. Aruna Asaf Ali Government Post Graduate College, India
- **Dr. Suresh Sankaranarayanan**
University of West Indies, Kingston, Jamaica
- **T C.Manjunath**
Visvesvaraya Tech. University
- **T V Narayana Rao**
Hyderabad Institute of Technology and Management, India
- **T. V. Prasad**
Lingaya's University
- **Taiwo Ayodele**
Lingaya's University

- **Totok R. Biyanto**
Infonetmedia/University of Portsmouth
- **Varun Kumar**
Institute of Technology and Management, India
- **Vellanki Uma Kanta Sastry**
Sreeneedhi
- **Dr. V. U. K. Sastry**
SreeNidhi Institute of Science and Technology (SNIST), Hyderabad, India.
- **Vinayak Bairagi**
Sinhgad Academy of engineering, India
- **Vitus S.W. Lam**
The University of Hong Kong
- **Vuda Sreenivasarao**
St.Mary's college of Engineering & Technology, Hyderabad, India
- **Y Srinivas**
GITAM University
- **Mr.Zhao Zhang**
City University of Hong Kong, Kowloon, Hong Kong
- **Zhixin Chen**
ILX Lightwave Corporation
- **Zuqing Zhu**
University of Science and Technology of China

CONTENTS

Paper 1: An Approach for Teaching of National Languages and Cultures through ICT in Cameroon

Authors: Marcellin Nkenlifack, Bethin Demsong, A. Teko Domche, Raoul Nangue

PAGE 1 – 10

Paper 2: Automatic Queuing Model for Banking Applications

Authors: Dr. Ahmed S. A. AL-Jumaily, Dr. Huda K. T. AL-Jobori

PAGE 11 – 15

Paper 3: Error Detection and Correction over Two-Dimensional and Two-Diagonal Model and Five-Dimensional Model

Authors: Danial Aflakian, Dr.Tamanna Siddiqui, Najeeb Ahmad Khan , Davoud Aflakian

PAGE 16 – 19

Paper 4: Developing Digital Control System Centrifugal Pumping Unit

Authors: Safarini Osama

PAGE 20 – 22

Paper 5: Image Compression of MRI Image using Planar Coding

Authors: Lalitha Y. S, Mrityunjaya V. Latte

PAGE 23 – 33

Paper 6: A Parallel and Concurrent Implementation of Lin-Kernighan Heuristic (LKH-2) for Solving Traveling Salesman Problem for Multi-Core Processors using SPC³ Programming Model

Authors: Muhammad Ali Ismail, Dr. Shahid H. Mirza, Dr. Talat Altaf

PAGE 34 – 43

Paper 7: Performance Evaluation of Mesh - Based Multicast Routing Protocols in MANET's

Authors: M. Nagaratna, V. Kamakshi Prasad, Raghavendra Rao

PAGE 44 – 52

Paper 8: Characterization of Dynamic Bayesian Network- The Dynamic Bayesian Network as temporal network

Authors: Nabil Ghanmi, Mohamed Ali Mahjoub, Najoua Essoukri Ben Amara

PAGE 53 – 60

Paper 9: Triple SV: A Bit Level Symmetric Block- Cipher Having High Avalanche Effect

Authors: Rajdeep Chakraborty, Sonam Agarwal, Sridipta Misra, Vineet Khemka, Sunit Kr Agarwal, J. K. Mandal

PAGE 61 – 68

Paper 10: Investigation on Simulation and Measurement of Reverberation for Small Rooms

Authors: Zhixin Chen

PAGE 69 – 73

Paper 11: Performance Analysis of Corporate Feed Rectangular Patch Element and Circular Patch Element 4x2 Microstrip Array Antennas

Authors: Md. Tanvir Ishtaique-ul Huque, Md. Al-Amin Chowdhury, Md. Kamal Hosain, Md. ShahAlam

PAGE 74 – 79

Paper 12: A Comparative Study of various Secure Routing Protocols based on AODV

Authors: Dalip Kamboj, Pankaj Kumar Sehgal

PAGE 80 – 85

Paper 13: The threshold EM algorithm for parameter learning in bayesian network with incomplete data

Authors: Fradj Ben Lamine, Karim Kalti, Mohamed Ali Mahjoub

PAGE 86 – 91

Paper 14: Emotion Classification Using Facial Expression

Authors: Devi Arumugam, Dr. S. Purushothaman Hossain

PAGE 92 – 98

Paper 15: Workshare Process of Thread Programming and MPI Model on Multicore Architecture

Authors: R. Refianti, A.B. Mutiara, D.T Hasta

PAGE 99 – 107

Paper 16: Hybrid Approaches to Image Coding: A Review

Authors: Rehna. V. J, Jeya Kumar. M. K

PAGE 108 – 115

Paper 17: Software Security Requirements Gathering Instrument

Authors: Smriti Jain, Maya Ingle

PAGE 116 – 121

Paper 18: The Development Process of the Semantic Web and Web Ontology

Authors: K.Vanitha, K.Yasudha, M.Sri Venkatesh, K.Ravindra, S.Venkata Lakshmi

PAGE 122 – 125

Paper 19: Solving the Vehicle Routing Problem using Genetic Algorithm

Authors: Abdul Kadar Muhammad Masum, Mohammad Shahjalal, Md. Faisal Faruque, Md. Iqbal Hasan Sarker

PAGE 126 – 131

Paper 20: Reconfigurable Efficient Design of Viterbi Decoder for Wireless Communication Systems

Authors: Swati Gupta, Rajesh Mehra

PAGE 132 – 136

Paper 21: Survey of Contrast Enhancement Techniques based on Histogram Equalization

Authors: Manpreet Kaur, Jasdeep Kaur, Jappreet Kaur

PAGE 137 – 141

Paper 22: Status of Wireless Technologies Used For Designing Home Automation System -A Review

Authors: Ashish J. Ingle, Bharti W. Gawali

PAGE 142 – 146

Paper 23: A Comparative Study of Wireless Technologies Used For Designing Home Automations System

Authors: Ashish J. Ingle, Bharti W. Gawali

PAGE 147 – 152

Paper 24: Image Compression Techniques Using Modified high quality Multi wavelets

Authors: M.Ashok, Dr.T.BhaskaraReddy

PAGE 153 – 158

Paper 25: On Algebraic Spectrum of Ontology Evaluation

Authors: Adekoya Adebayo Felix, Akinwale Adio Taofiki, Sofoluwe Adetokunbo

PAGE 159 – 168

Paper 26: Evaluation of SIGMA and SCTPmx for High Handover Rate Vehicle

Authors: Hala Eldaw Idris Jubara, Sharifah Hafizah Syed Ariffin

PAGE 169 – 173

An Approach for Teaching of National Languages and Cultures through ICT in Cameroon

Marcellin Nkenlifack¹, Bethin Demsong², A. Teko Domche³, Raoul Nangué²

¹LAIA - IUTFV - University of Dschang, LIMMS - National Polytechnic

²LAIA-IUTFV of Bandjoun - University of Dschang, Cameroon

³Faculty of Letters - University of Dschang, Cameroon

Email: marcellin.nkenlifack@gmail.com

Abstract—This article describes the input of ICT to the modernization of teaching national languages and cultures in order to promote cultural diversity as well as dissemination of scientific knowledge through national languages. This will also reinforce the understanding capacities of the population. This project will serve as the guideline towards development of scientific knowledge and know-how. It presents numerous psychological, pedagogic, scientific and social advantages, among which there is a sensitization of our languages and cultures, the deployment of a platform in some schools, the training of teachers in using ICT in language teaching, the distribution self-learning aids, the development of a website for analysis and dissemination of cultural data, of conservation of linguistic and cultural heritage, and worthiness of pre-requisites and local predispositions towards the emergence and development of technology. It will contribute to make concrete the introduction of teaching national languages in the school curricula in Cameroon.

Keywords-Local Languages; Culture; ICT; Learning Platform; TICELaCuN; Management Tools.

I. INTRODUCTION

A. State of the problem

One can easily remark at this era of globalization and ICT that roughly 80% of Internet network contents are made in English language. This domination does favorise neither cultural diversity, nor local languages representation. One can therefore legitimately question the pertinence of this quasi mono cultural tool [1] [2] [3] when we consider that linguistic and cultural diversities represent one of the eleven fundamental principles geared towards edification of information society as prescribed by world summit on information society (SMSI/wsis). Thus, for the populations to have access to universal information, putting the contents in local languages becomes worth noting. This therefore perfectly justifies the interest of this project and the need of mobilization of researchers in the domain of science and technology to serve the essential purpose of Internet access in multilingualistic and multicultural contexts [1] [3] [4]. To achieve it, populations should first of all master their local languages and cultures, then after, couple them with communication tools thanks to ICT, in the way of going beyond speeches to solve this problem of mono cultural information model.

B. Motivation for the project

Introducing national languages and cultures in the school curricula and advantages that modernization of these languages gives are worth in psychological, pedagogic and social levels as it will be shown in the follow lines.

At Psychologically Level:

- From childhood, intellectual awareness and development rely on language and logical activities. This awareness and development that guide our thought portray our languages and cultures. They constitute the base for the construction of our own way of seen the world, paradigms and models of perception of ourselves and the universe.
- Individual performances and productivities are not only based on simple technical, financial or organizational mechanisms, but they also deeply depend on psychological inputs, on what is called a “personal equation” on people who conceive and realize projects. This equation is gradually elaborated with the mastery of our languages and cultures.
- Mastering our languages will enable to avoid linguistic and cultural uprooting of the youth. It will also make them to be proud of cultural heritage, to have a mutual respect through the understanding of their join heritage. This togetherness inevitably accelerates national and African integration.
- Promote nationals languages world wide

At Pedagogical Level:

- Teaching in our national languages will facilitate learning process and general dissemination of scientific knowledge (even in other languages). It will stimulate a high sense of initiative and creativity of the target population.
- Our languages play an irreplaceable role in dissemination of scientific and technologic knowledge.
- Teaching in national languages is not a rejection of the importance of other foreign languages used for a great dissemination of scientific discoveries at the era of globalization; instead, it will facilitate their learning capacities.
- Appearing as a mirror, the face and the soul of a people and its culture or as its mark of existence, a language when taught will enrich and over all world cultural diversity.

- Using ICT will enable to make available dynamic soft modern tools useful in the learning and acquisition process.

At Social Level:

Teaching in national languages will help to:

- Avoid social and cultural uprooting of the target population in order to accelerate national and African integration;
- Possess dynamic soft modern tools useful to avoid the rapid erosion of our linguistic and cultural heritage;
- Initiate and develop a cooperative programme opened to the public. This programme should be focused on the analysis of cultural data ;
- Make Cameroon and African languages and cultures contribute to globalization

C. Objectives:

Our global objective is to promote linguistic and cultural diversity, to disseminate scientific discoveries and knowledge not only in official languages (French and English), but also in local languages. This combination will reinforce the general capacity of the target population.

This project is at the center of various national, sectorial, ministerial or thematic strategies of our country. The didactic dimension of it will lead to contribute to the consolidation of education as the fundamental mission of the country. In other words, it will greatly contribute to the reinforcement of the promotion of equality of chances to Cameroonian citizens with the use of new forms of teaching based on ICT. The operational phase of the display of this project will consist of introducing teaching local languages and cultures in official school curricula with the use of numerical, multimedia and interactive tools as means to teach languages, cultures, science and technology.

This project is geared towards a population made up of pupils, students, teachers, men in charge of promotion of cultures, linguists, researchers and neo-illiterates, to name a few.

Applying ICT in language teaching opens new ways to experimentation, to search new methods and tools that can favor learners' acquisition of language and intercultural skills.

When elaborating this project, we take into consideration a number of models focused on the nature of the partnership between schools, universities, civil society and the government. This models support the policy of innovation in education [5]. Matoussi corroborates by showing that in any didactic approach, a wrong choice of hypermedia teaching document to be used can impede the construction of learners' knowledge. In the same vein, Mattioli [7] presents a solution that can help learners from the University of Liège to follow a comprehensive distant training in foreign languages. This solution consists of making available to learners lectures prepared by lecturers and put in an e-learning platform. In the framework Leon-Grenoble tele-collaboration project, Tomé [8] gives priority to strategies and pedagogy practices leading to comprehension and oral productions, with the use of task and Web tools for learners' oral productions. A survey of

needs, advantages and constraints (cf [19] of integration of ICT high schools teachers training colleges is presented considering national environment and context.

In this work, the techniques that we propose are applied gradually on concrete examples in order to put into evidence their operationalization.

This article tackles applied research and is divided into six sections.

In section I, we introduce the work; Section II discusses the context, section III describes the methodology; section IV presents the results; section V focuses on openings and extensions while section VI concludes.

Note: this article follows the development of experimental works on ICTE and new forms of teaching whose previous results are described in [9], [10], [11] [12] [13].

II. CONTEXT

From a survey on its context, it appears that is of great interest, be it at international, Cameroonian or Regional levels. An important number of legal texts have been issued to protect and promote our languages and cultures.

A. International context

• At world level

Texts and recommendations have been made at world level to portray the general determination to achieve the previously stated objective, some of them are:

- The June 9th, 1996 universal declaration on linguistics rights in Barcelona – Spain

- Recommendations of the International Organization of *Francophonie* (OIF) on teaching French and partner languages (African languages) and those of the consultative committee on national languages held in Paris from 17th to 19 December 2005.

- The Convention on protection and promotion of cultural diversity expressions held in Paris (France) on October 20, 2005.

• At African level:

The recommendations on teaching mother languages taken in 1961 during the first African conference on education held in Addis Abebas (Ethiopia).

B. National context

The national context is also very rich. Many texts signed definitely open the ways to the promotion of locale languages and their introduction in various training modules of the youth.

Cameroon ratified since 2008 (decree N°2008/178) the UNESCO convention to safeguard immaterial cultural heritage as adopted in Paris on October 17, 2003.

At the same time, the 1996 fundamental law, the 1998 law on new directives of education, the 2001 law on directives of higher education, the 2004 laws regulating rules to be applied on Councils and Regions, the 2005 and 2007 texts appointing national and regional inspectors in charge of teaching and

promoting national languages and cultures, the 2008 texts creating the laboratory and Department in charge of teaching and promoting national languages and cultures in Higher Teachers Training College in Yaoundé and last but not the least the implementation on teaching national languages and cultures in five pilot government secondary schools, namely: Government High School Leclerc in Yaounde in the Center Region, Government High School Akwa in Douala in the Littoral Region, Government High School Bafang in the West Region, Government High School Njinikom in the North West Region and Government High School Garoua in the North Region.

This new philosophy led to the recruitment in 2009 of 40 students in the Department in charge of teaching and promoting national languages and cultures in Higher Teachers Training College in Yaoundé.

Many teams of actors and researchers are now mobilized to put into practice these new directives. It is worth noting the contribution of a number of partners to codify and standardize our languages in order to make them be used adequately in teaching and literacy programmes. They are: SIL (Société Internationale de Linguistique), CABTAL (Cameroon Association for Bible Translation and Literacy), ANACLAC (Association Nationale des Comités de Langues Camerounaises), language committees, Universities.

C. Regional Context

« Bamilékés » and « Bamoun » cultures are classified among the most original ones in Cameroon and Africa. About six languages committees are active in this vicinity. They are: (« M̀dumba », « Ghomala », « Fe'efe'e », « Ng̀mba », « Ngiembon », « Yemba »).

A number of languages in our country are not more only spoken but already written since a century for some. To illustrate it, we can point out that « Fe'efe'e » is written since 1928, that is already for 80 years. Many scientific works have been carried on in our languages and didactic materials have been produced to teach both in primary and secondary schools are available for « Fe'efe'e », « Ghomala » and « M̀dumba » languages. Some of them are effectively taught in some secondary schools since 1966. Many teachers have been trained both in their language and on efficient pedagogic methods. They could be more efficient if they master how to use ICT to avoid the destruction of their linguistic and cultural heritage.

III. METHODOLOGY

A. Process

Sensitization is worth in our process of implementation this philosophy. This sensitization is very important before starting the training phase of the target population on the interest of ICT in the acquisition and transmission of knowledge through the mastery of local languages and cultures.

We are going to give priority to technical, ergonomic and pedagogic aspects, to hypermedia documents (on line and/or off line) in training teachers. This should be based on learning in situation or in case study. It will lead young teachers to experience these pedagogies in situ using ICT in a transversal

project during the training sessions. This will be done via a training platform which provides a great chance of manipulation in managing the time allotted for training.

At the turning point of this process, there is the TICeLaCuN (*in French* – “TIC pour l'Enseignement des Langues et Cultures Nationales”) multimedia platform. The sides are built up with steps and modules. They cover:

- Knowledge acquisition modules from experts
- Knowledge structured into training scenario
- Feedback of knowledge acquisition interface to learners
- Evaluation module of learners' progress
- Production of self training material such as written papers, CD, DVD to be used on the platform
- Display of the platform in schools and communities
- Inventory, test and integration of existing solutions, of other tools and softwares... (SIL resources) after having divided them into lessons
- Development and putting on line of a dynamic Internet site available to the population. It should be meant to promote and develop national languages and cultures

A set of activities directed towards real life situations are given to learners during the learning process. He can consult whenever needed a glossary of terms related to the situation considered in relation to the cultural dimension of the chosen language to be taught.

Each module is backed by interactive and productive exercises (oral or written). These exercises are aimed at evaluation and the learner can check his level of acquisition of the competences targeted by the session.

By diversifying the modes of presentation of information, hyper Medias offer much for documentary research. However, their usage can have side effects if it does not respect the previously stated pedagogic and didactic strategies [6].

We have started a number of specific projects first of all by gathering the pluri-disciplinary researchers needed into groups. Our best wish is that the various results we arrived at should immediately be tested and got down to work gradually on the platform developed for the purpose. We can name a few:

- Specific keyboards for phones computers, TV panel controllers in national languages. [18]
- Text editors in local languages with a use of orthographic correctors
- Generation of special characters (in local languages) non UNICODE and development of pilots such as Linux, Windows for control (virtual keyboard) and display of characters on a screen when editing
- Translators (orthography, grammar, phonology) and numerical dictionaries in local languages
- Modules for vocal recognition (to teach and learn pronunciation)

- Didactic workshops on vocal recognition

With the various research programmes that go with this project, all the modules realized, specially the training platform, are updated in a dynamic way to integrate the results obtained or acquired from people initiated on.

It is from his reason that a team is now working at integrating m-learning techniques in the platform [4], other team is working on other aspects.

B. Operational Components of the Project

A survey has proved that this project scrupulously respects a well defined logic. Table 1 indicates the various components

of this project, the results expected and its measurement indicators while table 2 presents its physical display programme scheduled for five years.

C. Actors of the System

This system is made up of five different groups of actors. Figure 1 illustrates the role play of each category of actors in Cameroon context. It has already been hinted in [1].

Operationally, teachers and learners should work in a multimedia room equipped with computers connected to an Internet or a local network. These computers should be equipped with tools such as audio recorders, numerical photo device, video, microphones and earphones.

TABLE I. COMPONENTS OF THE PROJECT

N°	Components	Results	Measurement Indicators
1	Institutional and structural support Putting in place and rehabilitation of equipments Training of trainers and recruited network administrators	- multimedia centres built or rehabilitated -training of personnel and administrators	- Number of multimedia centers built or rehabilitated - Number of trainers trained - Number of platform administrators recruited or trained
2	Development of the platform for modernization of languages and cultures teaching	- operational platform - opening towards other modules	- operability and users-friendliness platform - Number of applicative layers offered - description of interactions with other research modules
3	Display, creation and enrichment of permanent contents	Scenarios and basic knowledge created	- Number of schools - Number and qualities of documents and media - Number of scenarii - Number of evaluations - Number of languages - Cultural heritage
4	Science of education and technology research projects applied to ICT, local languages and cultures	Research modules to facilitate languages teaching	- Number of research projects tested and appreciated positively - availability of the collaboration platform
5	Management of the project, of local personnel and of evaluation missions Consultations	- dissemination of information Control of resources management Missions meant for actors Control and evaluation structures	- distribution of budgetary package - Assessment of activities - missions specified and texts broadcasted - number of technical controls carried on

TABLE II. PHYSICAL DISPLAY PROGRAMME OF THE PROJECT

Phases & tasks to achieve	2010	2011	2012	2013	2014
Tasks/works	Analysis of the context and institutional framework	A survey of organizational and technical solutions Installation of basic Equipment	Display, equipment and solutions finding, beginning of experimentation Training	Installation of equipments Experimentation Assessment and preparation of a generalization plan	Installation of equipments Progressive Generalization and follow up of training sessions
Equipment	RAS	Basic equipment for development Passive equipments of pilot sites	Active equipment and Internet connection of pilot sites	Passive equipment of other sites	Active equipment and Internet connection of other sites
Consultation Services and Survey	Survey on context and institutional framework	Prior survey of technical and organizational solutions	Research and realization of basic scenarios and modules	Validation and feedback continuation of research in other modules	Continuation of development of complementary modules

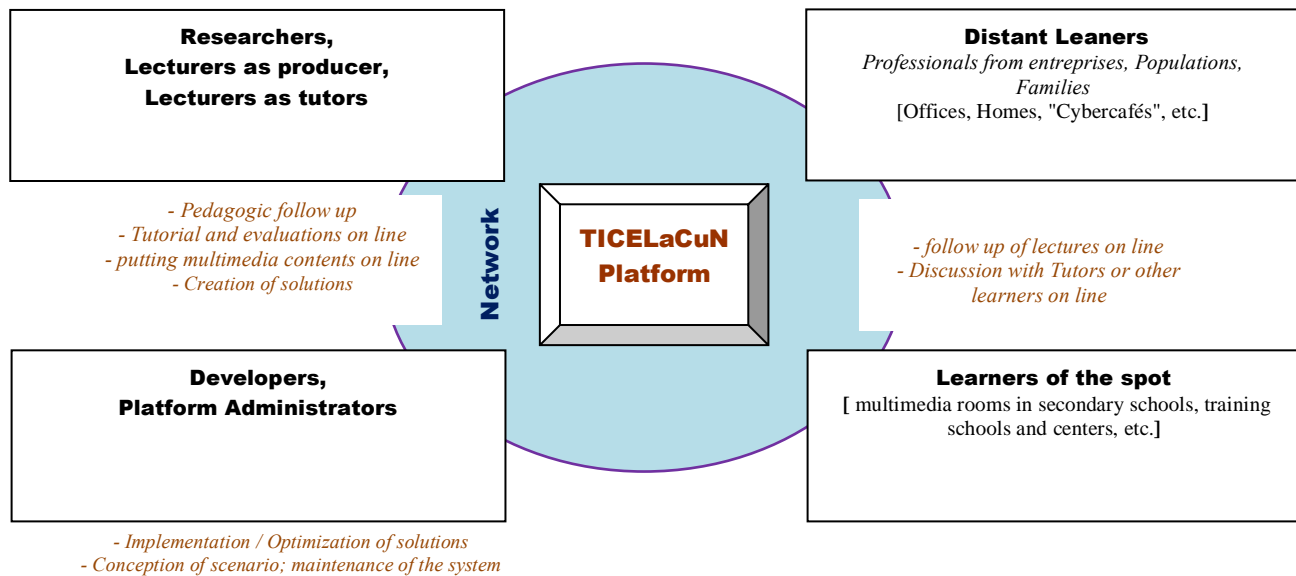


Figure 1. Various actors of the system

D. Technologies used and global architecture

We have based our research on a set of techniques and tools offered by New technologies and already discussed by many researchers in "E-learning" and "Web Services" domains [13] [14] [15] [3] [11]. We are going to put into action a set of applications integrated in our TICELaCuN platform. The online teaching – learning environment combines the two categories of tools usually found in ICT: asynchronous and synchronous tools.

In the following lines, we present the main technical components of our architecture with some guarantees it gives:

- Web access to available information such as lectures backups, directed work forms, Labs, charts, video
- Access to an important space of collaboration, share of ideas, classical communication integrated in our "numerical campus"
- A shared working platform; announcement space, classical or instantaneous messaging

Our strategy is basically focused on implementation and display of application thanks to free softwares such as:

- A secured Linux server (level of access, fireWall, Backup)
- Development and Communication tools such as Apache-MySQL-PHP, LDAP-SMB, WebMail-IMAP-SMTP
- Resources stocked on the platform based on Claroline kernel with its code deeply reviewed to adapt it to our need. These adjustments include evaluation modules, multiple connection control on the platform, chat, harmonization of authentication from LDAP (Lightweight Directory Access Protocol) in charge of centralization of resources input, the inter-operability and portability of the system. The platform of resources hosts various backups at various formats.

- A FilesServer that safely secures the stocking of directory of tutors and learners

Figure 2 presents the client-server architecture. It is of the « multi-tiers » type inspired from [11] [16]. The first layer is the interface, the second is the applicative layer and the third is the data stocking layer.

Our platform based on a basic technical kernel is dynamic. The description of this article geared towards computer science will not be taken in details; readers can report to [17] [11]. The TICELaCuN system is made up of a set of sub-systems presented as follow:

- The « Distant Learning System »: it offers a resources library to the learners registered such as multimedia backups, exercises and other didactic tools.
- The « Learning Management System » : It enables learners to register on line, to consult their marks on line, to submit and follow up the development of their petitions on time, just to list a few.
- The « Mail & SMS system » manages communication data between intervening actors. Messages are distributed automatically. The documents run by SIGES are equally transmitted by e-mail. The SMS module manages automatically alerts transmitted to tutors and learners (eg: submission of new documents, etc.).
- The global system users can use one account to log to every service offered by TICELaCuN. This is possible thanks to Universal LDAP directory.

Evidently, the access and communications between various modules and services make use of software buses.

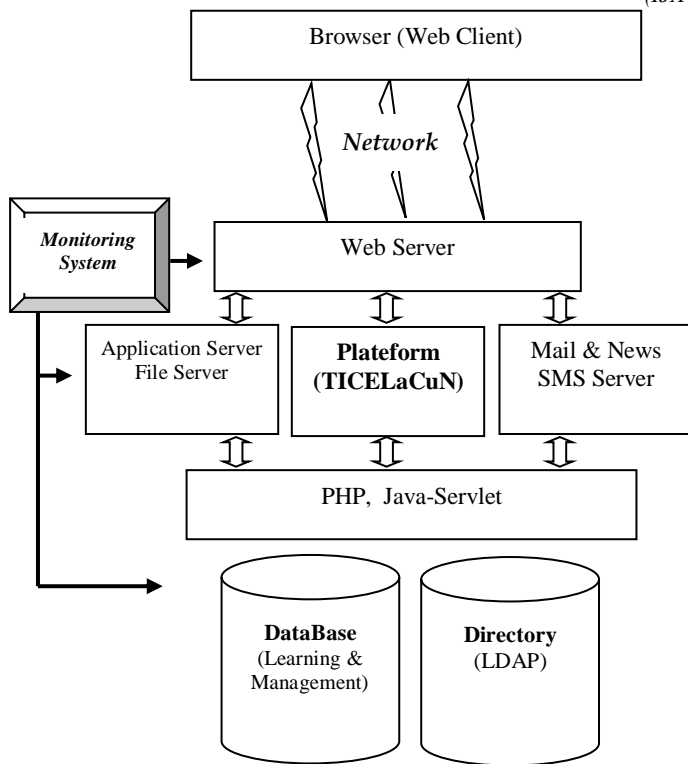


Figure 2. Architecture of the system

IV. RESULTS AND CONTRIBUTIONS OF THE PROJECT

A. State of fulfilment

The TICeLaCuN project is been set gradually and the setting up can already been observed. Terms of reference and various surveys have already been realized. They include:

- A survey on its impact
- Technical survey
- A survey on the risks
- A survey on the economy
- A survey and financial programming of works

As the real level of execution is concerned, we can name:

- The planning of all the tasks done
- Teams of correspondents at work
- Operational teams in activities
- The teams of researchers are been formed and are been

enlarged for, it is an important project embodying a variety of competences and human resources from various disciplinary domains.

Actually, a platform is been experienced and will permit to:

- create an online dictionary to learn a given language
- create an automatic translator of words in French and any chosen language

This project will enable to consolidate or to contribute to a better value of the requisites and predispositions in local languages to the development of technology.

B. Exploitation of results

This project of national scale will offer a framework for exchanges and free cooperation between specialists in local languages, sociologists, linguists, men in charge of cultures, researchers. It will permit to extend training to a larger number of people. It also stands as a solution to the lack of teachers in schools. Moreover, a lecturer could give his lectures independently to his/her geographical position.

The technology put in place will ease the updating of lectures' contents with a wider range of openings to exploitation.

We shall gradually sensitize the possible distant population via media and leaflets on the need to initiate days of national languages in schools and universities.

The project is backed by a dynamic web site for numerical archiving and preservation of national linguistic and cultural heritage. The contributions from the population are collected through the dynamic web site. Those of experts and correspondents pass through the platform displayed after seminar to train trainers.

The first modules of the platform are been experienced. Some extracts of them can be illustrated in [17] as presented afterwards. In figure 3, we have the page of translation from French to « ghomálá » (a local language spoken in the West Region of Cameroon) and figure 4 presents a page of learning the alphabet of the same language.

Table 3 presents the expected outputs and products of the first phase of the project. They are quantified in relation to the target population (men, women, young people and others) and their quantity.

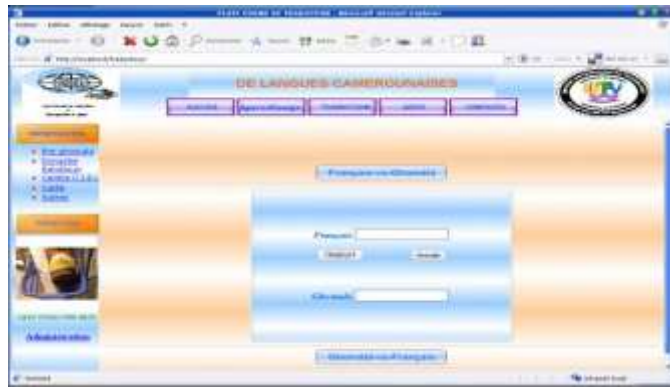


Figure 3. A translation page from French to “ghomálá” (a local language spoken in the West Region of Cameroon)



Figure 4. Page of learning alphabet in “ghomálá”

TABLE III. EXPECTED OUTCOMES AND PRODUCTS AWAITED FOR PHASE I OF THE PROJECT

Major outcomes (goods and services)	Quantity or values	Target beneficiaries			
		men	women	Young people	Others
• Training of trainers and leaders	150	50	50	50	
• Training of platform administrators	100	25	25	50	
• Production and distribution of CDROMs and DVD	500 000	150 000	150 000	200 000	All regions
• Display of TICELaCuN (TIC pour l'Enseignement des Langues et Cultures nationales) Platform	100 schools (government high schools and colleges...)	Total Access to schools	Total Access to schools	Total Access to schools	10 per region Schools, professionals, research institutions and homes
• Analysis and broadcasting on official site of numerical archiving and preservation of national cultural heritage	Accessible server via Internet and Intranets put in place	unlimited	unlimited	unlimited	The entire population
• Support of research through mobilization of researchers	Many teams planned at various levels of the project	30 researchers of different domains	15 researchers of different domains	40 developers And integrators	1 team to pilot and tens of correspondents and consultants
• Operationalization of many national languages	- phase 1 : 3 languages - phase 2 : more than 10 languages				An average of at least one language per Region

C. Projections : Display in schools

The projections planned for the progressive putting in place of the project in Cameroon in Regional Cameroon are presented in figure 5.

From the following chart, it is clearly seen that to cover the entire nation, it needs about five years.

				Potential=40	
			Potential=40	Confirmed=120	
		Potential=40	Confirmed=70		
	Potential=30	Confirmed=40			
Potential = 10	Confirmed=10				
Experimentation					
Sept. 2011	Sept. 2012	Sept. 2013	Sept. 2014	Sept. 2015	

Figure 5. Projections of display of the system in the nation

V. ANALYSIS OF IMPACT, OPENINGS AND PERSPECTIVES

Gradually as the project evolves, it becomes clear that we are managing to use systematically ICT to master our languages in training schools, research and homes. Standardization and harmonization of language teaching (official curricula) increases chances of success of students in official exams for, examination questions are common in the nation.

The majority of students in high schools and colleges registered in the platform are particularly motivated by their usage of new forms of teaching. They find these forms passionate thanks to the availability of operational pedagogic tools (teacher's guiding textbooks, Labs, individual training exercises, exams) and improvement of contents constantly updated.

Thus, we have succeeded a betting of mobilization of researchers (Doctorates and Masters) for the development of various applications.

We have presented the operational and technical components of the project, the carry on demonstrations [11] [12] [13] during which many opportunities were offered. Hence, from this project, the reflexion can be extended by researchers to:

- A profound survey of the influence of a language on development of science and technology;
- A thorough exploration of Internet and let its usage serve the development and interests of users while insuring the promotion of linguistic and cultural diversity;
- Analysis of the contribution of Internet to the reduction of gap between rich and poor countries, notably the numeral dissemination of technology and scientific information in local languages;
- Analysis of conditions of economical efficiency and

productivity of a multilingual Internet;

- Study how to make Internet affordable to all; how to overcome problems of equipments and make Internet affordable to people more or less literate;
- Development of new solutions and possibilities to create interfaces to give access to Internet to people who do not know how to use at least one of the major languages used in numerical network.

At a typical technical level, when we consider the technologies used or planned, the project opens new perspectives, with the possibilities of generalization of the usage of ICT through the development of supplementary management tools in other domains such as health, agriculture, virtual library, academics, etc.

VI. CONCLUSION

A language is the mirror, the face, the soul of the people and its culture, its mark of the existence. From our experiences, language teachers (as from their testimony) have a real framework required to efficiently train the learners by adapting their lectures to the needs and interests of learners in the country.

Though computers play a prominent role in on line teaching and learning process, the role of teachers cannot be minimized. We do not neglect the worries in [7]. They sustain the fear of computers and support the idea that computers dehumanize at consequently it discourages some people. But the general tendency of actors and target populations is a progressive motivation, thanks to positive contributions of the new forms of teaching-learning methods which make the learning process easy and exchanges as well as diversity among individuals.

This project offers important opportunities to the country, when considering its outcome as:

- Promotion of the development at social, human, economic and technological levels;
- Development through ICT and new forms of learning and teaching methods;
- Development of our capacities necessary to ease our integration on the global village while reducing the gaps between the rich and poor countries.

An actual asset on this project concerns free softwares. They provide:

- A better independence (technical, financial aspects, ...)
- More ease in the display
- More possibilities to update (GPL) the tools used
- More facilities of maintenance

The project will permit to overcome a number of challenges in future. It will provide a sustainable development with our languages and cultures through ICT.

ACKNOWLEDGMENT

This project has been conceived thanks to the expertise and support, be it direct or indirect of a number of partners and contribution of many structures already associated or to be associated to the project, notably:

- AUF (Agence Universitaire de la Francophonie),
- PNUD (Programme des Nations Unies pour le Développement),
- MINRESI (Ministère de la Recherche Scientifique et Technique)
- MINESUP (Ministère de l'Enseignement Supérieur du Cameroun)
- MINESEC (Ministère des Enseignements Secondaires) à travers ses Délégations Régionales et Départementales
- MINEDUB (Ministère de l'Education de Base)
- MINCULTURE (Ministère de la culture)
- University of Dschang / IUTFV Bandjoun (Internet Academy)
- Research Laboratories : LAIA (IUTFV), LIRIMA, LETS, LIMSS (National Polytechnic)
- Other Partners having exchanged with us during Seminars and Workshops: SIL, CABTAL, ANACLAC, CERDOLTOLA.

REFERENCES

- [1] Essono, L. (2008), « Enseignement des langues locales par Internet : Le Cameroun relève le défi », Revue en ligne Thot Cursus le monde de la formation à distance, mise à jour le vendredi 12 décembre 2008, <http://www.cursus.edu/?division=19&module=document&uid=66743&0=>
- [2] Onoholio S. (2009), « Lobbying Ingénieurs polytechniciens Mobilisation pour l'accès des langues africaines à Internet », Journal Le Messager, 7-12-2009
- [3] Drissi M. and Talbi M. (2009), « Dispositif de la formation à distance pour préparer les étudiants universitaires marocains à suivre des cours scientifiques en français – FOSEL (français sur objectifs spécifiques en ligne) », Revue africaine de didactique des sciences et des mathématiques, Numéro 4, 15 décembre 2009 : <http://www.radisma.infodocument.php?id=687>.
- [4] Lapalme, G. Brun, C. Dymetman, M. (2003). MDA-XML : une expérience de rédaction contrôlée multilingue basée sur XML, TALN 2003, Batz-sur-Mer, 11–14 juin 2003.
- [5] Laferrière T., Montane M., Gros B., Alvarez I., Bernaus M., Breuleux A., Allaire S., Hamel C., Lamon M. (2010), « Partenariats pour la coélaboration de connaissances : un modèle en émergence », Canadian Journal of Learning and Technology, V36(1) Fall / automne, 2010
- [6] Matoussi F., Simonneaux L. (2009), Didactique et Technologies de l'Information et de la Communication, ISDM N° 39, TICE Méditerranée Milano 2009, <http://isdms.univ-tln.fr>
- [7] Mattioli-Thonard A. (2009), « L'Enseignement Télématique des Langues: vers une bonne Distance », ISDM N° 39, TICE Méditerranée Milano 2009, 695, <http://isdms.univ-tln.fr>
- [8] Tomé M. (2009), « Compétences orales et outils de communication Web dans un projet de télécollaboration pour l'apprentissage du français langue étrangère », Journal of Distance Education, vol. 23, no. 1, 107-126, 2009
- [9] Marcellin Nkenlifack, Raoul Nangue, Bethin Demsong and Victor Kuete Fotso, ICT for Education: A Platform for Modernization of computer science teaching methods in secondary and high schools in Cameroon, International Journal of Advanced Computer Science and Applications, Vol. 2, No. 4, 2011
- [10] Marcellin Nkenlifack, Bethin Demsong and Raoul Nangue, Identité Numérique et Education : Enseignement des Langues Camerounaises grâce aux TIC, ISDM (Information Sciences for Decision Making), N° 41, 712, March 2011, <http://isdms.univ-tln.fr>
- [11] Nkenlifack M., Nangue R., Tchokomakoua M. (2009), «Projet TICLAC : TIC pour la Modernisation de l'Enseignement des Langues et Cultures nationales dans les établissements, Conférence internationale : ASAP 2009 sur la "Diversité culturelle et Internet multilingue en Afrique", 2 au 5 décembre 2009, Hôtel Hilton, Yaoundé-Cameroun
- [12] Nkenlifack M., Nangue R., Noulamo T. and Kwonche A. (2009), «Les TICE au service de la Formation Ouverte à Distance à l'Université de Dschang : Implémentation de SIEL (Système Intégré d'Enseignement en Ligne basé sur Internet)», Journal Langue et Communication, N° 07 novembre 2009, Revue scientifique internationale de recherche multidisciplinaire, ISSN 1560-3407
- [13] Fogue M. and Nkenlifack M. (2006), «Formation Ouverte à Distance : Nouvelle façon d'apprendre et d'enseigner, ETUDE DE CAS SUR LA DIVERSIFICATION DE L'ENSEIGNEMENT SUPÉRIEUR ET L'ADAPTATION AU MARCHÉ», Conf. Int., Thème "L'enseignement Supérieur au coeur des Stratégies de Développement en Afrique Francophone. Mieux Comprendre les Clefs du Succès", 13-15 Juin 2006, Ouagadougou, Burkina Faso : http://sitesources.worldbank.org/EDUCATION/Resourses/278200-1121703274255/1439264-1137083592502/Presentation_IUT_Dschang.ppt
- [14] Talla N., Tonye E., Dipanda A. and Ewoussoua L. (2010), «A model of Distance Learning of Technologies for Developing countries: Case of the Master (M2) in Telecommunications at the National Advanced School of Engineering in Cameroon», 10th African Conference on Research in Computer Science and Applied Mathematics CARI'2010, Côte d'Ivoire, Yamoussoukro, October 18 – 21, 2010
- [15] Meyong, C. (2010). Appropriation des innovations dans les écoles normales supérieures : une étude des besoins, des avantages et contraintes de l'intégration des TIC : Appropriation of the innovations in the Ecoles Normales Supérieures: a study of needs, advantages and constraints of the integration of ICT. frantice.net, Numéro 1 - juillet 2010. Récupéré du site de la revue : <http://www.frantice.netdocument.php?id=125>. ISSN 2110-5324
- [16] Koum G., Yekel A., Tampolla S. and Sanbong T. (2005), «Vocal Interaction in Web User Interface involving natural Language Processing», in Akono A., Tonye E., Dipanda A., Kokou Y. (ed.), Proc. Int. Conf. On Signal & Image Technology and Internet Based Systems, IEEE SITIS'2005, Yaounde, Cameroon, ISBN 2-9525435-0.
- [17] Mangui, A. Domche, S. (2008). Réalisation et Mise sur pied d'une plateforme web de traduction de langues camerounaises, Mémoire de fin d'études de DUT Informatique de Gestion, IUT FV de l'Université de Dschang, Cameroun, 2008.
- [18] Wishart J., McFarlane A. and Ramsden A. (2005), «Using Personal Digital Assistants (PDAs) with Internet Access to Support Initial Teacher Training in the UK», mLearn 2005, 4th World conference on mLearning, Cape Town, South Africa, 25 –28 October 2005. Available: <http://www.mlearn.org.za/CD/papers/Wishart.pdf>
- [19] Mvoto C. (2010), «Appropriation des innovations dans les écoles normales supérieures : une étude des besoins, des avantages et contraintes de l'intégration des TIC», frantice.net, Numéro 1 - juillet 2010. Récupéré du site de la revue : <http://www.frantice.netdocument.php?id=125>. ISSN 2110-5324

AUTHORS PROFILE



Dr. Marcellin NKENLIFACK is the Head of Computer Science Department at Fotso Victor University Institute of Technology, University of Dschang, and an Associate Professor. He is a holder of a M.A. Degrees in Computer Science and a Ph.D. in Computer Engineering and Control from National Polytechnic Institute, University of Yaounde I. He had been a visiting researcher at “Institut Scientifique et Polytechnique” Galilée – “Université de Paris 13” (2001), SUPELEC – Rennes – France (2003) and “Université Cheik Anta Diop” – Dakar, Senegal (2009). He has published more than 20 papers in reputed International journals and Conferences in the field of Software Engineering, Computer Applications in Industry and Engineering, Object oriented Modeling and Simulation, Meta-modeling, UML, Hybrid Control Systems, Distributed Control, Computer in Education, E-learning. He has been

awarded a Lecturer's award for 2003-2008 period for exceptional contributions towards developing e-learning at University of Dschang. He is an Editorial Board Member / Associate Editor / Reviewer of many international journals and conferences.

Bethin Demsong is a Head of Service in charge of General Affairs, IUT Fotso Victor of the University of Dschang, Cameroon, studying with the cycle of Master in Science of Language at the University of Dschang, Cameroon.

A. **Teko Domche** is Lecturer in Faculty of Letters, University of Dschang. He is co-authors of more than ten scientific papers in various journals.

Raoul Calvin Nangue is teaching and researching at Laboratory LAIA of the IUTFV of the University of Dschang. It is also a Doctorate in the “Department of Information and Communication Technology, School of ICT, Nelson Mandela Metropolitan University” in South Africa.

Automatic Queuing Model for Banking Applications

Dr. Ahmed S. A. AL-Jumaily

Department of Multimedia
IT College, Ahlia University
Manama, Bahrain

Dr. Huda K. T. AL-Jobori

Department of Information Technology
IT College, Ahlia University
Manama, Bahrain

Abstract—Queuing is the process of moving customers in a specific sequence to a specific service according to the customer need. The term scheduling stands for the process of computing a schedule. This may be done by a queuing based scheduler.

This paper focuses on the banks lines system, the different queuing algorithms that are used in banks to serve the customers, and the average waiting time. The aim of this paper is to build automatic queuing system for organizing the banks queuing system that can analyses the queue status and take decision which customer to serve. The new queuing architecture model can switch between different scheduling algorithms according to the testing results and the factor of the average waiting time. The main innovation of this work concerns the modeling of the average waiting time is taken into processing, in addition with the process of switching to the scheduling algorithm that gives the best average waiting time.

Keywords-Queuing Systems; Queuing System models; Queuing System Management; Scheduling Algorithms.

I. INTRODUCTION

Today banks are one of the most important units of the public. Since the foundational work of banks, many researchers try to get full advantage of any new technology to increase customer satisfaction. Therefore an active research has focused on analyzing the queues to optimize their operations and to reduce waiting time for customers [1,2,3].

This paper focuses on the bank lines system and the different queuing algorithms that used in banks to serve the customers. Most banks used standard queuing models. To avoid standing in a queue for a long time or in a wrong line, most banks use automatic queue system to give tickets to all customers. The customer can push a specific button in a tickets supplier device according to their needs.

The aim of this paper is to decrease customers waiting time by building a homogenous way that analyze the queue status and take decisions about which customer to serve by using the appropriate scheduling algorithm.

The rest of this paper is organized as follows. Section 2 consists of queuing systems characteristics, most common scheduling algorithms, and the queue models. Then our proposed queuing system model is shown in section 3. Experimental results are shown in section 4, followed by brief conclusions and suggestions for future work are shown in section 5. Then the references are shown in section 6.

II. QUEUING SYSTEMS

A queuing system consists of one or more servers that provide service to arriving customers. Figure 1 shows the characteristics of queuing system [4].

The population of customers may be finite (closed systems) or infinite (open systems). The arrival process describes how customers enter the system. The customers arrive to the service center in a random fashion.

Queue represents a certain number of customers waiting for service. The capacity of a queue is either limited or unlimited. Bank is an example of unlimited queue length.

The service is an activity requested by a customer, where each service takes a specific time. The scheduling algorithm is used to order the customers and to choose the next customer from the queue. The most common scheduling algorithms are [4,5]:

a) *FCFS (First Come First Serve):* The customers are served in the order of their arrival, which is most visibly fair because all customers think of themselves as equal.

b) *RSS (Random Selection for Service):* In this algorithm, customers are selected for service at random, so each customer in the queue has the same probability of being selected for service irrespective of his/her arrival in the service system.

c) *PRI (Priority Service):* The customers are grouped in priority classes according to some external factors. The customer with the highest priority is served first.

d) *SPF (Shortest Processed First):* The algorithm assumes that the service times are known in advance. When several customers are waiting in the queue, the SPF algorithm picks the shortest service time first.

The departure represents the way customers leave the system.

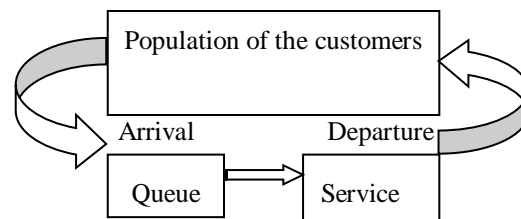


Figure 1: Simplest Queuing System

In queuing system, there are many types of queue models such as [5,6]:

- a) *SQ (Single Queue):* In this model each customer waits till the service point is ready to take him for servicing.
- b) *MQ (Multiple Queues):* In this model each customer tries to choose the shortest queue from a number of individual queues.
- c) *DQ (Diffuse Queue):* In this model each customer take a ticket from a ticket machine with single or multiple buttons each for specific service. After the customer registers his/her place in the queue by a ticket he/she will monitor the ticket number being served. The customers can not estimate when they will be served.

III. THE PROPOSED QUEUING SYSTEM MODEL

We know present a new technique for queue management system in banks. Our technique is to builds an automatic queuing system that can test the status of the queuing system such as DQ and choose the appropriate algorithm among more than one scheduling algorithms that already defined in the system such as FCFS and SPF to select the next customer to be served during a specific period of time.

Selecting the scheduling algorithm depends on the testing results to achieve the best waiting time for all the available customers that are waiting to be served.

To achieve this goal we add additional components to the traditional queuing management system as shown in figure 2.

The suggested queuing system consists of the following components:

- a) *Customer area:* In customer area the customer selects a service at the ticket dispenser via regular push buttons, and waits until his/her ticket number shown in a vision and/or audio notice for the number.
- b) *Queuing area:* In queuing area the system uses the queuing algorithm that is chosen by the testing area to select one of the waiting customers.
- c) *Testing area:* In testing area the system tests the status of the system according to the existing algorithms in the algorithms database and compares between all the result for the expected waiting and response time then selects the algorithm that gives the best waiting time.
- d) *Scheduling Algorithms Database area:* All the needed scheduling algorithms, the testing result, and the customers numbers, are stored in the scheduling algorithms database area. The testing result and the customer's numbers are saved temporarily.

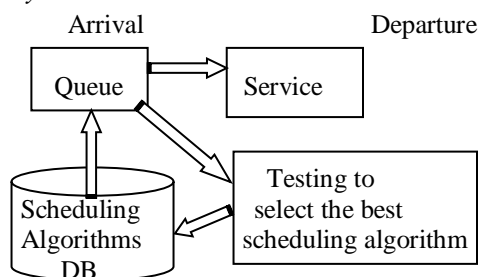


Figure 2: The new Queuing System

- e) *Service area:* In service area the system serves the customer according to the different services that a bank can give as open an account, transaction, send money, deposit funds, balance, etc. Each service needs a specific time.

IV. EXPERIMENTAL RESULTS

Simulations were carried to test the performance of the new proposed system. A database of two standard scheduling algorithms was developed to systematically evaluate the proposed system. For the purpose of illustrations, a comparison between the new system and the ordinary system (FCFS) that is used usually in most of the banks queuing systems.

In the proposed system, two scheduling algorithms are used (FCFS, SPF). For the purpose of calculation and reality a random number generation is used to generate a sequence of customers' arrival time and to choose randomly between three different services: open an account, transaction, and balance, with different period of time for each service: 15, 10, and 5 respectively.

The proposed system will test the queuing system using testing algorithm every specific period of time, let's conceder it 15 time unit, to select the appropriate scheduling algorithm i.e. either FCFS or SPF according to the average waiting time.

To test the proposed system we implement two case studies:

Case 1: After executing the random generator, a simulation snapshot for the queuing system is generated, the result are 20 customers with different arrival time starting from zero, and different service time as shown in table 1.

After implementing the ordinary queuing system and the proposed queuing system on the above snapshot, the resulted Gantt chart for the ordinary queuing bank system that uses only FCFS algorithm, as shown in figure 3.

The new queuing system calculates the waiting time for each customer, then calculates the total waiting time and the average waiting time according to the two algorithms (FCFS, SPF) each 15 time unit as shown in figure 4, it can switch between the two algorithms at the end of the time unit by selecting the algorithm with the minimum average waiting time.

TABLE 1: A SNAPSHOT FOR THE GENERATED QUEUING SYSTEM

Customer	Arrival Time	Service Time	Service Type
C1	0	10	Transaction
C2	5	15	Open account
C3	8	5	Balance
C4	15	10	Transaction
C5	17	5	Balance
C6	19	5	Balance
C7	20	10	Transaction
C8	25	5	Balance
C9	28	5	Balance

C10	30	10	Transaction
C11	40	15	Open account
C12	42	5	Balance
C13	43	5	Balance
C14	44	5	Balance
C15	110	15	Open account
C16	111	10	Transaction
C17	112	5	Balance
C18	113	5	Balance
C19	114	5	Balance
C20	115	10	Transaction

FCFS

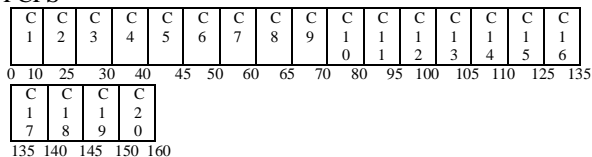
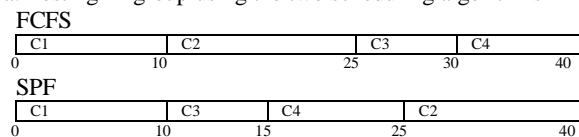
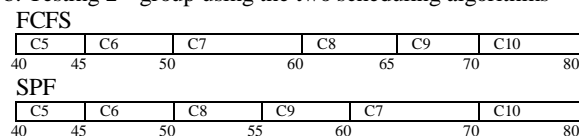


Figure 3: Ordinary queuing system Gantt chart

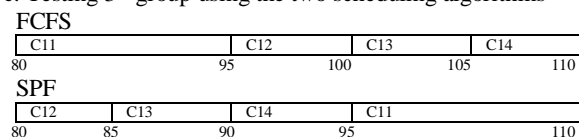
a. Testing 1st group using the two scheduling algorithms



b. Testing 2nd group using the two scheduling algorithms



c. Testing 3rd group using the two scheduling algorithms



d. Testing 4th group using the two scheduling algorithms

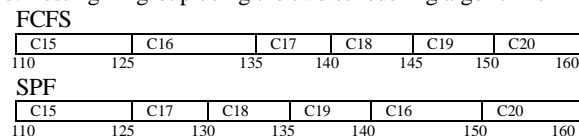


Figure 4: The new queuing system Gantt chart (a, b, c, d)

Through the extensive experiments conducted, the primary goal is to determine the ability of the new queuing system against the ordinary queuing system.

Figure 5 show that the new approach decreases the average waiting time, compared with the ordinary queuing system.

Equation 1 is used to calculate the waiting time for each customer [7]:

$$CWT_i = SSTC_i - ATC_i \quad (1)$$

Where:

CWT is a Customer Waiting Time
 SSTC is Start Serving Time for a Customer
 ATC is Arrival Time for a Customer
 i is The ith Customer number

The average waiting time for each group of customers is calculated using equation 2.

$$AWT = (\sum CWT_i) / TN \quad (2)$$

Where:

AWT is Average Waiting Time
 CWT is a Customer Waiting Time
 TN is total number of customers served
 i is the number of customer

Table 2 shows the average waiting time for the ordinary queuing system and the new queuing system.

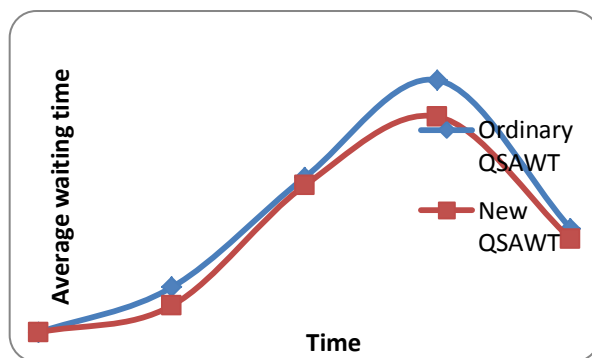


Figure 5: The different between the ordinary queuing system and the new queuing system

TABLE 2: THE AVERAGE WAITING TIME COMPARISON BETWEEN THE ORDINARY QUEUING SYSTEM AND THE NEW AUTOMATIC QUEUING SYSTEM

Time Slice	Ordinary Queuing System Average Waiting Time and Algorithm	New Automatic Queuing System Average Waiting Time and Algorithm	The Difference Between Ordinary and New Algorithm
1 st Group	9.25 / FCFS	5.5 / SPF	3.75
2 nd Group	31.83 / FCFS	30.16 / SPF	1.67
3 rd Group	52.75 / FCFS	45.25 / SPF	7.5
4 th Group	21.33 / FCFS	19.166 / SPF	2.164
Total Average waiting time	28.45	24.95	3.5

Case 2: After executing the random generator, a simulation snapshot for the queuing system is generated, the result are 12 customers with different arrival time starting from zero, and different service time as shown in table 3.

After implementing the ordinary queuing system and the proposed system on the above snapshot, we compare the results of waiting time and average waiting time. The results of comparison between them are shown in figure 6, figure 7, figure 8, and table 4 respectively.

TABLE 3: A SNAPSHOT FOR THE GENERATED QUEUING SYSTEM

Customer	Arrival Time	Service Time	Service Type
C1	0	15	Open account
C2	3	5	Balance
C3	9	15	Open account
C4	12	15	Open account
C5	14	10	Transaction
C6	18	5	Balance
C7	25	5	Balance
C8	28	5	Balance
C9	29	5	Balance
C10	42	10	Transaction
C11	43	10	Transaction
C12	44	5	Balance

FCFS

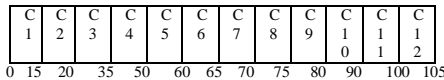
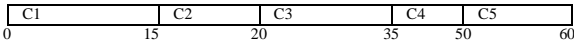


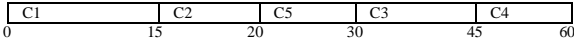
Figure 6: Ordinary queuing system Gantt chart

a. Testing first 15 time unit using the two scheduling algorithms

FCFS

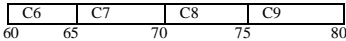


SPF

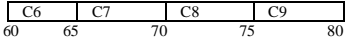


b. Testing 2nd 15 time unit using the two scheduling algorithms

FCFS

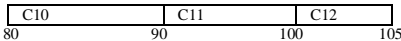


SPF



c. Testing 3rd 15 time unit using the two scheduling algorithms

FCFS



SPF

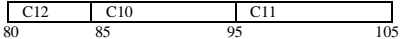


Figure 7: The new queuing system Gantt chart (a, b, c, d)

Table 4 shows the average waiting time for the ordinary queuing system and the new queuing system, it illustrate how the new queuing system fillips between the two different scheduling algorithms according to the average waiting time.

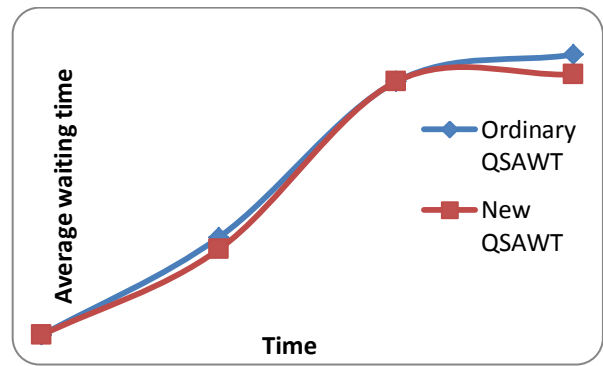


Figure 8: The different between the ordinary queuing system and the new queuing system

TABLE 4: RESULTS SHOWS THE AVERAGE WAITING TIME COMPARISON BETWEEN THE ORDINARY QUEUING SYSTEM AND THE NEW AUTOMATIC QUEUING SYSTEM

Time Slice	Ordinary Queuing System Average Waiting Time and Algorithm	New Automatic Queuing System Average Waiting Time and Algorithm	The Difference Between Ordinary and New Algorithm
1 st Group	16.4 / FCFS	14.4 / SPF	2
2 nd Group	42.5 / FCFS	42.5 / FCFS	0
3 rd Group	47 / FCFS	43.66 / SPF	3.34
Total Average waiting time	32.75	31.083	1.667

V. CONCLUSION AND FUTURE WORK

In a queue system, the balance between dealing with all customers fairly and the performance of the system is very important. Sometimes the performance of the system is more important than dealing with the customers fairly.

In this paper, we have presented a new technique for queuing system called automatic queuing system. The proposed technique showed improvements in average waiting time.

It will be more effect to add more factors in testing to take the right decision for choosing one of the available scheduling algorithms, such as throughput, utilization, and response time.

Also adding more scheduling algorithms to the system database will be useful.

REFERENCES

- [1] B. Goluby, and R. Preston McAfee, "Firms, queues, and coffee breaks: A flow model of corporate activity with delays", Springer-Verlag, vol.15, pp. 59-89, March 2011.
- [2] A. Mobarek, " E-banking practices and customer satisfaction- a case study in botswana", 20th Australasian Finance & Banking Conference, 2007.
- [3] O. Luštšik, "E-banking in estonia: Reasons and benefits of the rapid growth", University of Tartu, kroon and economy, vol. 3, pp.24-36, 2003.
- [4] K. Sanjay, Bose, "An introduction to queuing systems", Springer, 2002.

- [5] F. Mohamad, "Front desk customer service for queue management system", Master Thesis, University Malaysia Pahang, November, 2007.
- [6] A. Allen, "Probability, statistics, and queuing theory with computer science applications", Academic Press Inc., Second Edition, 1990.
- [7] A. Willig, "A short introduction to queuing theory", Technical University Berlin, Telecommunication Networks Group Sekr. FT 5-2, Berlin, July 21, 1999.

Error Detection and Correction over Two-Dimensional and Two-Diagonal Model and Five-Dimensional Model

Danial Aflakian 1 , Dr.Tamanna Siddiqui 2, Najeeb Ahmad Khan 3 ,Davoud Aflakian 4

Department of Computer Science

E-mails: a_danial85@yahoo.com, ja_zu_siddiqui@hotmail.com, nakhan@jamiahamdard.ac.in , davoud2007@yahoo.com

Abstract— In this research paper we discover two different schemes of error detection and correction which are based on parity-check code for optimal error detection and correction utilizing check bits without degrading the data rate too much. The scheme of the first method is obtained by arranging data in rows, to form a square, and then parity bits are added. The second scheme builds upon the first, by forming a square cube and the parity scheme is extended to this shape.

Keywords-component; Data Communication; Error detection and correction; Linear Block Coding; Parity check code.

I. INTRODUCTION

For transmission purposes, all signals consist of digital packets. To protect against data corruption, extra bits are added for error detection and correction. Corruption of data can occur due to the degradation of the signal due to noise or other impairments during transmission of signal from transmitter to receiver. Error detection [1] involves additional bits added to data at the transmitter end and sent as part of the packet. On reception, if the error scheme detects the data received is incorrect, then the receiver asks the transmitter to retransmit the data. In error correction, not only does the receiver detect the error, but is also able to recover correct data depending on the level of error correction implemented, i.e. the number of bits incorrect from which the error correction scheme is able to recover the correct data. The greater the level of error correction, the more bits required to be added to the data. There are two types of codes, the non-systematic and the systematic. A non-systematic code is one which accomplishes multiple error detection and correction through construction of a directory or catalog of word entries.

The first systematic error correction code was invented by W. Hamming [2]. There are many error correction schemes. One of the schemes involves dividing the data into blocks of k bits, called datawords, and adding r redundant bits. The resultant n bit blocks (consisting of $k + r$ bits each) are called codewords [3]. The method considered here consists of adding a single bit, known as a parity bit, to make either the number of 0's even or the number of 1's even (we consider making the number of 1's even in this article).

This scheme detects only an odd number of error bits. On reception, this scheme counts the number of 1's in the block.

If it is even, it considers the signal to be correct. If an even number of bits have been flipped during transmission, i.e. an even number of bits are incorrect on reception, this scheme does not detect an error.

The above method is called Simple parity check code, there are some methods which are based on simple parity check code known as Two-dimensional parity-check code, N-dimensional parity check code, three-dimensional parity-check code(S-codes families)[4] ,Multi-dimensional parity-check code theory[5], and Three and Four-dimensional Parity-check codes[6]. In Two-dimensional parity-check code, codewords are arranged separate rows to form a rectangle. Then, parity checking is also done for each column of the rectangle.

Four-dimensional parity-check code improves on Two-dimensional parity-check code by adding parity bits for the diagonal lines, as shown in figure 1, of the square or rectangle. For more information please refer to [6].

We studied four-dimensional and S-code and found that both are the same in the number of errors detected and corrected, but S-code's parity bits are more reliable and it has a better code transmission rate due to S-bits. We also discovered that S-code is more suited to a square shape, as this gives this scheme more reliability in the parity bits and makes it less complex.

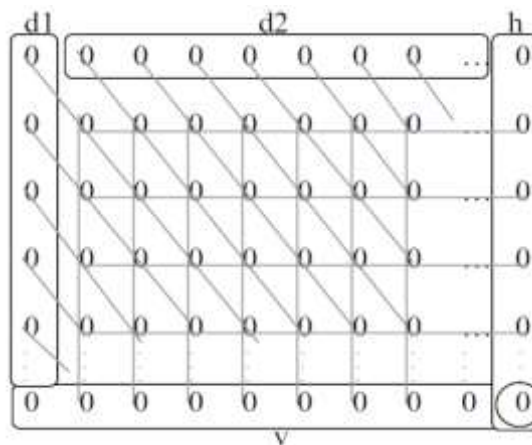


Figure 1, Four dimensional parity check code[6].

II. PROPOSED WORK

In this publication we improve on 4-dimensional parity-check code, which was published on 2004 which is final related work. We discovered two methods of improvements:

Case 1: Two-dimensional and Two-diagonal parity-check codes.

Case 2: Five-dimensional parity-check code.

A. Case 1: Two-dimensional and Two-diagonal parity-check code:

In this scheme, we add parity bits for the diagonals of the square to have the same bit rate of 4-dimensional parity-check code. This method involves five sequential steps, as follows:

- First Step: The top parity row is constructed as follows (see figure 2). Each parity bit in the top row is a parity bit for a fixed number of bits, the count of which is decided by the main diagonal. The diagonals being considered to construct the top parity row are those oriented from the top left to the bottom right. The main diagonal is taken from the top left corner to the bottom right corner (shown as a line in black in figure 2, with its parity bit also shown as black). Subsequent parity bits consist of two portions. The first portion consists of the diagonal below the parity bit, and the second portion consists of furthest diagonal below the main diagonal not used yet, e.g. the second parity bit is shown in yellow and its two portions are also shown as yellow lines in figure 2. Similarly each parity bit is shown in a different colour and its two portions are shown in the same colour in figure 2.

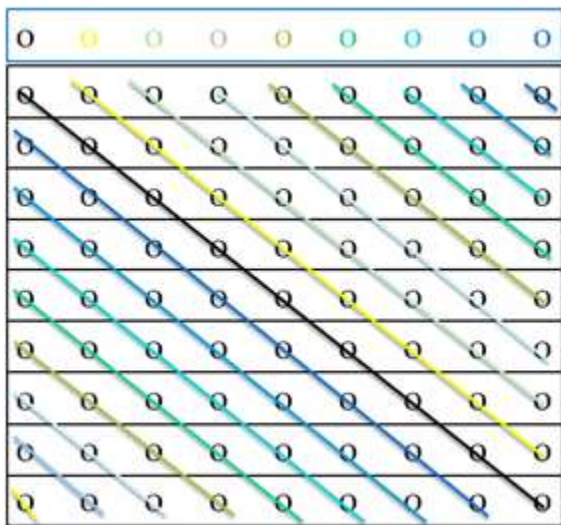


Figure 2, Top parity row.

- Second Step: The parity bits for the left column of parity bits are formed using the same method as step one, but consist of diagonals formed from bottom left to top right (as shown in figure 3).
- Third Step: The parity bits for the right column of parity bits are formed by taking each bit as the parity bit for its row of bits.

- Fourth Step: The parity bits for the bottom row of parity bits are formed by taking each bit as the parity bit for its column of bits.
- Fifth Step: Four bits are coloured red and inside red squares in figure 3. We use these bits as parity bits for others parity bits formed in steps one to four. The top right corner bit is the parity bit for the top row of parity bits. The bottom left corner bit is the parity bit for the left column of parity bits. The bottom right corner bit is the parity bit for the bottom row of bits, including the corner bit obtained in the previous calculation. The top left corner bit is the parity bit for the right column of parity bits, including the top right corner and bottom right corner bits. This scheme enables detection and correction of all errors in top parity row and left parity column. It detects odd number of errors in bottom parity row and right parity column. It also detects errors in the first three parity bit corners in red. The last calculated corner red bit (top left corner) has no parity bit associated with it and is critical in our error detection and correction scheme. One solution involves transmitting this top left corner parity bit thrice to ensure that there is no error in receiving it during transmission.

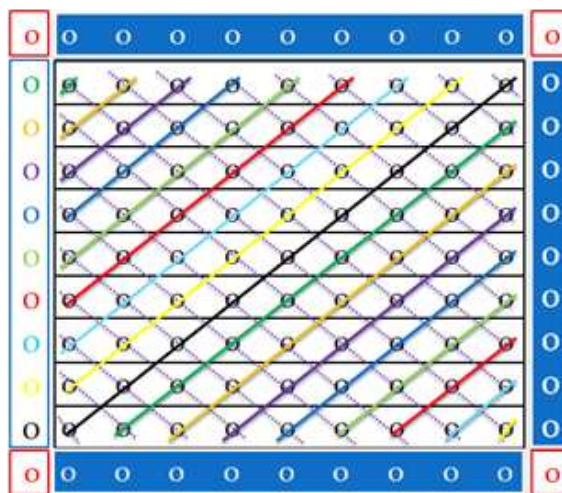


Figure.3: Two-dimensional and Two-diagonal parity-check code.

This scheme can detect 7 errors with 100% insurance (i.e. even if there is an error in parity bits). If there are 8 errors on vertices of a regular octagon, then the errors go undetected (as shown in figure 4). This scheme also corrects up to 4 errors. This error correction can also be improved upon by using the trial and error method of [7].

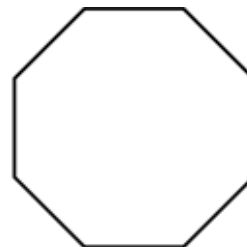


Figure 4, Undetectable 8-bit error pattern.

B. Case 2: Five-dimensional parity-check code

In this scheme a cube of data bits are formed. Then parity bits are present on five sides of the cube utilizing the following steps:

- First Step: The cube of data bits is divided into planes of squares. For each square, parity bits are formed using the scheme of Two-dimensional and Two-diagonal parity-check code.
- Second Step: In first step we obtained parity bit planes for four sides of the data cube. The fifth plane of parity bits is obtained as follows. We consider the forward facing face of cube (the only other remaining face is the back face), as seen in Figure 5. Each bit in this parity plane is calculated as the parity bit for the depth bits, except for the left column and top row. The left column parity bits are obtained by considering each bit the parity bit for its row in the parity plane. Similarly, each parity bit in the top row is obtained by considering it the parity bit of its column in the parity plane.
- Third Step: The common bit for the left column and top row is named as the share bit here. The share bit is got by taking the parity of its row, column and depth.

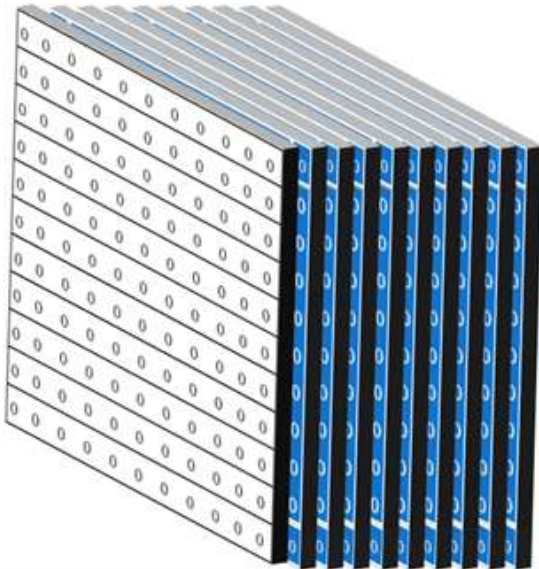


Figure 5, Five-dimensional parity-check code.

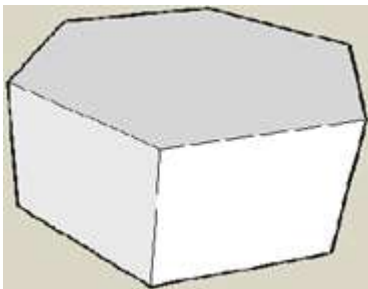


Figure 6, Undetectable 16-bit error pattern.

In this scheme, errors will go undetected if the errors form the shape of a regular octagonal prism (shown in figure 6). The probability of this happening is quiet low.

III. ANALYSIS

The advantage of proposed schemes can be demonstrated through overhead and code rate calculation.

A. Case1 overhead and code rate:

In case 1, the scheme uses data formed into a square, say of side of length L. Then:

$$\text{Number of information bits} = L^2$$

$$\text{Number of parity check codes} = L+L+L+L+4=4L+4$$

$$\begin{aligned} \text{Total number of bits (information bits +parity bits)} \\ = L^2+4L+4 \end{aligned}$$

$$\text{Overhead} = \frac{\text{No. of parity bits}}{\text{No. of information bits}} = \frac{4L+4}{L^2}$$

$$\text{Code Rate} = \frac{\text{No. of information bits}}{\text{Total number of bits}} = \frac{L^2}{L^2+4L+4}$$

If we compare four-dimensional parity-check code of [6] with case 1, we find that both have the same overhead and code rate, but our scheme makes a notable improvement in error detection and correction on information bits as well as parity bits.

B. Case2 overhead and code rate

This scheme uses a cube of data bits, say of side L. Then:

$$\text{Number of information bits} = L*L*L=L^3$$

$$\begin{aligned} \text{Number of parity bits} &= (L+L+L+L)*L+4L+(L+1)*(L+1) \\ &= 4L^2+4L+L^2+1+2L=5L^2+6L+1 \end{aligned}$$

$$\begin{aligned} \text{Total number of bits (information bits +parity bits)} \\ = L^3+5L^2+6L+1 \end{aligned}$$

$$\text{Overhead} = \frac{\text{No. of parity bits}}{\text{No. of information bits}} = \frac{5L^2+6L+1}{L^3}$$

$$\text{Code Rate} = \frac{\text{No. of information bits}}{\text{Total number of bits}} = \frac{L^3}{L^3+5L^2+6L+1}$$

Overhead and code rate is worse than previous methods, but error detection and correction is better.

C. Diagram of both cases

. In Figure 7, the vertical axis shows code rate and horizontal axis shows number of information bits. we replaced

L with some numbers to give comparisons. In figure 7, red indicates Two-dimensional parity-check code, blue indicates Four-dimensional parity-check code, green shows case 1, and violet shows case 2. We have shown case 2 separately, since it is not possible to compare its bit rates with others.

IV. CONCLUSION

In the Two-dimensional and Two-diagonal parity-check scheme we increase the number of errors detected and corrected by four-dimensional parity-check [6] by two, while maintaining the same overhead and code rates. The errors detected and corrected can be improved further by the trial and error method of [7]. Also it has a better detection on right column of parity bits and bottom row of parity bits. Errors on left column of parity bits and top row of parity bits are possible to correct.

For Five-dimensional parity-check code, up to 15 errors can be detected with the same level of error correction as the previous method. It is possible to improve on the error

detection and correction by using methods similar to trial and error method of [7].

REFERENCES

- [1] Shu Lin Daniel J. Costello Jr, "Error Control Coding: Fundamentals and Applications". Prentice Hall. ISBN 0-13-283796-X. , 1983.
- [2] R. W. Hamming, "Error detecting and error correcting codes", Bell System Tech. J. 29 , 1950 ,pp. 147-160.
- [3] Behrouz Forouzan, "Data communications and networking" ISBN-13:978-0-07-063414-5,2006.
- [4] Morris Rubinoff, "N-Dimensional Codes for Detecting and Correcting Multiple Errors", Communications of the ACM , Dec. 1961 .
- [5] Tan F.Wong and John M.Shea, "Multidimensional parity- check codes for bursty channels", Proceedings of the IEEE international Washington, DC , USA, June. 2001.
- [6] Naveen Babu Anne, Utthaman Thirunavukkarasu, Dr. Shahram Latifi, "Three and Four-dimensional Parity-check Codes" Proceedings of the International Conference on Information Technology: Coding and Computing (ITCC'04) 0-7695-2108-8/04, pp. 267-282, 2004.
- [7] Ashby, W. R, "Design for a Brain". Chapman & Hall (1960: Second Edition

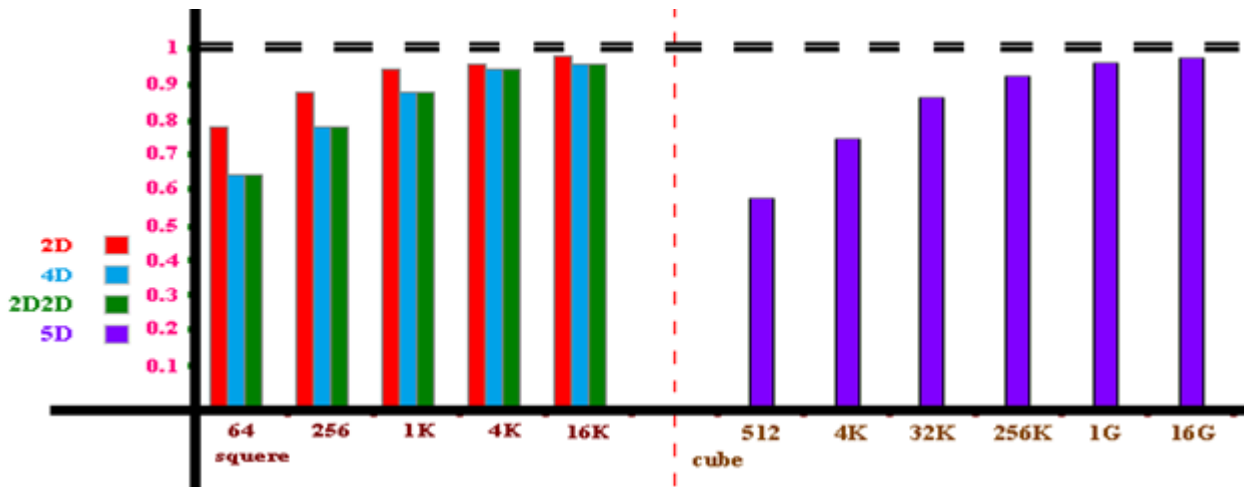


Figure 7, Code rate diagram for two proposed work schemes as well as Two and Four-dimensional parity-check codes.

Developing Digital Control System Centrifugal Pumping Unit

Digital Control Systems

Safarini Osama
IT Department
University of Tabuk,
Tabuk, KSA

Abstract— Currently, the leading Russian oil companies engaged in the development of automatic control systems (ACS) oil equipment, to improve its efficiency.

As an example of an object needed to optimize its work, a centrifugal pumping unit (CPU) can be specified. Frequency actuators provide an opportunity to run CPU in any algorithm, and many industrial controllers, are part of the automatic control system technological process (ACSTP), allow optimizing the operation of the centrifugal pumping unit and help determine the requirements for the development of digital automatic control system for CPU.

The development of digital automatic control systems for such a complex nonlinear control object like CPU has several features that should be considered when designing control systems for that object.

Keywords- ACS - Automatic Control System; CPU- Centrifugal Pumping Unit; PID- A proportional-integral-derivative.

I. INTRODUCTION

Modern status of oil producing companies is characterized by an increase in water content well product, which leads to increased costs of oil production.

One possibility to reducing costs is to use optimization methods of field equipment, through the development and implementation of optimal digital automatic control systems oilfield objects.

The solution of this problem consists of several stages and involves the development of models of control objects (primarily nonlinear) for the synthesis of regulators, for the simulation of control systems on digital computers, as well as developing methods for designing digital control systems and means to optimize their work.

II. DISCUSSION

In the synthesis of ACS CPU must consider several system requirements, determined by the characteristics of the controlled object and features of its operation. One such requirement is the frequency of the time discretization (sampling), which is mainly determined by the response time to emergencies. Frequency of issuing solutions of ACS is

governed by RD-35.240.00-KTN-207-08 JSC AK “Transneft”, according to which the processing of signals in the controller does not exceed 0.1s. Thus, the frequency of issuing control actions cannot be less than 10 Hz.

The second system requirement is a record of the presence of noise and interference in the measured values of management technological parameters. In practice, the pumping units are often located far away from the controller, which leads to significant levels of noise and interference in the measured values of adjustable parameters. A third feature to be considered in the design of ACS CPU is the presence of delays in information channels. Time delays of measured parameters and control signals lead to a significant reduction in the reserves stability of ACS CPU.

The next feature to be considered when designing the ACS CPU, The presence of an integral component of the control signal to the most widely used PID control algorithm [1] [2]. In the short-term disruptions in the supply voltage, important integral component of the PID can lead to disaster. It is therefore necessary to minimize the possibility of an integral component in the control signal and, furthermore, restricts its maximum value.

The fifth is particularly true nonlinear CPU as the object of control, making it necessary to change the controller parameters depending on the mode of operation.

As a parameter characterizing the mode of operation, for example, is chosen the rotation frequency of induction motor drive. To eliminate the problems associated with a step-change in the coefficients of the regulator [3], it is useful to determine their functionality depending on the mode of operation, for example, in the form of polynomials.

At the final stage of the development of ACS CPU, it is necessary to analyze the stability of the system. Low stability margins lead to instability and breakdown of equipment and armature CPU. Sustainable control system must meet engineering standards of quality, such as $\Delta\varphi \geq 45^\circ$, $\Delta L \geq 12$ dB where $\Delta\varphi$ and ΔL - system stability margins in phase and amplitude, respectively [4].

III. DESIGNING ACS CPU BASED ON SYSTEM FEATURES

As an example, the control system designed to meet the above functioning features, can lead the pressure of ACS to the output of CPU [5]:

$$\delta W_i = (P_i^{pr} - P_i) - K_D \cdot B_{1,i} \cdot (P_i - P_{i-1}) + B_{2,i} \cdot (\varphi_i - \varphi_{i-1}),$$

$$\begin{aligned} \delta W_{Int,i} &= \delta W_{Int,i-1} + \delta W_i \cdot \tau, \\ \delta W_i &= K_I \cdot \delta W_{Int,i} + K_P \cdot \delta W_i^p, \end{aligned} \quad (1)$$

Where - δW_i power, supplied to the engine in the current cycle control;

P_i^{pr} - Relative value of a given fluid pressure in the i-th step of control;

P_i, P_{i-1} - The relative fluid pressure on the current and previous steps of control;

φ_i, φ_{i-1} - The relative frequency of rotation of the CPU drive for current and previous steps of control;

τ - Duration of one cycle control.

The numerical values of the parameters $B_{1,i}$ and $B_{2,i}$ are determined in the process of design of ACS CPU.

The coefficients K_P , K_D and K_I are the coefficients of proportionality, differentiation and integration, respectively.

The value of the integration step ACS was chosen equal to the $\tau = 0.025$ sec. Thus, the frequency output of control influence ACS is 40 Hz.

In this case, reception, signal processing and issuance of the control action took three steps of control or 0.075 seconds, which satisfies the requirements of the regulations in 0.1 seconds.

The proposed implementation scheme ACS CPU (1) is based on the PID Act and is distinguished by the presence of additional feedback from the derivative rotation frequency of the drive of CPU.

The advantage of this structure is that it allows taking into account the dynamics of the drive motor and, thereby increasing the stability margins of the control system of fluid pressure.

To minimize the value of the integral component in the total control signal is necessary to obtain maximum transfer coefficient of the system while keeping the monotonic nature of the transition processes.

To do this, it is necessary to find the optimal value of the coefficients K_P , K_D and K_I by the method presented in [6]. The technique allows to determine the optimal coefficients ACS CPU considering engineering criteria for the quality of ACS.

At the first stage, the values of K_P , and K_D are determined, which provide the maximum value of static coefficient of transmission systems with a monotonic nature of the transition processes. In the second stage, the coefficient of the integrator K_I is determined, providing the highest system performance in the class of systems with monotonic transition processes

Minimizing the time of the transition process in the class of systems with monotonic processes is provided by the proposed definition of a minimum criterion of optimization. Then, the output value of the integrator is limited.

After finding the optimal coefficients for all the calculated modes of CPU according to [6], the coefficients K_P , K_D and K_I are converted into the functional dependence $K_P()$, $K_D()$ and $K_I()$ on the mode of CPU (as a mode of operation is the Frequency of rotation of the CPU drive).

For example, the coefficient of differentiation of the functional dependence of the frequency of rotation of the CPU drive will look like:

$$K_P(\varphi) = 0,3685 \varphi^2 - 1,4105\varphi + 9,6641 \quad (2)$$

IV. THE SIMULATION RESULTS

Experimental study of optimal digital ACS CPU, tailored to the characteristics, carried out by simulation in the Matlab 6.5. Studies were included to obtain the transition processes in the system mode $p = 100\%$ due to a step change of control action on the power supplied to the drive CPU. The results are shown in the table.

TABLE I. Simulation Results

$K_P = 70,2$ $K_D = 8,6$	$\Delta\varphi$	ΔL	transition process time
$K_I = 0$	83,6°	32,7 dB	2 c
$K_I = 103,8$	81,8°	32,7 dB	1 c

In the first stage Under certain optimal coefficients $K_P = 70,2$ and $K_D = 8,6$ and off the integrator transition processes time is 2 seconds. After a start operation of the integrator the found optimal value of the coefficient of integration stability margin in phase $\Delta\varphi$ decreased to 1.6, and the transition process time was reduced to 1 second.

Transition processes have monotonous periodic character. Stability margins optimal system developed to meet the considered system features a 3 times higher than specified in the design of quality criteria for $\Delta\varphi \geq 45^\circ$, $\Delta L \geq 12$ dB .

V. CONCLUSIONS AND SUGGESTIONS

This paper has proposed a method of designing a digital system that takes into account the CPU main features as a control object and the requirements of the regulatory system.

It is advisable on this basis to develop software that allows in the operation of the pump unit automatically determine the optimal parameters of the control system taking into account the system requirements and characteristics of the controlled object.

REFERENCES

- [1] Don Morrison. Is it time to replace PID? Applying model-predictive control at the single-loop level may yield the next big leap in performance gains. URL: <http://www.isa.org> // 01 March 2005
- [2] PID controller: From Wikipedia, the free encyclopedia URL:-http://en.wikipedia.org/wiki/PID_controller.
- [3] Minakov A.V., Belousov, G.G. Optimal software implementation of digital PID regulators with feedback for objects with low response time and transition characteristics of high-order. // Automation, telemechanization and communication in the oil industry. - Moscow: JSC "VNIIOENG", 2008. - № 4: URL:<http://vniiheng.mcn.ru/inform/-avtomatisation/sod4>.
- [4] Dorf, R. Bishop, R. Modern control systems. - Moscow: Laboratory of Basic Knowledge, 2002. URL: <http://www.twirpx.com/file/21901/>
- [5] Kuznetsova E.E. The method of designing digital pressure regulator at the output of the pump unit // Automation in industry. - 2009. - № 4. URL: <http://avtprom.ru/%C2%A0-metodika-proektirovaniya-tsifrovogore>.
- [6] Kuznetsova E.E., Lyantsev O.D., The method of determining the coefficients of PID regulator pump unit // Automation, telemechanization and communication in the oil industry. - Moscow: JSC "VNIIOENG", 2010. - № 4. URL: http://www.nefteavtomatika.ru/Publication127_13_159.aspx.

AUTHOR'S PROFILE



Dr. **Osama Ahmad Salim Safarini** had finished his PhD. from The Russian State University of Oil and Gaz Named after J. M. Gudkin, Moscow, 2000, at a Computerized-Control Systems Department. He obtained his BSC and MSC in Engineering and Computing Science from Odessa Polytechnic National State University in Ukraine 1996. He worked in different universities and countries . His research is concentrated on Automation in different branches.

Image Compression of MRI Image using Planar Coding

Lalitha Y. S

Department of Electronics & Communication Engg.
Appa Institute of Engineering & Technology

Mrityunjaya V. Latte

Principal, JSS Academy of Technical Education,
Bangalore, Karnataka, India Gulbarga, Karnataka, India.

Abstract-In this paper a hierarchical coding technique for variable bit rate service is developed using embedded zero block coding approach. The suggested approach enhances the variable rate coding by zero tree based block-coding architecture with Context Modeling for low complexity and high performance. The proposed algorithm utilizes the significance state-table forming the context modeling to control the coding passes with low memory requirement and low implementation complexity with the nearly same performance as compared to the existing coding techniques.

Keyword- image coding; embedded block coding; context modeling; multi rate services.

I. INTRODUCTION

With rapid development of heterogeneous services in image application the future digital medical images and video coding applications finds various limitations with available resource. The traditional multi-bit stream approach to the heterogeneity issue is very constrained and inefficient under multi bit rate applications. The multi bit stream coding techniques allow partial decoding at a various resolution and quality levels. Several scalable coding algorithms have been proposed in the international standards over the past decade, but these former methods can only accommodate relatively limited decoding properties. The rapid growth of digital imaging technology in conjunction with the ever-expanding array of access technologies has led to a new set of requirements for image compression algorithms. Not only are high quality reconstructed medical images required at medium-low bitrates, but also as the bit rate decreases, the quality of the reconstructed MRI image should degrade gracefully. The traditional multi-bit stream solution to the issue of widely varying user resources is both inefficient and rapidly becoming impractical. The bit level scalable codes developed for this system allow optimum reconstruction of a medical image from an arbitrary truncation point within a single bit stream. For progressive transmission, image browsing, medical image analysis, multimedia applications, and compatible trans coding, in a digital hierarchy of multiple bit rates, the problem of obtaining the best MRI image quality and accomplishing it in an embedded fashion i.e. all the encoded bits making compatible to the target bit rate is a bottleneck task for today's engineer. As medical images are of huge data set and encoding it for a lower bit rate results in loss of data, which intern results in very low image quality under compression. Coming to the transmission over a noisy channel this problem becomes more effective due to narrow bandwidth effect. Various algorithms were proposed for encoding and compressing the MRI image data before transmission. These algorithms show high-end

results under high bandwidth systems but show poor result under low data rate systems. The problem of transmission of MRI images over a low bit rate bandwidth can be overcome if the medical image data bits are such encoded and compressed that the data bit rate is made compatible to the provided low bit rate. Embedded zero tree wavelet algorithm is a proposed image compression algorithm which encode the bit in the bit stream in the order of importance which embed the bit stream in hierarchical fashion.

II. SYSTEM DESIGN

This work was motivated by success of two popular embedded coding techniques: zero-tree/block coding [1, 2, 3, 4] and context modeling of the sub band/wavelet coefficients [5, 6, 7]. Zero-tree/block coding takes advantage of the nature of energy clustering of sub band/wavelet coefficients in frequency and in space. These classes of coders apply a hierarchical set partitioning process to split off significant coefficients (with respect to the threshold in the current bit plane coding pass), while maintaining areas of insignificant coefficients. In this way, a large region of zero pixels can be coded into one symbol. It provides an efficient method to compactly represent a group of leading zeros of sub band/wavelet coefficients. The distinguished compression performances were demonstrated in [2, 3, 4]. Moreover, instead of all pixels, only a small number of elements in lists [2] needs to be processed in individual bit plane coding passes. Thus, processing speed for this class of coders is very fast. High compression efficiency achieved with context modeling was presented in [5, 6, 7]. In this class of coders, individual pixel of the DWT bit planes are coded using context based arithmetic coding. With help of the context models, strong correlation of sub band/wavelet coefficients within and across sub bands can be effectively utilized. Although simple context modeling was also employed in [2, 3, 4], the limited context information in those algorithm were insufficient to accurately predict the status of the current node. With carefully designed context models, some algorithms [6, 7] have been able to outperform the best zero-tree/block coders in PSNR performances. Nevertheless, unlike zero-tree/block coders, these algorithms needed to scan all sub band/wavelet coefficients at least once to finish coding of a full bit plane, with an implied higher computation cost. To combine advantages of these two coding techniques, ie, low computation complexity and effective exploitation of correlation of sub band coefficients, we propose an embedded medical image coding algorithm using Zero Blocks of sub band/ wavelet coefficients and context modeling, or EZBC for ease of reference. This zero block coding

algorithm is also based on the set partitioning technique. We adopted the adaptive quad tree splitting method introduced in [3] to separate the significant coefficients and code every block of zero pixels into one symbol. In this scheme, quad tree representations of DWT coefficients are first established for individual sub bands. The bottom level of the quad tree consists of the sub band/wavelet coefficients. The single node at the top tree level, or the root node, just corresponds to the maximum amplitude of the all DWT coefficients. To start with, the root is the only insignificant node to process. Each quad tree node splits into four insignificant descendent nodes of the next lower level once it tests as significant against the threshold of the current bit plane coding pass. The same splitting process is recursively applied to the individual descendent nodes until the bottom level of the quad tree is reached.

In this way, we can quickly zoom in to high-energy areas and regions of all zero pixels can be compactly represented. In EZBC, the context models were carefully designed for coding quad tree nodes at different tree levels and sub bands. Therefore, it retains the properties of compactness and low complexity of the zero block coders, and adds context information in an effective way, while the context information is also made effective use. Unlike the zero tree structure, each zero block only represents pixels from one sub band. Hence, EZBC is inherently applicable to resolution scalable applications. With the aid of inter band context, dependence of sub band/wavelet coefficients across scales can still be effectively utilized without having zero trees spanning several sub bands.

III. MEDICAL IMAGE CODING SYSTEM

Image compression addresses the problem of reducing the amount of data required to represent a digital medical image. Compression is achieved by the removal of one or more of three basic data redundancies: (1) coding redundancy, which is present when less than optimal (i.e., the smallest length) code words are used; (2) inter pixel redundancy, which results from correlations between the pixels of an medical image; and/or (3) psycho visual redundancy, which is due to data that is ignored by the human visual system (i.e., visually nonessential information). In this chapter We examine each of these redundancies, describe a few of the many techniques that can be used to exploit them, and examine two important compression standards – JPEG and JPEG 2000. These standards unify the concepts by combining techniques that collectively attack all three data redundancies. Medical Image compression systems are composed of two distinct structural blocks: an encoder and a decoder. Image $f(x, y)$ is fed into the encoder, which creates a set of symbols from the input data and uses them to represent the medical image. If we let n_1 and n_2 denote the number of information carrying units (usually bits) in the original and encoded medical images, respectively, the compression that is achieved can be quantified numerically via the compression ratio

$$C_R = \frac{n_1}{n_2} \quad (1)$$

To view and/or use a compressed (i.e., encoded) medical image, it must be fed into a decoder (see Fig.2.1), where a reconstructed output medical image, $\hat{f}(x, y)$, is generated. In general, $\hat{f}(x, y)$ may or may not be an exact representation of $f(x, y)$. If it is, the system is called error free, information preserving, or lossless; if not, some level of distortion is present in the reconstructed medical image. In the latter case, which is called lossy compression, we can define the error $e(x, y)$ between $f(x, y)$ and $\hat{f}(x, y)$, for any value of x and y as

$$e(x, y) = \hat{f}(x, y) - f(x, y) \quad (2)$$

so that the total error between the two medical images is

$$\sum_{x=0}^{M-1} \sum_{y=0}^{N-1} [y(x, y) - f(x, y)] \quad (3)$$

and the rms (root-means-square) error e_{rms} between $f(x, y)$ and $\hat{f}(x, y)$ is the square root of the squared error averaged over the $M \times N$ array, or

$$e_{rms} = \left[\frac{1}{MN} \sum_{x=0}^{M-1} \sum_{y=0}^{N-1} [y(x, y) - f(x, y)]^2 \right]^{1/2} \quad (4)$$

In the first stage of the encoding process, the mapper transforms the MRI input image into a (usually nonvisual) format designed to reduce inter pixel redundancies. The second stage, or quantizer block, reduces the accuracy of the mapper's output in accordance with a predefined fidelity Criterion- attempting to eliminate only psycho visually redundant data. This operation is irreversible and must be omitted when error-free compression is desired. In the third and final stage of the process, a symbol coder creates a code (that reduces coding redundancy) for the quantizer output and maps the output in accordance with the code.

IV. BIT PLANE CODING

Wavelet coefficient bit plane coding in EZBC follows a similar procedure to those adopted in other quad tree-based set partitioning coders. However, special care is given to list management and bit stream organization, which significantly influence efficiency of context modeling and code stream embedding, and scalable functionality of the resulting code stream. The EZW encoder is based on two important observations:

1) *Natural MRI images in general have a low pass spectrum. When a medical image is wavelet transformed the energy in the sub bands decreases as the scale decreases (low scale means high resolution), so the wavelet coefficients will, on average, be smaller in the higher sub bands than in the lower sub bands. This shows that progressive encoding is a very natural choice for compressing wavelet transformed medical images, since the higher sub bands only add detail.*

2) *Large wavelet coefficients are more important than small wavelet coefficients.*

These two observations are exploited by encoding the wavelet coefficients in decreasing order, in several passes. For every pass a threshold is chosen against which all the wavelet coefficients are measured. If a wavelet coefficient is larger than the threshold it is encoded and removed from the image, if it is smaller it is left for the next pass. When all the wavelet coefficients have been visited the threshold is lowered and the MRI image is scanned again to add more detail to the already encoded MRI image. This process is repeated until all the wavelet coefficients have been encoded completely or another criterion has been satisfied (maximum bit rate for instance).

The trick is now to use the dependency between the wavelet coefficients across different scales to efficiently encode large parts of the MRI images which are below the current threshold. It is here where the zero tree enters. So, let me now add some detail to the foregoing. (As most explanations, this explanation is a progressive one.)

The EZW encoder exploits the zero tree based on the observation that wavelet coefficients decrease with scale. It assumes that there will be a very high probability that all the coefficients in a quad tree will be smaller than a certain threshold if the root is smaller than this threshold. If this is the case then the whole tree can be coded with a single zero tree symbol. Now if the MRI image is scanned in a predefined order, going from high scale to low, implicitly many positions are coded through the use of zero tree symbols. Of course the zero tree rule will be violated often, but as it turns out in practice, the probability is still very high in general. The price to pay is the addition of the zero tree symbol to our code alphabet.

Quad tree Structure The bit plane coding process begins with establishment of the quad tree representations for the individual sub bands. The value of a quad tree (a) Quadtree buildup (b) Quadtree splitting node $Q_k[l](i, j)$ at position (i, j) , quad tree level l and subband k is defined by $Q_k[0](i, j) \square |c_k(i, j)|$, and

$$Q_k[l](i, j) \square \max\{Q_k[l-1](2i, 2j), Q_k[l-1](2i, 2j+1), Q_k[l-1](2i+1, 2j), Q_k[l-1](2i+1, 2j+1)\},$$

Where $c_k(i, j)$ is the subband coefficient at position (i, j) , subband k . That is, each bottom quadtree node is assigned to the magnitude of the subband coefficient at the same position. The quadtree node at the next higher level is then set to the maximum of the four corresponding nodes at the current level, as illustrated in Fig. 1 (a). By recursively grouping each 2×2 vector this way, the complete quad tree is built up for the individual subbands. The top quad tree node $Q_k[D_k-1](0, 0)$ is just equal to the maximal magnitude of all subband coefficients $\{c_k(i, j)\}_{i,j}$ from subband k , where D_k is the quadtree depth for subband k .

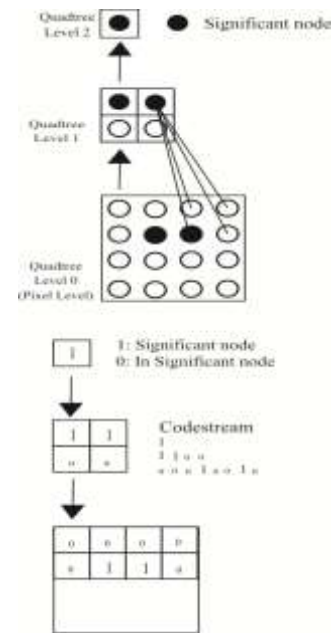


Fig. 1 Illustration of quad tree build up and decomposition.

Similar to the conventional bitplane coders, we progressively encode subband coefficients from the MSB toward the LSB. The individual bitplane coding pass n encodes bit n of all coefficients. The subband coefficients are thus effectively quantized by a family of embedded quantizers with a (dead-zone) quantization threshold $\tau_n = 2^n$ for bitplane level n . We define that a quadtree node Q tests significant with respect to a quantization threshold τ if $Q \geq \tau$. A quadtree Q is defined to be a significant node during the current bitplane pass n if

$$\begin{aligned} & - Q \geq \tau_{n+1}, \text{ or} \\ & - Q \in [\tau_n, \tau_{n+1}) \text{ and } Q \end{aligned}$$

has been tested, and an insignificant node otherwise. It should be noted that $Q \in [\tau_n, \tau_{n+1})$ is still considered as an insignificant node in the bitplane pass n until it has been coded/tested. A significant pixel (coefficient) is located by the testing and splitting operation recursively performed on the significant nodes up to the pixel (bottom) level of a quadtree, as shown in Fig. 1 (b). Given the coded quadtree splitting decisions, the decoder can duplicate the quadtree decomposition steps and the related significance information.

A parent-child relationship is defined in the quadtree structure. As opposed to the classic zerotree structure, this relationship is between nodes across the quadtree levels (rather than across resolution scales), as illustrated in Fig. 3.5. Each parent $Q_k[l](i, j)$ has four children from the same 2×2 block at the next lower quadtree level. These four child nodes are considered as siblings of each other. All the descendants of $Q_k[l](i, j)$ can be recursively traced from one quadtree level to the next lower in a similar way up to the pixel level.

Every quadtree node Q plays a dual role: It is an element with the value defined by (3.1) subjected to significance test. The established quadtree representation provides an additional

pyramidal description of the transformed medical image. The strong statistical dependencies among quadtree nodes, can be exploited to improve the performance of conditional entropy coding. Once a node Q tested insignificant, it indicates that all its descendants are insignificant, too. Hence, it also serves as a zero set defined in the conventional set partitioning coder and contains all its descendent coefficients as members. Each insignificant quadtree node Q [l] (i, j) thus effectively groups $2^l \times 2^l$ insignificant coefficients together. The hierarchical set partitioning with respect to a given test threshold is accomplished via recursive quadtree splitting.

Similar to other hierarchical coders, we utilize the ordered lists for tracking the significance status of the individual subband coefficient. LSP_k (list of significant pixels) contains a full list of significant pixels in subband k. All the insignificant coefficients are compactly gathered in the quadtree nodes which are maintained in arrays of the LINs (list of insignificant nodes). LIN_k[l], l = 0, ..., D_k - 1, contains a list of insignificant nodes from quadtree level l, subband k. A node (i, j) in LIN_k[l] thus indicates that $2^l \times 2^l$ subband coefficients

$$\begin{aligned} & \{ \{ c_k(i \cdot 2^l, j \cdot 2^l), c_k(i \cdot 2^l, j \cdot 2^l + 1), \dots, \\ & c_k(i \cdot 2^l, j \cdot 2^l + 2^l - 1) \}, \{ c_k(i \cdot 2^l + 1, j \cdot 2^l), \dots, \\ & c_k(i \cdot 2^l + 1, j \cdot 2^l + 2^l - 1) \}, \dots, \{ c_k(i \cdot 2^l + 2^l - 1, j \cdot 2^l), \dots, \\ & c_k(i \cdot 2^l + 2^l - 1, j \cdot 2^l + 2^l - 1) \} \} \quad (5) \end{aligned}$$

are all insignificant. Unlike other earlier set partitioning coders such as EZW, SPIHT and SPECK, the lists here are maintained separately for the individual subbands and quadtree levels. This strategy can effectively improve performance of context modeling and codestream embedding. Moreover, it is essential for efficient accommodation of resolution-scalable codestreams.

Bitplane Processing and Coding Initially, LIN_k[D_k-1] contains the single node from the top quadtree level and the other LIN_k lists and LSP_k are just empty for each subband k. It indicates that all the subband coefficients are insignificant before the first bitplane coding pass starts. The coding process begins with the MSB plane with the bit index given by

$$n_{\max} \square \left\lfloor \log_2(\max_{(k,i,j)} \{ |c_k(i, j)| \}) \right\rfloor \quad (6)$$

where $\lfloor \cdot \rfloor$ returns the largest integral value not greater than the input.

Because the quantization threshold is halved from bitplane to bitplane, more and more coefficients becomes significant as the bitplane coding process proceeds.

Two tasks are performed in each bitplane pass n:

- 1) 1. Reveal the new significant coefficients, $\{c_k(i, j) \in [2^n, 2^{n+1})\}$ with respect to the current threshold $\tau_n = 2^n$;
- 2) 2. Refine the old significant coefficients, $\{c_k(i, j) \geq 2^{n+1}\}$, collected from the previous bitplane passes.

Since all the insignificant coefficients with respect to the previous test threshold $\tau_n = 2^{n+1}$ were already compactly grouped by the quadtree nodes maintained in the LINs, the new significant coefficients can be fast located by significance test of the individual nodes from the LINs. If a node is tested insignificant, it remains in the same LIN. Otherwise, it splits into four children and each child is further tested. Once a child is tested insignificant, it is added to the LIN at the next lower level. Otherwise, it further splits into four grandchildren and each is tested in a similar way. This testing and splitting procedure is recursively performed on the significant descendants up to the pixel level. As soon as a pixel tested significant, it is appended to the LSP and its sign is encoded immediately. The refinement of old significant coefficients (so-called refinement pass) is simply accomplished by coding bit n of each coefficient in the LSPs gathered from the previous bitplane passes (not including the new significant coefficients from the current pass). The Boolean results of significance tests (true or false), the sign bits, and the refinement bits are all the required information for decoding of bitplane data. They are all encoded by context-dependent binary arithmetic coding, to be presented shortly. The bitplane coding process will stop once the desired coding bitrate or image quality is reached.

The quadtree build-up stage is not needed at the decoder as the significance information is already contained in the codestream. The bitplane decoder basically follows the same procedure as the bitplane encoder. Given the coded sequences of quadtree splitting decisions, the decoder can duplicate the quadtree decomposition steps taken by the encoder. The execution path within a subband for bitplane encoding is required to be strictly followed for bitplane decoding. However, since the quadtrees are independently established for the individual subbands, the bitplane decoding order among subbands is allow to be manipulated in various ways for some scalable coding applications.

In addition to the subband coefficients, the proposed algorithm also needs to deal with the quadtree nodes from the individual quadtree levels. At first look, it appears that the data size for processing and coding in each bitplane pass has been significantly expanded. Nevertheless, none of these quadtree nodes will be visited until their parents is already tested significant, except for the top quadtree nodes which do not have any parents. On the contrary, our experimental results show that the number of coded binary symbols in EZBC is in fact even smaller than that of pixels in the input medical image (at a typical lossy coding bitrate). That is, the average number of binary coding operation per pixel is less than one although the individual subband coefficient is encoded through multiple quantization and coding stages. It partially explains the high speed performance of this block-based set partitioning coding scheme.

Still, we need to visit every coefficient once for establishment of the quadtree representations of the decomposed medical image at the very beginning of the bitplane coding process. Nevertheless, our coding algorithm in fact is only concerned with the MSB index of a quadtree node (rather than the actual value) for significance test. This

quadtree buildup step can thus be efficiently implemented by the simple bitwise OR operation.

In order to have efficiently embedded codestreams, it is essential that the code data in the compressed file are ordered according to their relative efficiencies for distortion reduction. This basic concept is commonly called embedding principle. In the proposed algorithm, a fixed path for encoding of wavelet coefficient bitplane data is chosen as follows: The coding process advances in a bitplane-wise fashion from the most significant bit toward the least. In a given bitplane, the arrays of LINs are processed in an increasing order of quadtree level, as suggested by Islam and Pearlman in SPECK. That is, all the pixels in LIN[0] are processed first and all the nodes in LIN[1] are then processed next, followed by the processing's of LIN[2], LIN[3], and so on. In this way, the busy areas in the transformed medical image are updated earlier via a few quadtree splitting and coding steps, resulting in a good rate-distortion performance. The refinement of the previous significant coefficients from LSP is executed at last. In a significance test pass of a given quadtree level or a coefficient refinement pass, the subbands are visited from coarse to high resolution

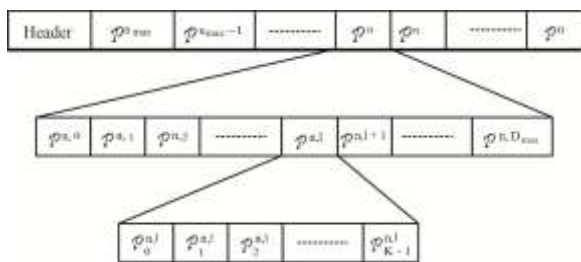


Fig. 2 Illustration of the hierarchical layout of a EZBC codestream.

A hierarchical layout of a EZBC codestream is depicted in Fig. 2, where p^n denotes the bitplane pass n , $p_k^{n,l}$ the sub-bitplane pass for processing the insignificant nodes in $LIN_k[l]$ (routine CodeLIN(k, l)), and $p_k^{n,D_{max}}$ the sub-bitplane pass for the refinement of the significant coefficients in LSP_k (routine CodeLSP(k)). Similar to the bitplane de-interleaving scheme widely adopted in the sequential bitplane coders, EZBC effectively partitions each bitplane into multiple sub-bitplane passes $\{p_k^{n,l}\}_{n,l,k}$ for providing an embedded codestream of fine granularity. However, unlike the multi-pass approach proposed in, EZBC does not need to scan the individual pixels more than once in each bitplane pass because all the involved pixels for the individual sub-pass were already organized in separate lists. Although our pre-defined data embedding order is not optimized for the best R-D performance (as compared to the algorithms), our empirical data show the resulting relative performance loss is mostly insignificant. The effectiveness of the proposed data embedding strategy is further evidenced by the smoothed R-D curves shown in our actual coding simulation results

It is worth mentioning that each bitplane pass could have been divided into even more sub-bitplane passes in our data

embedding scheme to further improve the R-D performance of the resulting codestream. It is simply accomplished by partitioning of the existing lists into smaller sub-lists and then processing each sub-lists via separate sub-bitplane coding passes. The resulting computational and storage costs are still the same because the total number of the nodes to be stored and processed in all the maintained lists is unchanged. For example, our empirical data show that the refinement of the significant coefficients from the previous bitplane coding pass reduces distortion more efficiently than the refinement of the significant coefficients from the other earlier bitplane coding passes (if exist). The PSNR performance can thus be slightly improved by partitioning the existing refinement pass into multiple sub-passes, each for the refinement of the significant coefficients from particular bitplane level(s). Nevertheless, it is observed that the granularity of the resulting codestream by the current algorithm is already fine enough in practical medical image coding applications.

A. Context-dependent entropy coding

As opposed to the conventional sequential bitplane coder, the proposed algorithm EZBC is required to process the bitplanes associated with the individual quadtree levels in each bitplane coding pass. A dual hierarchical pyramidal description, as previously shown in Fig. 3.1, is thus given by this quadtree representation of the decomposed medical images. Strong intraband correlation is clearly exhibited among quadtree nodes. The self-similarity is demonstrated across both quadtree and resolution levels. Such diverse statistical dependencies are exploited by context-dependent arithmetic coding in EZBC. Unlike most former set-partition coders, the lists in EZBC are separately maintained for the individual subbands and quadtree levels. Therefore, the independent probability models are allowed to be built up for significance coding of the nodes from different subbands and quadtree levels. As such, the unique statistical characteristics of the source samples associated with different subband orientations, sub-sampling factors and amplitude distributions will not be mixed up in the accumulated probability models.

Four classes of binary symbols are encoded in EZBC:

- 1) Significance test of a given quadtree node from LIN (in routine CodeLIN),
- 2) Significance test of a child (in routine CodeDescendants)
- 3) Sign bit of a newly significant coefficient, and
- 4) Refinement bit of a given coefficient from LSP.

These symbols are all encoded by context-based arithmetic coding with the distinct modeling strategies, to be respectively described in the following.

B. Significance coding

This subsection begins with a brief discussion that relates the proposed entropy coding algorithm to the APSG (alphabet partitioning and sample grouping) scheme. The utilization of inter- and intra-band correlation and dependence between subband levels in a subband-based quadtree representation is then respectively described, followed by a description of our context quantization/selection scheme.

Significance coding in the proposed algorithm is conditioned on the significance map defined by

$$\sigma(i, j) = \begin{cases} 1, & \text{if node } (i, j) \text{ is significant} \\ 0, & \text{otherwise} \end{cases} \quad (7)$$

Nevertheless, in contrast to the conventional sequential pixel-wise bitplane coding approach, significance coding of a quadtree node in EZBC jointly encodes a group of coefficients from a block region. The significance status of a contextual quadtree node compactly indicates local activity level in the corresponding block area. Hence, we can think of EZBC as a conditional block entropy coder that applies the APSG scheme on both source samples and modeling contexts. As such, block entropy coding and conditional entropy coding can be combined to exploit the strong subband dependency without suffering the complexity difficulties commonly associated with high-order source extension and context modeling. Although from a point of view of the conventional universal source coding, it was argued that there is no additional compression gain by blocking samples in conditional entropy coding. However, our block coding method here does not involve complex codebook design or any other computation-intensive procedures. On the contrary, the speed performance of the resulting coding system is substantially improved by compact grouping of subband coefficients. Besides, arithmetic coding of large areas of zero coefficients individually in conventional sequential bitplane coding is associated with a highly skew probability distribution, which is known to be penalized by a high learning cost.

C. Contextual Region

In Fig. 3 (a), we show the neighboring nodes included in the modeling contexts in our coder EZBC for significance coding. The eight spatial adjacent nodes from the same quadtree level are utilized to exploit intraband correlation. Such a contextual structure has been widely employed in many conventional bitplane coders, for significance coding of subband coefficients. The application of this model to significance coding of quadtree nodes is justified by the strong spatial dependency exhibited in the example MSB map in Fig. 3 (b).

To exploit the subband correlation across scales, we adopt the corresponding node from the next lower quadtree level (rather than from the current level) in the parent subband, indicated by 'F' in Fig. 3 (a). This choice is based on the fact that at a given quadtree level the related dimension in an input medical image for a quadtree node is doubled in the parent subband, as a result of sub-sampling operation in the subband transformation stage. The inter-band information is thus provided at the same spatial resolution by the parent subband, as demonstrated in Fig. 3(b).

D. Inter-/Intra- Band Modeling

The importance of the inter-band neighboring pixels lies in its ability to provide non-causal contextual information for conditional entropy coding. Such information is particularly valuable for efficient compression of the leading bitplanes since most spatial neighboring coefficients are still

insignificant. However, the complexity of the algorithm may be increased by a use of the inter-band neighbors for some imaging applications. It has been argued that the intra-band context model is capable of effective exploitation of

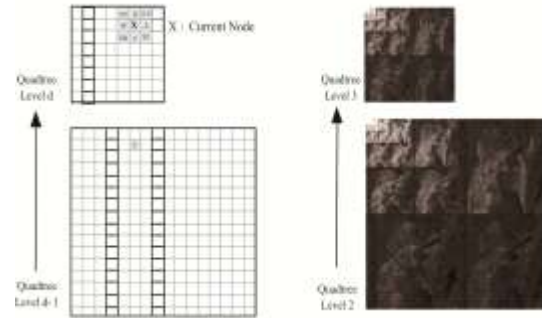


Fig. 3 Modeling contexts for conditional entropy coding of significance test. (a) Left: Neighbors included in the modeling contexts. (b) Right: Example MSB map of quadtree nodes from the decomposed MRI image.

Subband dependency combined with some efficient zero coding schemes. EBCOT, for instance, exhibits excellent compression performance combining quadtree decomposition, run-length coding with conventional context-based bitplane coding. Similar phenomenon was also observed during the development of EZBC. Our experimental results show that no PSNR improvement is made for significance coding of the individual pixels from LIN by inclusion of interband neighbors in the modeling context. The improvement for significance coding of a child pixel is also very limited. It is expected because the current pixel for significance test often already has some neighboring pixels tested significant when the quadtree decomposition operation proceeds to the bottom level. As a result, we only employ intraband modeling for conditional entropy coding of significance test at the pixel level.

On the other hand, it was also observed in our experimental results that the spatial dependency among quadtree nodes is decreasing as we move toward the higher quadtree levels. Recall that the value of a quadtree node is defined to be the maximal amplitude of all subband coefficients from its corresponding block region and the block size grows exponentially with the quadtree level. As is well known, the pixels with peak values are typically related to “singularity” in the input MRI image. Because of the energy clustering nature of subband coefficients, these medical image features are typically easily noticeable in the spatial contexts at the lower quadtree levels. Nevertheless, such clustering’s of high energy are restricted to the local region around the “peak pixels”. As the block size grows (or the quadtree level increases), this energy clustering phenomenon in the current block will become less likely reflected in the neighboring nodes if the peak pixel is not close to the block boundaries. Nevertheless, such an “anomaly” in space remains seen from the same corresponding area in the parent subband. Since the significance of a parent node is coded earlier during every bitplane pass, we can say that the parent node provides a look-ahead function into the region covered by the current node. In fact, our simulations indicate that the interband-only context model (containing a single neighboring node from the parent band) outperforms the

intraband-only context model (containing eight spatial neighboring nodes) at the 3rd level of the quadtree and higher.

The use of inter-band modeling is only optional in EZBC. An example application desirable for intraband modeling is highly scalable image coding presented.

E. Dependency between Quadtree Levels

The correlation between the adjacent quadtree levels is exploited to provide the inter-subband contextual information at the same spatial resolution. Within a given subband, the dependency also exists between the adjacent quadtree levels, directly attributed to the two properties associated with the basic mechanism of quadtree build-up and splitting:

- 1) When a parent remains insignificant, all its children are also insignificant;
- 2) After a parent tested significant, at least one of its four children will test significant in the subsequent descendant test

Property (i) is already utilized in a conventional zeroblock coder to compactly represent large numbers of insignificant pixels from block regions. Property (ii) implies that the chance of being testing significant is increasingly higher for the next child if none of its siblings have been tested significant yet. For example, without considering other contextual information, the probability that the first child tests significant is no less than 0.25. Had none of the past three siblings been tested significant, the fourth child is significant for sure and no significance testing and coding is required. This statistical characteristic is exploited in our context modeling scheme detailed in the next section.

F. Context Selection and Look-up tables

Although adaptive arithmetic coding is a universal coding scheme which allows the source statistics to learn on the fly, the related learning costs often turn out quite expensive for many practical instances. The compression efficiency can be substantially improved if prior knowledge about the source is effectively exploited in the context model design.

Unlike the conventional sequential bitplane coder which encodes subband samples one by one in each bitplane coding pass, EZBC processes coefficients in groups and hence has fewer samples to encode. Context dilution thus becomes an issue of great concern. Our context modeling scheme is based on the significance map which allows context quantization to be implicitly carried out. Instead of treating all the resulting context vectors (2^9 totally) as different conditional states, we carefully classify them into several model classes, similar to the context selection approach adopted in EBCOT and JPEG 2000. The look-up tables are then established accordingly to fast map a given context to the assigned model index. This strategy can further lower the model cost and enable the probability models to fast adapt themselves to varying local statistics.

The context classification, based upon the configurations of the significance map, is characterized by:

- 1) Orientations: identified by
 $H = \sigma(W) + \sigma(E)$, such that $0 \leq H \leq 2$,
 $V = \sigma(N) + \sigma(S)$, such that $0 \leq V \leq 2$,

$$HV = H + V, \text{ such that } 0 \leq HV \leq 4, \text{ and}$$
$$D = \sigma(NW) + \sigma(NE) + \sigma(SW) + \sigma(SE), \text{ such that}$$
$$0 \leq D \leq 4$$

where the relative positions of nodes 'W', 'E', 'N', 'S', 'NW', 'NE', 'SW',

'SW' are shown in Fig. 3.

- 2) Inter-band dependency: identified by

$$P = \sigma(F), \text{ such that, } 0 \leq p \leq 1,$$

where the position of node 'F' is shown in Fig. 3

- 3) Relative position v : index of the current child node as shown in Fig. 3. where

$$v \in \{00, 01, 10, 11\}.$$

- 4) Significance of the past coded siblings:

$$\sigma_{sb}(v) \triangleq \begin{cases} 1, & \text{if } v > 0 \text{ and } \sum_{i=0}^{v-1} (i) > 0 \\ 0, & \text{otherwise} \end{cases} \quad (8)$$

Where v is the index of the current child node.

The spatial correlation among quadtree nodes is exploited by the eight first order neighbors, as depicted in Fig.3. The structure features are summarized in horizontal, vertical and diagonal directions, respectively. It is well known that the MRI image attributes such as edges and corners are retained along the direction of lowpass filtering after subband transform. Hence, our context modeling scheme emphasizes the directional characteristics in accordance with the current subband orientation. For instance, the horizontal features are favored over the vertical and diagonal ones in the LH subband (horizontal lowpass filtering followed by vertical highpass filtering).

Since the inter-band dependency is not as useful at lower quadtree levels, we restrict the modeling contexts to the intraband neighbors for significance coding at the pixel quadtree level. It was mentioned that the coding statistics for significance test of the individual child are position-dependent. Hence, significance coding of each child is additionally conditioned on its relative position, v , and the significance status of its past coded siblings, σ_{sb} .

The look-tables are respectively designed for the subbands of LH and HH orientations. Following the idea of EBCOT, the coefficient matrix from the HL subband is transposed first before the bitplane coding process starts. In this way, the same set of look-up tables can be shared by both the HL and LH subbands. The transposition of the LH subband is avoided in the JPEG 2000 standard by transposing the look-up tables for the LH subband instead.

G. Refinement of significant coefficients

The same contextual intraband region shown in Fig. 3 is utilized for conditional coding of the refinement of the significant coefficients from LSP. The contextual information is characterized by significance map $\sigma^p(i, j)$, the significance status with respect to the quantization threshold at the previous bitplane level.

H. Context-dependent de-quantization

This section presents a new de-quantization algorithm that features a context-dependent strategy for reconstruction of

subband coefficients. A simple source statistical model is designed for each context with the model parameters estimated from the statistics accumulated at the decoder.

It is known that the optimal representation levels of a scalar quantizer should satisfy the following centroid condition

$$r_i^* = \frac{\int_{d_i}^{d_{i+1}} xf(x)dx}{\int_{d_i}^{d_{i+1}} f(x)dx} \quad (9)$$

Where r_i^* is the optimal reconstruction value for a given quantization interval $[d_i, d_{i+1}]$ and a probability density function (pdf) $f_X(x)$. However, the reconstruction values for the decoded coefficients are typically set to the midpoints of the corresponding quantization intervals in practice either for simplicity of implementation or for lack of knowledge about the source statistics. Such a choice is optimal for the source with uniform probability distribution over the individual decision intervals. For bitplane coding in particular, it is implicitly assumed that the positive and negative coefficients within the dead zone are equally likely and the reconstructed values of all the insignificant pixels are set to zero as a result.

The proposed de-quantization algorithm is based on the two experimental observations:

- 1) Subband coefficients exhibit strong spatial correlation in both signs and magnitudes
- 2) The statistics of bitplane samples bear strong resemblances within and across bitplane levels in a given subband and gradually grow into less skew probability distribution from bitplane to bitplane.

Observation (i) has been utilized for context-based arithmetic coding of the subband coefficients in EZBC. Similarly, the coded significant pixels can provide contextual information for reconstruction of their neighboring coefficients. Particularly, the signs of significant pixels are useful for predicting the signs of their neighboring insignificant coefficients which are distributed over the dead zone and are quantized to the zero symbols. Combined with observation (ii), we can estimate the source statistics on a given context using the related probability tables accumulated during the decoding process.

I. Reconstruction of significant coefficients

A simple statistical model is adopted for reconstruction of a significant subband coefficient $|c_i| \in [x_0, x_0 + \tau_i)$, as depicted in Fig. 4(a), where x_0 is the decoded value of $|c_i|$. The quantizer step size, τ_i , for c_i is given by

$$\tau_i = \begin{cases} 2^\alpha, & \text{if } c_i \text{ has been coded during the last pass } n \\ 2^{\alpha+1}, & \text{otherwise} \end{cases} \quad (10)$$

The estimated conditional probability

$$\hat{p}_0 = \hat{p}_r \left\{ |c_i| < x_0 + \frac{\tau_i}{2} \mid c_i \in [x_0, x_0 + \tau_i] c^i \right\} \quad (11)$$

given a context c^i is empirically determined by the related probability tables which were already accumulated during the decoding process. The definition of the contexts is the same as the one used for refinement coding of the significant coefficients. Uniform distribution is then assumed for each half of the quantization interval. The resulting reconstruction level, r_i , is computed by

$$\begin{aligned} \tau_i &= \int_{x_0}^{x_0+\tau_i} \hat{f}_x(x) dx \\ &= \frac{2\hat{p}_0}{\tau_i} \int_{x_0}^{x_0+\tau_i} x dx + \frac{2(1-\hat{p}_0)}{\tau_i} \int_{x_0+\tau_i/2}^{x_0+\tau_i} x dx \\ &= x_0 + \tau_i \left(\frac{3}{4} - \frac{1}{2} \hat{p}_0 \right) = x_0 + \tau_i \left(\frac{3}{4} - \frac{1}{2} \hat{p}_0 \right) \end{aligned} \quad (12)$$

where $\hat{f}_x(x)$ represents the estimated conditional probability density function for the magnitude of a significant coefficient c_i . We note that the reconstruction value r_i approaches the midpoint of the quantization bin, the conventional reconstruction value, as the probability distribution becomes less skew ($\hat{p}_0 \rightarrow 1/2$)

J. Reconstruction of insignificant coefficients

Our statistical model for reconstruction of insignificant subband coefficients $c \in (-\tau_i, \tau_i) \hat{p}_{sp} \rightarrow \frac{1}{2}, r \approx 0$ is depicted in Fig. 4 (b). The quantization threshold τ_i for c_i is equal to 2^n or 2^{n+1} , depending upon whether c_i has been visited during the last bitplane pass. The estimated conditional probabilities

$$\begin{aligned} \hat{p}_0 &= \hat{p}_r \left\{ |c_i| < \frac{\tau_i}{2} \mid c_i \in (-\tau_i, \tau_i) c^i \right\} \text{ and} \\ \hat{p}_{sp} &= \hat{p}_r \left\{ \zeta_i = 1 \mid c_i \in (-\tau_i, \tau_i) c^i \right\} \text{ for} \end{aligned}$$

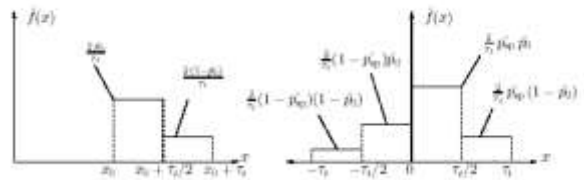


Figure 4 : The assumed conditional probability density function (pdf) for the subband coefficients.

- (a) Left: The conditional pdf model for significant coefficients $|c_i| \in [x_0, x_0 + \tau_i)$.
- (b) Right: The conditional pdf model for insignificant coefficients $c_i \in (-\tau_i, \tau_i)$.

The right half of the coordinate plane corresponds to $\zeta_i = 1$ (the sign prediction is correct). The given contexts C^i are empirically decided by the accumulated probability tables, where ζ_i denotes the correctness of sign prediction for c_i .

The definitions of the contexts for estimation of \hat{p}_0 and \hat{p}_{sp} are the same as the ones employed in significance coding of pixels and sign coding, respectively. Further, we assume the events $\left\{ |c_i| < \frac{\tau_i}{2} \mid c_i \in (-\tau_i, \tau_i), c^i \right\}$

and

$$\left\{ \zeta_i = l \mid c_i \in (-\tau_i, \tau_i), c^i \right\}$$

are statistically independent so that

$$p_r \left\{ |c_i| < \frac{\tau_i}{2} \mid \zeta_i = l \mid c_i \in (-\tau_i, \tau_i), c^i \right\} =$$

$$p_r \left\{ |c_i| < \frac{\tau_i}{2} \mid c_i \in (-\tau_i, \tau_i), c^i \right\}$$

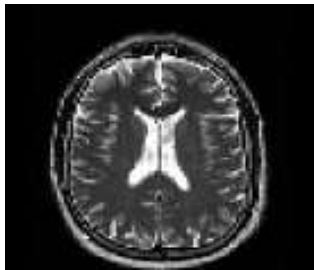
$$p_r \left\{ |c_i| < \frac{\tau_i}{2} \mid c_i \in (-\tau_i, \tau_i), c^i \right\}.$$

13)

V. RESULTS

The results at different bpp are shown in Figure 5.

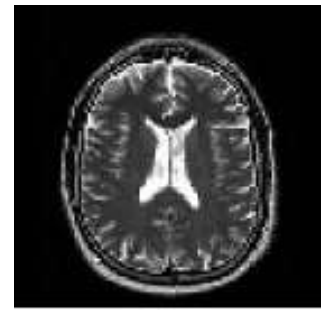
It is shown as the bit rate decreases, the quality of the reconstructed MRI image should degrade. The results are tabulated for two samples as in figure 6 and 7. The PSNR values for different bpp are shown in table 1.



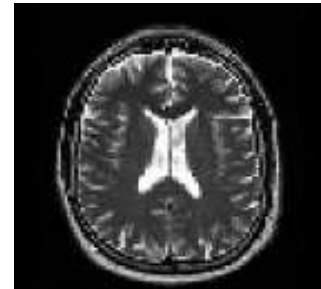
(a) Original MRI image sample 1



(c) Recovered image at 0.5 bpp

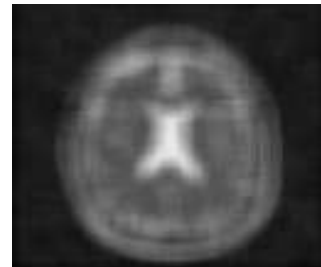


(i) Original MRI Image sample 2

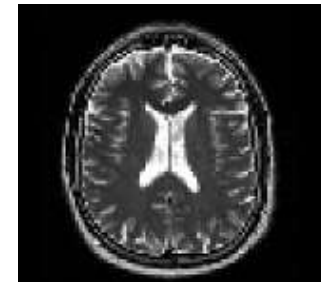


(ii) Recovered MRI image at 0.9 bpp

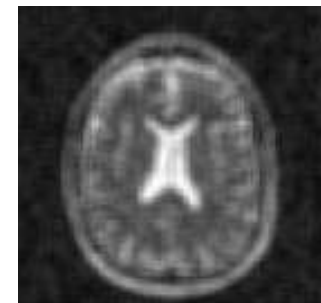
Figure 5. Recovered images with different Bits per pixel values.



(b) Recovered MRI image sample at 0.1 bpp



(d) Recovered MRI image sample at 0.9 bpp



(iii) Recovered image at 0.1 bpp



(iv) Recovered MRI image sample at 0.5 bpp

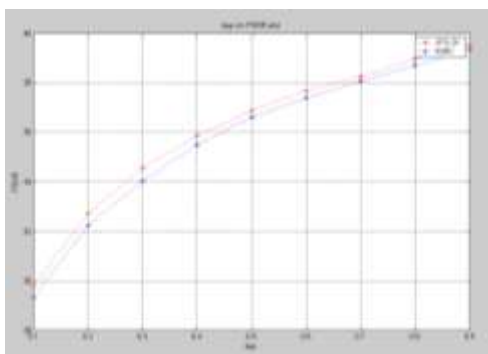


Fig. 6 PSNR v/s bpp plot for the given image

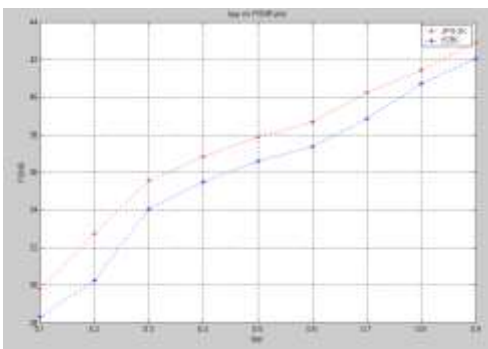


Fig. 7 PSNR v/s bpp plot for the given image

TABLE 1 PSNR V/S BPP PLOT FOR THE GIVEN LEAF IMAGE

Sample - 1			Sample - 2		
bpp	PSNR		bpp	PSNR	
	JPG - 3K	EZBC		JPG - 2K	EZBC
0.1	28.7871	28.2544	0.1	29.8107	28.3202
0.2	32.4212	32.1077	0.2	32.7202	30.2514
0.3	34.5121	34.0187	0.3	35.5479	34.0331
0.4	35.5643	35.3201	0.4	36.8422	35.4857
0.5	36.7434	36.1745	0.5	37.8623	36.5939
0.6	37.7332	37.5007	0.6	38.6650	37.3759
0.7	38.3265	38.0411	0.7	40.2581	38.8491
0.8	38.8021	38.6721	0.8	41.4390	40.7058
0.9	39.6411	39.2314	0.9	42.9218	42.0437

VI. CONCLUSION

This project implements an enhanced image coding system for medical image compression compared to the existing JPEG

2000 system. It is observed that EZW is able to achieve its good performance with a relatively simple algorithm. EZW does not require complicated bit allocation procedures like subband coding does, it does not require training or codebook storage like vector quantization does, and it does not require prior knowledge of the image source like JPEG does (to optimize quantization tables). EZW also has the desirable property, resulting from its successive approximation quantization.

One desirable consequence of an embedded bit stream is that it is very easy to generate coded outputs with the exact desired size. Truncation of the coded output stream does not produce visual artifacts since the truncation only eliminates the least significant refinement bits of coefficients rather than eliminating entire coefficients as is done in subband coding. From the obtained results it is concluded that embedded zero tree wavelet coding takes comparatively less (about 60%) time than the JPEG coding system. The coding also shows less percentage of error in medical image compare to the existing JPEG coding system. It is observed that image coded with embedded zerotree wavelet coding shows clearer image than other coding system.

REFERENCES

- [1] A. Said Pearlman, "A new, fast, and efficient image codec based on set partitioning in hierarchical trees," IEEE Trans. Circuits Syst. Video Technol., vol.6, no.3, 1996, pp.243-249.
- [2] D.Taubman, "High Performance scalable image compression with EBCOT", IEEE Trans. Image processing, vol.9, no.7, 2000, pp. 1158-1170.
- [3] M.Rabbani and R.Joshi, "An overview of the JPEG 2000 still image compression standard", Signal Processing: Image Communication, vol.17, no.1, 2002, pp.3-48.
- [4] S.-T. Hsiang and J.W.Woods, "Embedded image coding using zeroblocks and of subband/wavelet coefficients and context modeling", Proc. IEEE ISCAS'00, vol.3, Geneva Switzerland, may 2000, pp. 662-665.
- [5] J.M. Shapiro, "Embedded image coding using zerotrees of wavelet coefficients", IEEE Trans. on signal processing.vol.41, Dec.1993, pp. 3445-3462.
- [6] G.K. Wallace, "The JPEG still picture compression standard", Communications of the ACM, vol. 34, April 1991, pp.30-44.
- [7] W.P. Pennebaker and J.L. Mitchell. JPEG Still Image Data Compression Standard. New York: Van Nostrand Reinhold
- [8] J.Woods. ed., Subband Image Coding. Kluwer Academic Publishers. 1991.
- [9] M.Vetterli and J. Kovacevic, Wavelets and Subband Coding. Englewood Cliffs,NJ: Prentice-Hall, 1995.
- [10] M. Antonini.M. Barlaud, P. Mathieu, and I. Daubechies, "Image coding using wavelet transform", IEE Trans. Image Processing, vol. 1, pp. 205-220, 1992
- [11] S.-T. Hsiang and J. W. Woods, "Highly scalable and perceptually tuned embedded subband/wavelet image coding," in SPIE Conference on Visual Communications and Image Processing, vol. 4671, (San Jose, CA), Jan. 2002, pp. 1153-1164.
- [12] N. S. Jayant and P. Noll, Digital Coding of Waveforms. Englewood Cli.s, NJ: Prentice-Hall, 1984.
- [13] A. K. Jain, Fundamentals of Digital Image Processing. Englewood Cli.s, NJ: Prentice-Hall, 1989.
- [14] S. Rane, A. Aaron, and B. Girod, "Systematic Lossy Forward Error Protection for Error Resilient Digital Video Broadcasting," in Proc. VCIP 2004, San Jose, CA, USA.

- [15] A. Sehgal, A. Jagmohan, and N. Ahuja, "Wyner-Ziv coding of video: An error-resilient compression framework," IEEE Trans. Multi., vol. 6, no. 2, Apr. 2004, pp. 249–258.
- [16] C. Tillier and B. Pesquet-Popescu, "3D, 3-Band, 3-Tap Temporal Lifting For Scalable Video Coding," in Proc. ICIP 2003, Barcelona, Spain, 2003, Sept. 14-17.
- [17] C. Tillier, B. Pesquet-Popescu, and M. Van der Schaar, "Multiple Description Scalable Video Coding," in Proc. EUSIPCO 2004, Vienna, Austria, 2004, Sept. 6-10.
- [18] C. Tillier and B. Pesquet-Popescu, "A New 3-band MCTF Scheme For Scalable Video Coding," in Proc. PCS 2004, San Francisco, CA, USA, 2004, Dec. 15-17.
- [19] C. Brites, J. Ascenso and F. Pereira, "Improving Transform Domain Wyner-Ziv Video Coding Performance," in Proc. ICASSP 2006, Toulouse, France, 2006, May 14-19.

AUTHORS PROFILE



Lalitha Y.S was born on December 7, 1969 in India. She received B.E degree in Electronics and Communication Engineering and M.E. degree in Power Electronics from Gulbarga University Gulbarga, India, in 1991 and 2002 respectively. She is working as Professor in Appa Institute of Engineering & Technology, Gulbarga, India. Her research interests include image Processing, Wavelet Transform coding.



Mrityunjaya V Latte was born on April 25th 1964 in India. He received B.E. degree in electrical Engineering and M.E. degree in Digital electronics from S.D.M. College of Engineering & Technology, Dharwad, India in 1986 & 1995 respectively. He was awarded Ph.D. degree in 2004 for his work in the area of digital signal processing. He is working as Principal, JSS Academy of Technical Education, Bangalore, India. His research interests include coding, image processing and multiresolution transforms. He received a best paper award for his paper in a national conference NCSSS -2002 held at Coimbatore, India.

A Parallel and Concurrent Implementation of Lin-Kernighan Heuristic (LKH-2) for Solving Traveling Salesman Problem for Multi-Core Processors using SPC³ Programming Model

Muhammad Ali Ismail

Assistant Professor
Dept. of Computer & Info. Sys. Engg.
NED University of Engg. & Tech.
Karachi, Pakistan
maismail@neduet.edu.pk

Dr. Shahid H. Mirza

Professor
Usman Institute of Engg. & Tech.
Karachi, Pakistan
sh_mirza@uit.edu.pk

Dr. Talat Altaf

Professor & Dean (ECE)
Faculty of Elect & Comp Engg.
NED University of Engg. & Tech
Karachi, Pakistan
deanece@neduet.edu.pk

Abstract— With the arrival of multi-cores, every processor has now built-in parallel computational power and that can be fully utilized only if the program in execution is written accordingly. This study is a part of an on-going research for designing of a new parallel programming model for multi-core processors. In this paper we have presented a combined parallel and concurrent implementation of Lin-Kernighan Heuristic (LKH-2) for Solving Travelling Salesman Problem (TSP) using a newly developed parallel programming model, SPC³ PM, for general purpose multi-core processors. This implementation is found to be very simple, highly efficient, scalable and less time consuming in compare to the existing LKH-2 serial implementations in multi-core processing environment. We have tested our parallel implementation of LKH-2 with medium and large size TSP instances of TSPLIB. And for all these tests our proposed approach has shown much improved performance and scalability.

Keywords- TSP; Parallel Heuristics; Multi-core processors, parallel programming models.

I. INTRODUCTION

Multi-core processors are becoming common and they have built-in parallel computational power and which can be fully utilized only if the program in execution is written accordingly. Most software today is grossly inefficient for multi-core processors, as they are not written for the support of parallelism or concurrency. Writing an efficient and scalable parallel program is now much complex. Scalability embodies the concept that a programmer should be able to get benefits in performance as the number of processor cores increases. Breaking up an application into a few tasks is not a long-term solution. In order to make most of multi-core processors, either, lots and lots of parallelism are actually needed for efficient execution of a program on larger number of cores, or secondly, make a program concurrently executable on multi-cores [1, 2, 3].

The classical Travelling Salesman Problem (TSP) is one of the most representative irregular problems in combinatorial optimization. Despite its simple formulation, TSP is hard to

solve. The difficulty becomes apparent when one considers the number of possible tours. For a symmetric problem with 'n' cities there are $(n-1)!/2$ possible tours. If 'n' is 20, there are more than 10^{18} tours. For 7397-city problem in TSPLIB, there will be more than $10^{25,000}$ possible tours. In comparison it may be noted that the number of elementary particles in the universe has been estimated to be 'only' 10^{87} [5]. TSP has diversified application areas because of its generalized nature. TSP is being used to solve many major problems of nearly all engineering disciplines, medicine and computational sciences. [4, 6, 9].

Lin-Kernighan heuristic (LKH) is an implementation of local search optimization meta-heuristic [11, 12] for solving TSP [5, 7, 9, 10]. This heuristic is generally considered to be one of the most effective methods for generating optimal or near-optimal solutions for the symmetric traveling salesman problem. Computational experiments have shown that LKH is highly effective. Even though the algorithm is approximate, optimal solutions are produced with an impressively high frequency. LKH has produced optimal solutions for all solved problems including an 85,900-city instance in TSPLIB. Furthermore, this algorithm has improved the best known solutions for a series of large-scale instances with unknown optima, like 'World TSP' of 1,904,711-city instance. After the original algorithm (LK), its two successive variants LKH-1 and LKH-2 have also been proposed with further improvements in the original algorithm [7, 9, 13].

In this paper we have presented an efficient parallel and concurrent implementation of Lin-Kernighan Heuristic (LKH-2) for Solving Travelling Salesman Problem (TSP) using a newly developed parallel programming model, SPC³ PM, Serial, Parallel, and Concurrent Core to Core Programming Model developed for multi-core processors. It is a serial-like task-oriented multi-threaded parallel programming model for multi-core processors that enables developers to easily write a new parallel code or convert an existing code written for a single processor. The programmer can scale a program for use

with specified number of cores. And ensure efficient task load balancing among the cores [1].

The rest of the paper is organized as follows. In section II, the TSP problem and related solutions are discussed. In subsequent section III, the LKH-2 algorithm and its serial execution are analyzed in order to make it parallel and suitable for multi-core processors using SPC³ PM. Features and programming with SPC³ PM are highlighted in section IV. The parallel implementation of LKH-2 based on SPC³PM is presented in section V. In section VI, the experimental setup and results are discussed. Finally, conclusion and future work are given in section VII.

II. TRAVELLING SALESMAN PROBLEM AND RELATED SOLUTION

TSP is one of the most famous, irregular and classical combinatorial optimization problems. It has been proven that TSP is a member of the set of NP-complete problems. In TSP, a salesman is considered who has to visit n cities, the TSP asks for the shortest tour through all the cities such that no city is visited twice and the salesman returns at the end of tour back to the starting city.

Mathematically, let $G = (V, E)$ be a graph, where V is a set of n nodes and E is set of arcs. Let $C = [C_{ij}]$ be a cost matrix associated with E , where C_{ij} represents the cost of going from city i to city j . The problem is to find a permutation $(i_1, i_2, i_3, \dots, i_n)$ of the integers from 1 through n that minimizes the quantity $c_{i_1 i_2} + c_{i_2 i_3} + c_{i_3 i_4} + \dots + c_{i_n i_1}$. Using integer programming formulation, the TSP can be defined as

$$c = \min \sum_{i \in V} \sum_{j \in V} c_{ij} x_{ij}$$

$$\text{Such that } \sum_{j \in V} x_{ij} = 1, i \in V \text{ And } \sum_{i \in V} x_{ij} = 1, j \in V$$

$$\sum_{i \in S} \sum_{j \in S} x_{ij} \leq |S|-1, \forall S \subset V, S \neq \emptyset$$

$$\text{And } x_{ij} \in \{0,1\}, \text{ for all } i, j \in V.$$

Where $x_{ij} = 1$ if arc (i,j) is in the solution and 0 otherwise.

Properties of the cost matrix C are used to classify problems.

- If $c_{ij} = c_{ji}$ for all i and j , the problem is said to be symmetric; otherwise, it is asymmetric.
- If the triangle inequality holds ($c_{ik} \leq c_{ij} + c_{jk}$ for all i, j and k), the problem is said to be metric.
- If c_{ij} are Euclidean distances between points in the plane, the problem is said to be Euclidean. A Euclidean problem can be both symmetric and metric.

In order to find the optimal solution for any TSP based problem a number of solutions have been proposed, which can be classified into four classes as Exact, Heuristic, Meta-heuristic and hyper heuristics Algorithms.

A. Exact Algorithms

These algorithms are used when we want to obtain an exact optimal solution. In this, every possible solution is identified and compared for optimal solution. These algorithms are suitable for a smaller number of inputs. Brute-force method, Dynamic programming algorithm of Hell and Karp, Branch-and-Bound and Branch-and-Cut algorithm are some of the famous algorithms of this class [4, 5].

B. TSP Heuristics:

These heuristics are used when the problem size is large enough, time is limited or the data of the instance is not exact. In this class, instead of finding all possible solutions of a given problem, a sub optimal solution is identified. TSP heuristic can be roughly partitioned into two classes: 'Constructive heuristic' and 'Improvement heuristic'. Constructive heuristics build a tour from scratch and stop when one solution is produced. Improvement heuristics start from a tour normally obtained using a construction heuristic and iteratively improve it by changing some parts of it at each iteration. Improvement heuristics are typically much faster than the exact algorithm and often produce solutions very close to the optimal one. Greedy Algorithms, Nearest Neighbor, Vertex Insertion, Random Insertion, Cheapest Insertion, Saving Heuristics, Christofides Heuristics, Krap-Steele Heuristics, and ejection-chain method are the well known proposed heuristics algorithm of this class [4, 5, 6].

C. Meta-Heuristics

These are intelligent heuristics algorithms having the ability to find their way out of local optima. The Meta-heuristic approaches are the combination of first two classes. These Meta-heuristics contain implicit intelligent algorithms, ability to find their way out of local optima and possibility of numerous variants and hybrids. These heuristics are relatively more challenging to parallelize. Due to these reasons meta-heuristic approaches have drawn attention of many researchers.

Many of the well-known meta-heuristics have been proposed like Random optimization, Local search optimization, Greedy algorithm and hill-climbing, Best-first search, Genetic algorithms, Simulated annealing, Tabu search, Ant colony optimization, Particle swarm optimization, Gravitational search algorithm, Stochastic diffusion search, Harmony search, Variable neighborhood search, Glowworm swarm optimization (GSO) and Artificial Bee colony algorithm. However because of TSP nature, all these meta-heuristics cannot be used for solving TSP. Specific meta-heuristics used for solving TSP include Simulated Annealing, Genetic Algorithms, Neural Networks, Tabu Search, Ant colony optimization, and Local search optimization [4, 5, 6].

D. Hyper-Heuristics

This is an emerging direction in modern search technology. It is termed as Hyper-heuristic as it aims to raise the level of granularity at which optimization system can operate. They are broadly concerned with intelligently choosing the right heuristic or algorithm in given situation. A hyper-heuristic works at a higher level when compared with the typical application of meta-heuristics to optimize problems, i-e; a

hyper-heuristics could be taken as a heuristic or meta-heuristic which operates on other low level heuristics or meta-heuristics [4].

III. LIN-KERNIGHAN HEURISTIC AND SERIAL EXECUTION OF LKH-2 SOFTWARE

The Lin-Kernighan algorithm belongs to the class of so-called local search algorithms [5, 7, 9, 10]. A local search algorithm starts at some location in the search space and subsequently moves from the present location to a neighboring location. LKH has produced optimal solutions for all solved problems including an 85,900-city instance in TSPLIB. Furthermore, this algorithm has improved the best known solutions for a series of large-scale instances with unknown optima, like 'World TSP' of 1,904,711-city instance [5, 13].

The algorithm is specified in exchanges (or moves) that can convert one candidate solution into another. Given a feasible TSP tour, the algorithm repeatedly performs exchanges that reduce the length of the current tour, until a tour is reached for which no exchange yields an improvement. This process may be repeated many times from initial tours generated in some randomized way.

The Lin-Kernighan algorithm (LK) performs so-called k-opt moves on tours. A k-opt move changes a tour by replacing k edges from the tour by k edges in such a way that a shorter tour is achieved. Let T be the current tour. At each iteration step the algorithm attempts to find two sets of edges, $X = \{x_1, \dots, x_k\}$ and $Y = \{y_1, \dots, y_k\}$, such that, if the edges of X are deleted from T and replaced by the edges of Y, the result is a better tour. The edges of X are called out-edges. The edges of Y are called in-edges. The detail of LKH-2 software can be found in [7].

A. LKH-2 Software

LKH-2 software provides an effective serial implementation of the Lin-Kernighan heuristic Algorithm with General k-opt Sub-moves for solving the traveling salesman problem. It is written in visual C++. Computational experiments have shown that LKH-2 software is highly effective for solving TSP. This software has produced optimal solutions for all solved problems we have been able to obtain including a 85,900-city instance available in the TSPLIB. Furthermore, it has improved the best known solutions for a series of large-scale instances with unknown optima, among these a 1,904,711-city instance commonly known as World TSP. Similarly LKH-2- software also currently holds the record for all instances with unknown optima provided in the DIMACS TSP Challenge which provides many benchmark instances range from 1,000 to 10,000,000 cities. Its six versions 2.0.0, 2.0.1, 2.0.2, 2.0.2, 2.0.3, 2.0.4 and 2.0.5 have been released. For our study we have used its latest 2.0.5 version released in November 2010. This software can be downloaded free from [13].

B. Execution of LKH-2 software

For converting the serial LKH-2 software into parallel and make it suitable for multi-core processors the LKH heuristics and its LKH-2 software execution were analyzed in detail. On analyzing it is found that LKH-2 Software is written using

functional programming. Its complex computation is divided into ninety eight functions which can be called from the main program accordingly. This software also takes help of thirteen header files. On further exploration it was found that working of LKH-2 software can be broken into seven basic stages which may help in its parallelization. All the seven stages are discussed below. A flow chart representing the stages of LKH-2 software on the basis of the stages is shown in Fig. 1.

1) *Stage 1: Read parameter file:* This is the first step in LKH-2 software. A function is called to open the parameter file and to read the specified problem parameters in the file.

2) *Stage 2: Read Problem file:* In the next step, the specified problem file is read. In the TSP library all the instances and their related information is placed in an individual files using a standard format. This file is known as the problem file. The "ReadProblem function" in LKH-2 software reads the problem data in TSPLIB format for further processing.

3) *Stage 3: Partitioning of the problem:* After reading the problem, the large problem may be divided into number of sub-problems as defined in the parameter file using the parameter 'sub-problem size'. If sub-problem size is zero than no partitioning of the problem is done. Else by default the sub-problems are determined by sub-dividing the tour into segments of equal size. However LKH-2 software also provides five other different techniques to partition the problem. These include Delaunay Partitioning, Karp Partitioning, K-Means Partitioning, Rohe Partitioning and MOORE or SIERPINSKI Partitioning.

4) *Stage 4: Initialization of data structures and statistics variable:* After reading the problem and its partitioning, if done, the related data structures and statistics variables are initialized. The major statistical variables include minimum and maximum trials, total number and number of success trails, minimum and maximum cost, total Cost, minimum and maximum Time, total Time.

5) *Stage 5: Generation of Initial Candidate Set:* The "CreateCandidateSet" function and its sub-functions determines a set of incident candidate edges for each node. If the penalties (the Pi-values in the parameter file) is not defined, the "Ascent function" is called to determine a lower bound on the optimal tour using sub-gradient optimization. Else the penalties are read from the file, and the lower bound is computed from a minimum 1-tree. The function "GenerateCandidates" is called to compute the Alpha-values and a set of incident candidate edges is associated to each node.

6) *Stage 6: Find Optimal Tour :* This is main processing step where the optimal tour is found. After the creation of candidate set, the "FindTour" function is called for predetermined number of times (Runs). FindTour performs a number of trials, where in each trial it attempts to improve a chosen initial tour using the modified Lin-Kernighan edge exchange heuristics. If tour found is better than the existing tour, the tour and time are recorded.

7) *Stage 7: Update Statistics*: This step is called in two levels. Firstly this step is processed after every individual call for "FindTour" function to update the respective statistical variables. Finally it is processed at the end of total runs of "FindTour" function' to calculate and report the average statistics.

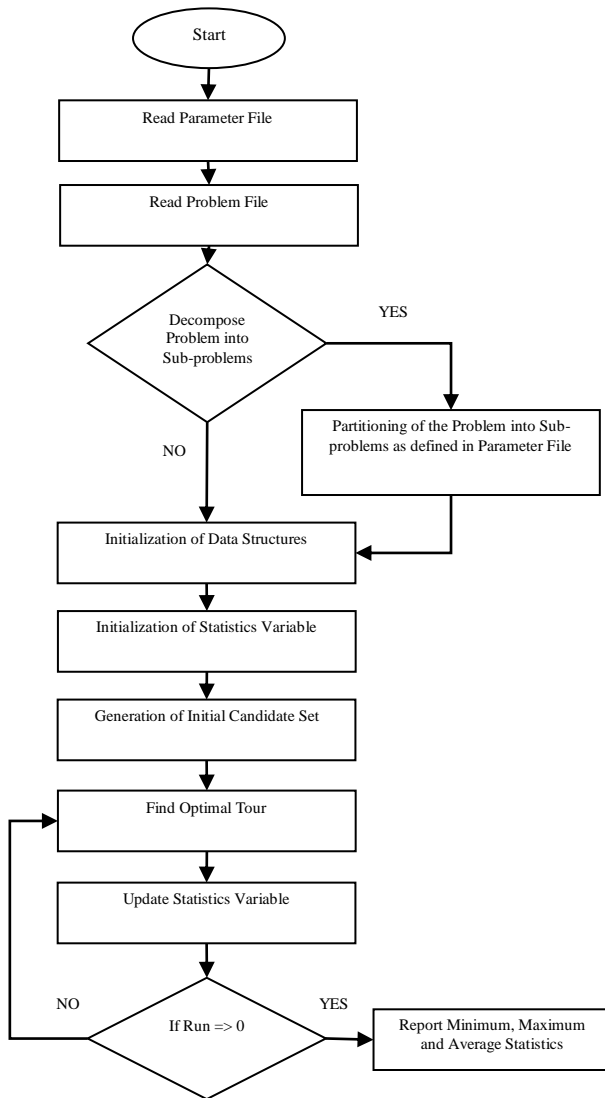


Figure1. Stages in Original serial LKH-2 software

IV. SPC³ PM (SERIAL, PARALLEL, AND CONCURRENT CORE TO CORE PROGRAMMING MODEL)

SPC³ PM, (Serial, Parallel, Concurrent Core to Core Programming Model), is a serial-like task-oriented multi-threaded parallel programming model for multi-core processors, that enables developers to easily write a new parallel code or convert an existing code written for a single processor. The programmer can scale it for use with specified number of cores. And ensure efficient task load balancing among the cores [1].

SPC³ PM is motivated with an understanding that existing general-purpose languages do not provide adequate support for parallel programming. Existing parallel languages are largely

targeted to scientific applications. They do not provide adequate support for general purpose multi-core programming whereas SPC³ PM is developed to equip a common programmer with multi-core programming tool for scientific and general purpose computing. It provides a set of rules for algorithm decomposition and a library of primitives that exploit parallelism and concurrency on multi-core processors. SPC³ PM helps to create applications that reap the benefits of processors having multiple cores as they become available.

SPC³ PM provides thread parallelism without the programmers requiring having a detailed knowledge of platform details and threading mechanisms for performance and scalability. It helps programmer to control multi-core processor performance without being a threading expert. To use the library a programmer specifies tasks instead of threads and lets the library map those tasks onto threads and threads onto cores in an efficient manner. As a result, the programmer is able to specify parallelism and concurrency far more conveniently and with better results than using raw threads.. The ability to use SPC³ PM on virtually any processor or any operating system with any C++ compiler also makes it very flexible.

SPC³ PM has many unique features that distinguish it with all other existing parallel programming models. It supports both data and functional parallel programming. Additionally, it supports nested parallelism, so one can easily build larger parallel components from smaller parallel components. A program written with SPC³ PM may be executed in serial, parallel and concurrent fashion. Besides, it also provides processor core interaction to the programmer. Using this feature a programmer may assign any task or a number of tasks to any of the cores or set of cores.

A. Key Features

The key features of SPC³ are summarized below.

- SPC³ is a new shared programming model developed for multi-core processors.
- SPC³ PM works in two steps: defines the tasks in an application algorithm and then arranges these tasks on cores for execution in a specified fashion.
- It provides Task based Thread-level parallel processing.
- It helps to exploit all the three programming execution approaches, namely, Serial, Parallel and Concurrent.
- It provides a direct access to a core or cores for maximum utilization of processor.
- It supports major decomposition techniques like Data, Functional and Recursive.
- It is easy to program as it follows C/C++ structure.
- It can be used with other shared memory programming model like OpenMP, TBB etc.
- It is scalable and portable.
- Object oriented approach

B. Programming with SPC³ PM

SPC³ PM provides a higher-level, shared memory, task-based thread parallelism without knowing the platform details

and threading mechanisms. This library can be used in simple C / C++ program having tasks defined as per SPC³ PM Task Decomposition rules. To use the library, you specify tasks, not threads, and let the library map tasks onto threads in an efficient manner. The result is that SPC³ PM enables you to specify parallelism and concurrency far more conveniently, and with better results, than using raw threads.

Programming with SPC³ is based on two steps. First describing the tasks as it specified rules and then programming it using SPC³ PM Library.

1) Steps involved in the development of an application using SPC³ PM

- The user determines that his application can be programmed to take advantage of multi-core processors.
- The problem is decomposed by the user following the SPC³ PM 'Task Decomposition Rules'.
- Each Task is coded in C /C++ as an independent unit to be executed independently and simultaneously by each core.
- Coding of Main Program using SPC³ PM Library to allow the user to run the program in serial, parallel or concurrent mode.
- Compilation of code using any standard C/C++ compiler.
- Execution of Program on a multi-core processor

2) Rules for Task Decomposition

The user can decompose the application / problem on the basis of following rules.

- The user should be able to breakdown the problem in various parts to determine if they can exploit Functional, Data or Recursive decomposition.
- Identify the loops for the loop parallelism and may be defined as Tasks.
- Identify independent operations that can be executed in parallel and may be coded as independent Tasks.
- Identify the large data sets on which single set of computations have to be performed. Target these large data sets as Tasks.
- Tasks should be named as Task1, Task2,..... TaskN. If a Task returns a value it should be named with suffix 'R' like TaskR1, TaskR2.... TaskRN.
- There is no limit on the number of Tasks.
- Each Task should be coded using either C/C++/VC++/C# as an independent function.
- A Task may or may not return the value. A Task should only intake and return structure pointer as a parameter. Initialize all the shared or private parameters in the structure specific to a Task. This structure may be shared or private.
- Arrange the tasks using SPC³ PM Library in the main program according to the program flow.

3) Program Structure

```
Define Task1
Define Task2
Define Task3
Define Task4
...
Define TaskN

Structure STRUCT_NAME
{
//The structure
//having private
//or global
//parameters
//associated with a
//specified task
}
STRUCT_NAME *P_TASK1

Structure STRUCT_NAME
{
//The structure
//having private
//or global
//parameters
//associated with a
//specified task
}
STRUCT_NAME *P_TASK2

Structure STRUCT_NAME
{
//The structure
//having private
//or global
//parameters
//associated with a
//specified task
}
STRUCT_NAME *P_TASK3

Structure STRUCT_NAME
{
//The structure
//having private
//or global
//parameters
//associated with a
//specified task
}
STRUCT_NAME *P_TASKN

Task1(LPVOID)
{
//performing
//some
//computation
}

Task2(LPVOID)
{
//performing
//some
//computation
}

Task3(LPVOID)
{
//performing
//some
//computation
}

TaskN(LPVOID)
{
//performing
//some
//computation
}

void main( void)
{
// any declaration;
// any piece of code ;

Serial (Task1, P_TASK1); //execution of task 1 in serial

// Any other code ;

Parallel (Task2, P_TASK2); //execution of task 2 in parallel

// any other code ;

Concurrent (Task3, P_TASK3, Task4, P_TASK4); //execution of task 3 and 4 concurrently
}
```

C. SPC³ PM Library

SPC³ PM provides a set of specified rules to decompose the program into tasks and a library to introduce parallelism in the program written using c/ c++. The library provides three basic functions.

- Serial
- Parallel
- Concurrent

1) *Serial*: This function is used to specify a Task that should be executed serially. When a Task is executed with in this function, a thread is created to execute the associated task in sequence. The thread is scheduled on the available cores either by operating system or as specified by the programmer. This function has three variants. Serial (Task i) {Basic}, Serial (Task i, core) {for core specification} and *p Serial (Task i, core, *p) {for managing the arguments with core specification}

2) *Parallel*: This function is used to specify a Task that should be executed in parallel. When a Task is executed with in this function, a team of threads is created to execute the associated task in parallel and has an option to distribute the work of the Task among the threads in a team. These threads are scheduled on the available cores either by operating system

or as specified by the programmer. At the end of a parallel function, there is an implied barrier that forces all threads to wait until the work inside the region has been completed. Only the initial thread continues execution after the end of the parallel function. The thread that starts the parallel construct becomes the master of the new team. Each thread in the team is assigned a unique thread id to identify it. They range from zero (for the master thread) up to one less than the number of threads within the team. This function has also four variants. Parallel (Task i) {Basic}, Parallel (Task i ,num-threads) {for defining max parallel threads}, Parallel (Task i, core list) {for core specification} and *p parallel (Task i, core, *p) {for managing the arguments with core specification}

3) *Concurrent*: This function is used to specify the number of independent tasks that should be executed in concurrent fashion on available cores. These may be same tasks with different data set or different tasks. When the Tasks are executed defined in this function, a set of threads equal or greater to the number of tasks defined in concurrent function is created such that each task is associated with a thread or threads. These threads are scheduled on the available cores either by operating system or specified by the programmer. in other words , this function is an extension and fusion of serial and parallel functions. All the independent tasks defined in concurrent functions are executed in parallel where as each thread is being executed either serially or in parallel. This function has also three variants. Concurrent (Task i, Taskj,Task N) {Basic}, Concurrent (Task i, core , Task j , core,) {for core specification} and Concurrent (Task i, core , *p, Task j , core, *p) {for managing the arguments with core specification}.

V. PARALLELIZATION OF LKH-2 SOFTWARE USING SPC³ PM

LKH-2 software is a serial code and cannot make most of multi-cores unless modified accordingly. This LKH-2 software code can be made suitable for multi-core processors by introducing parallelism and concurrency in it. Here it is

done using SPC³ PM.

SPC³ PM, Serial Parallel and Concurrent Core to Core programming Model provides an environment to decompose the application into tasks using its task decomposition rules and then execute these tasks in serial, parallel and concurrent fashion. As LKH-2 software is written in function style so we have to only restructure the some part of the code to make it suitable for SPC³ PM.

Working of LKH-2 software can be decomposed into seven stages as discussed in section III. Out of seven, the most important and computational intensive stages are its sixth stage that is finding of the optimal tour using LKH-2 algorithm and seventh stage, that is updating of the statistics accordingly. The other related time consuming step is to execute this stage multiple times as defined in the parameter file (runs). The rest of the stages do not demand much of time and computations and can be executed in serially.

LKH-2 software is parallelized by converting its tour finding and related routines (sixth stage) into tasks according to the SPC³ PM Task decomposition rules and executing them in parallel using parallel function of SPC³ PM Library. To execute this stage multiple times as defined in the parameter file (runs), concurrent function of SPC³ PM is used. This concurrent execution enables to execute this stage in parallel on the available cores. This approach of decomposition and execution of LKH-2 software makes it suitable for parallel execution on multi-core processors.

This two level parallel and concurrent execution of stages also makes this LKH-2 software scalable with respect to multiple-cores processors. The available cores are divided into sets equal to number of runs of stage six. Each set execute the stage concurrently and cores in each set execute the single task of finding the optimal tour in parallel. Number of sets and number of cores in each set is calculated using the following equations respectively.

$$\text{Number of Sets (S)} = \frac{\text{Number of Available Cores (N)}}{\text{Number of Runs}} \quad (1)$$

$$\text{Number of Cores in Each Set (C)} = \frac{\text{Number of Available Cores (N)}}{\text{Number of Sets (S)}} \quad (2)$$

For example, on a 24 cores processor with 8 runs of finding the tour task, the total 8 sets with 3 cores each are created. Each individual execution of the task is performed on each set concurrently. Whereas three cores in each set is responsible to execute the task with in a set in parallel.

A. Experimental Setup

For our study we have selected standard medium size and large size TSP instances of TSBLIB [5, 14, 15]. All the computational tests reported in this section, for both original and parallelized LKH-2 software code with SPC³ PM, run on the TSPLIB instances, have been made using the default values of parameters defined in LKH-2 software parameter file. These default values have proven to be adequate in many applications [5]. Each TSP instances for both original and parallelized LKH-2 software code with SPC³ PM, is given ten runs for calculating the optimal tour and for each respective TSP instance, three different execution times, i-e, the minimum execution time out of ten runs, average and total execution time required for all ten runs are then recorded.

For the execution of the algorithms, the latest Intel server 1500ALU with dual six core hyper threaded Intel Xeon 5670 processor is used. Thus total number of parallel threads that can be executed is $2 \times 2 \times 6 = 24$. Operating systems used is 64 bit windows 2008 server.

B. Result Analysis and Observations

Table1 shows the minimum, average and total execution time for original serial LKH-2 software for 10 runs of each medium size TSP instances.

TABLE1. Minimum, Average and Total execution time for original serial LKH-2 software for medium size TSP instances (10 runs each)

TSP Instance	Optimal Value	Average Root Gap	Min. Time (Sec)	Average Time (Sec)	Total Time (Sec)
pr1002	259045	0.00%	1	1	12
si1032	92650	0.00%	5	7	74
u1060	224094	0.01%	54	103	1026
vm1084	239297	0.02%	30	42	420
pcb1173	56892	0.00%	0	3	30
d1291	50801	0.00%	3	4	43
r11304	252948	0.16%	14	14	140
r11323	270199	0.02%	2	12	117
nrw1379	56638	0.01%	14	16	158
fl1400	20127	0.18%	3663	3906	39061
u1432	152970	0.00%	3	3	33
fl1577	22204	0.24%	1218	2189	21888
d1655	62128	0.00%	2	4	39
vm1748	336556	0.00%	20	22	220
u1817	57201	0.09%	68	119	1188
r11889	316536	0.00%	65	135	1348
d2103	79952	0.63%	146	162	1624
gr2121	2707	0.00%	25	30	303
u2319	234256	0.00%	1	1	10
pr2392	378032	0.00%	1	1	10

Table 2 shows the minimum, average and total time for the parallelized LKH-2 software using SPC³ PM for 10 runs of each medium size TSP instances.

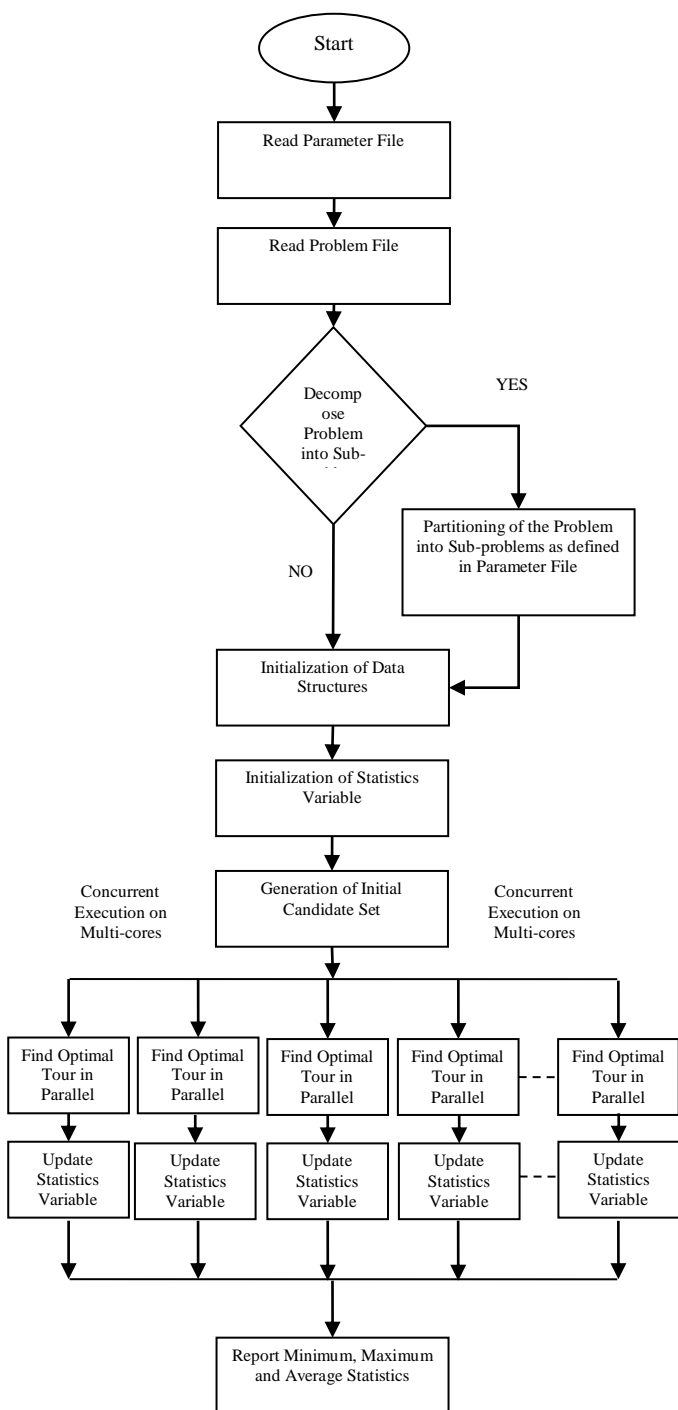


FIGURE2. Stages in parallelized LKH-2 software using SPC³ PM

VI. PERFORMANCE EVOLUTION

This section discusses the performance comparison of the parallelized LKH-2 software using SPC³ PM and the original LKH-2 software version 2.0.5. on various instances of TSP library. The LKH-2 is parallelized using SPC³ PM Task decomposition rules and SPC³ PM Library to make this serial code suitable for multi-core processors.

TABLE2: Minimum, Average and Total time for Parallelized LKH-2 software using SPC³ PM for each medium size TSP instances (10 runs each)

TSP Instance	Optimal Value	Average Root Gap	Min. Time (Sec)	Average Time (Sec)	Total Time (Sec)
pr1002	259045	0.00%	0	1	9
si1032	92650	0.00%	2	5	51
u1060	224094	0.01%	34	67	673
vm1084	239297	0.02%	15	27	271
pcb1173	56892	0.00%	0	2	20
d1291	50801	0.00%	2	3	31
rl1304	252948	0.16%	8	10	98
rl1323	270199	0.02%	2	8	77
nrw1379	56638	0.01%	8	11	112
fl1400	20127	0.18%	1883	2370	23695
u1432	152970	0.00%	2	2	22
fl1577	22204	0.24%	809	1422	14222
d1655	62128	0.00%	2	3	28
vm1748	336556	0.00%	11	16	159
u1817	57201	0.09%	44	81	811
rl1889	316536	0.00%	43	100	1001
d2103	79952	0.63%	106	137	1368
gr2121	2707	0.00%	15	22	219
u2319	234256	0.00%	1	1	7
pr2392	378032	0.00%	1	1	7

Following Fig. 3 based on tables 1 and 2, shows the comparison of minimum time between original serial LKH-2 software and parallelized LKH-2 software using SPC³ PM for the medium size TSP instances. Similarly, Fig. 4 and Fig. 5 show the comparison of average and total time between original serial LKH-2 software and parallelized LKH-2 software using SPC³ PM for 10 runs of each medium size TSP instances

From Fig. 3, for minimum execution time, it may clearly be observed that our parallelized LKH-2 software using SPC³ PM requires much lesser time that of the original LKH-2 software requires. It is so because the main function of finding the optimal tour using LKH algorithm is being executed in parallel on the available cores as defined in (2). In this case, 10 runs of each instance are executed concurrently on 20 cores. That is each run has a set of nearly 2 cores for its execution in parallel. Speedup obtained in our case ranges from 1.5 to 1.7, which is where much near to the ideal speedup which should be 2 in this case.

Similarly, from Fig 4, the same observation can be made that the average execution time for parallelized LKH-2 software using SPC³ PM requires much lesser time that of the original LKH-2 software requires. It is so, because all the required runs of an instance are running in parallel on their respective allocated set of 2 cores.

For the total execution time required for 10 runs of each instances, the parallelized LKH-2 software code shows much greater performance gain in comparison to original LKH-2 code. This is because of the concurrent execution of all required runs on the available cores. In this case as defined by (1), total 10 sets are created. Each set is responsible to execute a run of a given instance. Thus all the runs are executed concurrently on 24 core machine making most of the multi-core processor and reducing the total execution time remarkably. Whereas in serial execution of original LKH-2 software, next run of a TSP instance is executed only after the completion of the first run.

Table 3. shows the minimum, average and total time for original serial LKH-2 software for each large size TSP instances. Similarly, table 4 shows the minimum, average and total time for the parallelized LKH-2 software using SPC³ PM for each large size TSP instances. All the computational tests reported here are taken with default parameter file and having ten runs for each TSP instance.

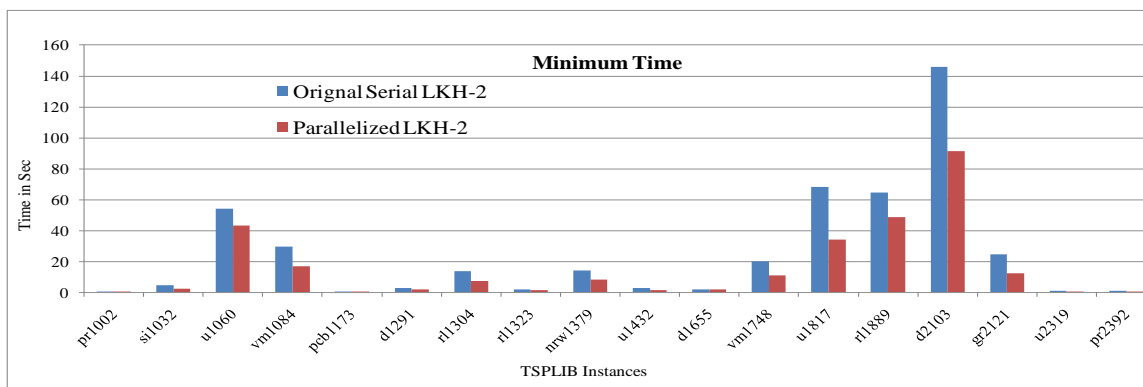


FIGURE 3. Comparison of minimum time between original serial LKH-2 software and parallelized LKH-2 software using SPC³ PM for the medium size TSP instances calculated for 10 runs

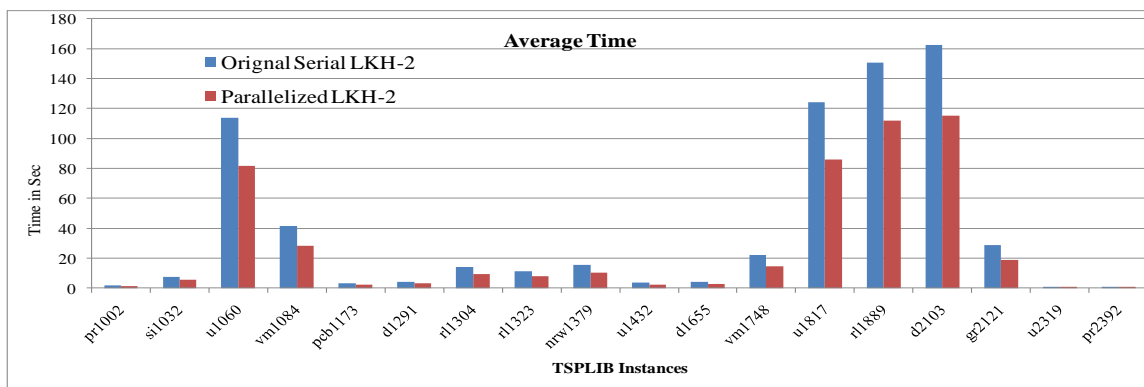


FIGURE 4. Comparison of average time between original serial LKH-2 software and parallelized LKH-2 software using SPC³ PM for the medium size tsp instances calculated for 10 runs

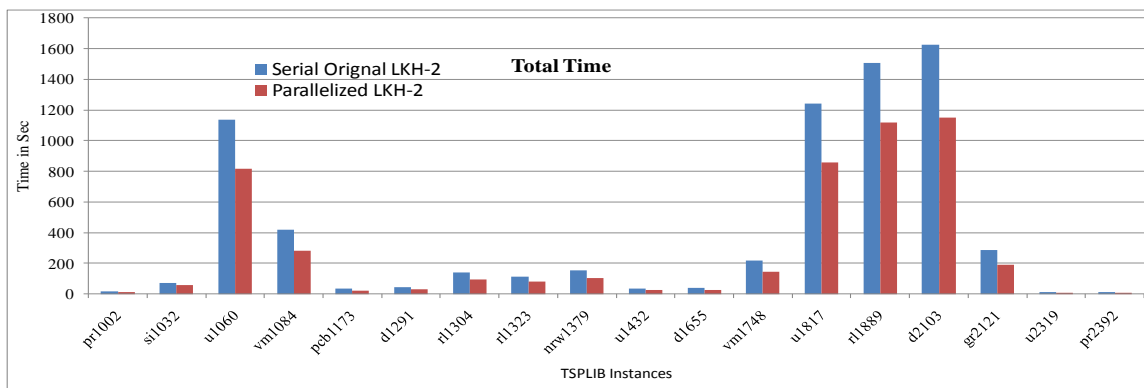


FIGURE 5. Comparison of total time between original serial LKH-2 software and parallelized LKH-2 software using SPC³ PM for the medium size TSP instances calculated for 10 runs

TABLE 3. Minimum, Average and Total execution time for original serial LKH-2 software for each large size TSP instances (10 runs each)

TSP Instance	Optimal Value	Avg. Root Gap	Min. Time (Sec)	Avg. Time (Sec)	Total Time (Sec)
pcb3038	137694	0.00%	430	499	4993
fl3795	[28723,28772]	0.31%	5114	6473	64725
fnl4461	182566	0.09%	2460	2759	27594
rl5915	[565040,565530]	0.37%	3220	3329	33286
pla7397	23260728	0.00%	1280	1544	15440

TABLE 4. Minimum, Average and Total time for Parallelized LKH-2 software using SPC³ PM for each large size TSP instances (10 runs each)

TSP Instance	Optimal Value	Avg. Root Gap	Min. Time (Sec)	Avg. Time (Sec)	Total Time (Sec)
pcb3038	137694	0.00%	279	365	540
fl3795	[28723,28772]	0.31%	3299	4474	7109
fnl4461	182566	0.09%	1507	1873	2675
rl5915	[565040,565530]	0.37%	1849	2420	3201
pla7397	23260728	0.00%	762	1107	1525

Following Fig. 6 based on tables 3 and 4 shows the comparison of minimum time between original serial LKH-2 software and parallelized LKH-2 software using SPC³ PM for the large size TSP instances. Similarly, Fig. 7 and Fig. 8 show the comparison of average and total time between original serial LKH-2 software and parallelized LKH-2 software using SPC³ PM for the large size TSP instances.

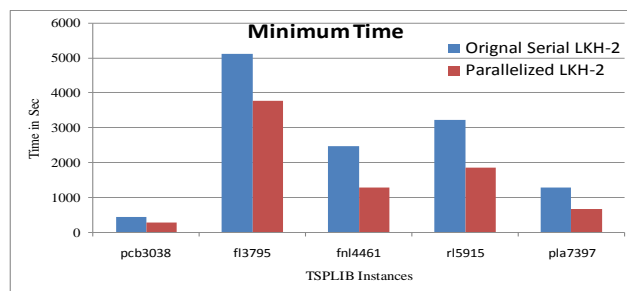


FIGURE 6. Comparison of minimum execution time between original serial lkh-2 software and parallelized LKH-2 software using SPC³ PM for the large size TSP instance calculated for 10 runs

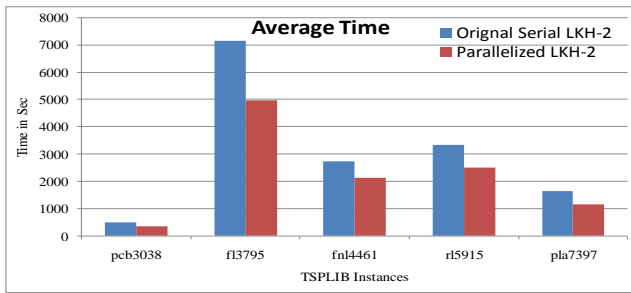


FIGURE 7. Comparison of average execution time between original serial lkh-2 software and parallelized LKH-2 software using SPC³ PM for the large size TSP instance calculated for 10 runs

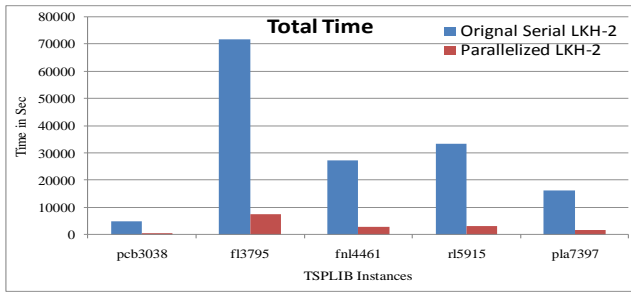


FIGURE 8. Comparison of total execution time between original serial lkh-2 software and parallelized LKH-2 software using SPC³ PM for the large size TSP instance calculated for 10 runs

From Fig. 6, 7 and 8, same observation can be made for large size TSP instance as that of the medium size TSP instance. The minimum, average and total execution time for parallelized LKH-2 software using SPC³ PM is found lesser than that of the original LKH-2 software requires.

VII. CONCLUSION AND FUTURE WORK

The results from this study show that the SPC³ PM (Serial, Parallel, and Concurrent Core to Core Programming Model) provides a simpler, effective and scalable way to parallelize a given code and make it suitable for multi-core processors. With the concurrent and parallel function of SPC³ PM, the programmer can transform a given serial code into parallel and concurrent executable form for making most of the multi-core processors.

The Lin-Kernighan Heuristic (LKH-2) for Solving Travelling Salesman Problem which is generally considered to be one of the most effective methods for generating optimal or near-optimal solutions for the symmetric traveling salesman problem is made further effective and less time consuming by introducing parallelism and concurrency in the algorithm with the help of SPC³ PM. Besides, the new parallel and concurrent implementation of the algorithm founds much more scalable and suitable for multi-core processors.

This SPC³ PM will be further worked out for introduction of some more parallel and concurrent functionality and synchronizing tools and will be applied to other standard and classical problems to meet the software challenges of multi-core era.

REFERENCES

- [1] M. A. Ismail, S.H. Mirza, T. Altaf, "Concurrent matrix multiplication on multi-core processors", Intl. J. of Comp. Sc. & Security, vol. 5(4), 2011, pp 208-220.
- [2] N. Vachharajani, Y. Zhang and T. Jablin, "Revisiting the sequential programming model for the multicore era", IEEE MICRO, Jan - Feb 2008.
- [3] M. D. McCool, "Scalable programming models for massively multicore processors", Proceedings of the IEEE, vol. 96(5), 2008.
- [4] F. Glover, G.A. Kochenberger, Handbook of Metaheuristics, Kluwer's international series, 2003, pp. 475-514.
- [5] D. L. Applegate, R. Bixby, V. Chvatal, W. J. Cook, The Travelling Salesman Problem, Princeton University Press, 2006, pp. 29, 59-78, 103, 425-469, 489-524.
- [6] E. Alba, Parallel Metaheuristics a new class of algorithms, Wiley, 2006.
- [7] K. Helsgaun, "General k -opt submoves for the Lin-Kernighan TSP heuristic", Math. Prog. Comp., vol. 1, pp. 119-163, 2009.
- [8] Lawler, E.L., Lenstra, J.K., Rinnooy Kan, A.H.G., Shmoys, D.B. (eds.): The Traveling Salesman Problem: A Guided Tour of Combinatorial Optimization. Wiley, New York, 1985.
- [9] S. Lin, B. W. Kernighan, "An effective heuristic algorithm for the traveling-salesman problem". Oper.Res. vol. 21, pp. 498-516, 1973.
- [10] K. Helsgaun, "An effective implementation of the Lin-Kernighan traveling salesman heuristic", EJOR 12, pp. 106-130, 2000.
- [11] H.H. Hoos, T. Stützle, Stochastic Local Search: Foundations and Applications. Morgan Kaufmann, Menlo Park, 2004.
- [12] D. S. Johnson, "Local optimization and the traveling salesman problem", LNCS, vol. 442, pp. 446-461, 1990.
- [13] <http://www.akira.ruc.dk/~keld/research/LKH/>
- [14] <http://www.tsp.gatech.edu/data/index.html>
- [15] <http://comopt.ifi.uni-heidelberg.de/software/TSPLIB95/>

AUTHORS PROFILE

Muhammad Ali Ismail received his B.E degree in Computer and Information Systems from NED University of Engineering and Technology, Pakistan in 2004. He did his M.Engg in Computer Engineering with specialization in Computer Systems and Design from the same university in 2007. Now he is pursuing his PhD research in the field of Multi-core Processors. His areas of interest include serial, parallel and distributed computer architectures, Shared memory, distributed memory and GPU programming, including generic and specific models and algorithms. He has received first prize Gold medal in all Pakistan competition for his cluster design. He is a member of IEEE (USA), IET (UK) & PEC.

Prof. Dr. Shahid Hafeez Mirza has 38 years of experience in teaching and research. He received his bachelor degree in Electrical Engineering from NED University of Engineering and Technology, Pakistan. He did his MS from USA. From UK he pursued his degree of doctorate. He has served department of Computer and Information System Engineering of NED University as a Chairman. He also remained the DEAN of faculty of Electrical and Computer Engineering. Now he is Senior Research fellow in the same university. His fields of interest include processor design, computer architecture and parallel processing. He is a member IEEE (USA) and member IET (UK).

Prof. Dr. Talat Altaf has 29 years of experience in teaching and research. He has B.Sc. Engineering (Honours) in Electrical Engineering and M.Sc. Engineering (Instrumentation) degrees from Aligarh Muslim University, Aligarh in 1976 and 1983 respectively. He pursued his Ph.D. degree from the University of Bradford, U.K. during 1990 till 1994. He has served the Department of Electrical Engineering of NED University as a Chairman during 1997 till 2007. He is presently the Dean of the Faculty of Electrical and Computer Engineering. His fields of interests are in the areas of Current Mode Circuits/Filters, Digital Signal Processing, Parallel Processing, Energy Conversion and Distributed Generation. He is a member of IEEE (USA), Circuits and Systems Society and Instrumentation and Measurement Society. He is also member of IET (U.K.), PEC, and Illumination Society of Pakistan.

Performance Evaluation of Mesh - Based Multicast Routing Protocols in MANET's

M. Nagaratna
Assistant Professor
Dept. of CSE
JNTUH, Hyderabad, India

V. Kamakshi Prasad
Prof & Additional Cont. of.
Examinations
School of Information Technology
JNTUH, Hyderabad, India

Raghavendra Rao
Professor & Head
Dept. of CSE
University of Hyderabad, India

Abstract— Multicasting is a challenging task that facilitates group communication among the nodes using the most efficient strategy to deliver the messages over each link of the network. In spite of significant research achievements in recent years, efficient and extendable multicast routing in Mobile Ad Hoc Networks (MANETs) is still a difficult issue. This paper proposes the comparison of ODMR and PUMA protocol. As per the simulation results PUMA is better than ODMR.

Keywords- MANET; multicast; QoS.

I. INTRODUCTION

An ad hoc mobile network is a collection of mobile nodes that are dynamically and arbitrarily located in such a manner that the interconnections between nodes are capable of changing on a continual basis [1]. The primary goal of an ad hoc network routing protocol is to provide an efficient route establishment between a pair of nodes so that messages may be delivered in a timely manner. Route construction should be done with a minimum of overhead and bandwidth consumption. Multicasting plays an important role for communication in a MANET, where group tasks are often deployed. For multicasting, a multicast group is constructed with one or more group members and multicast address is assigned to each group. In a MANET, the group members randomly spread and frequently move in the whole network, which causes more difficulty in packet delivery and group maintenance.

Quality of service (QoS) is an important consideration in networking, but it is also a significant challenge [3, 4, 9, 11]. QoS is more difficult to guarantee in MANETs than in other type of networks, because the wireless bandwidth is shared among adjacent nodes and the network topology changes as the nodes move. With the extensive applications of MANETs in many domains, the appropriate QoS metrics should be used. Therefore, QoS multicasting routing protocols face the challenge of delivering data to destinations through multi hop routes in the presence of node movements and topology changes. According to the topology, multicast routing protocols can be classified into tree-based and mesh-based. These protocols differ in terms of the redundancy of the paths between senders and receivers. Whereas tree-based protocols provide only a single path between senders and receivers, mesh-based protocols provide multiple paths. Examples of Mesh-based protocols are ODMR and PUMA. The rest of this

paper is organized as follows, section II presents about the ODMR protocol, section III presents about the PUMA protocol, section IV presents the Performance evaluation of two protocols, section V presents the simulation of NS, section VI presents simulation results of two protocols, section VII conclusions.

II. ON-DEMAND MULTICAST ROUTING PROTOCOL

Construction of a mesh it forms multiple routes and multicast packets are being delivered to destinations even the node movements and topology changes. ODMRP [2] uses the concept of forwarding group to establish a mesh for each multicast group. The forwarding group is set of nodes which are responsible for forwarding multicast data on shortest path between any member pairs. To maintain multicast group members a soft-state approach is used. Explicit control messages are not required to leave the group. ODMRP is more attractive in mobile wireless networks due to reduction of channel/storage overhead and the richer connectivity.

A. Mesh Creation and multicast Route:

This protocol establishes multicast routes and group memberships which are added to the source on- demand. If the node realizes it is in the path to the source and a segment of the forwarding group then it set the FG flag and it broadcast its own Join Reply. The Join Reply causes by every forwarding group member unless it reaches multicast source through the shortest path. In the forwarding group this process builds or adding the routes from sources to receivers and constructs a mesh. Forwarding group is set of nodes which are in charge of forwarding multicast packets and also it supports shortest paths between any member pairs. All nodes inside the multicast are members and also forwarding group nodes, forwarding group nodes forwards multicast data packets. If a multicast receiver is on the path between a multicast source and another receiver then it is said to be a forwarding group node. The mesh provides richer connectivity between multicast members as compared to multicast trees. Flooding redundancy among forwarding group helps to overcome node displacements and channel fading. Hence frequent reconfigurations are not required.

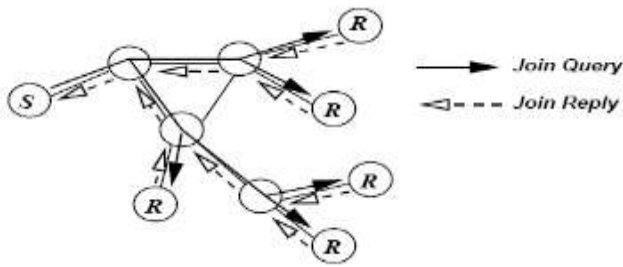


Fig 1. On-demand procedure for membership setup and maintenance

Fig 2 is an example to show the robustness of a mesh configuration. Three sources (S_1 , S_2 , and S_3) send multicast data packets to three receivers (R_1 , R_2 , and R_3) via three forwarding group nodes (A, B, and C). In case the route from S_1 to R_2 is $\langle S_1-A-B-R_2 \rangle$. In a tree configuration, if the link between nodes A and B breaks R_2 cannot receive any packets from S_1 until the tree is reconfigured but in ODMRP has a redundant route $\langle S_1-A-C-B-R_2 \rangle$ to deliver packets without going through the broken link between nodes A and B. Nodes R_2 and R_3 send their Join Replies to both S_1 and S_2 through I_2 , and R_1 sends its packet to S_1 through I_1 and S_2 through I_2 as shown in Fig 3.

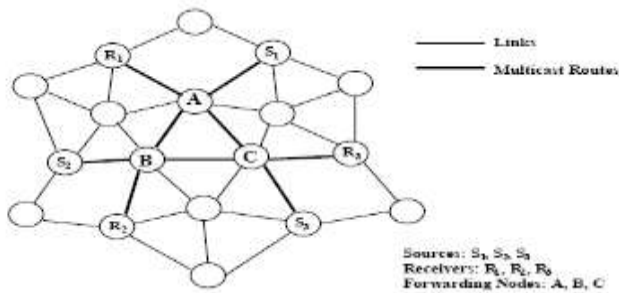


Fig 2. Mesh Configuration

When receivers send Join Replies to next hop nodes, an intermittent node I_1 set the FG Flag and built its own Join Reply as there is a next node ID entry in the Join Reply received from R_1 that verifies its ID. Note that the Join Reply built by I_1 having an entry for sender S_1 and not for S_2 as the next node ID for S_2 in the received Join Reply is not I_1 . At the same time node I_2 set the FG Flag and it builds its own Join Reply and sends its neighbors. However I_2 receives three Join Replies from the receivers, it broadcasts the Join Reply only once because the second and third table to hold no new source information. Channel overhead is

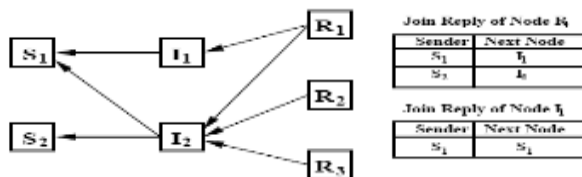


Fig 3. example of Join Reply forwarding

B. Data Forwarding:

After establishing the group and the route construction process a multicast source sends packets to receivers through selected routes and forwarding groups. Periodic control packets are delivered only when outgoing data packets are still present.

While receiving a multicast data packet a node forwards only if it is not a duplicate, set FG Flag for the multicast group which was not expired. This minimizes traffic overhead and to save sending packets through stale routes.

C. Soft State

In ODMRP to join or leave the group explicit control packets are need not be sent. In case a multicast source wants to leave group it immediately stops sending Join Query packets because it is not having any multicast data to sent to the group. From a specific multicast group a receiver no longer wants to receive it removes the corresponding entries from its Member Table and need not transmit the Join Reply for that group.

D. Selection of Timer Values:

The performance of the ODMRP is based on the timer values of route refresh interval and forwarding group timeout interval. The selection of soft state timers must be adaptive to network environment i.e. mobility pattern, capacity of the channel, type of traffic, load traffic, mobility speed etc. New route and membership information can be achieved frequently when small route refresh interval values are used at the cost of getting more packets and causes network congestion. In case where big route refresh values are selected even less control traffic is produced, nodes may not know up-to-date route information and multicast membership.

E. Unicast Capability:

The major strength of ODMRP is unicast routing capability. It can work with any unicast routing protocol and can also operate efficiently as unicast routing protocol. Therefore it need not require a separate unicast protocol. ODMRP offers the advantage of sharing the same optional software for both unicast and multicast operation reduced drastically when many multicast receivers share the same links to source.

III. PUMA

PUMA [6] supports any source to send multicast packets addressed to a given multicast group. PUMA does not need another unicast routing protocol because it can act as unicast protocol. PUMA implements a distributed algorithm to elect one of the receivers of a group as core of the group. The election algorithm used in PUMA is same as the spanning tree algorithm introduced by Perlman for internet works of transparent bridges [7]. Within a finite time router can find multiple paths to the core. All nodes on shortest paths between any receiver and the core collectively form the mesh.

A sender sends a data packet to the group along any of the shortest paths between the sender and the core. When the data packet reaches a mesh member, it is flooded within the mesh, and nodes maintain a packet ID cache to drop duplicate packets. PUMA uses single control message for all its functions, i.e. multicast announcement packet (MAP). Each MAP has a sequence number, group ID, core ID, distance to the core, mesh member flag, and a parent that states the preferred neighbor to reach the core. Successive MAPs have a higher sequence number than previous multicast announcements sent by the same core. With the information contained in such announcements, nodes elect cores, determine

the routes for sources outside a multicast group to unicast multicast data packets towards the group, notify about joining or leaving the mesh of a group and maintain the mesh.

A. Connectivity Lists and propagation of Multicast Announcements:

A node which is core of a group transmits multicast announcements periodically for that group. As the multicast announcement travels through the network, it establishes a connectivity list at every node in the network. Using connectivity lists, nodes will be able to establish a mesh, and route data packets from senders to receivers. A node stores the data from all the multicast announcements it receives from its neighbors in the connectivity list. Fresh multicast announcements overwrite entries with lower sequence numbers for the same group. For a given group, a node has only one entry in its connectivity list from a particular neighbor and it keeps only that information with the latest sequence number for a given core. Each entry in the connectivity list, it stores the multicast announcement, stores the time when it was received, and the neighbor from which it was received. Next the node generates its own multicast announcement based on the best entry in the connectivity list. For the same core ID and sequence number, multicast announcements with smaller distances to the core are considered. When all those fields are the same, the multicast announcement that arrived earlier is considered. After selecting the best multicast announcement, the node generates the fields of its own multicast announcement i.e. Core ID, Group ID, Sequence number, Distance to core, Parent, Mesh member. The connectivity list stores information about all the routes that exist to the core. When a core change occurs for a group then the node clears the entries of its old connectivity list and builds a new list, specific to the new core.

B. Mesh Establishment and Maintenance:

At the initial stage only receivers are considered as mesh members and their mesh member flag is set to TRUE in the MAP's. Non receivers consider themselves as mesh members if and only if they have at least one mesh child in their connectivity list. A neighbor in the connectivity list is a mesh child if (i) Its mesh member flag is set (ii) The distance to core of the neighbor is larger than the node's distance to core (iii) The multicast announcement corresponding to this entry was received in within a time period equal to two MAP intervals. If a node has a mesh child and is hence a mesh member, then it means that it lies on a shortest path from a receiver to the core.

C. Core Election:

When a new receiver wants to join a multicast group, it first finds whether it has received a MAP from core of that group. If the node has received it earlier, it adopts the core specified in the announcement it has received, and it starts transmitting MAP that specify the core for that group. It considers itself as the core of the group and starts transmitting MAP periodically to its neighbor stating itself as the core of the group and 0 distances to itself. Nodes propagate MAP based on the best multicast announcements they have received from their neighbors. A MAP with higher core ID is considered better than a multicast announcement with a lower core ID. Each connected component has only one core. If a receiver joins the

group before any other receivers, it declares itself as the core of the group. If several receivers join the group concurrently, then the one with the highest ID is declared as core of the group. The election is held in the partition which does not have the old core.

D. Forwarding Multicast Data Packets:

The parent field of connectivity list entry corresponds to the node from which the neighbor received its best MAP. This field allows nonmembers to forward multicast packets towards the mesh of a group. A node forwards a multicast data packet it receives from its neighbor. The packets are then flooded within the mesh and group members use a packet ID cache to detect and discard packet duplicates. The routing of data packets from senders to receivers is also used to update the connectivity list. When a nonmember transmits a packet, it expects its parent to forward the packet. This serves as an implicit acknowledgment of the packet transmission. If the node does not receive an implicit acknowledgment within ACK-TIMEOUT then it deletes the parent from its respective connectivity list.

IV. PERFORMANCE EVALUATION

The parameters used in calculating the performance of protocols [8,10] are Packet Delivery Ratio, Throughput, End-to-End Delay, Latency, no. of sent packets. Packet Delivery Ratio is the ratio of the data packets delivered to the destination. Throughput it is defined as the total amount of data a receiver R actually receives from all the senders of the multicast group divided by the time it takes for R to receive the last packet. End - to- End Delay this represents the average time it takes for a data packet to be transmitted from one forwarding node to another. Latency this represents the average time a data packet takes to travel from the transmitter to the receiver.

V. SIMULATION

The selected protocols are evaluated using Network simulator (NS-2) of 50-200 nodes incrementing by 50 nodes. Simulation runs for 100 seconds. The mobility model is selected as Random Way Point model. In this mobility model a node randomly selects a destination and it moves in the direction of the destination with a speed uniformly chosen between the minimal speed and maximal speed. After it reaches the destination, the node stays there for a pause time and then moves again. Each node moves randomly with a speed of 0-10 m/s and stays at the same place with a pause time 0-10s. The Distributed Coordinated Function (DCF) of IEEE 802.11 for wireless LANs is assumed as the MAC layer protocol. The Two Ray Ground model is selected for the propagation. A bandwidth of 2Mbps with a radio range of 250m is considered. 5 senders and 20 receivers were selected at random and the traffic senders send data packets of size 1460 Bytes each with a data rate of 10 packets/sec. we have chosen CBR as the type of communication and the maximum interface queue length is 250. The performance metrics considered are Throughput, Average End-to-End delay, Packet Delivery Ratio.

VI. SIMULATION RESULTS

Simulation results of ODMR and PUMA protocol for varying the node mobility and their group sizes.

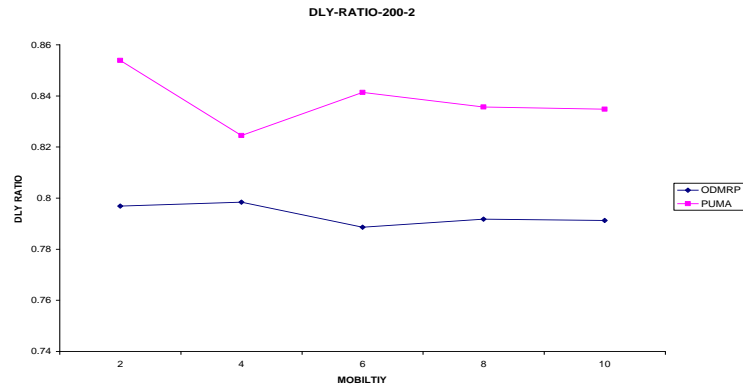


Fig 4. Packet delivery Ratio for 200 nodes and their group size is two

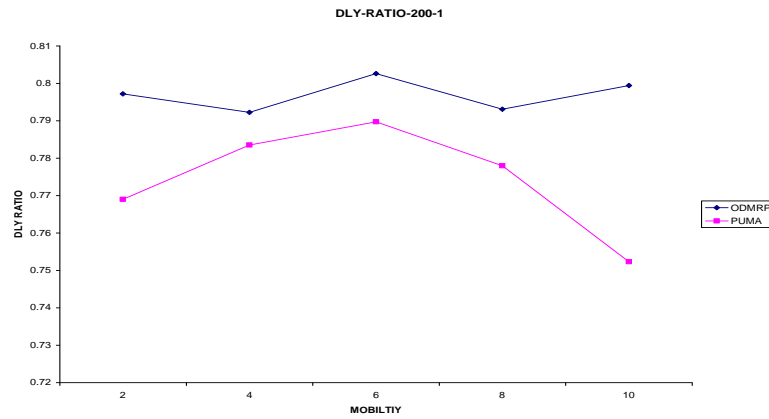


Fig 5. Packet delivery Ratio for 200 nodes and their group size is one

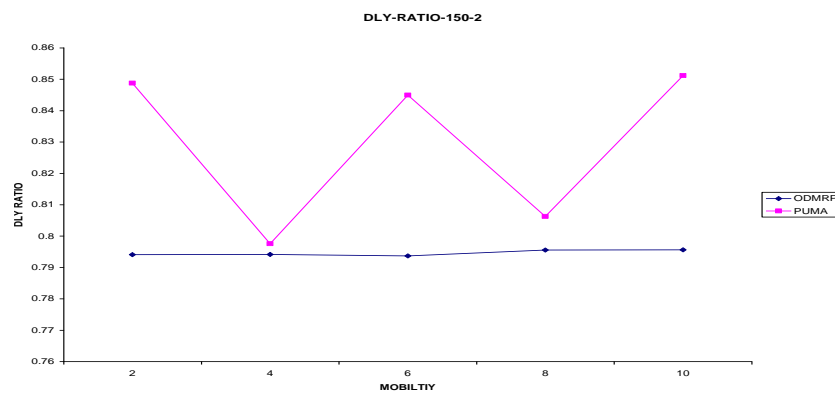


Fig 6. Packet delivery Ratio for 150 nodes and their group size is two

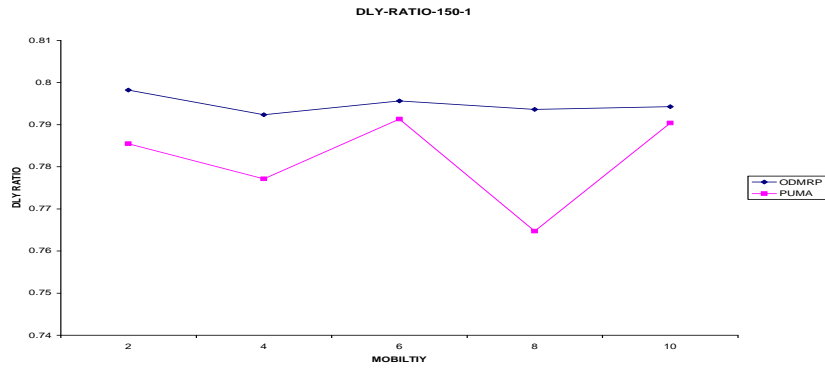


Fig 7. Packet delivery Ratio for 150 nodes and their group size is one

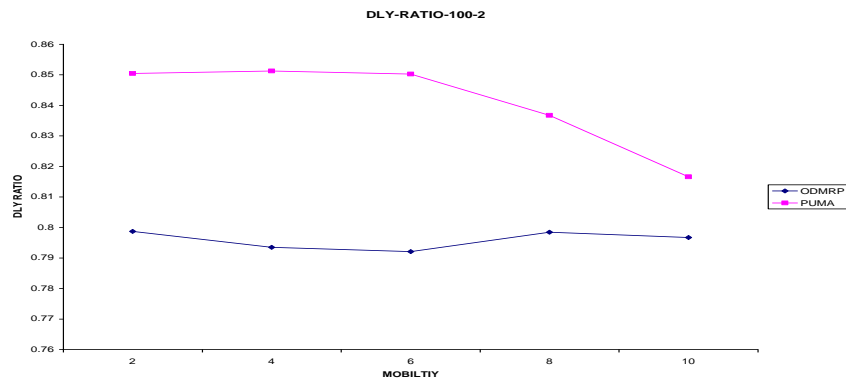


Fig 8. Packet delivery Ratio for 100 nodes and their group size is two

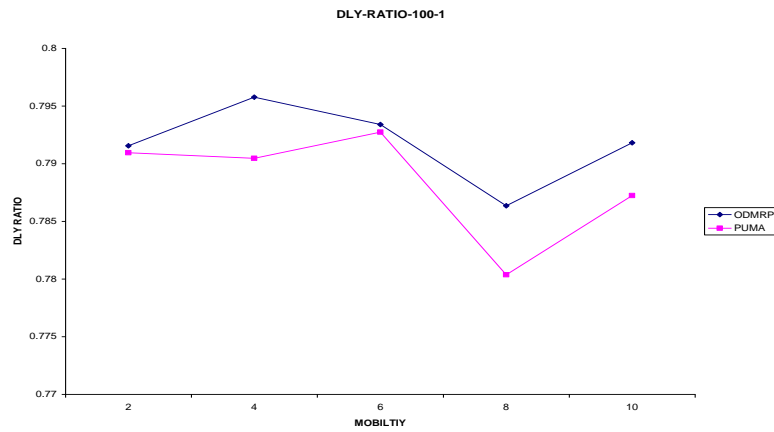


Fig 9. Packet delivery Ratio for 100 nodes and their group size is one

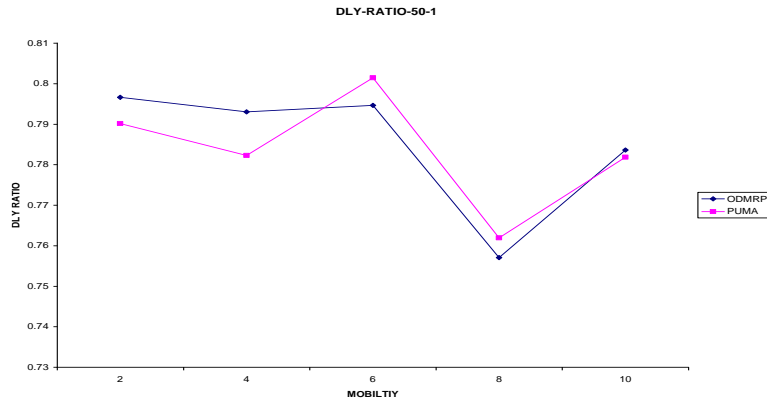


Fig 10. Packet delivery Ratio for 50 nodes and their group size is one

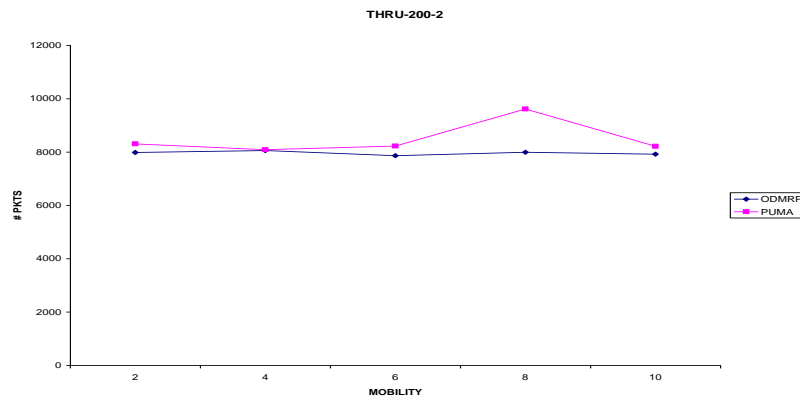


Fig 11. Throughput for 200 nodes and their group size is two

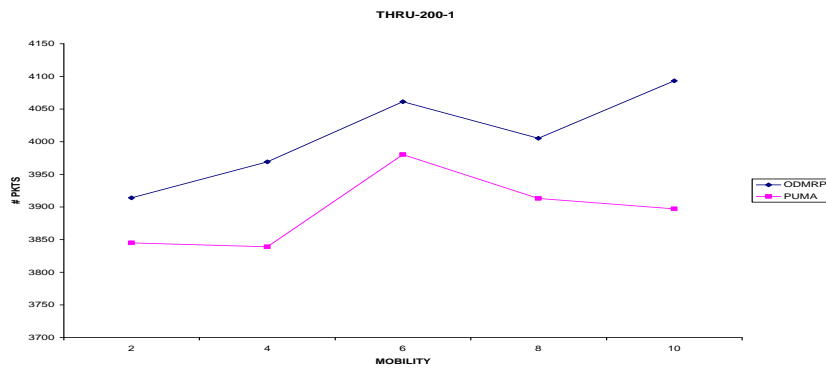


Fig 12. Throughput for 200 nodes and their group size is one

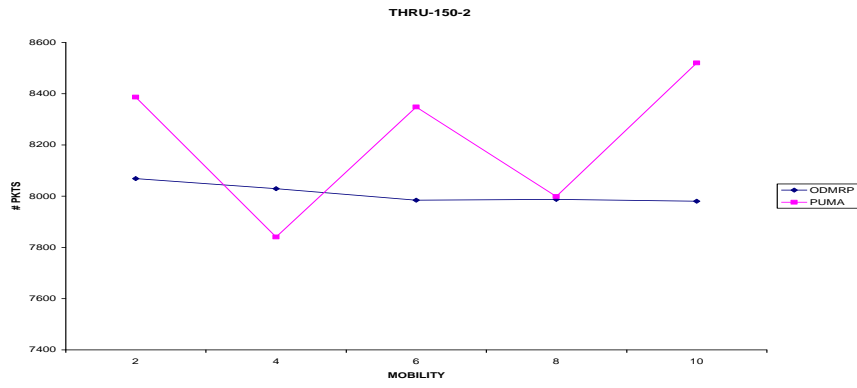


Fig 13. Throughput for 150 nodes and their group size is two

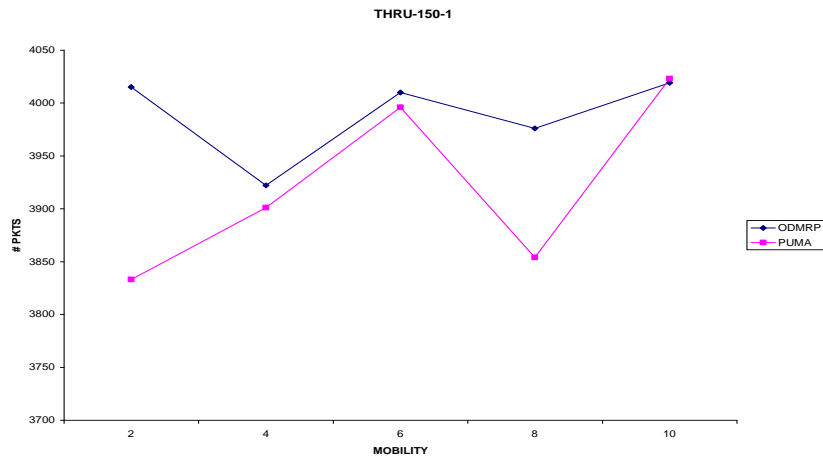


Fig 14. Throughput for 150 nodes and their group size is one

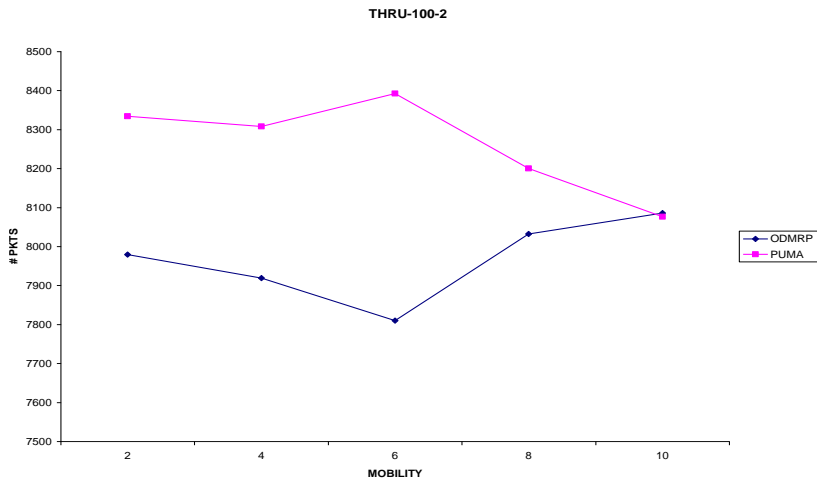


Fig 15. Throughput for 100 nodes and their group size is two

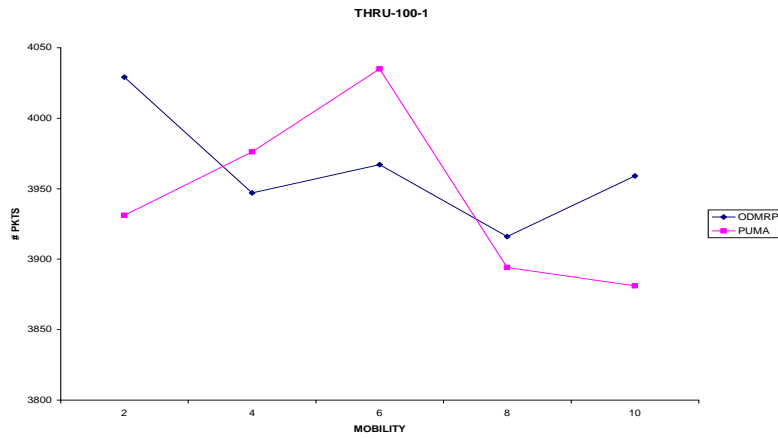


Fig 16. Throughput for 100 nodes and their group size is one

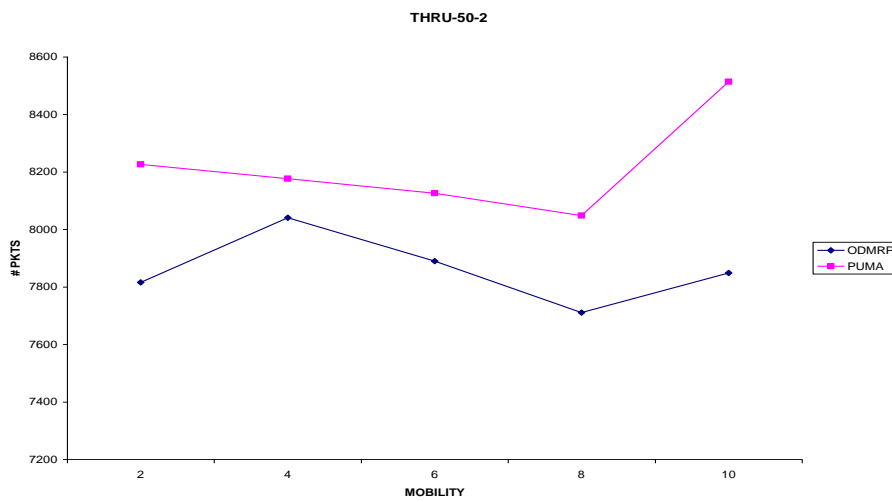


Fig 12. Throughput for 50 nodes and their group size is two

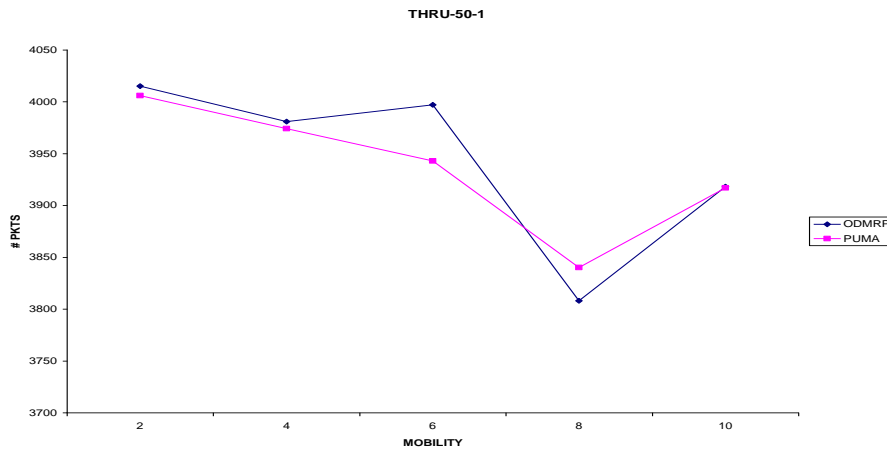


Fig 12. Throughput for 50 nodes and their group size is one

VII. CONCLUSIONS

This paper proposes the comparison of ODMR and PUMA protocol. As per the simulation results PUMA improves the

performance of ODMR. PUMA improves the throughput, packet delivery ratio by varying the node mobility and their group sizes.

REFERENCES

- [1] G. Santhi and Dr. A. Nachiappan , “Agent Based Adaptive Multicast Routing with QoS guarantees in MANETs”, 2010 Second International conference on Computing, Communication and Networking Technologies.
- [2] S. J. Lee, W. Su, and M. Gerla, “On-demand multicast routing protocol in multihop wireless mobile networks,” *ACM/Kluwer Mobile Networks and Applications*, Vol. 7, No. 6, 2002, pp. 441–453.
- [3] H. Chen, B. L. Sun, and Y. Zeng, “QoS Multicast Routing Algorithm in MANET: An Entropy-Based GA,” *Lecture Notes in Artificial Intelligence*, Vol. 4114, Springer Verlag, 2006, pp. 1279–1289.
- [4] C. R. Lin, “On-demand QoS Routing in Multihop Mobile Networks,” In: *Proceedings of IEEE INFOCOM 2001*, April 2001, pp. 1735–1744.
- [5] The Network Simulator NS-2: <http://www.isi.edu/ns-nam/ns/>.
- [6] Ravindra Vaishampayan, J.J. Garcia-Luna-Aceves
“Efficient and Robust Multicast Routing in Mobile Ad Hoc Networks”, 2004 IEEE International Conference on Mobile Ad-hoc and Sensor Systems.
- [7] R. Pedman, “An algorithm for distributed computation of a spanning tree in an extended lan:” in *ACM Special Interest Group on Data Communication (SIGCOMM)*. 1985, pp. -53.
- [8] S.-J. Lee, W. Su, J. Hsu, M. Gerla and R. Bagrodia. A Performance Comparison Study of Ad-Hoc Wireless Multicast Protocols. In *Proceedings of IEEE INFOCOM 2000*, pages 565–574, March 2000.
- [9] Qi Xue, Aura Ganz, Ad Hoc QoS On-demand Routing (AQOR) In Mobile Ad Hoc Networks, *Journal of Parallel and Distributed Computing*, Volume 63, Issue 2, February 2003, pp.: 154-165.
- [10] S. Corson, J. Macker, Mobile Ad hoc Networking (MANET): Routing Protocol Performance Issues and Evaluation Considerations, RFC2501.
- [11] G.I. Ivascu, S.Pierre and A. Quintero, QoS Support based on a Mobile Routing Backbone for Ad Hoc Wireless Networks, *IWCMC’06*, July 3-6, 2006, Vancouver, Canada, pp.: 121-126.

Characterization of Dynamic Bayesian Network

The Dynamic Bayesian Network as temporal network

Nabil Ghanmi
National School of Engineer of
Sousse
Sousse - Tunisia

Mohamed Ali Mahjoub
Preparatory Institute of Engineer of
Monastir
Monastir - Tunisia

Najoua Essoukri Ben Amara
National School of Engineer of
Sousse
Sousse - Tunisia

Abstract— In this report, we will be interested at Dynamic Bayesian Network (DBNs) as a model that tries to incorporate temporal dimension with uncertainty. We start with basics of DBN where we especially focus in Inference and Learning concepts and algorithms. Then we will present different levels and methods of creating DBNs as well as approaches of incorporating temporal dimension in static Bayesian network.

Keywords- DBN; DAG; Inference; Learning; HMM; EM Algorithm; SEM; MLE; coupled HMMs.

I. INTRODUCTION

The majority of events encountered in everyday life are not well described based on their occurrence at a particular point in time but rather they are described by a set of observations that can produce a comprehensive final event. Thus, time is an important dimension to take into account in reasoning and in the field of artificial intelligence in general. To add the time dimension in Bayesian networks, different approaches have been proposed. The common names used to describe this new dimension are "temporal" and "dynamic".

II. BASICS

A. Definition

Bayesian networks represent a set of variables in the form of nodes on a directed acyclic graph. It maps the conditional independencies of these variables. They bring us four advantages as a data modeling tool [16,17,18]

A dynamic Bayesian network can be defined as a repetition of conventional networks in which we add a causal one time step to another. Each Network contains a number of random variables representing observations and hidden states of the process.

We consider a dynamic Bayesian network composed of a sequence of T hidden state variables (a hidden state of a DBN is represented by a set of hidden state variables) and a sequence of T observable variables where T is time limit of the studied process.

In order that the specification of this network is complete, we need to define the following parameters:

- The transition probability between states $P(x_t/x_{t-1})$

- The conditional probability of hidden states knowing observation $P(y_t/x_t)$
- The probability of the initial state $P(x_1)$

The first two parameters must be determined for each time $t = 1, \dots, T$. These parameters can be invariant or not over time.

B. Inference

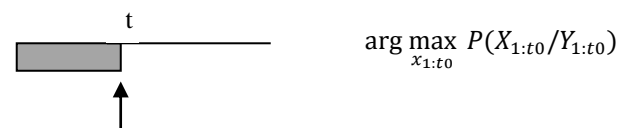
The general problem of inference for DBNs is to calculate $P(X_{t_0}^i/Y_{t_1:t_2})$ where $X_{t_0}^i$ is the i^{th} hidden variable at time t_0 and $Y_{t_1:t_2}$ represents all observations between times t_1 and t_2 .

There are several interesting cases of inference, they are illustrated below. The arrow indicates t_0 : that we try to estimate. Shaded regions correspond to observations between t_1 and t_2

Filtering: this is to estimate the belief state at time t_0 knowing all the observations until this moment:



Decoding (Viterbi): decoding problem is to determine the most likely sequence of hidden states knowing the observations up to time t_0 :



Prediction: This is to estimate a future observation or state knowing the observations up to the current time t_0



Smoothing (offline): is to estimate a past state knowing the observations up to the current time T



There are several algorithms for inference in Dynamic Bayesian Networks. We can classify these algorithms according to their accuracy, in two broad classes:

A. Exact Inference:

1) Forward-Backward Algorithm:

The algorithm proceeds in two steps:

- a) *Forward step: forward propagation of probabilities*
- b) *Backward step: backward propagation of probabilities*

FORWARD ALGORITHM:

We consider a dynamic Bayesian network B. We wish to calculate the probability $P(Y_{1:T})$ of occurrence of the sequence of observation $Y_{1:T}$. This probability is:

$$P(Y_{1:T}) = \sum_{\text{possible paths}} \left[\left(\prod_{t=1}^{T-1} P(x_{t+1}/x_t) P(y_{t+1}/x_t) \right) P(x_{T+1}/x_T) \right] \quad (1)$$

Applying directly this formula, the computation time is $O(TN^2)$. For this, we consider the forward variable defined by:

$$\alpha_t(x_t) = P(Y_{1:t}, x_t) \quad (2)$$

which expresses the probability of observing the sequence $Y_{1:t}$ while lying in state x_t . This variable can be computed inductively:

Initialisation :

$$\alpha_1(x_1) = P(x_1)$$

Induction :

$$\alpha_{t+1}(x_{t+1}) = P(y_{t+1}/x_{t+1}) \left(\sum_{x_t} P(x_{t+1}/x_t) \alpha_t(x_t) \right) \quad (3)$$

Thus, we can calculate $\alpha_T(x_T) = P(Y_{1:T}, x_T)$, this naturally leads us to:

$$P(Y_{1:T}) = \frac{\alpha_T(x_T)}{\sum_{x_t} \alpha_t(x_t)} \quad (4)$$

BACKWARD ALGORITHM:

It is also possible to perform the calculation in reverse, using the backward algorithm.

For this, we define the backward variable as follows:

$$\beta_t(x_t) = P(Y_{t+1:T}/x_t) \quad (5)$$

This variable expresses the conditional probability of observation from time t +1 until the last observation time T, given the values of the hidden states at time t. Its calculation follows the following procedure:

Initialisation :

$$\beta_T(x_T) = 1$$

Induction :

$$\beta_{t-1}(x_{t-1}) = \sum_{x_t} P(x_t/x_{t-1}) \cdot P(y_t/x_t) \cdot \beta_t(x_t) \quad (6)$$

Thus, we can calculate the expected probability:

$$P(Y_{1:T}) = \sum_{x_1} \beta_1(x_1) \cdot P(y_1/x_1). \quad (7)$$

The complexity of this algorithm is, as the forward algorithm in $O(TN^2)$.

From these two factors (forward and backward) propagation probabilities, we can explore other terms that are useful for inference and learning of Dynamic Bayesian networks:

- **Smoothing:** this is to calculate $P(x_t/Y_{1:T})$ where $t < T$. From equations (4) and (6), we can determine the following equation:

$$\gamma_t = P(x_t/Y_{1:T}) = \frac{\alpha_t(x_t)\beta_t(x_t)}{\sum_{x_t} \alpha_t(x_t)\beta_t(x_t)} \quad (8)$$

γ_t is called smoothing operator. We can also derive higher order smoothing equations. For example, a smoothing of the first order is defined as follows:

$$\begin{aligned} \xi_{k,k-1}(x_t, x_{t-1}) &= P(x_t, x_{t-1}/Y_{1:T}) \\ &= \frac{\alpha_{t-1}(x_{t-1})P(x_t, x_{t-1})P(y_t/x_t)\beta_t(x_t)}{\sum_{x_t} \alpha_t(x_t)\beta_t(x_t)} \end{aligned} \quad (9)$$

These terms may be used to easily calculate the probabilities of hidden states from the neighboring nodes.

- **Prediction:** this is to calculate $P(x_{t+1}/Y_{1:t})$ et $P(y_{t+1}/Y_{1:T})$. We can easily determine:

$$P(x_{t+1}/Y_{1:t}) = \frac{\sum_{x_t} P(x_{t+1}/x_t) \alpha_t(x_t)}{\sum_{x_t} \alpha_t(x_t)} \quad (10)$$

Similarly, one can determine:

$$P(y_{t+1}/Y_{1:t}) = \frac{\sum_{x_{t+1}} \alpha_{t+1}(x_{t+1})}{\sum_{x_t} \alpha_t(x_t)} \quad (11)$$

- **Decoding :** is to determine the sequence of hidden states $\hat{X}_{1:T}$ such as :

$$\hat{X}_{1:T} = \arg \max_{X_{1:T}} P(X_{1:T}/Y_{1:T}) \quad (12)$$

This task can be solved using the dynamic programming algorithm of Viterbi. We can start with the following equation:

$$\delta_{t+1}(x_{t+1}) = \max_{X_{1:t}} P(X_{1:t+1}/Y_{1:t+1}) \quad (13)$$

Considering the topology of the DBN, we can deduce:

$$\begin{aligned} \delta_{t+1}(x_{t+1}) &= P(y_{t+1}/x_{t+1}) \max_{x_t} \left[P(x_{t+1}/x_t) \max_{x_{1:t-1}} P(X_{1:t}/Y_{1:t}) \right] \\ &= P(y_{t+1}/x_{t+1}) \max_{x_t} [P(x_{t+1}/x_t) \delta_t(x_t)] \end{aligned} \quad (14)$$

We can now easily deduce that:

$$\max_{x_{1:T-1}} P(X_{1:T-1}/Y_{1:T-1}) = \max_{x_{T-1}} \delta_{T-1}(x_{T-1}) \quad (15)$$

To find $\hat{X}_{1:T}$, we must introduce the argument x_t that maximizes $\delta_{t+1}(x_{t+1})$ as follows:

$$\psi_{t+1}(x_{t+1}) = \arg \max_{x_t} [P(x_{t+1}/x_t) + \delta_t(x_t)] \quad (16)$$

And we have:

$$\hat{x}_t = \psi_{t+1}(\hat{x}_{t+1}) \quad (17)$$

Note that if we want to use the Viterbi algorithm to decode the sequence of hidden states, we must have a complete observation y_1, \dots, y_T . If the number of observations is not sufficient, a less optimal solution known as the truncated Viterbi algorithm can be used.

2) Junction Tree Algorithm:

The Junction Tree Algorithm [1] is an algorithm similar to the Baum-Welch algorithm used in HMM. It involves transforming the original network into a new structure called junction tree and apply a type inference algorithm used for static Bayesian networks. This tree is obtained by following these steps:

- **Moralization:** connecting parents and eliminating directions.
- **Triangularization:** selectively adding arcs to the graph morale (not to have cycles of order 4 or more).
- **Junction Tree** : is obtained from the triangulated graph by connecting the cliques such that all cliques on the path between two cliques X and Y contain $X \cap Y$

B. Approximate inference:

When the dimension of Bayesian networks increases, the computing time is increasingly important. When the conditional probability tables are derived from data (learning), these tables are not accurate. In this case it is not worth wasting time by making exact inference on probabilities not precise, hence the use of approximate inference methods. Among the approximate inference methods that often work well in practice, we give:

1) Variational methods

The simplest example is the approximation by the average (mean-field approximation) [2], which exploits the law of large numbers to approximate large sums of random variables by their average. The approximation by the average product of a lower probability. There are other, more stringent, resulting in a lower and upper.

2) Monte Carlo

The easiest Monte Carlo Method [3] is the Importance Sampling (IS) that produces a large number of samples x from $P(X)$ the unconditional distribution of hidden variables) then we give weight to samples based on their likelihood $P(Y/X)$ (where y is the observation). This forms the basis of Particulate Filter which is simply the Importance Sampling adapted to a dynamic Bayesian network.

3) Loopy Belief propagation

We apply the algorithm of Pearl [4] to the original graph even if it contains loops. In theory, one runs the risk of double counting certain words but it was shown that in some cases (for example, a single loop), events are counted twice and thus cancel out fairly between them to give the correct answer .

4) Learning:

Learning is to estimate the probability tables and conditional distributions CPTs CPDS. This task is based on the EM algorithm (Expectation Maximization) algorithm or the GEM (General Expectation Maximization) for DBNs.

Let M be a Dynamic Bayesian network with parameter θ , learning aims to determine $\hat{\theta}$ such the posterior probability of the observations is maximal, then either:

$$\hat{\theta} = \arg \max_{\theta} [P(Y, X/\theta)] \quad (18)$$

EM Algorithm: This algorithm includes:

- an evaluation step of expectation (E), which calculates the expectation of the likelihood taking into account the recent observed variables,
- a maximization step (M), where an estimated maximum likelihood parameters by maximizing the likelihood found in step E.

C. Pruning

This task is based on the possibility of change in time, of RBD's structure. This is usually omitted for its complexity. Pruning the network consists in perform one of the following operations:

- a) Delete one or more states of a given node
- b) Remove a connection between two nodes
- c) Remove one or more network nodes

This can be exact (lossless) or approximate

III. DIFFERENT LEVELS OF CREATING DBN

To describe a dynamic Bayesian network, we must specify its topology (the graph structure) as well as all the tables of conditional probability distribution. You can learn them both (the graph and distributions) from experimental data.

However, it is more difficult to learn a structure to learn its parameters.

It is possible that some nodes are hidden during the experiments (values that we can't observe), or missing data. In this case, learning becomes more complicated settings. From these considerations, there are 4 possible cases of learning [5]:

TABLE I. METHODS OF DETERMINATION OF DBN STRUCTURE AND PARAMETERS

Structure	Observability	Method
Known	Full	Simple statistics : MLE
Known	Partial	EM or Gradient Ascent Algorithm
Unknown	Full	Search through model space
Unknown	Partial	Structural EM

A. Known structure /Full observability

The DBN's structure is known, it remains to estimate the parameters of the network using the method of maximum likelihood estimation. We look for parameters θ describing the model assumptions that maximize the likelihood of observations Y :

$$l(Y, \theta) = P(Y/\theta) \quad (19)$$

In general, it instead uses the log likelihood (log-likelihood)

$$L(Y, \theta) = \log(P(Y/\theta)) \quad (20)$$

B. Known structure /Partial observability

When certain variables are not observable, the likelihood surface becomes multimodal and we must use iterative methods such as EM or gradient increasing to find local maxima of the function ML / MAP. The principle of the EM algorithm is to associate a problem with an incomplete data problem for which complete data for a simple solution exists for the maximum likelihood estimate. This procedure needs to use an inference algorithm to compute the parameters for each node. These algorithms are explained in section II.3

C. Unknown structure / Full observability

There are several techniques for learning DBN structure from observed data. These techniques help to create the network structure by adding or deleting edges between any two nodes or reversing the direction of an existing arc. These changes must be made in order to maintain and acyclic directed graph.

To accomplish the task of structural learning, we need [6]:

- an algorithm to find the different possible structures
- a metric for comparing the possible structures to each other

The structure learning algorithms can be classified into two broad categories.

- The first class of algorithms using heuristic search methods to construct the graph and evaluates it using scores (scoring methods). This procedure is repeated until the improvement between two consecutive models is not significant.
- The second class of algorithms to create the network structure by analyzing the independence relations between nodes. These independence relations are measured using several types of tests of conditional independence (eg mutual information between two nodes can be considered as a criterion for conditional independence)

According to Cheng et al. [7], when comparing the two types of algorithms, we can conclude that the first class of algorithms are faster than the second if the network is densely connected, but can't find the best solution for most models corresponding to real processes of the heuristic nature of these algorithms. The second class of algorithms can produce, under some assumptions, an optimal or near optimal solution especially when the data are not numerous.

D. Unknown Structure /Partial Observability

The EM algorithm is developed to make learning network settings, so it must be adjusted to perform structural learning from incomplete data. The structural EM (SEM) is one of the most popular techniques that are developed for this purpose. SEM has the same E-step EM algorithm for completing the data using observations and the current structure of the network. The M-step involves two parts: In the first, it recalculates as already explained, the maximum likelihood to determine the parameters. In the second part, it uses these parameters to evaluate any other candidate structure similar to the current structure.

IV. DIFFERENT APPROACHES FOR INCORPORATING TIME IN BAYESIAN NETWORK

Dynamic Bayesian Networks (DBN) are an extension of Bayesian networks that represent the temporal or spatial evolution of random variables. There are several models for incorporating time into network representation. These models can be classified into three broad categories:

- Models that use static BNs and formal grammars to represent the temporal dimension (temporal probabilistic networks (TPNs))
- Models that use a mixture of several probabilistic frameworks
- Models that use temporal nodes in the static BNs to represent temporal dependencies

The first two models are developed for specific objectives and have a very limited use. We will therefore focus on the third model.

A. Probabilistic Temporal Networks (PTN)

1) Definition

A probabilistic temporal network (PTN) is defined as a model, representing the time information while fully embracing probabilistic semantics. In a PTN, the nodes of the

graph are the temporal aggregates and the arcs are causal and / or temporal relations

This type of network uses grammatical rules to express temporal dependencies in the structure of Bayesian networks: The conservation of the structure of static Bayesian networks allow reuse of powerful techniques for inference of BNs this specific type of networks. Grammar introduce temporal relations between events

2) Temporal Reasoning

In PTN, temporal reasoning is based on interval algebra [8] which was introduced by James F. Allen in 1983. This is a calculation that defines the possible relationships between time intervals and provides a table of composition that can be used as a basis for reasoning on descriptions of temporal events.

The 13 following basic relations capture possible relationships between two intervals are illustrated in the following table:

TABLE II. ALLEN'S INTERVAL ALGEBRA

Relation	Illustration	Interprétation
X < Y Y > X		X Precede Y
X m Y Y mi X		X meets Y
X o Y Y oi X		Overlaps X by Y
X s Y Y si X		X starts Y
X d Y Y di X		X during Y
X f Y Y fi X		X finishes Y
X = Y		X is equal to Y

B. DBN as a mixture of several probabilistic structures

Dynamic Bayesian networks generalize hidden Markov models (HMM) and linear dynamical systems (LDS) by representing the hidden states (and seen) as state variables, with complex interdependencies. The HMMs are used to represent discrete states and the LDS are used to represent states (variables) continuous. The combination of these two structures to create a mixed-state DBN. This type of model

was introduced and applied to the recognition of human gestures [9]

C. Pure Probabilistic DBN

In this section we consider a DBN as a graph whose nodes represent states and arcs represent conditional dependencies (causal) between states of a band as well as temporal dependencies between the states belonging to two consecutive time slices

1) Extension of BNs toward DBNs

A static Bayesian network can be extended in many ways to represent temporal process. These extensions can be classified into five categories:

- 1- Adding the history of a node to explicitly express the temporal aspect in the Bayesian network.
- 2- Select from a library of pre-developed Bayesian network, the RB appropriate to the current state.
- 3- Changing dynamics of the network structure.
- 4- Repeat the traditional network for each time step by introducing Bayesian networks to represent events.
- 5- Repeat the classical Bayesian network by adding arcs representing the time dependencies of a time slice to another.

The networks of the first category may be regarded as mere static BNs which is added an additional node to represent past information in time. The second class of Bayesian networks is the object of an idea that has been used in early work on DBNs by Singhal et al. They use a bunch of BNs (COBRA) developed locally and every time the system selects the Bayesian network corresponding to its beliefs about the current state of real objects studied, hence the dynamic (temporal) aspect of this class

We will describe in more detail, the three other types of extension of BNs to the DBN:

2) Dynamic change in the structure of DBNs

Changes in the structure of a DBN can be:

- Changing network settings (values of the table of conditional probabilities CPT) of a time slice to another
- Adding or deleting new nodes and / or arcs to the structure of BN.

The structural changes of a DBN (addition or deletion of edges or nodes) is a complex problem and can not be generalized easily. In the following, we are interested in changing parameters (CPT) system.

In [10] Zweig and Russell presented a model that uses decomposition techniques to represent dynamic situations real. These dynamic processes can be decomposed into several sequences. Such decomposition can be used in speech recognition or recognition of manuscripts. They found it more suitable to represent dynamic processes (temporal) creating a RB (a subnet) at each stage in the evolution of the process to model the whole process by a single BN. Each sub-network must be learned from observations at the appropriate time.

3) DBNs for events representation

In such networks, we use information obtained from states belonging to two consecutive time slots in order to deduce the events that took place between the two points of time. Structure of these networks is presented in the following diagram:

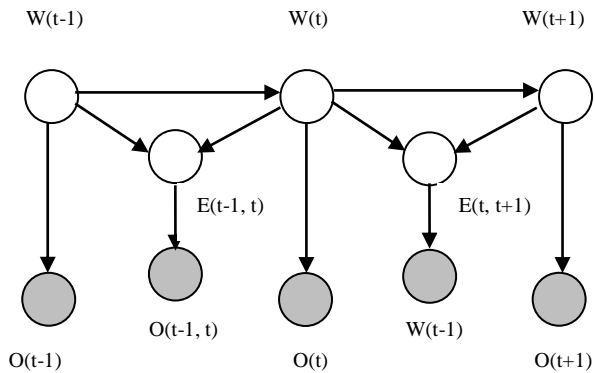


Figure 1. General structure of a dynamic belief network

In such networks, there are three types of nodes W, O and E which represent respectively:

- The random variables (corresponding to states of the real process)
- Observations
- Events

Dynamic Bayesian networks are a repetition of the traditional network in which we add a causal link (representing the time dependencies) of a time step to another. The network topology is the same for the different time slots. Arcs and probabilities that form these models have the same interpretations as for a statistical system based on a classic SNL. Thus, a DBN is completely defined by giving the couple (B_1, B_2) , with:

- B_1 is a BN which defines the a priori probability $P(X_1)$ (initial state)
- B_2 is the temporal Bayesian Network with two time slices (2TBN: two-slice Temporal Bayes Net) which defines $P(X_t, X_{t-1})$ using a directed acyclic graph DAG as follows:

$$P(X_t/X_{t-1}) = \prod_{i=1}^N P(X_t^i/C(X_t^i))$$

Where X_t^i represent le i^{th} node at time t and $C(X_t^i)$ is the parent of X_t^i in the graph.

V. FROM HMMs TO DBNs

The main difference between the HMM and dynamic Bayesian networks is that in an RBD the hidden states are represented as distributed by a set of random variables $(X_t^1, X_t^2, \dots, X_t^n)$. Thus, in an HMM, the state space consists of a single random variable X_t .

Figure 2 shows a HMM represented in its graphical form with a dynamic Bayesian network. The gray nodes represent observed nodes and nodes in white are the hidden nodes.

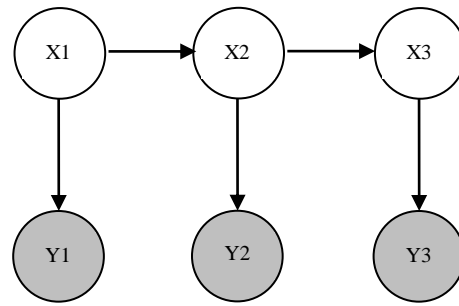


Figure 2. HMM represented as an instance of RBD unrolled over three time steps

In Figure 2, following the notations used in the literature on the HMM, the node X_1 represents the initial state π with $\pi(i) = p(X_1 = i)$. The transition matrix is represented by tables of transition probabilities between nodes X_t et X_{t+1} with

$$A(i, j) = P(X_t = j/X_{t-1} = i)$$

Finally, the observation matrix is found in probability tables between nodes X_t and Y_t with

$$B(i, j) = P(Y_t = j/X_t = i)$$

Thus, the specification of an HMM as a dynamic Bayesian network is simply given by the probability tables for $P(X_1)$, $P(X_t/X_{t-1})$ et $P(Y_t/X_t)$. Assuming that the model is invariant over time (transition matrix and observation are fixed over time) then the giving of $P(X_1)$, $P(X_2/X_1)$ et $P(Y_1/X_1)$ are sufficient.

The major advantage of dynamic Bayesian networks over HMM is that it is very easy to create alternatives to HMM simply giving another structure more or less complex DBN. The formalism and algorithms remain the same [11]. If you change the tables of probability distributions (discrete tables) by continuous distributions (eg Gaussian), then it also becomes possible to represent models based on Kalman filters [12]. It is also possible to combine these different models simply by hanging them DBN and thus provide more complex models.

VI. REPRESENTATION OF HMMs AS DBNs

There are several variants of HMM, which were proposed in response to specific classes of problems and to overcome limitations in traditional HMMs.

In this section, we will present the variations of the most widely used HMM (shown in Figure 3). The coupled HMM (Figure 3 (a)) is probably the most natural structure, which can process, simultaneously and with good efficiency, multiple data streams from the same observations. For this, we will briefly introduce other representations and will be presented in more detail the coupled HMMs in the next section.

Figure 4 (b) is a specific coupling of HMM described in [13] as an event coupled HMM. The motivation for this representation is to model a class of loosely coupled time series where only the occurrence of events are coupled in time.

The representation of events coupled with HMMs is obviously limited by its narrow structure and this structure is for a very specific class of applications.

Input / Output HMM (Figure 4 (c)) [15] represents a promising alternative to the use of a hidden Markov model. This variant allows to map an input sequence and output sequence. The main difference with traditional HMMs is indeed the first is the distribution $P(y_1^T)$ of the output sequence $y_1^T = \{y_1, y_2, \dots, y_T\}$ when the second shows the distribution conditional $P(y_1^T / u_1^T)$ of the output sequence given an input sequence $u_1^T = \{u_1, u_2, \dots, u_T\}$. This allows for spot monitoring or recognition of sequences online. The inputs and outputs can be discrete or continuous, scalar or vector.

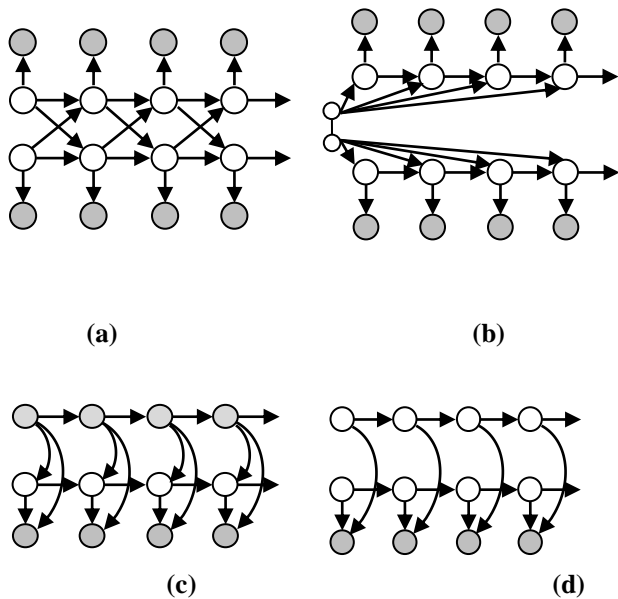


Figure 3: different variants of HMM: The empty circles represent the hidden states and the gray circles represent the observations (slightly gray circles in Figure (d) represent the input nodes). (a) coupled HMMs, (b) event coupled HMM, (c) factorial HMM, (d) input-output HMM.

The factorial HMM (Figure 3 (d)) [14] is a model used to represent systems in which the hidden states are made from a set of decoupled dynamical systems and with only one observation available.

VII. COUPLED HMM

A. Definition

In a coupled HMM, each hidden variable (state) is connected to his own observation. It is also connected to its two nearest neighbors in the time slice with the exception of the following variables belonging to chains border, each with a single nearest neighbor (see Figure 4).

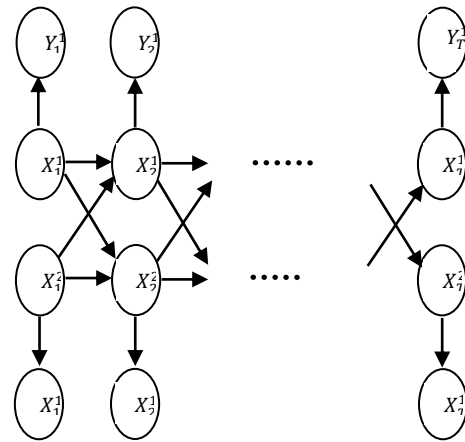


Figure 4. Coupling of two HMMs

B. Parameters of coupled HMMs

Let a CHMM model formed with L coupled HMMs. This model is fully described giving the following parameters:

- initial probabilities:

$$\pi = \{\pi_j^{(l)}\}, \quad 1 \leq l \leq L, \quad 1 \leq j \leq N^{(l)}$$

$N^{(l)}$ is the number of states (hidden nodes) of the chain l

- Transition probabilities:

$$A = \{a_{ij}^{(l,l')}\}, \quad 1 \leq l, l' \leq L, \quad 1 \leq i \leq N^{(l)}, 1 \leq j \leq N^{(l')}$$

$$\sum_{j=1}^{N^{(l')}} a_{ij}^{(l,l')} = 1$$

- Probability of observation

$$B = \{b_j^{(l)}(k)\}, \quad 1 \leq l \leq L, \quad 1 \leq j \leq N^{(l)}, \quad 1 \leq k \leq M$$

$$\sum_{j=1}^{N^{(l)}} b_j^{(l)}(l) = 1$$

C. Extension of the forward-backward algorithm for CHMM:

In the same way as for traditional HMMs, we use the Forward-backward algorithm to calculate $P(O / \lambda)$ in the case of L coupled HMMs. There, in this case each observation o_t is a vector $(o_t^1, o_t^2, \dots, o_t^L)$. Since L HMMs are coupled, the variables forward and backward should be defined jointly for all HMMs. In other words, we define the forward variable α_t as follows:

$$\alpha_t(j_1, j_2, \dots, j_L) = P(o_1, o_2, \dots, o_t, S_{t,j_1}, S_{t,j_2}, \dots, S_{t,j_L} / \lambda)$$

And the backward variable β_t as follows:

$$\beta_t(j_1, j_2, \dots, j_L) = P(o_{t+1}, \dots, o_T / S_{t,j_1}, S_{t,j_2}, \dots, S_{t,j_L}, \lambda)$$

Therefore, we can calculate inductively the two variables as follows:

$$\alpha_t(j_1, j_2, \dots, j_L) = \begin{cases} \prod_l \pi_{j_l}^{(l)} \cdot b_{j_l}^{(l)}(o_1^l), & t = 1 \\ \sum_{i_1, i_2, \dots, i_L} \left(\alpha_{t-1}(i_1, i_2, \dots, i_L) \prod_l b_{j_l}^{(l)}(o_t^l) \cdot \sum_{i_l'} a_{i_l' j_l}^{(l, t)} \right), & t > 1 \end{cases}$$

$$\beta_t(i_1, i_2, \dots, i_L) = \begin{cases} 1, & t = T \\ \sum_{j_1, j_2, \dots, j_L} \left(\beta_{t+1}(j_1, j_2, \dots, j_L) \prod_l b_{j_l}^{(l)}(o_{t+1}^l) \cdot \sum_{i_l'} a_{i_l' j_l}^{(l, t)} \right), & t < T \end{cases}$$

And the likelihood function $P(O / \lambda)$ can be calculated as follows:

$$P(O / \lambda) = \sum_{j_1, j_2, \dots, j_L} \alpha_T(j_1, j_2, \dots, j_L)$$

D. EM algorithm for learning parameters of CHMM

As in the case of traditional HMMs, the two basic steps of the EM algorithm as described in [3] are:

- Estimation step:

Given the observations O , the parameters to estimate λ and the objective function $L(\lambda; O, S)$, we construct an auxiliary function:

$$Q(\lambda; \hat{\lambda}) = E_s [L(\lambda; O, S) / O, \hat{\lambda}]$$

that represents the expectation of the objective function of all sequences of possible states, given the observations O and the current parameters estimated

- Maximization step:

In the exact EM algorithm, the role of this step is to estimate the new parameters $\hat{\lambda}_{new}$ as follows:

$$\hat{\lambda}_{new} = \arg \max_{\lambda} Q(\lambda; \hat{\lambda})$$

VIII. MOTIVATION OF USING CHMM

According to its definition, a coupled HMM can be viewed as a collection of HMMs, one for each data stream, where the

discrete nodes at time t for each HMM are conditioned by the discrete nodes at time $t-1$ of all HMMs linked.

The characteristics of handwritten characters can perform a joint analysis of the image of a character according to the two preferred directions: vertical ("column") and horizontal ("lines"). So we will use the coupled HMM (CHMM) to couple two HMMs: one can handle comments on the columns and the second will be used to handle comments on the lines

IX. REFERENCES

- [1] ZWEIG G., Speech Recognition with Dynamic Bayesian networks, Bayesian networks, PhD thesis, University of California, Berkeley, 1998.
- [2] N. Lawrence. Variational Inference in Probabilistic Models. PhD thesis, University of Cambridge, U.K., 2000.
- [3] W. Gilks, S. Richardson, and D. Spiegelhalter. Markov chain monte carlo in practice. Interdisciplinary Statistics. Chapman & Hall, 1996.
- [4] J. Pearl. Probabilistic reasoning in intelligent systems: Networks of plausible inference. Morgan Kaufmann, second edition in 1991, 1988.
- [5] K. Muphy, S.Mian: Modelling Gene Expression Data using Dynamic Bayesian Network, Technical Report, Computer Science Division, University of California, Berkeley, CA, 1999
- [6] T.A. Stephenson, An Introduction to Bayesian Network Theory and Usage, IDIAP Research Report 00-03, 2002
- [7] J. Cheng, D. A. Bell, W. Liu, Learning Belief Networks from Data: An Information Theory Based Approach, Proceedings of the sixth ACM International Conference on Information and knowledge Management
- [8] J.F.Allen, Maintaining Knowledge about Temporal Intevals, Comm. ACM, vol.26, 1983
- [9] V. Pavlovic, B. Frey, and T.S. Huang, Time series classification using mixed-state dynamic Bayesian networks, in Proc. IEEE CVPR, 1999
- [10] G.Zweig, S. Russel, Compositional Modelling With DPNs, Report N. UCB/CSD-97-970, 1997
- [11] Smyth P., Heckerman D. and Jordan M. Probabilistic Independence Networks for Hidden Markov Probability Models. Technical Report MSR-TR-96-03, Microsoft Research, 1996
- [12] K. Murphy, Dynamic Bayesian Networks: Representation, Inference and Learning, PhD thesis University of California, Berkely, 2002.
- [13] T. T. Kristjansson, B. J. Frey, and T. Huang. Event-coupled hidden Markov models. In Proc. IEEE Int. Conf. On Multimedia and Exposition, volume 1, pages 385–388, 2000
- [14] E. Sanchez, Réseaux Bayésiens Dynamiques pour la Vérification du Locuteur, PhD thesis Telecom Paris, Mai 2005
- [15] Y. Bengio and P. Frasconi. Input-Output HMMs for sequence processing. IEEE Trans. Neural Networks, 7(5):1231–1249, September 1996.
- [16] K. Jayech, MA Mahjoub "New approach using Bayesian Network to improve content based image classification systems", *IJCSI International Journal of Computer Science Issues*, Vol. 7, Issue 6, November 2010.
- [17] K. Jayech, MA Mahjoub "Clustering and Bayesian Network to improve content based image classification systems", *International Journal of Advanced Computer Science and Applications- a Special Issue on Image Processing and Analysis*, May 2011.
- [18] MA Mahjoub, K. kalti "Software Comparison dealing with Bayesian networks" Lecture Notes in Computer Science (LNCS), 2011, Volume 6677, Advances in Neural Networks – ISSN 2011 Pages 168-177.

Triple SV: A Bit Level Symmetric Block Cipher Having High Avalanche Effect

Rajdeep Chakraborty
Department of Computer Science & Engineering
Netaji Subhash Engineering College
Kolkata, West Bengal, India

Sonam Agarwal
Department of Computer Science
Netaji Subhash Engineering College
Kolkata, West Bengal, India

Sridipta Misra, Vineet Khemka, Sunit Kr Agarwal
Department of Information Technology
Netaji Subhash Engineering College
Kolkata, West Bengal, India

J. K. Mandal
Department of Computer Science and Engineering
University of Kalyani
Kalyani, West Bengal, India

Abstract— The prolific growth of network communication system entails high risk of breach in information security. This substantiates the need for higher security for electronic information. Cryptography is one of the ways to secure electronic documents. In this paper, we propose a new block cipher, TRIPLE SV (3SV), with 256-bit block size and 112-bit key length. Generally, stream ciphers produce higher avalanche effect but Triple SV shows a substantial rise in avalanche effect with a block cipher implementation. The CBC mode has been used to attain higher avalanche effect. The technique is implemented in C language and has been tested for feasibility.

Keywords- Avalanche Effect; Block Cipher; Cipher Block Chaining (CBC) mode; Cryptography.

I. INTRODUCTION

With the transformation of classical [1] methodology in business to conventional methodology, security of electronic documents is in need. A Cipher is something that converts the actual document into a format that cannot be recognized by anyone except the sender and intended receiver. One of the vital considerations for a good cipher is its *avalanche effect*. This effect obviates the brute force attack to a greater extent. Modern techniques of encryption either use a single symmetric key or two asymmetric keys. The algorithm is called as Symmetric Key Cryptography if only one key is used on both ends of the communication and it is called as a Public Key Cryptography if two distinct keys are used. The proposed technique is based on Private Key Cryptography in Cipher Block Chaining mode [1,2] with high avalanche effect i.e. a one-bit change in a plaintext affects all following cipher-text blocks [2,3].

The Section II of this paper deals with the proposed technique. A concept of key-generation [1] is given in Section III. Results and comparisons are illustrated in Section IV. Conclusions are drawn in Section V.

II. TRIPLE SV (3SV)

The Triple SV is a block cipher that uses secret key encryption. This algorithm takes a fixed-length string of plaintext bits and transforms it through a series of complicated operations into another cipher-text bit string of the same length. The proposed block size is 256 bits.

The Key comprises 112 bits. Fig. 1 summarizes the overall structure of Triple SV.

A. Modes of Operation

Like other block ciphers, Triple SV by itself is not a secure means of encryption but must instead be used in one of the several modes of mode of operation, like Electronic codebook (ECB), Cipher-block chaining (CBC), Propagating cipher-block chaining (PCBC), Cipher feedback (CFB), and Output feedback (OFB). We have designed and implemented Triple SV in CBC mode

In the CBC mode, each block of plaintext is XORed with the previous cipher-text block before being encrypted. This way, each cipher-text block is dependent on all plaintext blocks processed up to that point. Also, to make each message unique, an initialisation vector must be used in the first block.

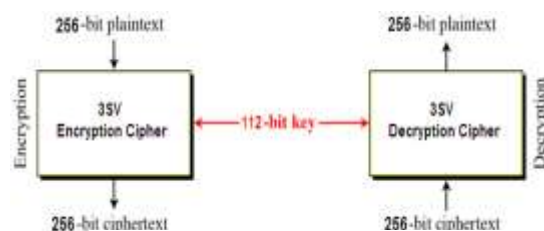


Figure 1. Overview of the Triple SV

A one-bit change in a plaintext affects all following cipher-text blocks. A plaintext can be recovered from just two adjacent blocks of cipher-text. As a consequence, decryption can be parallel zed, and a one-bit change to the cipher-text

causes complete corruption of the corresponding block of plaintext, and inverts the corresponding bit in the following block of plaintext. Fig. 2 and Fig. 3 represent the encryption and the decryption process of CBC mode.

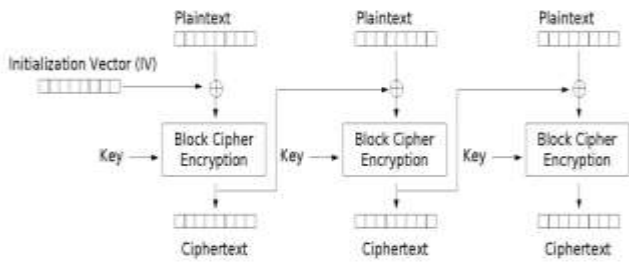


Figure 2. The Cipher Block Chaining (CBC) mode (encryption)

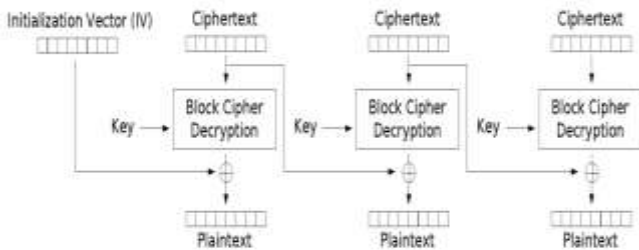


Figure 3. The Cipher Block Chaining (CBC) mode (decryption)

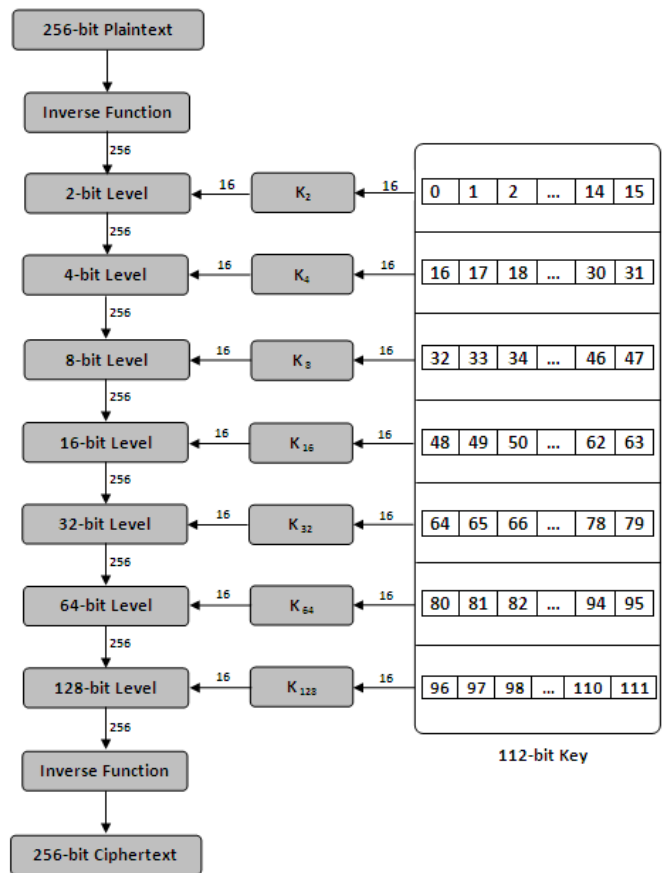


Figure 4. Triple SV Encryption Overview

B. Encryption

The algorithm's overall structure (for encryption) is shown in Fig. 4. There are basically seven similar levels of processing. In addition there is also an initial and final inversion operation. The seven similar levels of processing have identical structure but differ in the number of consecutive n bits out of the input 256 bits to each level, which are coupled together and treated as a single entity while being processed inside each level. The values that n take in the 7 distinct levels are 2, 4, 8, 16, 32, 64, 128, (i.e. $2^{(\text{level number})}$), respectively. Hence the seven levels of processing are named as 2-bit level, 4-bit level, 8-bit level, 16-bit level, 32-bit level, 64-bit level, and 128-bit level, respectively.

1) n-Bit Level Structure

Fig. 5 explains the entire construct of the n -bit level. Each level basically comprises three major functions, namely, Far Swapping, Near Swapping and Expansion Function, and a XOR Function.

The 256-bit input to the level first undergoes an n -bit far swap. The 256-bit output of the n -bit far swap is then introduced to an n -bit near swap, which again generates a 256-bit output.

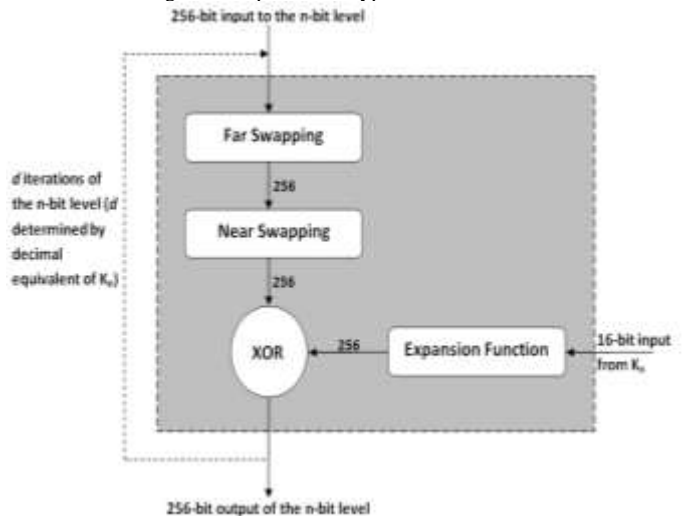


Figure 5. n-BIT Level Structure (Encryption)

Meanwhile, the 16-bit string, K_n enters the level and get expanded into a 256-bit string with which the 256-bit output of the near swap gets XORed to produce a 256-bit intermediate. This intermediate is again fed into the same level to carry out the procedure all over again. This iterative operation of the level continues for d time, where d is a positive integer, the value of which is determined by the decimal equivalent of the string K_n .

After d complete iterations of the level, the 256-bit output is the output of that level and is carried to the next n -bit level for similar series of operations.

- a) *n*-Bit Far Swap Function: The n -bit far swap function has been diagrammatically depicted in Fig.6. The n -bit far swap function is a simple function. Firstly, the 256-bit of the incoming string are grouped into distinct n -bit groups, where n is 2, 4, 8, 16, 32, 64, or 128, depending on the level at which we are operating. The groups are formed by starting from the first bit and grouping together the first n consecutive bits, then the next n consecutive bit, and so on. These distinct n -bit groups behave as individual entities at that particular level.

For n -bit far swapping, the first n -bit group gets swapped (interchanged) the last (farthest) n -bit group. The second n -bit group gets swapped with the penultimate n -bit group, and so on.

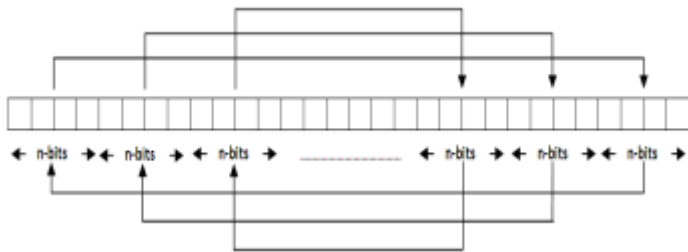


Figure 6. n-Bit Far Swap Function

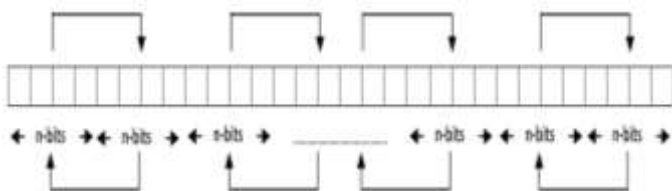


Figure 7. n-Bit Near Swap Function.

- b) *n*-Bit Near Swap Function: The n -bit near swap function is quite similar to n -bit far swapping function, with a subtle change in swapping pattern, as demonstrated in Fig. 7. For n -bit near swapping, the first n -bit group gets swapped (interchanged) the second (nearest) n -bit group. The third n -bit group

gets swapped with the fourth n -bit group, and likewise the penultimate n -bit group is swapped with the ultimate n -bit group.

- c) *Expansion Function (for encryption)*: The Expansion Function, in comparison to the earlier functions is a little more complex. For a certain n -bit level, the Expansion Function transforms the 16-bit string, K_n into a 256-bit string, which is used as an input to the XOR Function. Fig. 8 summarizes the expansion function for encryption.

The function takes the 16-bit K_n string as input. Next, it determines the number of iteration of the particular level (a). Then the K_n is given a left-rotations and the modifies string makes the first 16 bits of the expanded string. Next, another left-rotation is given to the first 16-bits to produce the next 16-bits, and so on.

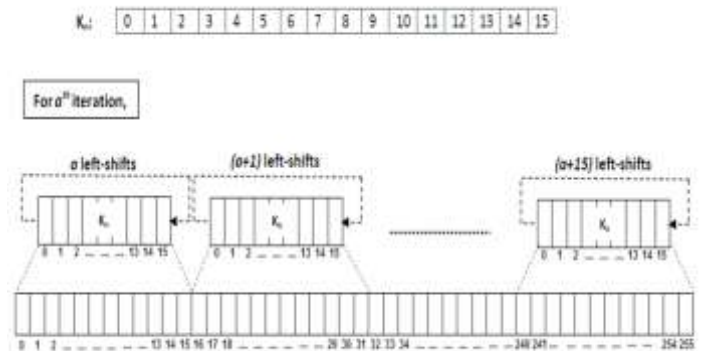


Figure 8. Expansion Function (for encryption)

Sixteen such modifications of the 16-bit string finally produce the 256-bit string for that particular level and that particular iteration. Thus, a 256-bit output is generated by the expansion function, which then gets XORed with the 256-bit output of the n -bit near swapping of that particular iteration of the level.

C. Decryption

The decryption algorithm is just the reverse of the encryption algorithm. In case of decryption, the 256-bit cipher text fed to the cipher first undergoes 128-bit level, then 64-bit level and so on till 2-bit level. Fig. 9 shows the decryption algorithm.

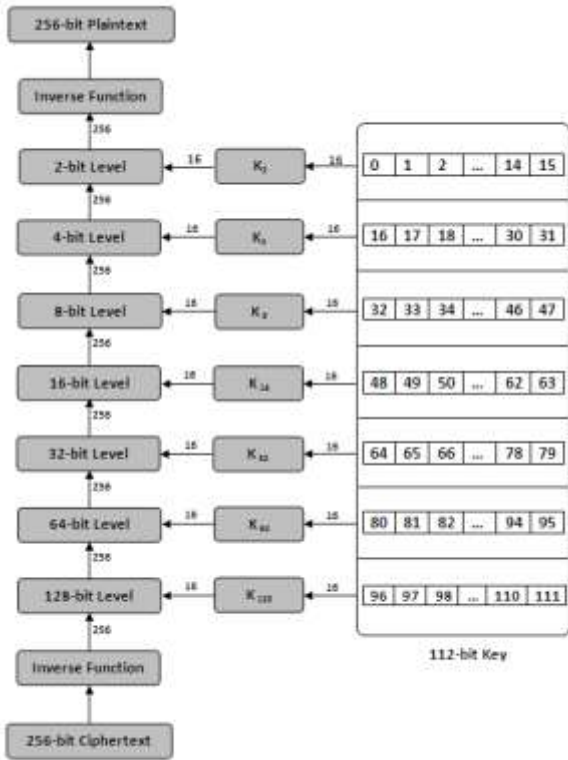


Figure 9. Triple SV Decryption Overview

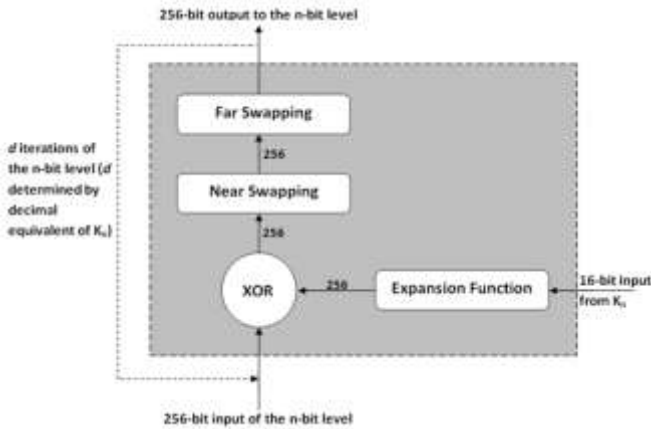


Figure 10. n-Bit Level Structure (Decryption)

Even the order of operations inside each level is reversed with the expansion function operating first, then the n-bit near swap and then the n-bit far swap, as depicted in Fig. 10.

All the individual function retains exactly the same functionality as in case of encryption. The only function that gets a little modified in case of decryption is the Expansion Function.

Fig. 11 clearly explains the functioning of the expansion function in case of decryption.

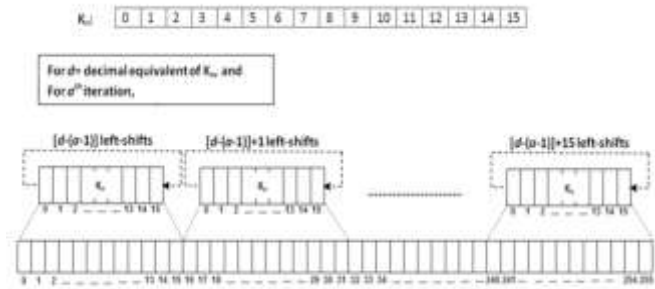


Figure 11. Expansion Function (for Decryption)

III. KEY STRUCTURE

Key length is one of the two most important security factors of any encryption algorithm—the other one being the design of the algorithm itself. The effective key length of Triple SV is 112 bits, giving 2^{112} possible combinations. The 112-bit key is completely user defined and is provided by the user in the form of numbers of iteration that each of the n-bit levels would have while the encryption or decryption process progresses. The 112 bits of the key have been logically divided into seven 16-bit binary sequences, each of which relates to a particular n-bit level. The association is elucidated below.

- Bit number 1 to 16 form string K2, and is associated with 2-bit level.
- Bit number 17 to 32 form string K4, and is associated with 4-bit level.
- Bit number 33 to 48 form string K8, and is associated with 8-bit level.
- Bit number 49 to 64 form string K16, and is associated with 16-bit level.
- Bit number 65 to 80 form string K32, and is associated with 32-bit level.
- Bit number 81 to 96 form string K64, and is associated with 64-bit level.
- Bit number 97 to 112 form string K128, and is associated with 128-bit level.

IV. RESULTS AND COMPARISONS

A. The Avalanche Effect:

Calculation of Avalanche Effect,

$$\text{Avalanche Effect} = \frac{\text{No. of flipped bits in ciphertext}}{\text{No. of bits in the ciphertext}} \times 100\%$$

Avalanche Effect refers to a desirable property of any cryptographic algorithm where, if an input is changed slightly (for example, flipping a single bit) the output changes significantly (e.g., more than half the output bits flip).

Table I compares the avalanche effect ratio for 3SV, TDES and RSA algorithm and Fig.12 gives the graph of the same which are obtained after calculating the respective Avalanche Effect by making a change of a few (approx 3) characters in each file.

It is observed that the proposed technique is showing an average avalanche ratio percentage of 95.77%, which is way higher than that obtained using Triple DES or RSA. High avalanche ratio ensures higher security from brute force attack.

The results [4] shown in Fig. 13, Fig. 14, Fig. 15 are obtained after calculating the respective Frequency Distributions of the source file 'ANSI.DOC' and the corresponding encrypted files using Triple SV, RSA and Triple DES.

B. Frequency Distribution

TABLE I. COMPARISON OF AVALANCHE RATIO FOR 3SV, TDES AND RSA ALGORITHM

Index	Filename	File Type	Size (In Kb)	Avalanche Ratio		
				3SV	TDES	RSA
1	POINT	CPP	1	0.9860	0.9874	0.1651
2	Wuident	TEXT	1.2	0.9902	0.1427	0.1381
3	winword2	DOC	1.72	0.9977	0.0403	0.0042
4	Footer	HTML	1.73	0.9739	0.1496	0.1221
5	VCIRC	CPP	2.46	0.9873	0.1827	0.0712
6	CIRCLE	CPP	3	0.9850	0.0763	0.2144
7	Options	BMP	3.8	0.7337	0.2502	0.0105
8	Default	HTML	4.31	0.9797	0.0958	0.0948
9	Winword	DOC	4.5	0.9715	0.1939	0.0124
10	safe_easier	HTML	7.5	0.9844	0.0573	0.0981
11	best_road	HTML	8.16	0.9820	0.0976	0.0577
12	GREP2MSG	C	9	0.9854	0.0364	0.0357
13	desktop_icon_04	BMP	9.05	0.9766	0.1021	0.0234
14	start_windows	HTML	10	0.9824	0.0247	0.1349
15	WINWORD8	DOC	10.5	0.9718	0.2341	0.0719
16	TASM2MSG	CPP	17.2	0.9854	0.0361	0.0455
17	ANSI	DOC	23	0.9874	0.0394	0.0070
18	Greenstone	BMP	25.9	0.9884	0.0101	0.0060
19	Dberr	TEXT	27	0.9858	0.7562	0.0062
20	eula.txt	TEXT	32	0.9868	0.0205	0.0075
21	Setup	BMP	234	0.9773	0.0343	0.0087
22	CLASSLIB	DOC	255	0.9853	0.0006	0.0011
23	watermark_300x	BMP	351	0.7295	0.0251	0.0183
24	Nbtlog	TEXT	443	0.8425	0.0004	0.0003
25	Setuplog	TEXT	758	0.9865	0.0003	0.0013

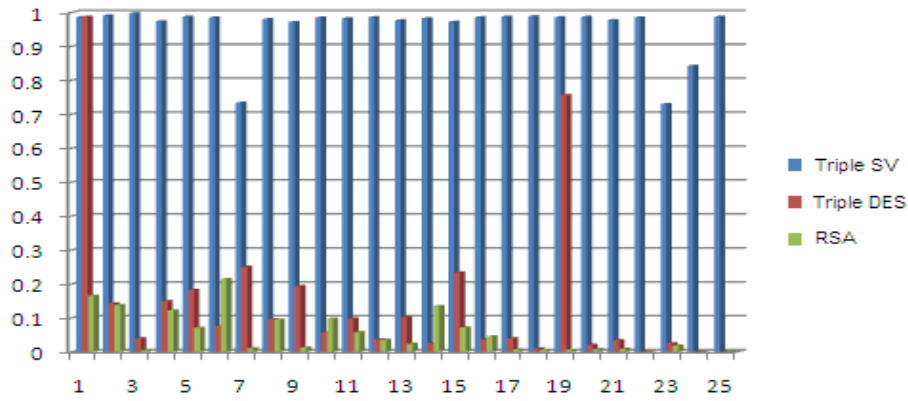


Figure 12. Graph for Comparison of Avalanche Ratio for 3SV, TDES & RSA

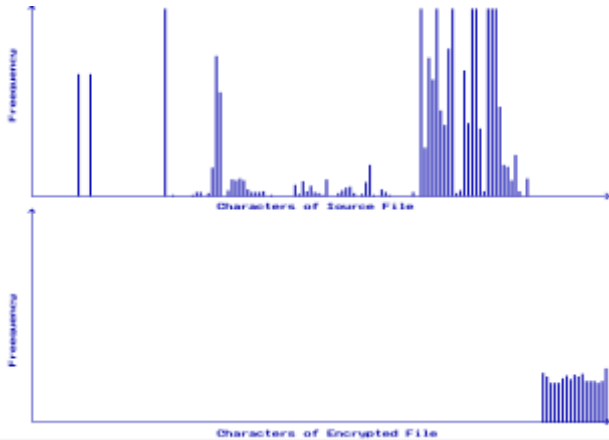


Figure 13. Graph for Distribution of Characters for Source file 'ANSI.DOC' and Triple SV

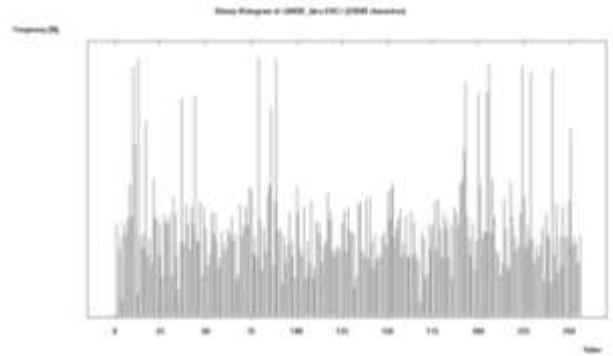


Figure 14. Graph for Distribution of Characters for RSA

From Fig. 13, it is substantiated that the frequency distribution of the proposed technique is well distributed over a range that is exclusive to the range of the source file. This makes statistical cryptanalysis [1,5,6,7] immensely improbable.

Figure 15. Graph for Distribution of Characters for TDES

C. Non-Homogeneity Test

Another way to analyse the technique is to test the non-homogeneity of the source and the encrypted file. The Chi-Square test has been performed for this purpose. Table II and Fig. 16 show the file size and the corresponding Chi-Square values for ten different files. The Chi-Square values for the proposed technique are comparatively lower than those obtained by RSA or TDES. The value of degree of freedom is on an average 127. Hence the source and the corresponding encrypted files are considered to be heterogeneous.

D. Time Complexity Analysis

This section compares the time complexity of the Triple SV with that of RSA and TDES by taking the encryption and decryption times into consideration.

The graphical analysis of the encryption and decryption time of Triple SV, RSA and TDES has been depicted in Fig. 17 and Fig. 18 respectively where x-axis represents the 25 test files (of increasing sizes varying from 1 KB to 758 KB) and y-axis represents the time taken for encryption/decryption (in seconds). The time complexity of the proposed technique is well comparable to RSA and TDES.

V. CONCLUSIONS

The cryptographic algorithm, Triple SV is a symmetric block cipher using a 256-bit block and 112-bit key. From the above discussions it can be inferred that Triple SV is potentially a promising algorithm, which can find its efficient implementation in different fields. Triple SV has a way better Avalanche Effect than any of the other existing algorithms and

hence can be incorporated in the process of encryption of any plain text. The high avalanche ratio and a key size of 112 bits ensure sound security from brute force attacks. The implementation in CBC mode ensures low predictability and tougher cryptanalysis. Even the time complexity of the proposed algorithm is considerably viable and even better than RSA and TDES at many instances.

TABLE II. THE CHI SQUARE VALUES AND DEGREE OF FREEDOM FOR TRIPLE SV, TRIPLE DES AND RSA ALGORITHMS

Index	Filename	File Type	Size (In KB)	Chi-Square Value			Degree Of Freedom		
				3SV	TDES	RSA	3SV	TDES	RSA
1	POINT	CPP	1	1221	15417	15281	127	248	251
2	Wuident	TEXT	1.2	1443	60322	34433	126	254	255
3	winword2	DOC	1.72	2365	2413761	2457	101	223	245
4	Footer	HTML	1.73	2072	30826	24387	127	254	255
5	VCIRC	CPP	2.46	2923	39301	59753	127	255	255
6	CIRCLE	CPP	3	3071	57862	52331	127	255	255
7	Options	BMP	3.8	5019	841431	39438	127	254	254
8	Default	HTML	4.31	5143	45397	37919	127	255	254
9	Winword	DOC	4.5	9476	1314485	89517	125	252	255
10	safe_easier	HTML	7.5	8917	124503	119531	127	255	254
11	best_road	HTML	8.16	9694	144300	98956	127	255	255
12	GREP2MSG	C	9	10693	352680	295390	127	255	255
13	desktop_icon_04	BMP	9.05	8289	863031	76607	127	255	254
14	start_windows	HTML	10	11507	151721	114562	127	255	255
15	WINWORD8	DOC	10.5	11498	6891550	88675	127	254	255
16	TASM2MSG	CPP	17.2	20424	491314	52537	127	255	255
17	ANSI	DOC	23	26159	369304	374085	127	255	255
18	Greenstone	BMP	25.9	30007	330192	319512	127	255	255
19	Dberr	TEXT	27	31450	268039	263938	127	255	255
20	eula.txt	TEXT	32	33595	406353	286747	127	255	254
21	Setup	BMP	234	268322	42142512	7993738	127	255	255
22	CLASSLIB	DOC	255	300645	3929874	2622070	127	255	255
23	watermark_300x	BMP	351	242589	5249601	4218862	127	255	254
24	Nbtlog	TEXT	443	524360	5484097	3694341	123	255	255
25	Setuplog	TEXT	758	897065	5551341	5395921	127	255	255

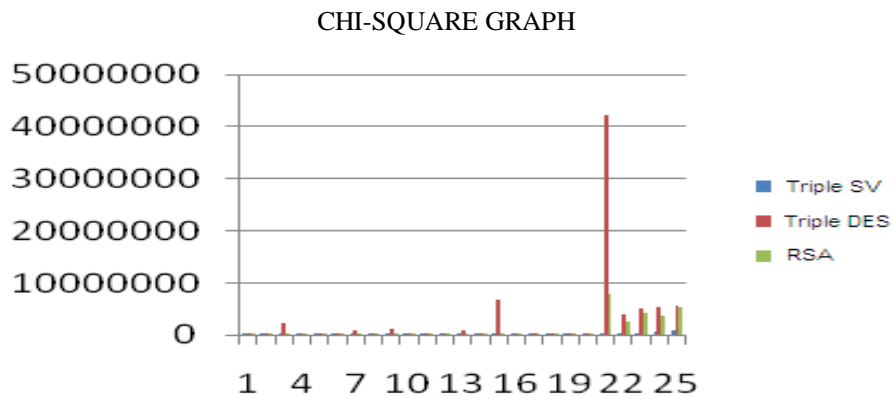


Figure 16. Graph for Comparison of Chi Square Values for Triple SV, Triple DES and RSA

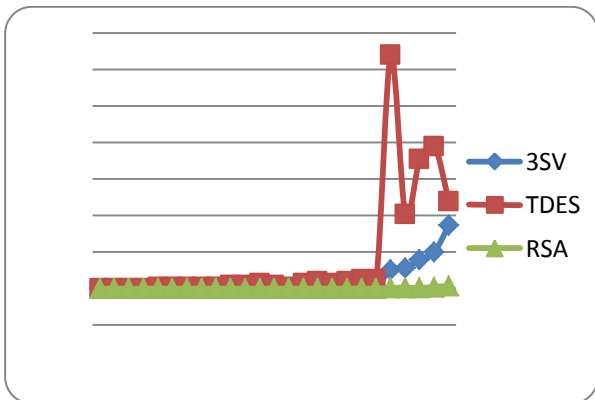


Figure 17. Graph for Comparison of Time Complexity for Encryption Time for Triple SV, Triple DES & RSA

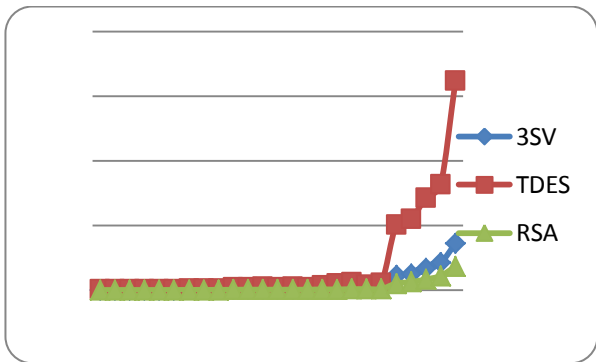


Figure 18. Graph for Comparison of Time Complexity for Decryption time for 3SV, TDES & RSA

ACKNOWLEDGMENT

The authors would like to acknowledge the Department of Computer Science and Information Technology, Netaji Subhash Engineering College, garia, Kolkata, India and the Department of Computer Science and Engineering, University of Kalyani, Kalyani, Nodia, West Bengal, India.

REFERENCES

- [1]. B. Schneier, "Applied cryptography" John Wiley & Sons Inc., New York, New York, USA, 2nd edition, 1996.
- [2]. http://en.wikipedia.org/wiki/Block_cipher_modes_of_operation#Cipher-block_chaining_28CBC.29
- [3]. Sriram Ramanujam and Marimuthu Karupiah, "Designing and algorithm with high avalanche effect," *International Journal of Computer Science and Network Security*, VOL.11 No.1, January 2011.
- [4]. The software cryptographic tools for educational purpose available at <http://www.cryptool.com/>.
- [5]. W. Stallings, "Cryptography and Network Security: Principles and Practices," Prentice Hall, Upper Saddle River, New Jersey, USA, Third Edition, 2003.
- [6]. U.S. Department of Commerce/National Institute of Standard and Technology, FIPS PUB 197, Specification for the Advanced Encryption Standard (AES), November 2001. Available at <http://csrc.nist.gov/encryption/aes>.
- [7]. A. J. Menezes, P. C. van Oorschot, and S. A. Vanstone. "Handbook of Applied Cryptography", CRC Press, Boca Raton, Florida, USA, 1997.
- [8]. http://en.wikipedia.org/wiki/Data_Encryption_Standard.
- [9]. Rajdeep Chakraborty, Dr. J.K.Mandal, "A Microprocessor-based Block Cipher through Rotational Addition Technique (RAT)", ICIT – 2006 18-21 December, 2006, Bhubaneswar, INDIA.
- [10]. "Data Encryption Standard," Federal Information Processing Standards Publication No. 46, National Bureau of Standards, January 15, 1977.

Investigation on Simulation and Measurement of Reverberation for Small Rooms

Zhixin Chen

ILX Lightwave Corporation
Bozeman, Montana, USA

Abstract—This paper investigates the simulation of reverberation in a small room using image source method, Schroeder model, and Gardner model. It then compares the simulation results with measurement of reverberation in the real measurement room. It shows a large difference between the simulation and the real measurement of reverberation due to the over-simplified representation of the sound source, receiver, and room surfaces in the models. A reverberation simulation model including the real measurement of the source, receiver, and room surfaces will be developed to better match the real measurement of reverberation.

Keywords-Digital Signal Processing; Reverberation; Room Acoustics; Embedded Systems.

I. INTRODUCTION

Reverberation in a room is the result of many reflections of sound that occurs in that room. Reverberation can be separated into direct sound, early reflections, and late reverberations [1]. Room reverberation has been modeled in many applications. For example, it can be used to help predict the acoustical characteristics of the new finished spaces, to help create a virtual studio effect without building the actual room, or to help compare the effect of different absorbing materials and treatments.

Reverberation also has extensive uses in our daily life. For example, when we try to speak to a group of people outdoors, we need to speak louder than when we speak in a room. The reason is that when we speak indoors, the room reverberation helps keep sound energy localized in the room, raising sound pressure level and distributing sound throughout it. On the other hand, when we speak outdoors, many of the reflective surfaces are missing and much of the sound energy is lost.

Although reverberation is almost always around us, we still need to create reverberation effects in some cases because sometimes we are in environments with very little or poor reverberation. In the reverberation effect creation, it is often mistakable that a simple delay device with feedback can produce reverberation. Actually, a simple delay unit can only simulate reflections with a fixed time interval between them, but it cannot produce a very important characteristic of reverberation, that is, the rate of arriving reflections changing over time. There has been a lot of research on the simulation of reverberations [2-7]. However, most of the research focuses on creating reverberation effects for recorded or live music in large concert halls. Moreover, most of the research does not compare the simulation results with the real measurement of reverberation.

In this paper, we investigate the simulation of reverberation in a small room using the popular image source method, Schroeder model, and Gardner model. We then compare the simulation results with real measurement of reverberation in the real measurement room. It shows that there is a big difference between the simulation and the real measurement of reverberation due to the simple representation of the source, receiver, and room surfaces in the models.

The remaining part of this paper is organized as follows. First, the fundamentals of reverberation are reviewed. Next, the reverberation simulations using digital signal techniques, including the image source method, Schroeder model, and Gardner Model are described. Then, the measurement and simulation of reverberation in a real measurement room are compared. Finally, the paper is concluded with a summary of results.

II. FUNDAMENTALS OF REVERBERATION

In this section, the fundamentals of reverberation, including reverberation time and the methods to create reverberation effects are reviewed.

A. Reverberation Time

Reverberation time is a key parameter to characterize reverberation in a room. It is defined as the time required for reflections of a direct sound to decay by 60 dB below the level of the direct sound. The reverberation time is controlled primarily by the room size and the absorption coefficients of the room surfaces. The room surfaces determine how much energy is lost in each reflection. Highly reflective materials, such as tile floors, brick walls, and concrete windows, increase reverberation time. Absorptive materials, such as curtains, heavy carpet, and people, reduce reverberation time.

Wallace Clement Sabine was the first person to develop methods to estimate reverberation time. He found that reverberation time is proportional to the dimensions of room and inversely proportional to the amount of absorption. The equation he proposed is:

$$R_T = \frac{0.161 \cdot V}{S \cdot \bar{a}}, \quad (1)$$

where V is the volume of the room in cubic meters, S is the total surface area of the room in square meters, and \bar{a} is the average absorption coefficient in the room. According to this equation, typical small rooms have reverberation time from 100 to 500 milliseconds.

B. Methods to Create Reverberation Effects

It is often desirable to create reverberation effects for recorded or live music. Many methods are available to create reverberation effects, among which the most common way is to use spring reverberators, plate reverberators, or digital reverberators [8].

In the old days, spring reverberators or plate reverberators were often used to create reverberation effects. Spring reverberators provide a relatively simple and inexpensive method for creating reverberation effects. A spring reverberator uses a transducer at one end of a spring and a pickup at the other end to create and capture vibrations with a metal spring. Many musicians have made use of spring reverberator by rocking them back and forth, creating a thundering, crashing sound caused by the springs colliding with each other.

Plate reverberators were not used widely as spring reverberators because they are much more expensive. A plate reverberator uses an electromechanical transducer, similar to the driver in a loud speaker, to create vibration in a large plate of sheet material. A pickup captures the vibrations as they bounce across the plate, and the result is output as an audio signal.

Nowadays, the common way to implement reverberation is to use digital reverberators which use various signal processing techniques in order to create reverberation effects. Since reverberation is essentially caused by a very large number of echoes, simply reverberation algorithms use multiple feedback delay circuits to create a large, decaying series of echoes. A more detailed description of these computer models will be provided and the simulation results of the models will be presented in next section.

III. SIMULATION AND MEASUREMENT OF DIGITAL REVERBERATORS

Early digital reverberation techniques tried to simulate the room reverberation by using two types of IIR filters so that the output would gradually decay [1, 7]. One is the comb filter, which gets its name from the comb-like notches in its frequency response. The other is the allpass filter, which has the nice property that all frequencies are passed equally, reducing a coloration of the sound. Much of the early work on digital reverberation was done by Schroeder [1]. One of his well-known reverberator designs used four comb filters and two allpass filters. However, this design did not create the increasing arrival rate of reflections. Some improvements were made by Gardner [7].

The popular image source method can also be combined with these reverberation algorithms to create reverberation effects [7, 9]. Typically, a FIR filter made using the image source method is used to create the direct sound and early reflections, and IIR filters using the reverberation algorithms are used to create late reverberation. The early reflection and late diffuse reverberation are then combined to form the reverberation.

A. Image Source Method

The image source method has been a popular technique to simulate room acoustics [10-12]. The simulation of sound propagation from a source to a receiver within a rectangular room using the image source method is shown in Figure 1. The sound propagation is modeled as the superposition of the direct sound and a number of reflected sounds from the source to the receiver.

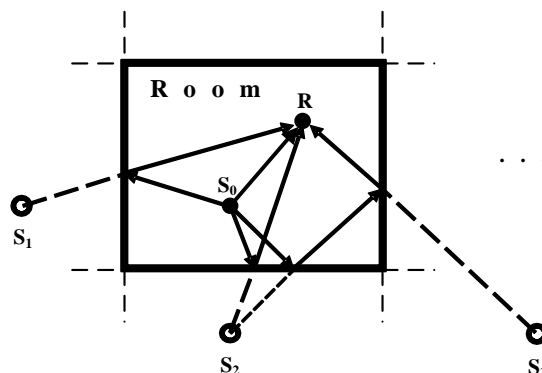


Figure 1: Simulation of sound propagation between two points in a rectangular room using image source method.

Image source method can be used to make the FIR filter by considering the composite contributions of each nearby virtual source to the receiver. The FIR tap delay lengths correspond to the sound travel time between the nearby virtual source and the listener. The FIR coefficient amplitudes are proportional to the reciprocal of distance to the nearby virtual source. The effects of absorption on the FIR coefficient amplitude should also be included since all reflections reduce the amplitude of the nearby virtual source by a factor of the reflection coefficient of the wall material. Actually, if an adequate amount of virtual source is considered, the image source method can also be used to calculate the whole reverberation.

B. Digital Reverberation Algorithms

Early work on simulating reverberation focused on the design of digital filters to model room responses. This work was based on the assumption that the perceptual difference between a real room and a greatly simplified simulation could be made small. As mentioned previously, Schroeder's initial reverberator design consisted of comb filters and allpass filters. A comb filter is a simple delay with feedback and its time domain impulse response of a comb filter is an exponentially decaying pulse train, which is shown in Figure 2.

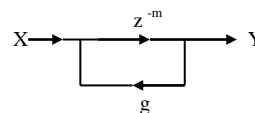


Figure 2: Flow graph of the comb filter

An allpass filter is just like a comb filter with a feed forward path around the delay, which is shown in Figure 3. In the all pass filter, the zeroes cancel the influence of the poles

on the magnitude of the frequency response, resulting in a flat frequency response. However, the allpass filters affect the phase of signals.

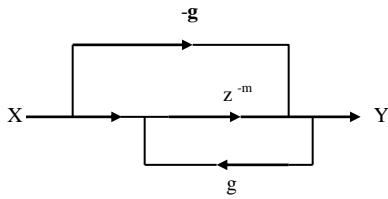


Figure 3: Flow graph of the allpass filter

The flow graph of one reverberator designed by Schroeder is shown in Figure 4. This reverberator consists of four parallel comb filters feeding into two serial allpass filters. The parallel comb filters are used to simulate the echoes occurring between walls in a room since in the frequency domain, the peaks caused by the comb filters correspond to the normal modes of the room. However, the parallel comb filters do not supply a sufficient buildup of echoes for realistic diffuse reverberation. In order to increase the echo density, the output of the comb filters is fed into two allpass filters in series. Each allpass filter has a multiplicative effect on the number of echoes, but prevents coloration by taking advantage of the flat frequency response of the allpass filters [1].

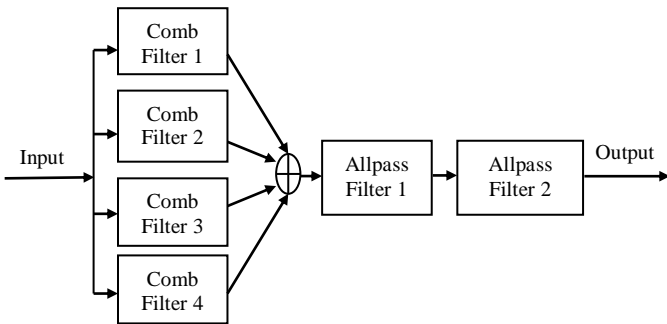


Figure 4: Block diagram of Schroeder's reverberator

Instead of using allpass filters in series as in the Schroeder reverberator, Gardner managed to combine them in a way that led to an exponential buildup of echoes as occurs in real rooms. He used a nested allpass filter, which embeds an allpass filter into the delay element of another allpass filter [7]. In a nested allpass system shown in Figure 5, the echoes generated by the inner allpass filters will be recirculated to their inputs via the outer feedback path. The number of echoes generated in response to an impulse will therefore increase over time as what we expected rather than remaining constant as with a standard allpass filter.

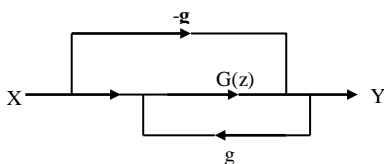
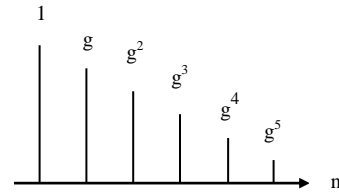


Figure 5: Flow graph of the nested allpass filter. Here $G(z)$ is also an allpass filter.



C. Simulation and Measurement of Reverberation

In this sub-section, the simulations of room reverberation using the popular image source method and the digital reverberation models are shown. A real measurement of reverberation is also presented. The subjective comparison between the simulations and the measurement is then performed.

Before the room reverberation was modeled, the measurement room dimensions, the source position, and the receiver position were measured. The layout of the measurement room is shown in Figure 6. The rectangular measurement room is 3.37 meters long, 3.03 meters wide, and 2.39 meters high. The sound source is localized in the position of (0.31, 0.28, 1.02) meters and the receiver is in the position of (1.57, 1.49, 1.02) meters. The reflections coefficients are 0.90 for the walls, 0.85 for the ceiling, and 0.85 for the floor. The temperature in the measurement room was 19° C, giving a sound velocity of 342.8 m/s.

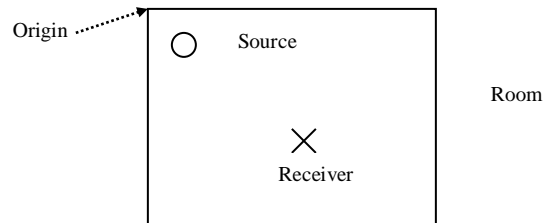


Figure 6: The layout of the measurement room

A MATLAB program was developed to implement the image source method to simulate the reverberation of the room. The reflection order was set to 20, resulting in 68921 virtual sources, which is sufficient to simulate the reverberation. The simulated reverberation result is shown in Figure 7. It is shown that the reverberation decays very quickly.

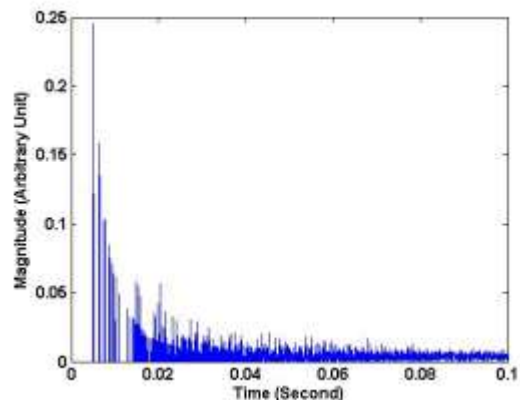


Figure 7: Reverberation simulation using the image source method

Then, the image source method was used to simulate the direct sound and early reflections of the room. The first 20 milliseconds of the direct sound and early reflections generated by the image source method were extracted and then fed into the IIR filters to simulate the late reverberations. The IIR filters were implemented using Schroeder model and Gardner model respectively. The direct sound, early reflections, and late reverberation were then combined to form the whole reverberation. The reverberation results using these two models are shown in Figure 8 and Figure 9 respectively. It is shown that the magnitude of the late reverberation decrease exponentially for both models, but it is hard to tell which one is better by just looking at the simulation of reverberation.

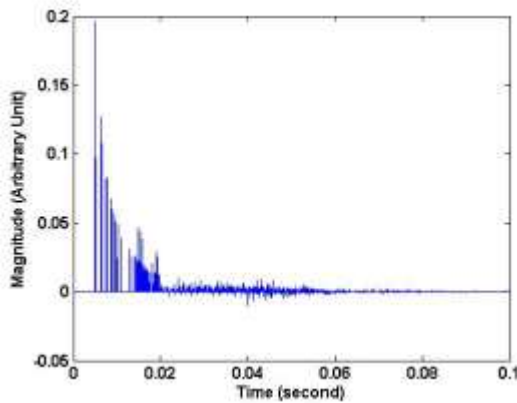


Figure 8: Reverberation simulation using Schroeder model

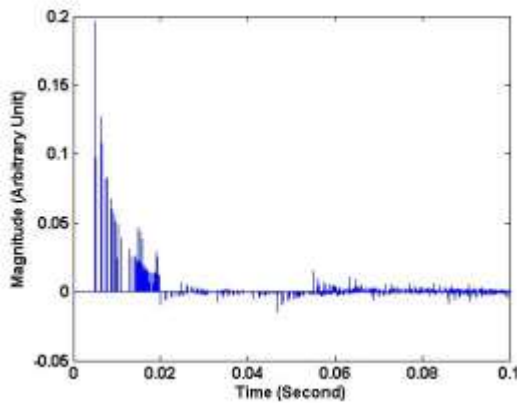


Figure 9: Reverberation simulation using Gardner model

The reverberation in the real measurement room was also measured using the SMAART software [13]. Here the sound generated from the speaker acts as the sound source and a high quality microphone acts as the receiver. The measurement of the room reverberation is shown in Figure 10. It can be seen that the direct sound and some early reflections are very similar to the simulation results. However, the late

reverberations are stronger than that simulated by the image source method or the two models. It should also be noticed that there are some energy components among the early reflections, which seem to be the joint effects of the measurement errors, the polar responses of the speaker or microphone, and the scattering of the room surfaces.

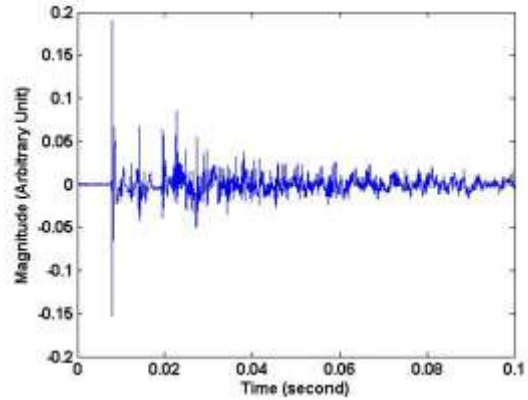


Figure 10: Reverberation measurement of the real room

The quality of the reverberation simulation can now be judged subjectively by listening to the output sound signal of the reverberator. Both male speech and female speech were fed into the two reverberators, the system using the image source method, and the system with the real measurement of reverberation. By listening to the output sound of these systems, we found that the real room has stronger reverberations than any of the simulation systems. It appeared that the Gardner model had a result more similar to the real room, which also showed that the Gardner model has a better performance than the image source method and the Schroeder model in modeling room reverberation.

IV. CONCLUSION

This paper briefly reviewed the fundamentals of reverberation and its simulation methods. It then compared the simulation and the measurement of reverberation. It showed that the simulations using the image source method, Schroeder model, and Gardner Model have similar results. But they differed substantially from the real measurement of reverberation. The difference might be due to the over-simplified representation of the source, receiver, and room surfaces in the reverberation models. A reverberation model that includes the real measurement of the source, receiver, and room surfaces is being developed to better match the real measurement of reverberation.

REFERENCES

- [1] M. R. Schroeder, "Natural sounding artificial reverberation," *J. Audio Eng. Soc.*, vol.10, no. 3, 1962.
- [2] L. Savioja, "Modeling techniques for virtual acoustics," Ph.D. dissertation, Helsinki University of Technology, Espoo, Finland, 1999.
- [3] M. Kleiner, B. I. Dalenbäck, and P. Svensson, "Auralization-an overview," *J. Audio Eng. Soc.*, vol. 41, pp. 861-875, 1993.
- [4] U. P. Svensson and U. R. Kristiansen, "Computational modelling and simulation of acoustic spaces," 22nd Int. Conf. on Virtual, Synthetic and Entertainment Audio, Espoo, Finland, pp. 11-30, June 2002.

- [5] C. L. Christensen and J. H. Rindel, "Predicting acoustics in classrooms," *InterNoise 2005*, pp. 1782, 2005.
- [6] J. A. Moorer, "About this reverberation business", *Computer Music Journal*, vol. 3, no. 2, pp. 13 - 28, June 1979.
- [7] W.G. Gardner, "The virtual acoustic room", M.S. MIT, 1992.
- [8] Scott Lehman, "Reverberation", *Harmony Central*, 1996.
<http://www.harmony-central.com/Effects/Articles/Reverb>
- [9] Sean Browne, "Hybrid reverberation algorithm using truncated impulse response convolution and recursive filtering", *University of Miami*, 2001.
- [10] B. M. Gibbs and D. K. Jones, "A simple image method for calculating the distribution of sound pressure levels within an enclosure," *Acustica*, vol. 26, pp. 24-32, 1972.
- [11] J. B. Allen and D. A. Berkley, "Image method for efficiently simulating small-room acoustics," *J. Acoust. Soc. Am.*, vol. 65, no. 4, pp. 943-950, 1979.
- [12] J. Borish, "Extension of the image model to arbitrary polyhedra," *J. Acoust. Soc. Am.*, vol. 75, no. 6, pp. 1827-1836, 1984.
- [13] P. D. Henderson, "Getting started with SmaartLive: basic measurement setup and procedures," *SIA Software Company, Inc.*
<http://www.siasoft.com/pdf/Getting-Started-SmaartLive.pdf>.

AUTHORS PROFILE

Zhixin Chen is a Firmware Engineer in ILX Lightwave Corporation. He holds a BS degree from Xiamen University in China, a MS degree from Xiamen University in China, and a Ph.D. degree from Montana State University in USA, all in Electrical and Computer Engineering. His research interest and working experience are in the area of acoustics, audio, and speech processing, multimedia communication, and embedded system design for high power current source, temperature controller, and optical power meter.

Performance Analysis of Corporate Feed Rectangular Patch Element and Circular Patch Element 4x2 Microstrip Array Antennas

Md. Tanvir Ishtaique-ul Huque¹, Md. Al-Amin Chowdhury², Md. Kamal Hosain³, Md. Shah Alam⁴
^{1,2,3}Dept. of Electronics and Telecommunication Engineering,
⁴Dept. of Electrical and Electronic Engineering,
Rajshahi University of Engineering & Technology, Rajshahi-6204, Bangladesh.

Abstract— This paper present simple, slim, low cost and high gain circular patch and rectangular patch microstrip array antenna, with the details steps of design process, operate in X-band(8 GHz to 12 GHz) and it provides a mean to choose the effective one based on the performance analysis of both of these array antennas. The method of analysis, design and development of these array antennas are explained completely here and analyses are carried out for 4x2 arrays. The simulation has been performed by using commercially available antenna simulator, SONNET version V12.56, to compute the current distribution, return loss response and radiation pattern. The proposed antennas are designed by using Taconic TLY-5 dielectric substrate with permittivity, $\epsilon_r = 2.2$ and height, $h = 1.588$ mm. In all cases we get return losses in the range -4.96 dB to -25.21 dB at frequencies around 10 GHz. The gain of these antennas as simulated are found above 6 dB and side lobe level is maintained lower than main lobe. Operating frequency of these antennas is 10 GHz so these antennas are suitable for X-band application.

Keywords- microstrip array antenna; rectangular patch; return loss; X band; circular patch.

I. INTRODUCTION

The term “Microstrip” comes because the thickness of this metallic strip is in micro-meter range. Microstrip patch antennas are popular, because they have some advantages due to their conformal and simple planar structure. They allow all the advantages of printed-circuit technology. A vast number of papers are available on the investigation of various aspects of microstrip antennas [1, 5, 6, 7, 8, 12, 13]. The key features of a microstrip antenna are relative ease of construction, light weight, low cost and either conformability to the mounting surface or, at least, an extremely thin protrusion from the surface. These criteria make it popular in the field of satellite and radar communication system. Different Radar systems such as synthetic aperture radar (SAR), remote sensing radars, shuttle imaging radar and other wireless communication systems operate in L, Ku, C and X bands [11, 12, 14, 15]. Microstrip antennas are the first choice for this high frequency band such as X-band due to its light weight, low cost, and robustness. In this paper the designed microstrip antennas are also best suited for X band applications. The extended AM

broadcast band or simply “X band” is a segment of the microwave radio region of the electromagnetic spectrum. X-band radar frequency sub-bands are used in civil, military and government institutions for weather monitoring, air traffic control, maritime vessel traffic control, defense tracking, and vehicle speed detection for law enforcement. In radar engineering, its frequency range is specified by the IEEE at 8.0 to 12.0 GHz. X band is used in radar applications including continuous-wave, pulsed, single-polarization, dual-polarization, synthetic aperture radar, and phased arrays. In Ireland, Libya, Saudi Arabia and Canada, the X band 10.15 to 10.7 segment is used for terrestrial broadband. Portions of the X band are assigned by the International Telecommunications Union (ITU) exclusively for deep space telecommunications. The primary user of this allocation is the American NASA Deep Space Network (DSN) [16].

Microstrip patch elements are available in various configuration. But the most common is the rectangular patch element and after the rectangular patch element the next most well known configuration is the circular patch element. This paper presents the design procedure, characteristic and the corresponding performance analysis of both the rectangular and circular patch microstrip array antennas and provides a mean to choose the effective one based on their performance parameters to get the efficient radiation efficiency. In this paper we have also investigated the performance of corporate feed array in case of both the rectangular patch element and circular patch element, because it provides better directivity as well as radiation efficiency and reduce the beam fluctuations over a band of frequencies compared to the series feed array [5, 9]. Here all of these antennas are designed to support 10 GHz operating frequency and their corresponding simulations have been done by using the SONNET version V12.56 simulator. The proposed antennas are designed by using Taconic TLY-5 dielectric substrate with permittivity, $\epsilon_r = 2.2$ and height, $h = 1.588$ mm. These designed antennas are promising to be a good candidate for the X-band wireless applications due to the simplicity in structure, ease of fabrication and high gain and high efficiency.

II. MICROSTRIP ANTENNA DESIGN

Microstrip patch antennas consist of very thin metallic strip (patch) placed on ground plane where the thickness of the

metallic strip is restricted by $t \ll \lambda_0$ and the height is restricted by $0.0003\lambda_0 \leq h \leq .05\lambda_0$ [2, 5]. The microstrip patch is designed so that its radiation pattern maximum is normal to the patch. For a rectangular patch, the length L of the element is usually $\lambda_0/3 < L < \lambda_0/2$. There are numerous substrates that can be used for the design of microstrip antennas and their dielectric constants are usually in the range of $2.2 \leq \epsilon_r \leq 12$. To implement the microstrip antennas usually Fr-4 ($\epsilon_r = 4.9$), Rogers TMM 4 ($\epsilon_r = 4.5$), Taconic TLY-5 ($\epsilon_r = 2.2$), Alumina (96%) ($\epsilon_r = 9.4$), Teflon (PTFE) ($\epsilon_r = 2.08$), Arlon AD 5 ($\epsilon_r = 5.1$) dielectric materials are used as the substrate [1, 2, 5, 10].

The Performance of the microstrip antenna depends on its dimension. Depending on the dimension the operating frequency, radiation efficiency, directivity, return loss and other related parameters are also influenced [3]. Here, in this paper, the investigation is made on two types of microstrip patch elements. They are

- Rectangular patch element
- Circular patch element.

A. Rectangular Patch Element

For an efficient radiation a practical width of the Rectangular patch element becomes [2, 3, 5]

$$w = \frac{1}{2f_r \sqrt{\mu_0 \epsilon_0}} \times \sqrt{\frac{2}{\epsilon_r + 1}} \quad (1)$$

And the length of the antenna becomes [2, 3, 5]

$$L = \frac{1}{2f_r \sqrt{\epsilon_{eff}}} \sqrt{\epsilon_0 \mu_0} - 2\Delta L \quad (2)$$

Where,

$$\Delta L = 0.41h \frac{\epsilon_{eff} + 0.3}{\epsilon_{eff} - 0.258} * \frac{\left(\frac{w}{h} + 0.264\right)}{\left(\frac{w}{h} + 0.8\right)} \quad (3)$$

And

$$\epsilon_{eff} = \frac{\epsilon_r + 1}{2} + \frac{\epsilon_r - 1}{2\sqrt{1 + 12\frac{h}{w}}} \quad (4)$$

Where, λ is the wave length, f_r (in Hz) is the resonant frequency, L and W are the length and width of the patch element, in cm, respectively and ϵ_r is the relative dielectric constant. In the following Fig. 1, the antenna has been designed to cover specific 10 GHz operating frequency where the antenna dimension is in mm range and the quarter wavelength transformer method [2, 5] is used to match the impedance of the patch element with the transmission line.

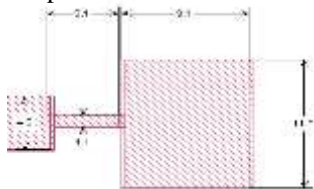


Figure 1. Single element Rectangular microstrip patch antenna.

B. Circular Patch Element

Other than the rectangular patch, the next most popular configuration is the circular patch or disk. For rectangular patch elements there are two degrees of freedom to control whereas for the circular patch elements there is one degree of freedom to control. Thus it is more convenient to design as well as to control the radiation pattern of the circular patch element.

From [12, 14] the first order approximation of the physical radius of the circular patch element becomes.

$$a = \frac{F}{\sqrt{\left\{1 + \frac{2h}{\pi \epsilon_r F} \left[\ln\left(\frac{\pi F}{2h}\right) + 1.7726\right]\right\}}} \quad (5)$$

Where

$$F = \frac{8.791 \times 10^9}{f_r \sqrt{\epsilon_r}}$$

Thus the effective area of the circular patch element is given by [12]

$$A_{eff} = \pi a^2 \left\{1 + \frac{2h}{\pi \epsilon_r F} \left[\ln\left(\frac{\pi F}{2h}\right) + 1.7726\right]\right\} \quad (6)$$

Where, f_r (in Hz) is the resonant frequency, h (in cm) is the thickness of the substrate, a is the effective radius of the circular patch element and ϵ_r is the relative dielectric constant.

In the following Fig. 2, the antenna has been designed to cover specific 10 GHz operating frequency where the antenna dimension is in mm range and the quarter wavelength transformer method [2, 5] is used to match the impedance of the patch element with the transmission line.

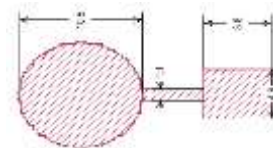


Figure 2. Single element circular microstrip patch antenna.

III. MICROSTRIP ARRAY ANTENNA DESIGN

Microstrip antennas are used not only as single element but also very popular in arrays. Microstrip arrays radiate efficiently only over a narrow band of frequencies and they can't operate at the high power levels of waveguide, coaxial line, or even stripline [1]. Antenna arrays are used to scan the beam of an antenna system, to increase the directivity and perform various other functions which would be difficult with any one single element. In the microstrip array, elements can be fed by a single line or by multiple lines in a feed network arrangement. Based on their feeding method [2, 5] the array is classified as

- Series feed network

- Corporate feed network

Series-feed microstrip array is formed by interconnecting all the elements with high impedance transmission line and feeding the power at the first element. Because the feed arrangement is compact the line losses associated with this type of array are lower than those of the corporate-feed type [5]. The main limitation in series-feed arrays is the large variation of the impedance and beam-pointing direction over a band of frequencies [5].

The corporate-feed network is used to provide power splits of $2n$ (i.e. $n = 2; 4; 8; 16; \text{etc.}$). This is accomplished by using either tapered lines or using quarter wavelength impedance transformers [5, 6]. In this paper the patch elements are connected by using the quarter wavelength impedance transformer method.

Corporate-feed arrays are general and versatile. This method has more control of the feed of each element and is ideal for scanning phased arrays, multiband arrays. Thus it provides better directivity as well as radiation efficiency and reduce the beam fluctuations over a band of frequencies compared to the series feed array [5, 9]. The phase of each element can be controlled by using phase shifters while amplitude can be adjusted using either amplifiers or attenuators [2, 8].

In this paper we have investigated the performance of corporate feed array in case of both the rectangular patch element and circular patch element.

A. Rectangular Patch Microstrip Array

In this paper we have designed the 8-elements rectangular patch Microstrip array antenna, as shown in Fig. 3, to cover 10 GHz operating frequency. Here the power is fed to the antenna by using the Microstrip transmission line method [2, 3] and the patch elements are matched together as well as with the transmission line with the quarter wavelength transformer method for the maximum power transmission.

The radiated field of the E -plane for a single element rectangular patch can be expressed by using the following formula [2, 10].

$$E = j \frac{k_0 W V_0 e^{-jk_0 r}}{r \pi} \left\{ \frac{\sin(\frac{k_0 h}{2} \cos \varphi)}{\frac{k_0 h}{2} \cos \varphi} \right\} \cos(\frac{k_0 L_e}{2} \sin \varphi) \quad (7)$$

Here, r is the radius of the patch antenna, L_e is the extended length, $V_0 = hE_0$ is the voltage across radiating slot of the patch, h is the substrate height, $K_0 = 2\pi/\lambda$ and r is the far field distance from the antenna.

The array factor as given in [4, 8] as

$$FA = \frac{\sin^2(N\pi(d_x/\lambda)\sin\theta)}{N^2 \sin^2(\pi(d_x/\lambda)\sin\theta)} \quad (8)$$

Here, d_x is the element spacing and N is the number of elements. Combining array factor and element voltage radiation pattern we get the total element normalized power radiation pattern [2, 4, 5] that is

$$20\log(|E/FA|) \quad (9)$$

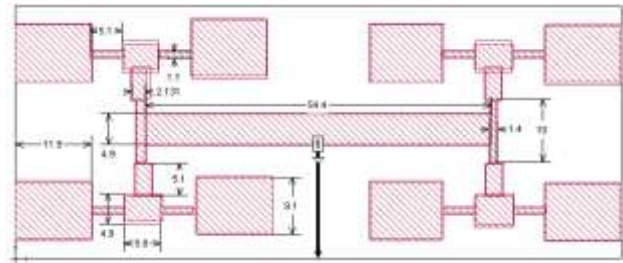


Figure 3. 8-elements corporate-feed rectangular microstrip array antenna.

B. Circular Patch Microstrip Array

Here the 8-elements circular patch Microstrip array antenna, as shown in Fig. 4, is designed to operate at 10 GHz frequency and similar to the previous one the power is fed to the antenna by using the Microstrip transmission line method and the patch elements are matched together as well as with the transmission line with the quarter wavelength transformer method for the maximum power transmission.

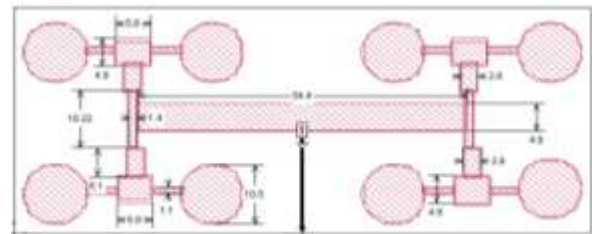


Figure 4. 8-elements corporate-feed circular microstrip array antenna.

The radiated field of the E -plane for a single element circular patch can be expressed by using the following formula [2, 5].

$$E = -jV_0 \frac{ak_0 e^{-jk_0 r}}{2r} \cos \phi J_1'(k_0 a \sin \theta) \quad (10)$$

Here, θ is the beam pointing angle measured from the broadside direction, $V_0 = hE_0$ is the voltage across radiating slot of the patch, $K_0 = 2\pi/\lambda$, J_1 is the Bessel function of first order and r is the far field distance from the antenna. The array factor as given in [14] as

$$AF = A_0 \frac{\sin(\frac{N\psi}{2})}{N \sin(\frac{\psi}{2})} \quad (11)$$

Where

$$\psi = \alpha + \beta d \sin(\theta) \cos(\varphi)$$

$$\beta d = (\frac{2\pi}{\lambda})S$$

Here, α is the phase difference between elements, N is the number of array elements and S is the spacing between circular patch elements. Now we can get the normalized power radiation pattern by combining the element radiation pattern and array factor [5].

IV. SIMULATION RESULT & DISCUSSION

A. Rectangular Microstrip Array Antenna Parameters

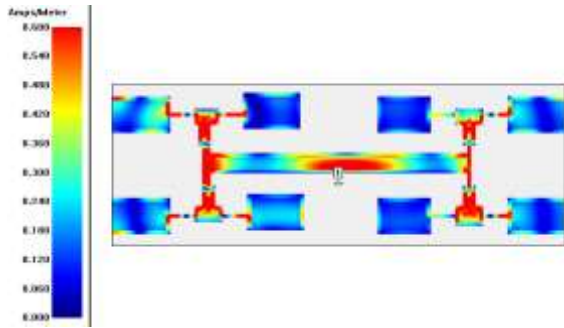


Figure 5. Current distribution of 8-elements rectangular microstrip array antenna.

In this paper, it is considered that the substrate permittivity of the antenna is $\epsilon_r = 2.2$ (Taconic TLY-5), height is 1.588 mm and resonance frequency of the antenna is 10 GHz. After simulation, as shown in Fig. 6, we found that, return loss is -25.21 dB at 10 GHz and it is maximum.

The simulated gain of the antenna, according to Fig. 7, is found around 6 dB at $\theta=0^\circ, \phi=0^\circ$ at the operating frequency 10 GHz. Fig. 8 shows that the HPBW and the FNBW for this simulated antenna are in the range 70° & 142.10° respectively.

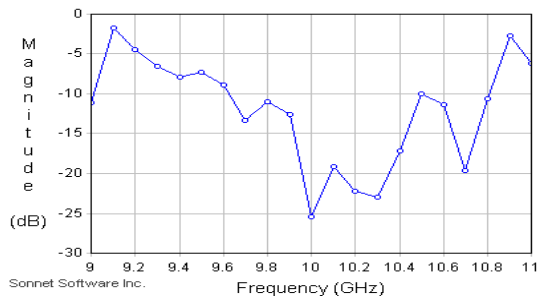


Figure 6. Return loss of the 8-elements rectangular microstrip array.

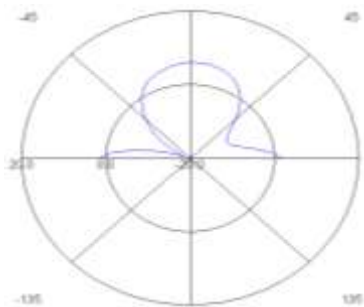


Figure 7. Radiation (Polar plot) pattern of the 8-elements rectangular microstrip array antenna.

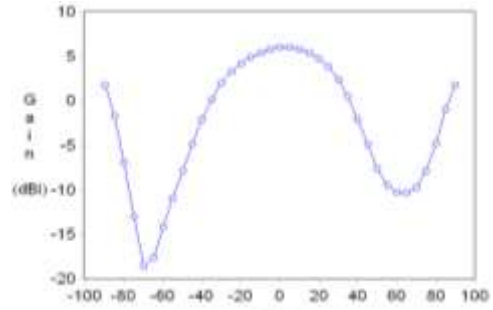


Figure 8. Radiation (Rectangular plot) pattern of the 8-elements rectangular microstrip array antenna.

B. Circular Microstrip Array Antenna Parameters

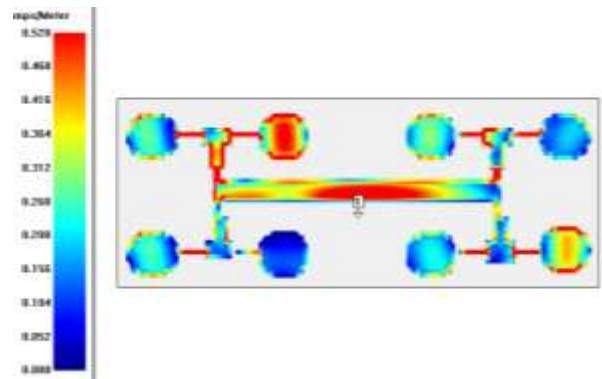


Figure 9. Current distribution of the 8-elements circular microstrip array antenna.

Here, the substrate permittivity of the antenna is 2.2 (Taconic TLY-5), height is 1.588 mm and resonance frequency of the antenna is 10 GHz. After simulation, as shown in Fig. 10, we found that, return loss is -4.96 dB at 10 GHz and it is maximum that is -6.91 dB at 9.8 GHz operating frequency. The simulated gain of the antenna, according to Fig. 11, is found around 7.21 dB at $\theta=0^\circ, \phi=0^\circ$ for the operating frequency 10 GHz.

Fig. 12 shows that the HPBW and the FNBW for this simulated antenna are in the range 89° and 130° respectively and Fig. 9 gives us the concept of current distribution of this array antenna which states that current density at each element of circular array antenna is much higher than that of the rectangular one as shown in Fig. 5.

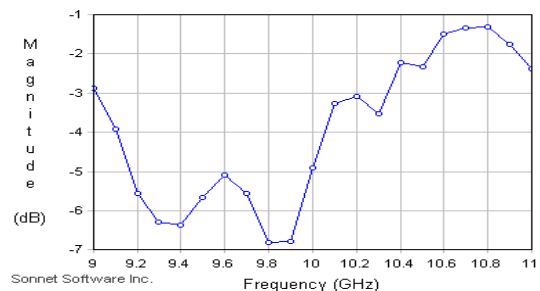


Figure 10. Return loss of the 8-elements circular microstrip array antenna.

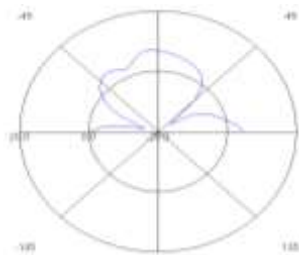


Figure 11. Radiation (polar plot) pattern of the 8-elements circular microstrip array antenna.

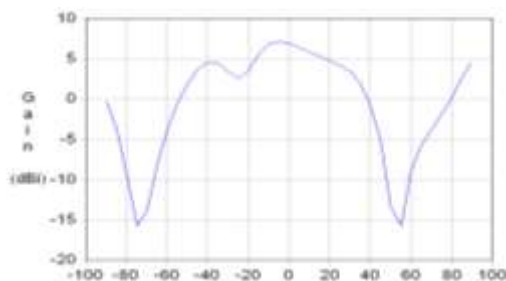


Figure 12. Radiation (rectangular plot) pattern of the 8-elements circular microstrip array antenna.

C. Comparison Between These two Array Antennas

After observing the performance analysis of both of these array antennas, it is convenient to say that the circular patch microstrip array antenna provides better performance than the rectangular patch Microstrip array antenna. Circular microstrip array antenna has the higher directive gain as well as the narrow beam width which seem to be a suitable criteria to design a transceiver antenna. Moreover its one degree of freedom to control reduce the design complexities. It also shows a remarkable achievements in case of current distribution. The current density for the rectangular microstrip array antenna, as shown in Fig. 5, at each patch element is not less than 0.12 amp/m and it is maximum up to 0.356 amp/m . Whereas the current density for the circular microstrip array antenna, as shown in Fig. 9, at each patch element is not less than 0.156 amp/m and it is maximum up to 0.52 amp/m . Thus the circular Microstrip array occupies lower transmission loss and it's the higher current density at each element provides better radiation efficiency than the rectangular microstrip array.

TABLE I. PERFORMANCE ANALYSIS BETWEEN RECTANGULAR AND CIRCULAR MICROSTRIP ARRAY ANTENNAS

Performance Parameter	Feeding Types	
	Rectangular (4x2)array	Circular (4x2)array
Physical area(mm ²)	95.6x34.2	92.8x35.82
Degree of freedom to control	Two	One
FNBW	142.10 ⁰	130 ⁰
Simulated gain(dB)	Around 6	7.21

Transmission line loss	Higher	Lower
Return loss(dB)	-25.21	-4.96

V. CONCLUSION

The unique feature of this microstrip antenna is its simplicity to get higher performance. In many applications basically in radar and satellite communication, it is necessary to design antennas with very high directive characteristics to meet the demand of long distance communication and the most common configuration to satisfy this demand is the array form of the microstrip antenna. After the rectangular patch the next most popular configuration is the circular patch and in our investigation, comparing the circular patch microstrip array antenna with the rectangular one, we have found that the circular microstrip array has some advantages such as small dimensions, light weight, higher directivity, higher current density and easy manufacturing. The physical area of the circular patch is 16% less than that of the rectangular patch [5].

Here designed array antennas covers 10 GHz operating frequency and it would also be possible to design the bands, operating any other system such as in WLAN, WiMax, WBAN or other wireless systems, by changing the dimension of the patch element. In future, we can investigate the spiral elements which seems to have more radiation efficiency for both the series feed and corporate feed networks and at the same time we can merge two different patch elements operating at two or more different frequencies by using quarter wavelength transformer method within an array network configuration to get multiband support.

REFERENCES

- [1] R. J. Mailloux, J. F. McIlvanna, N. P. Kernweis, "Microstrip array technology", IEEE Trans. Antenna Propagation Magazine, Vol. 29, No. 1, pp. 25-27, 1981.
- [2] C. A. Balanis, Antenna Engineering, 2nd ed., Wiley, 1982.
- [3] T. A. Millikgan, Modern Antenna Design, 2nd ed. , IEEE Press, John Wiley & Sons inc., 2007.
- [4] M. I. Skolnik, Introduction to RADAR System, 3rd ed., McGraw Hill Higher Education, 2000.
- [5] R. Garg, P. Bhartia, I. Bahl, A. Ittipiboon, Microstrip Antenna Design Handbook, Artech House inc., 2001.
- [6] R. J. Milloux, Electronically Scanned Arrays, Morgan & Claypool, 2007.
- [7] W. L. Stutzman , "Estimating directivity and gain of antennas", IEEE Antennas and Propagation Magazine, Vol. 40, No. 4,pp 7-11, August, 1998.
- [8] H. J. Visser, Array and Phased Array Antenna Basics, John Wiley & Sons Ltd., 2005.
- [9] Muhammad Mahfuzul Alam, Md. Mustafizur Rahman Sonchoy, and Md. Osman Goni, "Design and Performance Analysis of Microstrip Array Antenna", Progress In Electromagnetic Research Symposium Proceedings, Moscow, Russia, August 18-21, 2009.
- [10] Md. Shihabul Islam and Md. Tanvir Ishtaique-ul Huque, "Design and Performance Analysis of Microstrip Array Antenna", B.Sc.

Engineering thesis, Dept. of ETE, Rajshahi University Of Engineering & Technology(RUET), Rajshahi, Bangladesh, April, 2010.

- [11] Gi-cho Kang, Hak-young Lee, Jong-kyu Kim, Myun-joo Park, "Ku-band High Efficiency Antenna with Corporate-Series-Fed Microstrip Array", IEEE Antennas and Propagation Society International Symposium, 2003.
- [12] T. F. Lai, Wan Nor Liza Mahadi, Norhayatision, "Circular Patch Microstrip Array Antenna for KU-band", World Academy of Science, Engineering and Technology, vol. 48, pp. 298-302, 2008.
- [13] K. Shambavi, C. Z. Alex , T. N. P. Krishna, "Design and Analysis of High Gain Millimeter Wave Microstrip Antenna Array for Analysis of High Gain Millimeter Wave Microstrip Antenna Array for Wireless Application", Journal of Applied Theoretical and Information Technology(JATIT), 2009.
- [14] Asghar Keshtkar, Ahmed Keshtkar and A. R. Dastkhosh, "Circular Microstrip Patch Array Antenna for C-Band Altimeter System", International Journal of Antenna and Propagation, article ID 389418, doi:10.1155/2008/389418, November, 2007.
- [15] M. F. Islam, M. A. Mohd. Ali, B. Y. Majlis and N. Misran, "Dual Band Microstrip Patch Antenna for Sar Applications", Australian Journal of Basic and Applied Sciences, 4(10): 4585- 4591, 2010.
- [16] http://en.wikipedia.org/wiki/X_band

AUTHORS PROFILE

Md. Tanvir Ishtaique-ul Huque was born in 1988 in Bangladesh. He received his B.Sc. Engineering degree from the Rajshahi University of

Engineering & Technology (RUET) in 2010. Now he is working as a part time teacher in the Dept. of Electronics and Telecommunication Engineering of RUET. His research interests include the antenna application of the wireless body area network(WBAN) and next generation wireless communication system.

Md. Al-Amin Chowdhury was born in 1988 in Bangladesh. he has completed his B.Sc. in Electronic and Telecommunication Engineering from Rajshahi University of Engineering & Technology(RUET) in 2010. He has keen interest to research on the optical fiber, different types of antennas. He wants to do his further study in USA on the communication field. World is becoming closer and closer due to the remarkable achievements in the communication field. He wants to receive the sound and proper knowledge in communication field so that he can contribute to the next generation demands in the communication sectors.

Md. kamal Hosain was born in 1982 in Bangladesh. He received his B.Sc. Engineering degree from the khulna University of Engineering & Technology(KUET) in 2001 and now he working as a Lecturer in the Dept. of Electronics and Telecommunication Engineering(ETE) of RUET. His research interests include the antenna and its application on the biomedical devices.

Md. Shah Alam was born in Rangpur, Bangladesh, on June 24, 1982. He received the B.Sc. degree in Electrical and Electronic Engineering from Rajshahi University of Engineering & Technology, Rajshahi, Bangladesh, in 2006. He is going to be completed his M.SC degree from the same institution on July, 2011. From 2007 to 2009, he was a Lecturer with the Rajshahi University of Engineering & Technology, Rajshahi, Bangladesh and currently he is working there as an Assistant Professor. His research interests involve Electromagnetic and Nanotechnology.

A Comparative Study of various Secure Routing Protocols based on AODV

Dalip Kamboj

Department of Information Technology,
MMEC, Maharishi Markandeshwar University,
Mullana, Haryana, India

Pankaj Kumar Sehgal

Department of Information Technology,
MMEC, Maharishi Markandeshwar University,
Mullana, Haryana, India

Abstract— The paper surveyed and compared various secure routing protocols for the mobile ad hoc networks (MANETs). MANETs are vulnerable to various security threats because of its dynamic topology and selfconfigurable nature. Security attacks on ad hoc network routing protocols disrupt network performance and reliability. The paper significantly based on base routing protocol AODV and Secure protocol based on AODV. The comparison between various secure routing protocols has been made on the basis of security services and security attacks. From the survey it is quite clear that these protocols are vulnerable to various routing attacks. A multifence secure routing protocol is still required to fulfill the basic security services and provide solution against various attacks.

Keywords—ad hoc network; basic security services; security attack.

I. INTRODUCTION

Wireless networks have become increasingly popular in the past few decades, particularly with in the 1990's when they are being adapted to enable mobility and wireless devices became popular. Networks that support the ad hoc architecture are typically called wireless ad hoc networks or mobile ad hoc networks [1]. Such networks are typically assumed to be self-forming and selfhealing. This is because the typical applications of such networks require nodes to form networks quickly without any human intervention. Given the wireless links and mobility of nodes, it is possible that nodes may lose connectivity to some other nodes. This can happen if the nodes move out of each other's transmission range. As a result, it is possible for portions of the network to split from other portions of the network. In some applications it is also possible that some nodes may get completely disconnected from the other nodes, run out of battery, or be destroyed. For these reasons, nodes in a MANET cannot be configured to play any special role either in the way nodes communicate or in the way of providing communication services. This leads to a symmetric architecture where each node shares all the responsibilities. The network needs to be able to reconfigure itself quickly to deal with the disappearance (or reappearance) of any node and continue operating efficiently without any human intervention. Routing in such networks is particularly challenging because typical routing protocols do not operate efficiently in the presence of frequent movements, intermittent connectivity, network splits and joins. In typical routing protocols such events generate a large amount of overhead and require a significant amount of time to reach stability after some of those events.

Routing is an important function in any network [1], be it wired or wireless. The protocols designed for routing in these two types of networks, however, have completely different characteristics. Routing protocols for wired networks typically do not need to handle mobility of nodes within the system. These protocols also do not have to be designed so as to minimize the communication overhead, since wired networks typically have high bandwidths. Very importantly, the routing protocols in wireline networks can be assumed to execute on trusted entities, namely the routers. These characteristics change completely when considering ad hoc wireless networks. In ad hoc network the device will have to act a router as well. Ad hoc wireless network routing protocols [2] can be classified into the three major categories viz table driven routing protocol, reactive or on-demand driven routing protocol and hybrid routing based on the routing information update mechanism. In the table driven routing protocols, every node maintains the network topology information in the form of routing tables by periodically exchanging routing information. Routing information is generally flooded in the whole network. Whenever a node requires a path to a destination, it runs an appropriate path-finding algorithm on the topology information it maintains. For example DSDV [5], WRP [6], CGSR [7], STAR [8], OLSR [9], FSR [10], HSR [10] and GSR [11]. The Reactive or On-demand routing protocols do not maintain the network topology information. They obtain the necessary path when it is required, by using a connection establishment process. Hence these protocols do not exchange routing information periodically. For example DSR [12], AODV [13], ABR [14], SSA [15], FORP [16], PLBR [17]. The Hybrid routing protocols combine the best features of the above two categories. Nodes within a certain distance from the node concerned, or within a particular geographical region, are said to be within the routing zone of the given node. For routing within this zone, a table-driven approach is used. For example CEDAR [18], ZRP [19] and ZHLS [20].

The above protocols do not provide any security mechanism against basic security services viz authentication, confidentiality, integrity, authentication, non-repudiation and availability. These protocols are also vulnerable to various security attacks such as Rushing attack, Sybil attack, Black Hole attack, Wormhole attack, Blackmail attack, Replay attack and Routing table poisoning attack. Many protocols have been introduced to provide basic security services and mitigate against security attacks. For example SAODV [21], SAR [23],

A-SAODV [24], MS-AODV [25], RAODV [26], TAODV [27], ISAODV [28] and SecAODV [29], SRPM [3], SecureAODV [4] and CBRP [22].

The rest of the paper explained as follow. The section II provides the information of the base routing protocol i.e. Ad hoc on demand distance vector routing protocol (AODV). The section III provides the information of secure routing protocol based on AODV. The section IV describes the comparisons based on basic security services. The section V describes the comparison on basis of various security attacks. The section VI describes the conclusion of this paper.

II. AD-HOC ON-DEMAND DISTANCE VECTOR ROUTING (AODV)

AODV was an improvement on DSDV [5] because it typically minimizes the number of required broadcasts by creating routes on a demand basis. AODV [13] routing protocol uses reactive approach for finding routes, that is, a route is established only when it is required by any source node to transmit data packets. The protocol uses destination sequence numbers to identify the recent path. The source node and the intermediate nodes store the next node information corresponding to each data packet transmission. The source node floods the Route REQuest (RREQ) packet in the network when a route is not available for the desired destination. It may obtain multiple routes to different destinations from a single RREQ. A node updates its path information only if the destination sequence number of the current packet received is greater than the last destination sequence number stored at the node. A RREQ carries the destination identifier(DestID), the source identifier(SrcID), the source sequence number (SrcSeqNum) and destination sequence number (DestSeqNum), the broadcast identifier (BcastID), and the time to live (TTL) field. DestSeqNum shows the freshness of the route that is selected by the source node. When an intermediate node receives a RREQ, it either forwards it or prepares a route reply (RREP) if it has a valid route to the destination. The validity of a route at the intermediate node is determined by comparing the sequence number at packet. If a RREQ is received multiple times, which is indicated by BcastID-SrcID pair, then the duplicate copies are discarded. A timer is used to delete this entry in case a RREP is not received before the timer expires. This helps in storing an active path at the intermediate node as AODV does not employ source routing of the data packets like DSR [12]. When a node receives a RREP packet, information about the previous node from which the packet was received is also stored in order to forward the data packet to this next node as the next hop towards the destination.

III. SECURE ROUTING PROTOCOLS BASED ON AODV

Although there are several some routing protocol are based on AODV. Some are selected for survey and comparison for this paper. There are SAODV, A-SAODV, MS-AODV,

RAODV, TAODV, ISAODV and SecAODV. The following subsections describe the protocols in detail.

A. Secure Ad-hoc on demand distance vector Routing (SAODV)

A secure version of AODV [13] called Secure AODV (SAODV). It provides features such as integrity, authentication, and nonrepudiation of routing data. It incorporates two schemes for securing AODV. The first scheme involves nodes signing the messages e.g. Route Request (RREQ), Route Reply (RREP). This allows other nodes to verify the originator of the message. This scheme can be used for protecting the portion of the information in the RREQ and RREP messages that does not change once these messages are created. However, RREQ and RREP messages also contain a field (namely the hop count) that needs to be changed by every node. Such mutable information is ignored by the creator of the message when signing the message. The second scheme of SAODV [21] is used for protecting such mutable information. This scheme leverages the idea of hash chains. Signing routing messages implies that the various nodes need to possess a key pair that makes use of an asymmetric cipher. In addition, nodes in the network also need to be aware of the authentic public keys of the other nodes.

B. Security Aware Ad hoc Routing (SAR)

SAR [23] protocol integrates the trust level of a node and the security attributes of a route to provide the integrated security metric for the requested route. A Quality of Protection (QoP) vector used is a combination of security level and available cryptographic techniques. It uses the timestamps and sequence numbers to stop the replay attacks. Interception and subversion threats can be prevented by trust level key authentication. Attacks like modification and fabrication can be stopped by verifying the digital signatures of the transmitted packet. The main drawbacks of using SAR are that it required excessive encrypting and decrypting at each hop during the path discovery. The discovered route may not be the shortest route in the terms of hop-count, but it is secure.

C. Adaptive SAODV (A-SAODV)

A-SAODV [24] optimizes the routing performance of secured protocols with help of a threshold mechanism. A-SAODV is a multithreaded application. In that protocol the cryptographic operations are performed by a dedicated thread to avoid blocking the processing of other message and other thread to all other functions. Every node has queue of routing message to be signed or verify and the length of the queue implies the load state of the routing thread. Whenever a node processes a route request and has enough information to generate a RREP on behalf of destination, it first checks its routing message queue length. If the length of the queue is below a threshold then it reply otherwise, it forwards the RREQ without replying. The value of threshold can be changed during execution. The A-SAODV [24] also maintains a cache of latest signed and verified message in order to avoid signing and verifying the same message twice. This adaptive reply decision has a significant improvement on the performance of SAODV [21].

D. More Stable Ad-hoc On-demand Distance Vector Routing (MS-AODV)

MS-AODV [25] works according to existing AODV [13] in case of sending RREQ and REPLY packets. Packet formats are almost same. For measuring stability added some extra fields in the neighbor management table of the node and in the packets. In MS-AODV the forward path and reverse path setup are almost same as existing AODV [13] with a difference that Forward path setup is delayed. Each node stores its all neighbor's stability in Neighbor Management Table. Stability measurement is based on path stability which outperforms over all other parameters of stability measurement. Before sending data packet into the Reverse Path Setup, AODV [13] protocol discovers the routing path from source to destination. Source broadcasts RREQ packets to its neighbors and these packets are forwarded from node to node until the desired destination receives this packet. As the node forwards packets it updates its routing table as well as its stability table which is used for comparing stability of adjacent links. Thus several reverse paths are created from source to destination. Into the MS-AODV [25] the Forward Path Setup is different from existing AODV [13] protocol. In existing AODV, the destination sends REPLY packet as soon as it receives first RREQ packet. But in MS-AODV [25], as the destination needs to determine the most stable path, it needs to wait for a short while so that it can receive RREQ packet within this period as much as possible. RREQ packets arrive through multiple paths between source and destination. In each RREQ packet, the destination gets the cumulative stability of the path from the source to the destination. After comparing those values, the destination decides which path to be used for data communication and hence sends a REPLY packet to that path in reverse direction.

E. Reliable Ad-hoc On-demand Distance Vector Routing (RAODV)

The existing AODV [13] has been extended to RAODV [26] by adding two types of control packets: Reliable Route Discovery Unit (RRDU) and RRDU Reply (RRDU_REP). The RRDU messages are control packets sent by the source node along with RRDU-ID, to the destination at regular intervals and RRDU_REP message is the response of RRDU by the destination to the source node. RRDU_REP can only be generated by the destination. There is no impersonation i.e. no node other than the destination, can generate RRDU_REP on behalf of the destination. Reliability List (RL) field is also adding in the routing table entry. An entry in the RL has Source address, a field called Forward Data Packet Count (FDPC) and RRDU-ID, i.e. the triplet (Source address, FDPC, RRDU-ID). The Routing Table entry format of RAODV is same as that of AODV [13] except for the additional RL field. RAODV uses RREQ, RREP messages for route discovery and RERR, HELLO messages for route maintenance which is similar in AODV [13]. In addition, RAODV also uses RRDU and RRDU_REP to help discover the path and for reliability maintenance. In RAODV [26] the path discovery can be thought of as consisting of two phases. The phase I is same as AODV [13]. Whenever a node wishes to communicate with another node it looks for a route in its table. If a valid entry is found for the destination it uses that path else the node

broadcasts the RREQ to its neighbors to locate the destination. The neighbor nodes again broadcast RREQ to their neighbors. The process continues until either the destination or an intermediate node with a fresh route to the destination is located. A reverse path is created for the source at each intermediate node. It must be noted that several reverse paths may be created in this process. The source receives RREPs from all these paths. But in AODV [13], it selects the one with minimum hop count and others are discarded. But in Phase II the source node sends an RRDU packet to all the nodes from which it gets the RREPs. Now since replies to RRDU, i.e. RRDU_REP packets are generated only by the destination and there is no impersonation, the source node will receive a unique RRDU_REP and the path discovery is completed.

F. Trusted Ad-hoc On-demand distance vector Routing (TAODV)

TAODV [27] is secure routing protocol which uses cryptography technologies recommended to take effect before nodes in the establish trust relationships among one another. The main salient feature of TAODV [27] is that using trust relationships among nodes, there is no need for a node to request and verify certificates all the time. TAODV (Trusted AODV) has several salient features: (1) Nodes perform trusted routing behaviors mainly according to the trust relationships among them; (2) A node who performs malicious behaviors will eventually be detected and denied to the whole network. (3) The performance of the System is improved by avoiding requesting and verifying certificates at every routing step. That protocol greatly reduces the computation overheads. Assume that the keys and certificates needed by these cryptographic technologies have been obtained through some key management procedures before the node performs routing behaviors. Some extra new fields are added into a node's routing table to store its opinion about other nodes' trustworthiness and to record the positive and negative evidences when it performs routing with others. The main advantages of embedding trust model into the routing layer of MANET, save the consuming time without the trouble of maintaining expire time, valid state, etc. which is important in the situation of high node mobility and invalidity. Trusted AODV [27] are mainly three modules in the whole TAODV system: basic AODV [13] routing protocol, trust model, and trusted AODV routing protocol. Based on trust model, the TAODV routing protocol contains such procedures as trust recommendation, trust combination, trust judging, cryptographic routing behaviors, trusted routing behaviors, and trust updating.

G. Intrusion Detection Ad-hoc On-demand distance vector Routing (ISAODV)

The Intrusion Detection Systems (IDS) has been used for the support of secure Ad Hoc On Demand Distance Vector (AODV) routing, named IDS-based Secure AODV (IS-AODV [28]), in wireless ad hoc and vehicular network scenarios. The (IS-AODV) is based on the detection of behavior anomalies on behalf of neighbor hosts, with passive reactions, aiming to create a cluster whose route paths will include only safe nodes, eventually. That protocol is implemented by adopting an IDS solution and the concept of Statistically Unique and Cryptographically Verifiable (SUCV) identifiers, for IPv6-

based MANETs. IS-AODV [28] is based on SUCV and mutual verification of nodes behaviors during the path creation process. SUCV identifiers (or Crypto-based IDs, CBIDs) are used to realize a secure binding between IPv6 addresses and cryptography keys, without requiring any trusted Certification Authority (CA) or a Key Distribution Center (KDC). IS-AODV is different from SecAODV [29], because it uses the IDS as the basis for the implementation of secure AODV routing. In IS-AODV, in order to control the behavior of neighbors during the route discovery and data forwarding phases, each node monitors the traffic whose path includes the node itself: when a node N perceives a suspect behavior from a neighbor host, the IDS reaction is passive, that is, the information is not advertised to local nodes, and the node N does not rely/assist any suspect neighbor-node communication. In addition, unlike SecAODV [29], the ISAODV scheme does not require any cryptography operation in the intermediate nodes. The IS-AODV mechanism introduces a low-overhead additional field for standard AODV [13] Route Request (RREQ) and Route Reply (RREP) messages. A public key cryptography is used by end-nodes only (possibly replaced by more lightweight symmetric cryptography, after a safe path is found), to verify the signature of routing and data packets. This allows the end-to-end packet verification.

H. Secure AODV (SecAODV)

SecAODV and the snooping IDS complement each other in being able to detect most of the prevalent attacks. SecAODV [29] is a highly adaptive distributed algorithm designed for IPv6-based MANETs that does not require: (1) prior trust relations between pairs of nodes (e.g. a trusted third party or a distributed trust establishment), (2) time synchronization between nodes, or (3) prior shared keys or any other form of secure association. The protocol provides on-demand trust establishment among the nodes collaborating to detect malicious activities. A trust relationship is established based on a dynamic evaluation of the sender's "secure IP" and signed evidence, contained in the SecAODV [29] header. This routing protocol enables the source and destination nodes to establish a secure communication channel based on the concept of "Statistically Unique and Cryptographically Verifiable" (SUCV). The SecAODV implements two concepts. (1) Secure binding between IPv6 addresses and the RSA key generated by the nodes themselves, and independent of any trusted security service (2) Signed evidence produced by the originator of the message and signature verification by the destination, without any form of delegation of trust. The SecAODV protocol adds security features to the basic AODV [13] mechanisms, but is otherwise identical. A source node S that requests communication with another member of the MANET referred to as destination initiates the process by constructing and broadcasting a signed route request message

RREQ. Upon successful verification, the node updates its routing table with S's address and the forwarding node's address. If the message is not addressed to it, it rebroadcasts the RREQ. When D receives the RREQ, it constructs a signed route reply message (RREP) addressed to then source node S, which includes the D's public key.

IV. COMPARISONS ON BASIC SECURITY SERVICES

The table I provide a comparison on basic security services viz Confidentiality, Integrity, Authentications, Nonrepudiation and Availability. The Confidentiality ensures that certain information is only readable or accessible by the authorized [30] party. Basically, it protects data from passive attacks. The principal of confidentiality specifies that only the sender and the recipients should be able to access the contents of a message. Confidentiality gets compromised if an unauthorized person is able to access a message. The Integrity defines when the contents of the message are changed after the sender sends it, but before it reaches the intended recipient, we say that the integrity of message is lost. Integrity [30] guarantees that the authorized parties are only allowed to modify the information or messages. It also ensures that a message being transmitted is never corrupted. As with confidentiality, integrity [1] can apply to a stream of messages, a single message or selected fields within a message. The Authentication [30] ensures that the access and supply of data is done only by the authorized parties. Authentications mechanisms help establish proof of identities. It is concerned with assuring that a communication is authentic. In the case of a single message, such as a warning or alarm signal, the function is to assure the recipient that the message is from the source that it claims to be from. Without authentication [1], an adversary could masquerade as a node, thus gaining unauthorized access to resource and sensitive information and interfering with the operations of the other nodes. The authentication process ensures that the origin of an electronic message or document is correctly identified. The Nonrepudiation are the situations [30] where a user sends a message and later on refuses that she had sent that message. Nonrepudiation prevents either sender or receiver from denying a transmitted message. Thus, when a message is sent, the receiver can prove that the message was in fact sent by the alleged sender. On the other hand, after sending a message, the sender can prove that the message was received by the alleged receiver. Nonrepudiation is useful for detection and isolation of compromised nodes. The Availability defines the network resources should be available to authorized entities without excessive delays. The principle of the availability [1] states that resources should be available to authorized parties at all times. For example, due to the intentional actions of an unauthorized user C, and authorized user A may not be contact a server computer B. This would be defeat the principle of availability.

TABLE I. COMPARISON STUDY BASED ON BASIC SECURITY SERVICES

Performance Parameters type	SAODV [21]	A-SAO DV [24]	MS-AODV [25]	RAO DV [26]	TAO DV [27]	ISAOD V [28]	SAR [23]
Central trust authority	CA required	CA required	NOT required	NOT required	NOT required	NOT required	CA/KDC required
Authentication	Yes	Yes	No	Yes	Yes	Yes	Yes
Confidentiality	No	No	No	No	No	Yes	Yes
Integrity	Yes	Yes	No	Yes	Yes	Yes	Yes
Nonrepudiation	Yes	Yes	No	Yes	Yes	Yes	Yes
Availability	No	No	No	No	No	No	No

V. COMPARISONS ON BASIS OF VARIOUS SECURITY ATTACKS

The table II provides a comparison study based on various security attack viz rushing attack, Sybil attack, black hole attack, wormhole attack, Blackmail attack, replay attack and Routing table poisoning. There are various types of attacks on ad hoc network which are describing following: In Rushing attack [1], the attacker simply forwards all control packets (but not data packets) received at one node (the attacker) to another node in the network. The rushing attacker may employ a wormhole to rush packets. This attack [2] impacts more on reactive routing protocol. The protocol defends it by using randomized selection of route request message. Every node is expected to collect a threshold number of route requests. The Sybil attack assumed that every physical device has only one radio and device is incapable of simultaneously transmitting and receiving on more than one channel. The node allocates a channel to each of its neighbors to verify if any of its neighbors are Sybil [1] identities. The neighboring node is expected to transmit a message on the allocated channel. The verifier node then picks random channels for listening. If no message is heard on the channel selected then the corresponding node identity is assured to be a Sybil identity. In a Black hole attack a malicious node injects false route replies to the route requests it receives, advertising itself as having the shortest path to a destination [31]. These fake replies can be fabricated to divert network traffic through the malicious node for eavesdropping, or simply to attract all traffic to it in order to perform a denial of service attack by dropping the received packets. A Wormhole attack typically requires the presence of at least two colluding nodes in an ad hoc network. The malicious nodes need to be geographically separated in order for the attack to be effective. In this attack, a malicious node captures packets from one location and “tunnels” these packets to the other malicious node, which is assumed to be located at some distance. The second malicious node is then expected to replay the “tunneled” packets locally. The Blackmail attack is relevant against routing protocols that use mechanisms for the identification of malicious nodes and propagate messages that try to blacklist the offender [32]. An attacker may fabricate such reporting messages and try to isolate legitimate nodes from the network. The security property of non-repudiation can prove to be useful in such cases since it binds a node to the messages it generated. A Replay attack occurs when an attacker copies a stream of messages between two parties and replays the stream to one or

more of the parties. Unless mitigated, the computers subject to the attack process the stream as legitimate messages, resulting in a range of bad consequences, such as redundant orders of an item. Routing table poisoning attack is classified as internal attack, as selfish node or set of misbehaving node implement this attack for purpose to save the battery life or exploit the routing.

TABLE II. COMPARISON STUDY BASE ON VARIOUS SECURITY ATTACKS

Security Attack	SAODV [21]	A-SAO DV [24]	MS-AOD V [25]	RAO DV [26]	TAO DV [27]	SAO DV [28]	SecAODV [29]	SAR [23]
Black-Hole	No	No	No	Yes	No	No	No	No
Wormhole	No	No	No	Yes	No	No	No	No
Blackmail	NA	NA	NA	NA	NA	NA	NA	NA
Denial of Services	No	No	No	No	No	No	No	No
Replay	Yes	Yes	Yes	Yes	Yes	Yes	Yes	Yes
Rushing attacks	No	No	No	Yes	No	No	No	No
Routing table poisoning	Yes	Yes	Yes	Yes	Yes	Yes	Yes	Yes

VI. CONCLUSION

Secure Routing is one of the most basic and important tasks in MANETs. This paper reviewed various secure routing protocols based on AODV. From the comparative studies it is quite clear that these protocols are vulnerable to various routing attacks.

It has been observed none of secure routing protocol provides the availability service. Two protocols ISAODV and SAR provide the Confidentiality, Integrity, Authentications, Nonrepudiation. Only one protocol MSAODV does not provide any basic security services.

All the secure protocols provides the protection against replay and routing table poisoning attack but does not provide the protection against black-hole attack, blackmail attack, rushing attack and DoS. Only RAODV provides the protection against black-hole attack, wormhole attack, rushing attack.

In nutshell, there is no single mechanism which can provide basic security services and protection against various security attacks. So, there is a requirement of a multifence mechanism which can provide basic security services as well mitigate against various security attacks.

REFERENCES

- [1] Farooq anjum and Petros Mouchtaris, "Security for wireless ad hoc networks," John Wiley, 2007.
- [2] C.Siva Ram Murthy and B. S. Manoj, "Ad hoc wireless networks: Architecture and Protocols". Prentice Hall Publishers, ISBN 013147023X, May 2004.
- [3] S. Khan and K.K. Loo, "SRPM Analysis in the Presence of Sinkhole attack in Hybrid Wireless Mesh Networks," In International Journal of Research and Reviews in Ad Hoc Networks Vol. 1, No. 1, March 2011.
- [4] Suman Deswal and Sukhbir Singh, "Implementation of Routing Security Aspects in AODV," In International Journal of Computer Theory and Engineering, Vol. 2, No. 1 February, 2010.

- [5] C. E. Perkins and P. Bhagwat, "Highly Dynamic Destination-Sequenced Distance-vector-Routing (DSDV) for Mobile Computers," SIGCOMM, UK, pages 234-244, 1994.
- [6] S. Murthy and J.J. Garcia-Luna-Aceves, "An Efficient Routing Protocol for Wireless Network", In ACM Mobile Networks and Applications Journal, Special Issue on Routing in Mobile Communication Networks, vol. 1, no. 2, pages 183-197, October 1996.
- [7] C. C. Chiang, H. K. Wu, W. Liu, and M. Gerla, "Routing in Clustered Multi-Hop Mobile Wireless Networks with Fading Channel," Proceedings of IEEE SICON 1997, pp. 197-211, April 1997.
- [8] J.J. Garcia-Luna-Aceves and M. Spohn, "Source-Tree Routing in Wireless Networks," Proceedings of IEEE ICNP, Pages 273-282, October 1999.
- [9] T. Clausen and P. Jacquet, eds, "Optimized Link State Routing Protocol (OLSR)," IETF RFC 3626, October 2003.
- [10] A. Iwata, C. C. Chaing, G. Pei, M. Gerla, and T.W. Chen, "Scalable Routing Strategies for Ad Hoc Wireless Networks," In IEEE Journal on Selected Areas in Communications, vol. 17, no. 8, pp. 1369-1379, August 1999.
- [11] T.W. Chen and M.Gerla, "Global state Routing: A New Routing Scheme for Ad Hoc Wireless Networks," Proceeding of IEEE ICC 1998, pp. 171-175, June 1998.
- [12] D. Johnson and D. Maltz., "Dynamic source routing in ad-hoc wireless networks routing protocols," In Mobile Computing, pages 153-181. Kluwer Academic Publishers, 1996.
- [13] C.E.Perkins and E.M.Royer, "Ad hoc On-Demand Distance Vector Routing," Proc. 2nd IEEE Workshop of Mobile Comp. Sys. and Apps., pages 90-100, Feb. 1999.
- [14] C.-K. Toh., "Associativity-based routing for ad-hoc mobile networks," Wireless Personal Communications, 4(2):103-139, 1997.
- [15] R.Dube, C.D.Rais, K.Y. Wang and S.K. Tripathi, "Signal Stability-Based Adaptive Routing for Ad Hoc Mobile Networks," IEEE Personal Communications Magazine, Pages 36-45, February 1997.
- [16] W. Su and M.Gerla, "IPv6 Flow Handoff in Ad Hoc Wireless Networks Using Mobility Prediction," Proceeding of IEEE GLOBECOM, Pages 271-275, December 1999.
- [17] R.S. Sisodia, B.S. Manoj, and C. Siva Ram Murthy, "A Preferred Link-Based Routing Protocol for Ad Hoc Wireless Networks," In Journal of Communication and Networks, vol. 4, no. 1, pp. 14-21, March 2002.
- [18] P. Sinha, R. SivaKumar, and V. Bharghavan, "CEDAR : A Core Extraction Distributed Ad Hoc Routing Algorithm," In IEEE Journal on Selected Areas in Communications, vol. 17, no. 8, pp. 1454-1466, August 1999.
- [19] Z. J. Haas, "The Routing Algorithm for the Reconfigurable Wireless Networks," Proceedings of ICUPC 1997, vol. 2. pp. 562-566, October 1997.
- [20] M. Joa-Ng and I. T. Lu, "A Peer-to-Peer Zone Based Two Level Link State Routing for Mobile Ad Hoc Networks," IEEE Journal on Selected Areas in Communications, vol. 17, no. 8, pp. 1415-1425, August 1999.
- [21] Manel Guerrero Zapata, "Secure Ad hoc On-Demand Distance Vector (SAODV) Routing," draft-guerrero-manet-saodv-06.txt, September 5, 2006.
- [22] Seyed Amin Hosseini Seno, Rahmat Budiarto and Tat-Chee Wan, "A Secure Mobile Ad hoc Network Based on Distributed Certificate Authority," In King Fahd University of Petroleum and Minerals 2010, 15 January 2011.
- [23] R. Kravets, S. Yi, and P. Naldurg, "A Security-Aware Routing Protocol for Wireless Ad Hoc Networks," In ACM Symp. On Mobile Ad Hoc Networking and Computing, 2001.
- [24] R Alekha Kumar Mishra and Bibhu Dutta Sahoo, "A Modified Adaptive-Saodv Prototype For Performance Enhancement In Manet," In International Journal Of Computer Applications In Engineering, Technology And Sciences (Ij-Ca-Ets), Volume 1 : Issue 2 , Page: 443, April '09 – September '09.
- [25] Tamanna Afroze, Saikat Sarkar, Aminul Islam and Asikur Rahman, " More Stable Ad-hoc On-Demand Distance Vector Routing Protocol," In 978-1-4244-2800-7/09/\$25.00 ©2009 IEEE.
- [26] Sandhya Khurana, Neelima Gupta and Nagender Aneja, "Reliable Ad-hoc On-demand Distance Vector Routing Protocol," In Proceedings of the International Conference on Networking, International Conference on Systems and International Conference on Mobile Communications and Learning Technologies (ICNICONSMCL'06) 0-7695-2552-0/06 \$20.00 © 2006 IEEE.
- [27] Xiaoqi Li, Michael R. Lyu, and Jiangchuan Liu, "A Trust Model Based Routing Protocol for Secure Ad Hoc Networks," In IEEEAC, 0-7803-8155-6 © 2004 IEEE.
- [28] Luciano Bononi and Carlo Tacconi, "Intrusion detection for secure clustering and routing in Mobile Multi-hop Wireless Networks," In © Springer-Verlag Published online: 10 July 2007.
- [29] Anand Patwardhan , Jim Parker, Anupam Joshi, Michaela Iorga and Tom Karygiannis, "Secure Routing and Intrusion Detection in Ad Hoc Networks," To appear in the Proceedings of the 3rd International Conference on Pervasive Computing and Communications (PerCom 2005), Kauai Island, Hawaii, 2005.
- [30] Atul Kahate, Cryptography and Network Security, Tata Mcgraw Hill Education private Limited, 2008.
- [31] Mohammad Al-Shurman and Seong-Moo Yoo, Seungjin Park, "Black Hole Attack in Mobile Ad Hoc Networks," ACMSE'04, April 2-3, 2004, Huntsville, AL, USA.
- [32] Patroklos g. Argyroudīs and donal o'mahony, "Secure Routing for Mobile Ad hoc Networks," IEEE Communications Surveys & Tutorials Third Quarter 2005.

The threshold EM algorithm for parameter learning in bayesian network with incomplete data

Fradj Ben Lamine

Department of computer science
Faculty of science of Monastir
Monastir – Tunisia

Karim Kalti

Department of computer science
Faculty of science of Monastir
Monastir – Tunisia

Mohamed Ali Mahjoub

Preparatory Institute of Engineer of
Monastir
Monastir – Tunisia

Abstract—Bayesian networks (BN) are used in a big range of applications but they have one issue concerning parameter learning. In real application, training data are always incomplete or some nodes are hidden. To deal with this problem many learning parameter algorithms are suggested foreground EM, Gibbs sampling and RBE algorithms. In order to limit the search space and escape from local maxima produced by executing EM algorithm, this paper presents a learning parameter algorithm that is a fusion of EM and RBE algorithms. This algorithm incorporates the range of a parameter into the EM algorithm. This range is calculated by the first step of RBE algorithm allowing a regularization of each parameter in bayesian network after the maximization step of the EM algorithm. The threshold EM algorithm is applied in brain tumor diagnosis and show some advantages and disadvantages over the EM algorithm.

Keywords- bayesian network; parameter learning; missing data; EM algorithm; Gibbs sampling; RBE algorithm; brain tumor.

I. INTRODUCTION

Machine Learning is now considered among the essential tools for making decisions and solving problems that affect the uncertainty. This science allows automation of methods that helps the expert to take an effective decision in several areas. This work is functional by means of artificial intelligence that combines the concepts of learning, reasoning and problem-solving. In recent years, Bayesian networks have become important tools for modeling uncertain knowledge. They are used in various applications such as information retrieval [6], data fusion [5], bioinformatics [11], and medical diagnostics [2].

Bayesian networks [(Jensen, 1996)] are graphical models that can apply these concepts in daily life by modeling a given problem as a causal structure as a graph indicating the independence between the different actors of the problem and using qualitative state which is in the form of conditional probability tables. The clarity of the semantics and comprehensibility by humans are the major advantages of using Bayesian networks for modeling applications. They offer the possibility of causal interpretation of models of learning.

The concepts of learning in bayesian network are devised into two types; the first one is to learn the parameters when the structure is known. The second one is to learn the structure and the parameters at the same moment. In this paper, we assume that the structure is known. The parameter learning in this case is divided into two categories. If the training data are

complete this problem is resolved by statistic approach or a bayesian approach. In real application, to find complete training data is difficult for various reasons. When data are incomplete two classical approaches are usually used to determine the parameters of a bayesian network that include EM algorithm [1] and Gibbs Sampling [3].

Other methods are suggested to deal with the disadvantages of these classical approaches. The most robust is the RBE algorithm [8]. In order to regularize the learning problem, some modifications are needed to reduce the search space and help escape from local maxima.

These problems in learning parameter in bayesian network motivate us to add some modification in the existing parameter learning algorithm where the network structure is known and the data are incomplete.

II. LEARNING BAYESIAN NETWORK PARAMETERS

A bayesian network is defined by a set of variables $\chi = \{X_1, X_2, \dots, X_n\}$ that represent the actors of the problem and a set of edge that represent the conditional independence between these variables. If there is an arc from X_i to X_j then X_i is called parent of X_j and is noted by $pa(X_j)$. Each node is conditionally independent from all the other nodes given its parents. The conditional distribution of all nodes is described as:

$$P(\chi) = \prod_{i=1}^n P(X_i | pa(X_i)) \quad (1)$$

Each node is described by a conditional probability table which we denote by the vector θ . The entire vector is composed by a set of parameters value $\theta_{i,j,k}$ and it's defined by:

$$\theta_{i,j,k} = P(X_i = x_k | pa(X_i) = x_j) \quad (2)$$

Where $i=1 \dots n$ represents the range of all variables, $k=1 \dots r_i$ describes all possible states taken by X_i and $j=1 \dots q_i$ ranges all possible parent configurations of node X_i .

The process of learning parameters in bayesian network is discussed in many papers. The goal of parameter learning is to find the most probable θ that explain the data. Let $D = \{D_1, D_2, \dots, D_N\}$ be a training data where $D_1 = \{x_1[1], x_2[1], \dots, x_n[1]\}$ consists of instances of the bayesian network nodes. Parameter learning is quantified by the log-likelihood function denoted as

$L_D(\theta)$. When the data are complete, we get the following equations:

$$L_D(\theta) = \log \left\{ \prod_{l=1}^N P(x_1[l], x_2[l], \dots, x_n[l]; \theta) \right\} \quad (3)$$

$$L_D(\theta) = \log \left\{ \prod_{i=1}^n \prod_{l=1}^N P(x_i[l] | pa(x_i[l]); \theta) \right\} \quad (4)$$

The equation (3) and (4) are not applied where the training data is incomplete.

A. Learning parameter with complete data

In the case where all variables are observed, the simplest method and most used is the statistical estimate. It estimates the probability of an event by the frequency of occurrence of the event in the database. This approach (called maximum likelihood (ML)) then gives us:

$$P(X_i = x_k | pa(X_i) = x_j) = \theta_{i,j,k} = \frac{N_{i,j,k}}{\sum_k N_{i,j,k}} \quad (5)$$

Where $N_{i,j,k}$ is the number of events in the database for which the variable X_i is in state x_k and his parents are in the configuration x_j .

The principle, somewhat different, the Bayesian estimation is to find parameters most likely knowing that the data were observed. Using a Dirichlet distribution as a priori parameters which are written as:

$$P(\theta) \propto \prod_{i=1}^n \prod_{j=1}^{q_i} \prod_{k=1}^{r_i} \theta_{i,j,k}^{\alpha_{i,j,k}-1} \quad (6)$$

where $\alpha_{i,j,k}$ are the parameters of the Dirichlet distribution associated with the prior distribution.

The approach to maximum a posteriori (MAP) gives us:

$$P(X_i = x_k | pa(X_i) = x_j) = \theta_{i,j,k} = \frac{N_{i,j,k} + \alpha_{i,j,k} - 1}{\sum_k N_{i,j,k} + \alpha_{i,j,k} - 1} \quad (7)$$

B. Learning parameter with incomplete data

In most applications, databases are often incomplete. Some variables are observed only partially or never. The classical approaches are EM, Gibbs sampling and RBE algorithms. These algorithms are approximate except RBE which determinate a low bound and an upper bound for each parameter in the bayesian network.

The method of parameter estimation with incomplete data and the most commonly used is based on the iterative Expectation-Maximization (EM) proposed by Dempster [1] and applied to the RB in [7].

The EM above is as follows: repeat the steps expectation and maximization until the convergence. Each iteration ensures that the likelihood function increases and eventually converges to a local maximum. By cons, when we have multiple nodes admitting a large number of missing

data, the method of learning by the EM method converges quickly to a local maximum. In the first step, the algorithm starts by depending arbitrary quantities on missing data. The second steps consist of employing the expectation entries and maximizing them with respect to the unknown parameters. The results of the second step are used as arbitrary quantities in the next expectation step. The algorithm converges when the difference between successive estimates is smaller than a fixed threshold or the number of iterations is bigger than a fixed maximum iteration.

Algorithm Expectation Maximization EM (input : DAG, data base D, E function that calculate expectation)

output : $\theta_{i,j,k}$

Begin

1. $t=0$
2. Randomly initialize the parameters
3. Repeat
4. Expectation
use the current parameters $\theta_{i,j,k}^{(t)}$ to estimate missing parameters :
 $E^{(t)}(N_{i,j,k}) = \sum p^{(t)}(X_i=x_k | pa(X_i)=x_j)$
For i from 1 to N
5. Maximization
use estimate date to apply the learning procedure
(for example the maximum likelihood)
 $\theta_{i,j,k}^{(t+1)} = E(N_{i,j,k}) / E(N_{i,j})$
6. $t=t+1$
Until convergence ($\theta_{i,j,k}^{(t+1)} = \theta_{i,j,k}^{(t)}$)

End

Algorithm : EM algorithm

The second algorithm is Gibbs sampling [3] introduced by Heckerman. Gibbs sampling is described as a general method for probabilistic inference. It can be applied in all type of graphical models whether the arcs are directed or not and whether the variables are discrete or continuous. Gibbs sampling is a special case of MCMC (Markov Chain Monte Carlo). It generates a string of samples with accepting or rejecting some interesting points. In other words, Gibbs sampling consists in completing the sample by inferring the missing data from the available information. In learning the parameters, Gibbs sampling is a method that converges slowly or has no solution if the number of hidden variables is very large.

The third algorithm is Robust Bayesian Estimator RBE [8]. It's composed of two steps Bound and Collapse [10]. The first step consists of calculating a lower bound and an upper bound for each parameter in the bayesian network. The second step uses a convex combination to determine the value of $\theta_{i,j,k}$.

RBE is considered a procedure that runs through all the data D recorded observations about the variables and then it allows to bound the conditional probability of a variable X_i . This procedure begins by identifying the virtual frequencies following:

- $n(X_i = x_k | ?)$: calculating the number of observations where the variable X_i takes the value x_k and the value of $pa(X_i)$ is not completely observed.
- $n(? | pa(X_i) = x_j)$ calculating the number of observations where parents $pa(X_i)$ takes the value x_j and the value of X_i is missing.
- $n(? | ?)$: calculating the number of observations where both values of X_i and $pa(X_i)$ are unknown and the value of $pa(X_i)$ can be completed as x_j .

These frequencies help us to calculate the minimum and maximum number of observations that may have characteristics $X_i = x_k$ and $pa(X_i) = x_j$ in the database D :

$$n_{\min} = n(? | pa(X_i) = x_j) + n(X_i = x_k | ?) + n(? | ?) \quad (8)$$

is the minimum number of observations with characteristics $X_i = x_k$ and $pa(X_i) = x_j$.

$$n_{\max} = n(? | pa(X_i) = x_j) + \sum_{(h \neq k)} n(X_i = x_k | ?) + n(? | ?) \quad (9)$$

is the maximum number of observations with characteristics $X_i = x_k$ and $pa(X_i) = x_j$.

Virtual frequencies defined above can be set to zero, which is called the Dirichlet distribution with parameters $\alpha_{i,j,k}$. We define the lower bound of the interval by:

$$\min_{i,j,k} = \frac{\alpha_{i,j,k} + n(X_i = x_k | pa(X_i) = x_j)}{\alpha_{i,j} + n(pa(X_i) = x_j) + n_{\min}} \quad (10)$$

And the upper bound by:

$$\max_{i,j,k} = \frac{\alpha_{i,j,k} + n(X_i = x_k | pa(X_i) = x_j) + n_{\max}}{\alpha_{i,j} + n(pa(X_i) = x_j) + n_{\max}} \quad (11)$$

A detailed example mentioned in [8] shows the use of these equations in calculating conditional probabilities by determining the minimum and maximum bounds of the interval. This phase of determining $\min_{i,j,k}$ and $\max_{i,j,k}$ depends only on the frequency of observed data in the database and virtual frequencies calculated by completing the records. The major advantage of this method is the independence of the distribution of missing data without trying to infer.

To find the best parameters for this method, a second phase is necessary. It estimates the parameters using a convex combination from each distribution calculated for each given node. This convex combination can be determined either by external knowledge about the missing data, or by a dynamic estimate based on valid information in the database. A description of the execution of this phase is articulated in [10].

III. THE THRESHOLD EM ALGORITHM FOR PARAMETER LEARNING IN BAYESIAN NETWORK WITH INCOMPLETE DATA

The set of parameter in bayesian network using EM algorithm is approximate. In addition, the use of the bound

step of the RBE algorithm gives a lower bound and an upper bound for each parameter in the network which is defined by :

$$\min_{i,j,k} \theta_{i,j,k} \leq \theta_{i,j,k} \leq \max_{i,j,k} \theta_{i,j,k} \quad (12)$$

Our work consists of performing the optimization of the bayesian network parameter using the EM algorithm and verifying the bound step of the RBE algorithm.

For doing that, the threshold EM algorithm consists of verifying the constrain mentioned in equation (12) after the two steps of the EM algorithm.

Let $\theta_{i,j,k}^{(t)}$ be the maximized parameter after the execution of the two steps of the EM algorithm. The threshold EM algorithm is composed by three steps. The first two steps are the same as the EM algorithm. The third step consists of the regularization of $\theta_{i,j,k}^{(t)}$ with the constraint mentioned in equation (12). The main actions used in this step consists of:

- 1) If $\theta_{i,j,k}^{(t)} \leq \min_{i,j,k}$ then the $\theta_{i,j,k}^{(t)}$ is equal to $\min_{i,j,k}$.
- 2) If $\theta_{i,j,k}^{(t)} \geq \max_{i,j,k}$ then the $\theta_{i,j,k}^{(t)}$ is equal to $\max_{i,j,k}$.
- 3) If $\min_{i,j,k} < \theta_{i,j,k}^{(t)} < \max_{i,j,k}$ then the $\theta_{i,j,k}^{(t)}$ is saved like it's.

These changes provide a disagree of the probabilities constraint defined in equation (13) :

$$\sum_k \theta_{i,j,k} = 1 \quad (13)$$

So, it's necessary to make a normalization step to verify the equation (13). This step is described by the use of the equation (14).

$$\theta_{i,j,k}^{(t+1)} = \frac{\theta_{i,j,k}^{(t)}}{\sum_{k'} \theta_{i,j,k'}^{(t)}} \quad (14)$$

These new calculating parameters are used like an input in the next step of the threshold algorithm. This principle is repeated until convergence. The stopping points are the same as the EM algorithm.

The third step is used to force the solution to be between the bounds calculating by the bound step of the RBE algorithm. In the worst case, the solution is moving toward the directions of reducing the violations of the constraint mentioned in equation (12).

Now, we are ready to present the threshold EM algorithm for parameter learning in bayesian network with missing data as summarized in table 1.

IV. EXPERIMENTS

Repeat until it converges

Step1: Expectation step to compute the conditional expectation of the log-likelihood function.

Step2: Maximization step to find the parameter $\theta^{(t)}$ that maximize the log-likelihood.

Step3: Regularization step to get the parameter into the interval calculating by the bound step of the RBE algorithm:

For each variable i , parent configuration j , value k

If $\theta_{i,j,k}^{(t)} \leq \min_{i,j,k}$ then $\theta_{i,j,k}^{(t)} = \min_{i,j,k}$.

If $\theta_{i,j,k}^{(t)} \geq \max_{i,j,k}$ then $\theta_{i,j,k}^{(t)} = \max_{i,j,k}$.

If $\min_{i,j,k} \leq \theta_{i,j,k}^{(t)} \leq \max_{i,j,k}$ then the $\theta_{i,j,k}^{(t)}$ is saved like it's.

Step4: Normalization step based on equation (14)

$$\theta^{(t)} = \theta^{(t+1)}$$

Go to step1

Return $\theta^{(t)}$

Algorithm 1. The threshold EM algorithm

We describe in table 2 an example of using the threshold algorithm in one iteration :

TABLE I. AN EXAMPLE

Min	0,0566	0.07
Max	0.5	0.5
$\theta_{i,j,k}^{(t)}$	0.6206	0.3794
Regularization	0.5	0.3794
Normalization	0.5686	0.4314

We see that the new parameter calculating in one step reduces the violations of the constraint mentioned in equation (12).

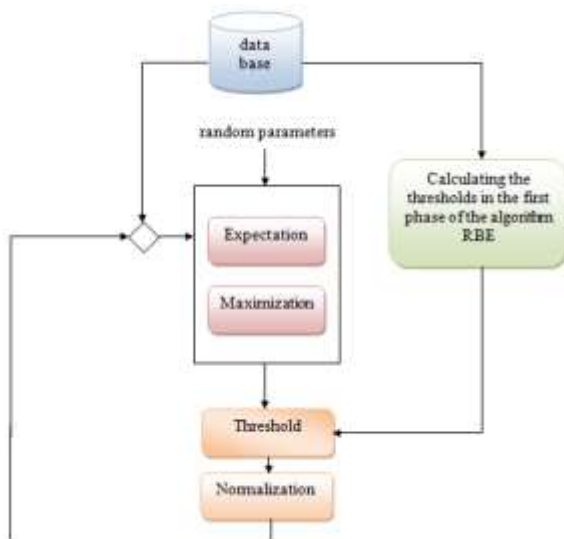


Figure 1. The threshold EM algorithm

During this section, we compare our algorithm to the EM algorithm. We apply this work in brain tumor diagnosis. We use the Bayesian Network Toolboxes (BNT) by Murphy to test our algorithm. The bayesian network as shown in Fig1 is created in these experiments. Then, 72 instances are collected from a real diagnosis and we mention that not all the variables are instanced.

The dataset use to learn the bayesian network parameters is composed by 72 instances of each node tacked from a real cases collected by a specialist in brain tumor diagnosis. All these nodes are discrete and takes between two and 8 values. The percentage of the missing data in this dataset is equal to 37.16%. The majority of missing data is in the intermediate nodes of the bayesian network. The causes of the missing data are the quality of IRM images or the doctor forgot to mention all the details in this report.

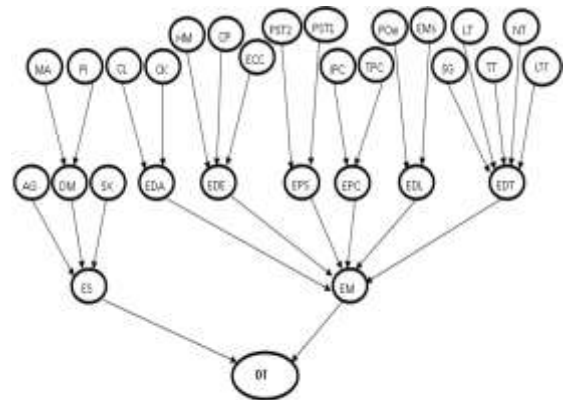


Figure 2. The Bayesian Network structure

The different meanings of names used in the figure are detailed in Table II and III.

TABLE II. TABLE TYPE STYLES

Node name	signification
AG	Age
CK	Cystic component
CL	Calcification
CP	Composition
DM	Medical record
DT	Decision Tumor
ECC	Flooding Corpus Callosum
EDA	State Auxiliary Data
EDE	State data encephalic
EDL	Liquide state data
EDT	Tumor state data
EM	Radiologic state
Ems	Mass effect
EPC	State taking contrast
EPS	Signal taking state

We show in Figure 3 the comparison between EM algorithm and the threshold EM algorithm (TH_EM)

concerning the log-likelihood function which is defined as follows :

$$LL(D|\theta) = \log L(D|\theta) = \sum_{i=1}^n \sum_{j=1}^{q_i} \sum_{k=1}^{r_i} N_{i,j,k} \log \theta_{i,j,k} \quad (15)$$

where :

n is the node number.

q_i is node i parents configuration number.

r_i the number state of node i

$N_{i,j,k}$ is the number of cases where the node i is in state k and its parents are in configuration j .

$\theta_{i,j,k}$ is the parameter value where node i is in state k and its parents are in configuration j .

TABLE III. TABLE TYPE STYLES

Node name	signification
ES	State clinic
HM	Hemorrhage
IPC	Importance of taking Contrast
LT	Tumor location
LTT	Tumor limit
MA	Diseases auxiliary
NT	Tumor number
PI	first Infection
Poe	Edema presence
PST1	Making the Signal in T1
PST2	Making the signal in T2
SG	seat
SX	Sex
TPC	Type of taking Contrast
TT	Tumor size

Equation 15 allows to give the performance parameters calculated in the Bayesian network. The Log-Likelihood gives the parameters that best describe the training set. This value is updated at each iteration in the EM algorithm.

We show in this graphic that these functions are already the same. The log-likelihood of the TH_EM algorithm is lower than the log-likelihood of the EM algorithm.

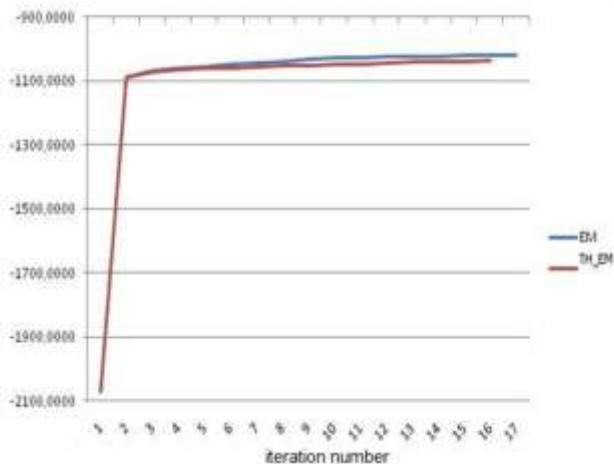


Figure 3. Comparison of the log-likelihood between TH_EM and EM algorithms

This test is applied when we fix the same starting points in the two algorithms. We see that the convergence of our algorithm is quickly than EM algorithm. This result is shown in 70% of cases when we change the starting points of the two algorithms (figure 4). In addition, we see that the probability distribution in each node is modified. Each probability is between the two bounds calculating with the first step of the RBE algorithm or error rate become smaller. One advantage of our algorithm consists of the absence of zero probability in each probability distribution.

The convex combination of the two bounds calculated in the first step of the RBE algorithm external information to get the parameters of any bayesian networks. This task becomes difficult when you have a complex structure. Our proposed method deletes the use of this information to get the conditional probability tables of our bayesian network.

V. CONCLUSION

In real application, training data in Bayesian network are always incomplete or some nodes are hidden. Many learning parameter algorithms are suggested foreground EM, Gibbs sampling and RBE algorithms. In order to limit the search space and escape from local maxima produced by executing EM algorithm, this paper presents a learning parameter algorithm that is a fusion of EM and RBE algorithms. This algorithm incorporates the range of a parameter into the EM algorithm. The threshold EM algorithm is applied in brain tumor diagnosis and show some advantages and disadvantages over the EM algorithm

REFERENCES

- [1] A. P. Dempster, N. M. (1977). Maximum likelihood from incomplete data via the EM algorithm. *The Royal Statistical Society Series B*, vol. 39, 1–38.
- [2] Basilio Sierra, I. I. (2000). Medical Bayes Networks. DOI: 10.1007/3-540-39949-6_2 .
- [3] Geman, S. G. (1984). Stochastic relaxation, Gibbs distribution and the Bayesian restoration of images. *IEEE Transactions on Pattern Analysis and Machine Intelligence*, vol. 6, 721–741.
- [4] Jensen, F. (1996). An introduction to bayesian network. *UCL press, UK* .
- [5] Ji, Y. Z. (May 2005). Active and dynamic information fusion for facial expression understanding from image sequence. *IEEE Transactions on Pattern Analysis and Machine Intelligence*, vol. 27, no. 5, 699–714.
- [6] L. M. de Campos, J. M.-L. (2004). Bayesian networks and information retrieval: an introduction to the special issue. *Information Processing and Management*, 727–733.
- [7] Lauritzen, S. (1991). The EM algorithm for graphical association models with missing data. *Technical Report TR-91-05, Departement of Statistics, Aalborg University* .
- [8] M. Ramoni and P. Sebastiani. (2001). Robust learning with missing data. *Machine Learning*, vol. 45, no. 2, 147–170.
- [9] Marco Ramoni, P. S. (1997). Bayesian inference with missing data using bound and collapse.
- [10] Marco Ramoni, P. S. (1997). The use of exogenous knowledge to learn bayesian network from incomplete databases.
- [11] P. JM, B. J. (2005). Growing bayesian network models of gene networks from seed genes. *Bioinformatics*, 224–229.

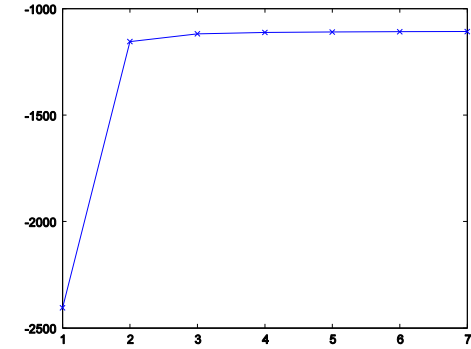
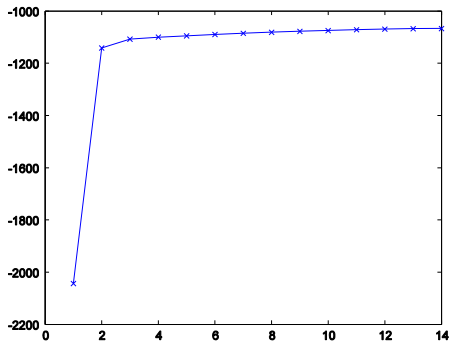
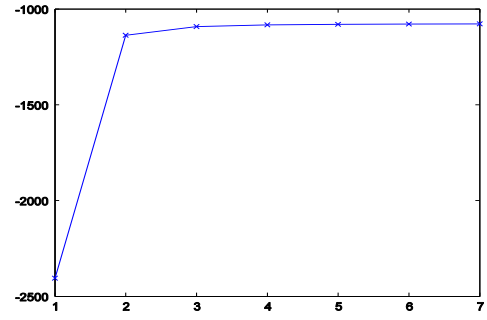
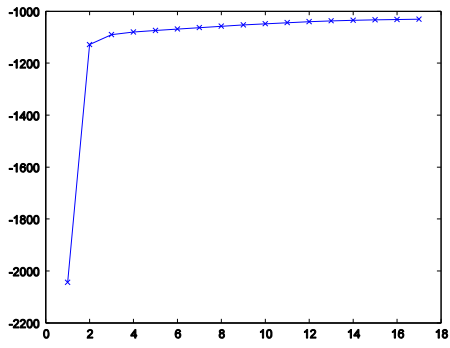


Figure 4. Log-likelihood with different starting points

Emotion Classification Using Facial Expression

Devi Arumugam

Research Scholar, Department of Computer Science,
Mother Teresa Women's University,
Kodaikanal, India.

Dr. S. Purushothaman B.E, M.E., Ph.D(IIT-M)

Principal,
Sun College of Engineering and Technology,
Sun Nagar, Erachakulam, Kanyakumari,
India.

Abstract— Human emotional facial expressions play an important role in interpersonal relations. This is because humans demonstrate and convey a lot of evident information visually rather than verbally. Although humans recognize facial expressions virtually without effort or delay, reliable expression recognition by machine remains a challenge as of today. To automate recognition of emotional state, machines must be taught to understand facial gestures. In this paper we developed an algorithm which is used to identify the person's emotional state through facial expression such as angry, disgust, happy. This can be done with different age group of people with different situation. We Used a Radial Basis Function network (RBFN) for classification and Fisher's Linear Discriminant (FLD), Singular Value Decomposition (SVD) for feature selection.

Keywords - Universal Emotions; FLD; SVD; Eigen Values; Eigen Vector; RBF Network.

I. INTRODUCTION

Human beings express their emotions in everyday interactions with others. Emotions are frequently reflected on the face, in hand and body gestures, in the voice, to express our feelings or liking. Recent Psychology research has shown that the most expressive way humans display emotions is through facial expressions. Mehrabian [1] indicated that the verbal part of a message contributes only for 7% to the effect of the message as a whole, the vocal part for 38%, while facial expressions for 55% to the effect of the speaker's message.

Emotions are feeling or response to particular situation or environment. Emotions are an integral part of our existence, as one smiles to show greeting, frowns when confused, or raises one's voice when enraged. It is because we understand other emotions and react based on that expression only enriches the interactions. Computers are "emotionally challenged". They neither recognize other emotions nor possess its own emotion [2].

To enrich human-computer interface from point-and-click to sense-and-feel, to develop non intrusive sensors, to develop lifelike software agents such as devices, this can express and understand emotion. Since computer systems with this capability have a wide range of applications in different research arrears, including security, law enforcement, clinic, education, psychiatry and Telecommunications [4]. There as been much research on recognizing emotion through facial expressions.

In emotional classification there are two basic emotions are there, Love-fear. Based on this we classify the emotion into

positive and negative emotions. The six basic emotions are angry, happy, fear, disgust, sad, surprise. One more expression is neutral. Other emotions are Embarrassments, interest, pain, shame, shy, anticipation, smile, laugh, sorrow, hunger, curiosity.

In different situation of emotion, Anger may be expressed in different ways like Enraged, annoyed, anxious, irritated, resentful, miffed, upset, mad, furious, and raging. Happy may be expressed in different ways like joy, greedy, ecstatic, fulfilled, contented, glad, complete, satisfied, and pleased. Disgust may be expressed in different ways like contempt, exhausted, peevd, upset, and bored.

In emotional expression face, If we are angry, the brows are lowered and drawn together, Vertical lines appear between the brows, lower lid tensed, eyes hard stare or bulging, lips can be pressed firmly together with corners down or square shape as if shouting, nostrils may be dilated, the lower jaw juts out.

If we are happy, corners of the lips are drawn back and up, mouth may or may not be parted, teeth exposed, a wrinkle runs from outer nose to outer lip, cheeks are raised, lower lid may show wrinkles or be tense, crows feet near the outside of the eyes. Disgust has been identified as one of the basic emotions. Its basic definition is "bad taste" secondarily to anything which causes a similar feeling, through the sense of smell, touch and even of eyesight. The well defined facial expression of disgust is characterized by furrowing of the eyebrows, closure of the eyes and pupil constriction, wrinkling of the nose, upper lip retraction and upward movement of the lower lip and chin, drawing the corners of the mouth down and back

This research describes a neural network based approach for emotion classification. We learn a classifier that can recognize three basic emotions.

II. RELATED WORK

There are several approaches taken in the literature for learning classifiers for emotion recognition [2] [6].

In the static Approach, the classifier classifies each frame in the video to one of the facial expression categories based on the tracking results of that frame. Bayesian network classifiers were commonly used in this approach. Naïve Bayes classifiers were also used often. Because of this unrealistic approach some used Gaussian classifiers.

In the Dynamic Approach, these classifiers take into account the temporal pattern in displaying facial expression. Hidden Markov Model (HMM) based classifiers for facial

expression recognition has been previously used in recent works. Cohen and Sebe [4] further advanced this line of research and proposed a multi-level HMM classifier.

This field has been a research interest for scientists from several different tracks like computer science, engineering, psychology, and neuroscience [1]. In this paper, we propose a complete emotional classification using facial expression. The network is well trained with the various emotions of the face with different age group of people from different situation. When given an input, the RBF network with the help of FLD, trained with various emotions of the face expression with that of training examples and produces the output.

This Existing research was developed by Paul Ekman [3]. He is a psychology perspective. In the early 1990s the engineering community started to use these results to construct automatic methods of recognizing emotions from facial expressions in images or video [4] based on various techniques of tracking [5]. An important problem in the emotion recognition field is the lack of agreed benchmark database and methods for compare different methods performance. Cohn-kanade database is a step in this direction [2].

Since the early 1970, Paul Ekman and his colleagues have performed extensive studies of human facial expression [7]. They found evidence to support universality in facial expressions. These “Universal facial expressions” are those representing happiness, sadness, anger, fear, surprise, and disgust. They studied facial expressions in different cultures, including preliterate cultures, and found much commonality in the expression and recognition of emotions on the face. However, they observed differences in expressions are governed by “display rules” in different social contexts. For Example, Japanese subjects and American subjects showed similar facial expressions while viewing the same stimulus film. However, in the presence of authorities, the Japanese viewers were more reluctant to show their real expressions. On the other hand, babies seem to exhibit a wide range of facial expressions without being taught, thus suggesting that these expressions are innate.

Ekman and Friesen [3] developed the Facial Action Coding System (FACS) to code facial expressions where movements on the face are described by a set of action units (AU s). FACS provides the mechanisms to detect facial movements by human coders. Action Units are a set of actions that corresponds to muscle movement such as raising lower lips, blinking, Biting lip, blow. Each AU has some related muscular basis. FACS consists of 44 action units. It does not contain any emotion specific so it must be sent to other system to recognise the emotions. This system of coding facial expressions is done manually by following a set of prescribed rules. The inputs are still images of facial expressions, often at the peak of the expression. This process is very time-consuming. Ekman's work inspired many researchers to analyze facial expressions by means of image and video processing. By tracking facial features and measuring the amount of facial movement, they attempt to categorize different facial expressions.

Recent work on facial expression analysis and recognition [8] has used these “basic expressions” or a subset of them. In [9], Pantic and Rothkrantz provide an in depth review of many

of the research done in automatic facial expression recognition in recent years. The work in computer-assisted quantification of facial expressions did not start until the 1990s.

Mase [10] used optical flow (OF) to recognize facial expressions. He was one of the firsts to use image-processing techniques to recognize facial expressions. Lanitis [11] used a flexible shape and appearance model for image10 coding, person identification, pose recovery, gender recognition, and facial expression recognition. Black and Yacoub [12] used local parameterized models of image motion to recover non-rigid motion. Once recovered, these parameters were used as inputs to a rule-based classifier to recognize the six basic facial expressions.

Yacoub and Davis [13] computed optical flow and used similar rules to classify the six facial expressions. Rosenblum, Yacoub, and Davis [14] also computed optical flow of regions on the face then applied a radial basis function network to classify expressions. Essa and Pentlands [15] used an optical flow region-based method to recognize expressions. Donato et al. [16] tested different features for recognizing facial AUs and inferring the facial expression in the frame. Otsuka and Ohya [17] first computed optical flow, then computed the 2D Fourier transform coefficients, which were used as feature vectors for a hidden Markov model (HMM) to classify expressions. The trained system was able to recognize one of the six expressions near real-time (about 10 Hz). Furthermore, they used the tracked motions to control the facial expression of an animated Kabuki system [18]. Martinez [19] introduced an indexing approach based on the identification of frontal face images under different illumination conditions, facial expressions, and occlusions.

A Bayesian approach was used to find the best match between the local observations and the learned local features model and an HMM was employed to achieve good recognition even when the new conditions did not correspond to the conditions previously encountered during the learning phase. Oliver et al. [20] used lower face tracking to extract mouth shape features and used them as inputs to an HMM based facial expression recognition system (recognizing neutral, happy, sad, and an open mouth). These methods are similar in that they first extract some features from the images, then these features are used as inputs into a classification system, and the outcome is one of the pre selected emotion categories. They differ mainly in the features extracted from the video images and in the classifiers used to distinguish 11 between the different emotions.

III. PROBLEM DEFINITION

There are three main factors to construct a Facial Expression Recognition system, namely face detection, facial feature extraction, and emotion classification. An ideal emotion analyzer should recognize the subjects regardless of gender, age, and any ethnicity.

The system should be invariant to different lightening conditions and distraction as glasses, changes in hair style, facial hair, moustache, beard, etc. and also should be able to “fill in” missing parts of the face and construct a whole face. It should also perform robust facial expression analysis despite

large changes in viewing condition, rigid movement, etc. A good reference system is the human visual system [4]. The current systems are far from ideal and they have a long way to achieve these goals.

IV. THE SYSTEM SETUP

The design and implementation of the Emotion classification using facial expression System can be subdivided into three main parts: Image Detection, Recognition technique which Includes Training of the images, Testing and then result of classification of images.

A. Image Detection

We used Canon Power shot SD 1000-canon digital camera. Images are stored in .jpg format. Most systems detect face under controlled conditions, such as without facial hair, glasses, any rigid head movement. Locating a face in a generic image is not an easy task, which continues to challenge researchers. Once detected, the image region containing the face is extracted and geometrically normalized. References to detection methods using neural networks and statistical approaches can be found.

We used real time database instead download the images from existing databases. This is because of noise free and easy use. We are using Radial basis function network which is capable of handling noisy images also. Its gives better result than back propagation neural network. For Face Data, The face slides are part of the facial emotion database assembled by Ekman and Friesen [21]. In Proposed method, the pictures in the database were tested on different age group of people from my relatives. We used four individual's one child, one adult, one middle aged women, one aged women. They are expressing one of the six emotions - happy, sad, fear, anger, surprise, disgust. We used three basic emotions such as happy, anger, disgust. We asked them to express their emotions for different situations. Figure 1, Figure 2, Figure 3 shows some of the training images.

B. Recognition technique

It aims at modelling the face using some mathematical representation in such a way the feature vector can be fed into a classifier. The overall performance of the system mainly depends on the correct identification of face or certain facial features such as eyes, eyebrows and mouth. After the face is detected, there are two ways to extract the features: Holistic Approach, Analytic Approach. In Holistic, raw facial image is subjected for feature extraction. While in analytic, some important facial features are detected. Here we used Holistic Approach, as that it means we send a raw image as an input without any feature selection. We fix the block size as fifty. The images are fed into fifty rows and fifty columns.

C. Statistical Method

After reading the image, the image must be analysed for duplication. So that correlation of the matrix will be find. Since the correlation matrix for each image is square, we can



Figure 1. Angry expression for different situations.



Figure 2. Disgust expression in different situations



Figure 3. Happy expression in different situations

Calculate Eigen vector and Eigen value for each matrix. These are very important so that it gives useful information about the data.

1) Eigen Vectors and Eigen Value :

In Eigen vectors any vector change in magnitude but not in direction is called as Eigen vector. In Eigen values, the magnitude that the vector is changed is called an Eigen value.

$$A x = \lambda x \quad (1)$$

Where A is n x n matrix. X is the length of n column vector. λ is a scalar. It's an Eigen value and x is the Eigen vector.

“The Eigen values for angry image1:” 0.1369, 0.1371, 0.1372, 0.1373, 0.1371, 0.1368, 0.1366, 0.1375, 0.1382, 0.1285, 0.1394, 0.1402, 0.1406, 0.1408, 0.1412, 0.1417, 0.143”. “The Eigen values for angry image2:” 0.1368, 0.1371, 0.1374, and 0.1372. “The Eigen values for angry image3:” 0.1367, 0.1371, 0.1375 and 0.1371. It is important to notice that these eigenvectors are both unit eigenvectors that is their lengths are both 1. This is very important for FLD. In math packages, when asked for eigenvectors, will give you unit eigenvectors. It turns out that the eigenvector with the highest Eigen value is the linear Component of the data set [22]. After getting the Eigen values we calculate the mean values for all the images, in order to get highest Eigen values. The highest Eigen value must contain important feature about the data. So we select ten highest Eigen values from all the images.

2) Fisher's Linear Discriminant:

It can reduce the number of variable in the input by projecting data onto a possibly uncorrelated and low dimensional space. It reduces the number of features in the input to a manageable level. Some variable with information that is not related to facial expression can be excluded during the projection on low dimensional space. This helps the network to prevent from learning unwanted details in the input. The above property can improve the network classifier's performance and generalization. By minimizing within class variance and maximizing between class variance. The most famous example of dimensionality reduction is principal component analysis. This technique searches for direction in the data that have largest variance and subsequently project the data onto it. That removes some of the noisy directions. There are many issues with how many directions one needs to choose. It is a unsupervised technique [23].

When compare with Principle Component Analysis, Independent Component Analysis, and FLD gives maximum percentage of the output. It is best for classification, improves the performance and reduction technique. Fisher Linear Discriminant Analysis considers maximizing the following objective.

$$J(w) = w^T S_B w / w^T S_W w \quad (2)$$

Where S_B is the “between class scatter matrix” and S_W is the “within class scatter matrix”. Then we find two matrixes which contain specific information of the data.

3) Singular Value Decomposition:

The Singular Value Decomposition (SVD) is one of the most important tools of numerical signal processing. It plays an interesting, fundamental role in many different applications. SVD in digital applications provides a robust method of storing large images as smaller, more manageable square ones. This is accomplished by reproducing the original image with each succeeding nonzero singular value. To reduce storage size, by using fewer singular values [25]. The SVD of a face image has good stability in which it defined that whenever a small

perturbation is added to a face image, a large variance of its singular values (SV) didn't occur. Since it has stated that singular value represent algebraic properties of an image. Hence, SV features possess algebraic and geometric invariance as an instance [26]. The theory of SVD states that any matrix A of size m x n can be factorized into a product of unitary matrices and a diagonal matrix, as the following [24].

The diagonal elements of Σ are called the singular values of A and are usually ordered in descending manner. We use the orthogonal matrix U as the projection vectors. U and V matrices are inherently orthogonal in nature. These directions are encoded in U and V matrices. This method called as FLD+SVD method. In contrast to eigenvector calculations involved in conventional algorithms, the SVD has several advantages. Computationally efficient and it is robust under noise conditions.

$$[U, S, V] = \text{svd}(sw) \quad (4)$$

$$sw = U * S * V^T \quad (5)$$

Using the formula in mat lab, we can find the svd of sw. Using this value we can find Phi 1 vector and Phi2 vector.

φ1 vector	φ2 vector
0.2173	-0.0192
0.1899	-0.0356
0.2097	-0.0754
0.2019	-0.0942
.	.
.	.

We concatenate the results so as to convert high dimensional data into two dimensional data. First of all, we read all the images (four persons with three different situations for three basic emotions). After reading the image, correlation of the images can be finding. Then we find Eigen vectors, Eigen values for all the images in order to get original data. After, Using FLD and SVD feature selection is done. Now we get the graph for all emotions. Figure 4 and figure 6 describe the different emotional graph and their corresponding values.

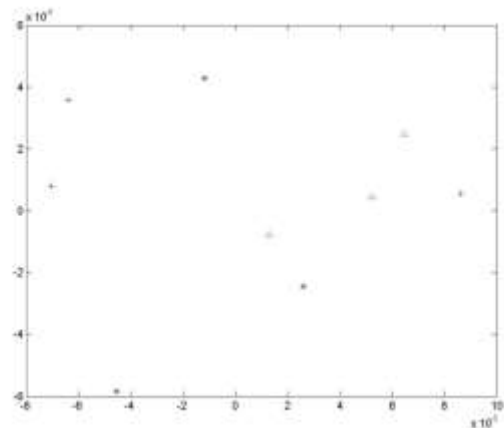


Figure 4. Above Graph for different emotions * for Angry emotion, + For disgust emotion, ^ For happy emotion

Angry	-0.0012	0.0043	
	-0.0045	-0.0058	*
	0.0026	-0.0024	
Disgust	-0.0072	0.0008	
	0.0086	0.0006	+
	-0.0064	0.0036	
Happy	0.0064	0.0025	
	0.0052	0.0042	^
	0.0013	-0.0008	

Figure 5. Graph has been plotted using above measurement

D. Neural networks

A neural network have been used in the field of image processing, it provides an optimistic result in terms of quality of outcome and ease of implementation. Neural network proved itself to be invaluable in applications where a function based model or parametric approach to information Processing is difficult to formulate. The description of neural network can be summarized as a collection of units that are connected in some pattern to allow communication between the units. These units are referred as neurons or nodes generally. The output signals feed to other units along the connections which known as weight. The weights usually excite or inhibit the signal that is being communicated. One of the specialty of neural networks is that the *hidden units* factors. The function of the *hidden units* or *hidden cells* or also called *hidden neurons* is to intervene between the external input and the network output. The network which implemented neural network in it actually has the ability to extract higher order statistics by adding one or more hidden layers [27].

Hence, this characteristic is particularly valuable when the size of the input layer is large, specifically in the face recognition field [28].

E. Radial Basis Function Network

It's a two layer, Hybrid feed forward learning network. It is fully connected network. This is becoming an increasing popular neural network with diverse applications and is probably the main rival to the multi layered perceptron. Much of the inspiration for RBF network has come from traditional statistical pattern classification techniques. It's mainly used as classification tool. It's used by broom head and Lowe in 1988.

Each hidden neuron has a symmetric radial basis function as an Activation Function. The purpose of the hidden neurons is to cluster the input data and reduce dimensionality. Train input data in order to minimize the sum of square errors and find the optimal weights between hidden neurons and output nodes. These optimal weights can classify effectively the test data into correct classes. Figure 5 describes the basic architecture of RBF network.

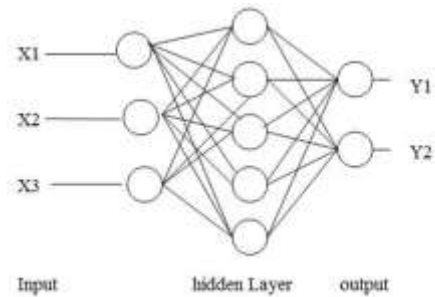


Figure 6. Shows basic architecture for radial basis function network

F. Training Phase

We present the network with training examples, which consist of a pattern of activities for the input units together with the desired pattern of activities for the output units. We determine how closely the actual output of the network matches the desired output. We change the weight of each connection so that the network produces a better approximation of the desired output. The input to the training phase is a collection of images showing human faces. These images are also called as Face images. These face images are then passed through a feature extraction step. In the feature extraction step key attributes of the images are computed and stored as a vector called feature vector. We get phi 1 vector and phi2 vector. These feature vectors define or represent the most important properties observed in the face image. Highest Eigen values are chosen.

There are two advantages of this step. First, the size of the data is reduced from the entire image to only a few selected important features. Second, the selection of features gives more structured information than just basic pixel values of the images. Thus the feature vectors can be considered as the minimal set that is adequate to represent the face image. The training could be done on face images showing a selected class of emotion or the entire set of emotions. If the training is done for selected class of emotions then the model is build for each class of emotion. Hence in this case three basic emotions mentioned earlier a separate will be build for each of three emotions. The input images for a particular model will be only the images that show the corresponding emotion. If the training is desired for building a single model for the entire set of emotions then the entire set of face images is used for the training space. In our case after the training the radial basis functional network will get the separate values for each emotion.

Now training has been done. We conclude that the value for Angry Emotion is nearly 0.1, the value for Disgusted Emotion is nearly 0.2 and the value for Happy Emotion is nearly 0.3. Figure 7 shows the approximate results for the three basic

emotion

Inode for Angry Emotion	Angry	
-0.0012 0.0043	0.1000	
-0.0045 -0.0058	0.1000	=0.1
0.0026 -0.0024	0.1000	
Inode for Disgust Emotion	Disgust	
-0.0012 0.0043	0.1000	
-0.0045 -0.0058	0.1000	
0.0026 -0.0024	0.1000	= 0.2
-0.0070 0.0008	0.2000	
-0.0071 0.0008	0.2000	
Inode for Happy Emotion	Happy	
-0.012 0.0043	0.1000	
-0.0045 -0.0058	0.1000	=0.3
0.0026 -0.0024	0.2000	
-0.0070 -0.0008	0.3000	

Figure 7. Shows the approximate results for three basic emotions.

G. Testing phase

This phase can be performed to measure the classification rate. The inputs to this phase are the models that were build during training phase and the test images for which the emotions are to be recognized. Here again only the face region is used as rest of the image do not contribute information about the emotion. In a typical real time scenario the input image would be detected face image from an earlier face detection phase.

The first step here again would be a feature extraction phase where the key features from the face image are extracted. The extraction method must be same as the one used in the training phase. The output of this step is the feature vector of the face image that would then be subjected to a testing step. In the testing step the feature vector is tested against the models built during the training phase. The output of the testing step is a score that indicated the emotion that is detected by the model.

This score is usually in the form of distance or probability and it defines which model was best suited for the feature vector extracted in the previous step. In the testing step there are two possible ways that can be employed. The first possibility is in the case when one model was built per class of emotion. Here the feature vector is tested against all the models and their scores then define which model was the most suited one. The second possibility is the case when only one model was built for the entire set and a single score defines the possible emotion detected. During testing a simple image the approach can correctly classify it as the correct emotion expressed. In another case the approach can also wrongly classifies a sample image as the correct emotion expressed. These cases constitute false positives. It could also be the case that the approach wrongly classifies a sample images as incorrect emotion expressed. These cases constitute false negatives.

V. EXPERIMENTAL RESULTS

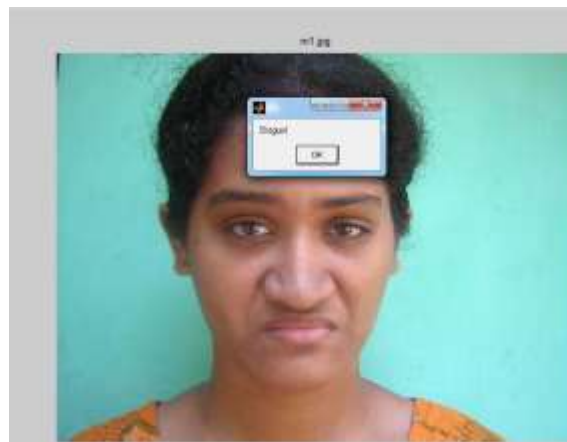


Figure 9. Shows the result for disgust image.



Figure 8. Shows the result for happy image



Figure 10. Shows result for angry image.

VI. CONCLUSION

In this paper we have presented an approach to expression recognition in the static images. This emotion analysis system implemented using FLD, SVD for feature selection and RBF

network for classification. This paper is designed to recognize emotional expression in human faces using the average values calculated from the training samples. We evaluated that the system was able to identify the images and evaluate the expressions accurately from the images

VII. FUTURE WORK

In this paper we classify the emotional expression for three basic emotions. This gives accurate performance. In future we may include other expression also. We proceed with Video images also.

ACKNOWLEDGMENT

I wish to thank Professor Dr. S. Purusothaman for his extreme support and guidance. I also thank my family and colleagues for their valuable feedback and thoughtful suggestions.

REFERENCES

- [1] A. Mehrabian, Communication without words, psychology today, vol. 2, no. 4, pp. 53-56, 1968.
- [2] Nicu Sebe, Michael S. Lew, Ira Cohen, Ashutosh Garg, Thomas S. Huang, "Emotion recognition using a Cauchy naïve bayes classifier", ICPR, 2002.
- [3] P. Ekman, W.V. Friesen, "Facial action coding system: investigator's guide", Consulting Psychologists Press, Palo Alto, CA, 1978.
- [4] G. Littlewort, I. Fasel, M. Stewart Bartlett, J. Movellan "Fully automatic coding of basic expressions from video", University of California, San Diego.
- [5] M.S. Lew, T.S. Huang, and K. Wong, Learning and feature Selection in Stereo Matching, IEEE Transactions on Pattern Analysis and Machine Intelligence, vol. 16, no. 9, 1994.
- [6] Ira Cohen Nicu Sebe, Larry Chen, Ashutosh Garg, Thomas Huang, "Facial Expression Recognition from Video Sequences: Temporal and Static modeling Computer Vision and Image Understanding(CVIU) special issue on face recognition.
- [7] P. Ekman. Strong evidence of universals in facial expressions: A reply to Russell's mistaken critique. Psychological Bulletin, pp. 268-287, 1994.
- [8] Y. Tian, T. Kanade, J. Cohn, "Recognizing action units for facial expression analysis", Carnegie-Mellon University, IEEE Transactions on pattern recognition and machine intelligence vol. 23, No. 2, February 2001 pp. 97-115.
- [9] Maja Pantic, Leon J.M. Rothkrantz, "Automatic analysis of facial expressions: the state of art", IEEE Transactions on pattern Recognition and Machine Intelligence, Dec. 2000, pp. 1424-1444.
- [10] K. Mase, Recognition of facial expression from optical flow. IEICE Transactions pp. 3474-3483, 1991
- [11] A. Lanitis, C.J. Taylor, and T.F. Cootes, "A unified approach to coding and interpreting face images", In International Conference on Computer Vision, pp. 368-373, 1995.
- [12] M.J. Black and Y. Yacoob, "Tracking and recognizing rigid and non rigid facial motions using local parametric models of image motion", International Conference on Computer Vision, pp. 374-381, 1995.
- [13] Y. Yacoob and L.S. Davis, "Recognizing human facial expressions from long image sequences using optical flow". IEEE Transactions on Pattern Analysis and Machine Intelligence, pp. 636-642, June 1996.
- [14] M. Rosenblum, Y. Yacoob, and L.S. Davis, "Human expression recognition from motion using a radial basis function network architecture", IEEE Transactions on Neural Network, pp. 1121-1138, September 1996.
- [15] I.A. Essa and A.P. Pentland, "Coding, analysis, interpretation, and recognition of facial expressions", IEEE transactions on Pattern Analysis and Machine Intelligence, pp. 757-763, 1997.
- [16] G. Donato, M.S. Bartlett, J.C. Hager, P. Ekman, and T.J. Sejnowski, Classifying facial actions. IEEE Transactions on Pattern Analysis and Machine Intelligence, pp. 974-989, 1999.
- [17] T. Otsuka and J. Ohya, "Recognizing multiple persons facial expressions using HMM based on automatic extraction of significant frames from image sequences", In IEEE International Conference on Image Processing, pp. 546-549, 1997.
- [18] T. Otsuka and J. Ohya, "A study of transformation of facial expressions based on expression recognition from temporal image sequences", Technical report, Institute of Electronic, Information, and Communications Engineers (IEICE), 1997.
- [19] A Martinez. Face image retrieval using HMMs. In IEEE Workshop on Content-based Access of Images and Video Libraries, pp. 35-39, 1999.
- [20] N. Oliver, A. Pentlands, and F. Berard, "LAFTER: A real-time face and lips tracker with facial expression recognition", Pattern Recognition, pp. 1369- 1382, 2000.
- [21] P. Ekman and W. Friesen. Pictures of facial affect. 1976.
- [22] Dr. S. Santhosh Baboo and V.S. Manjula, "face emotion analysis using gabor features in image database for crime investigation", International Journal of Data Engineering (IJDE), volume 2, issue 2, 2011.
- [23] Max Welling Notes to explain Fisher Linear Discriminate Analysis, university of Toronto. 2001.
- [24] S. Noushath, Ashok Rao, G. Hemantha Kumar, "SVD based algorithms for robust face and object recognition in robot vision applications", 24th international Symposium on Automation & Robotics in Construction (ISARC 2007) construction Automation Group, I.I.T. Madras.
- [25] Mandep Kaur, Rajeev Vashisht, Nirvair Neeru, "Recognition of Facial Expressions with principal component analysis and singular value decomposition", International Journal of computer Applications(00975-8887), volume 9-No.12, November 2010.
- [26] Y. Wang, T. Tan and Y. Zhu, "Face Verification based on Singular Value Decomposition and Radial Basis Function Neural Network", National Laboratory of Pattern Recognition Institute of Automation, Chinese Academy of sciences, Beijing.
- [27] Thaahirah S.M. Rasied, Othman O. Khalifa and Yuslina Binti Kamarudin, "Human Face Recognition based on singular Valued Decomposition and Neural Network", GVIP 05 Conference, 19-21 December 2005, CICC, Cairo, Egypt.
- [28] P. Picton, neural Networks, Second Edition, Palgrave. 2000.

Workshare Process of Thread Programming and MPI Model on Multicore Architecture

R. Refianti¹, A.B. Mutiara², D.T Hasta³

Faculty of Computer Science and Information Technology, Gunadarma University,
Jl. Margonda Raya No.100, Depok 16424, Indonesia

Abstract—Comparison between OpenMP for thread programming model and MPI for message passing programming model will be conducted on multicore shared memory machine architectures in order to find which has a better performance in terms of speed and throughput. Application used to assess the scalability of the evaluated parallel programming solutions is matrix multiplication with customizable matrix dimension. Many research done on a large scale parallel computing which using high scale benchmark such as NSA Parallel Benchmark (NPB) for their testing standardization [2]. This research will be conducted on a small scale parallel computing that emphasize more on the performance evaluation between MPI and OpenMP parallel programming model using self created benchmark. It also describes how workshare processes done on different parallel programming model. It gives comparative result between message passing and shared memory programming model in runtime and amount of throughput. Testing methodology also simple and has high usability on the available resources.

Keywords-MPI; OpenMP; SMP; Multicore; Multithreading.

I. INTRODUCTION

The growth of multicore processors has increased the need for parallel programs on the largest to the smallest of systems (clusters to laptops). There are many ways to express parallelism in a program. In HPC (High Performance Computing), the MPI (Message Passing Interface) has been the main tool for parallel message passing programming model of most programmers [1,3].

A multi-core processor looks the same as a multi-socket single-core server to the operating system. (i.e. before multi-core, dual socket servers provided two processors like today's dual core processors) Programming in this environment is essentially a matter of using POSIX threads. Thread programming can be difficult and error prone. OpenMP was developed to give programmers a higher level of abstraction and make thread programming easier. Accordance to multicore trend growth, parallel programming using OpenMP gains popularity between HPC developers. Together with the growth of thread programming model on shared memory machines, MPI which has been intended for parallel distributed systems since MPI-1, also has improved to support shared memory systems. The principal MPI-1 model has no shared memory concept, and MPI-2 has only a limited distributed shared memory concept. Nonetheless, MPI programs are regularly run on shared memory computers. MPI performance for shared memory systems will be tested on cluster of shared memory

machines. OpenMP will be used as a reference on the same multicore systems with MPI clusters (both MPI and OpenMP will have an equal amount of core works)[2].

Application used as a testing is $N \times N$ rectangular matrix multiplication with adjustable matrix dimension N ranging from 10 to 2000. For OpenMP, a single multicore machine with two worker cores will be used to calculate the matrix. For the MPI, two multicore machines with three worker cores will be used (one as a master process who decompose the matrix to sub - matrix and distribute it to two other worker process and compose the final result matrix from the sub - matrix multiplication done by its two worker process).

Parameter results which can be obtained from this test are amount of floating point operation per second (FLOPS) which in this case is matrix multiplication, Program Running Time, and Speedup. For MPI, two machines are used for testing having quite similar performance (Memory and CPU performance). MPI testing is done via LAN cable medium transmission to achieve best run time performance and minimizing time communication between processes.

There is already related research topic in this area. One of them did the testing by using certain parallel benchmark such as NAS Parallel benchmark (NPB) to standardize the evaluation on large clusters and ten to hundreds of CPU cores [2], which can produce large speedup and throughput.

This research is simpler compared than the previous research which uses tens or hundreds machine resources and complicated benchmark. This research focused on how does different parallel programming model can affect the program performance. Testing in this research done by using a self created benchmark which counts the program running time and matrix multiplication operation per second.

This research describes how workshare processes done on different parallel programming model. This research gives comparative result between message passing and shared memory programming model in runtime and amount of throughput. Testing methodology also simple and has high usability on the available resources.

Problem covered in this research are:

- How does different parallel programming model influence parallel performance on different memory architecture?

- How does workshare construct differ between shared and distributed shared memory systems?

Objectives of this research are:

- Evaluating parallel performance between thread and message passing programming model.
- Evaluating parallel algorithm workshare between threads and message passing programming model.

Testing experiment conducted on a single multicore shared memory machine which consist of two cores for thread programming model (OpenMP). And two identical multicore shared memory machines with two cores on each machine for message passing programming model without expressing thread safety level. Matrix Multiplication Program used for testing also has a limited dimension which is 2000, because of the machine power limitation. Testing parameters generated are amount of floating point operation per second (FLOPS) which in this case is matrix multiplication, Program Running Time, and Speedup.

II. FUNDAMENTAL THEORY

Parallel computing is a form of computation in which many calculations are carried out simultaneously, operating on the principle that large problems can often be divided into smaller ones, which are then solved concurrently ("in parallel"). Parallel computing is done by a certain amount of parallel computers. Each of parallel computer may has different CPU core and memory architecture

Parallel computers can be roughly classified according to the level at which the hardware supports parallelism. Currently there are three types which are shared memory (which usually has multiple core processor), distributed memory (clusters, MPPs, and grids), and Distributed shared memory (cluster of Shared memory systems).

A. Shared Memory Systems

In computer hardware, shared memory refers to a (typically) large block of random access memory that can be accessed by several different central processing units (CPUs) in a multiple-processor computer system. A shared-memory parallel computer whose individual processors share memory (and I/O) in such a way that each of them can access any memory location with the same speed; that is, they have a uniform memory access (UMA) time. Each of individual processor in shared memory system has a small and fast private cache memory. Cache memory used to supply each core processor with data and instruction at high rates. This is because fetching data done from processor to main memory directly is slower than fetching it from cache memory.

The issue with shared memory systems is that many CPUs need fast access to memory and will likely cache memory [4], which has two complications:

- CPU-to-memory connection becomes a bottleneck. Shared memory computers cannot scale very well. Most of them have ten or fewer processors.
- Cache coherence: Whenever one cache is updated with information that may be used by other processors, the

change needs to be reflected to the other processors; otherwise the different processors will be working with incoherent data. Such coherence protocols can, when they work well, provide extremely high-performance access to shared information between multiple processors. On the other hand they can sometimes become overloaded and become a bottleneck to performance.

However, to avoid memory inconsistency as already mentioned above, there is a cache memory which can be shared to all processor. Shared cache memory can be used for each core processor to write and read data. Figure.1 gives information about cache memory.

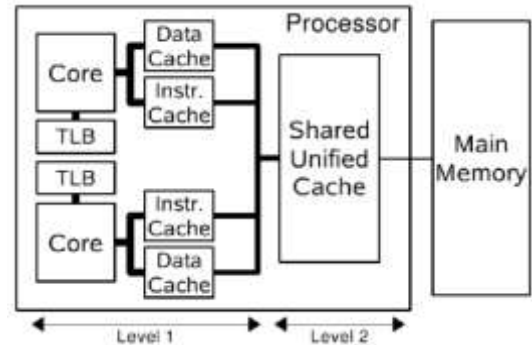


Figure 1. Block diagram of a generic, cache-based dual core processor

B. Distributed Memory

In computer science, distributed memory refers to a multiple-processor computer system in which each processor has its own private memory. In other words each processor will resides on different computer machine. Computational tasks can only operate on local data, and if remote data is required, the computational task must communicate with one or more remote processors [5]. In a distributed memory system there is typically a processor, a memory, and some form of interconnection that allows programs on each processor to interact with each other. The interconnection can be organized with point to point links or separate hardware can provide a switching network. The network topology is a key factor in determining how the multi-processor machine scales. The links between nodes can be implemented using some standard network protocol (for example Ethernet), etc. Figure.2 shows distributed memory systems architecture.

In contrast, a shared memory multi processor offers a single memory space used by all processors. Processors do not have to be aware where data resides, except that there may be performance penalties, and that race conditions are to be avoided.

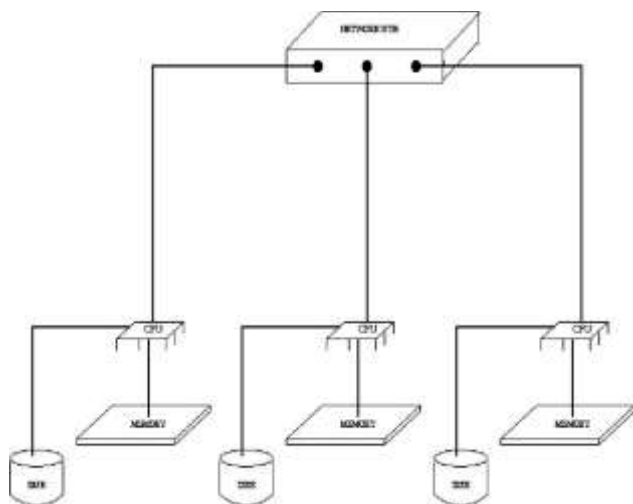


Figure 2. An illustration of a distributed memory system of three computers

C. Distributed Shared Memory

Distributed Shared Memory (DSM), also known as a distributed global address space (DGAS), is a term in computer science that refers to a wide class of software and hardware implementations, in which each node of a cluster has access to shared memory in addition to each node's non-shared private memory. The shared memory component is usually a cache coherent SMP machine. Processors on a given SMP can address that machine's memory as global. The distributed memory component is the networking of multiple SMPs. The SMPs know only about their own memory - not the memory on another SMP. Therefore, network communications are required to move data from one SMP to another. Figure.3 describes about distributed shared memory.

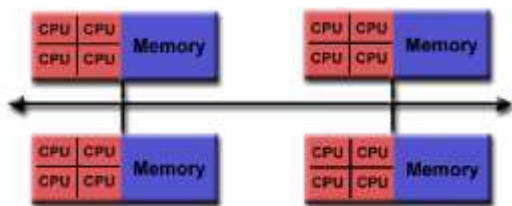


Figure 3. An illustration of a distributed shared memory system

D. Parallel Programming Models

All of those parallel hardware classifications need programming language which has a capability to share or divided the work among processors. Concurrent programming languages, libraries, APIs, and parallel programming models have been created for programming parallel computers. These can generally be divided into classes based on the assumptions they make about the underlying memory architecture which are shared memory, distributed memory, or shared distributed memory [6]. A parallel programming model is a set of software technologies to express parallel algorithms and match applications with the underlying parallel systems. It encloses the areas of applications, programming languages, compilers, libraries, communications systems, and parallel I/O.

Parallel models are implemented in several ways: as libraries invoked from traditional sequential languages, as

language extensions, or complete new execution models. They are also roughly categorized for two kinds of systems: shared-memory system and distributed-memory system, though the lines between them are largely blurred nowadays.

Shared memory programming languages communicate by manipulating shared memory variables through threads. Threads used as subtasks which carry instruction process to one / more core processor. However, one thread only can carry one instructions process at a certain time. In other words, multiple threads can carry multiple instruction process. Distributed memory uses message passing. POSIX Threads and OpenMP are two of most widely used shared memory APIs, whereas Message Passing Interface (MPI) is the most widely used message-passing system API. Shared memory systems use threads whereas distributed memory systems use message passing task and communication carried out by message passing over network transmission. A programming model is usually judged by its expressibility and simplicity, which are by all means conflicting factors. The ultimate goal is to improve productivity of programming.

1) OpenMP

OpenMP (Open Multi-Processing) is an application programming interface (API) that supports multi-platform shared memory multiprocessing programming in C, C++ and FORTRAN on much architecture, including UNIX and Microsoft Windows platforms. It consists of a set of compiler directives, library routines, and environment variables that influence run-time behavior [7]. OpenMP is an implementation of multithreading, a method of parallelization whereby the master "thread" (a series of instructions executed consecutively) "forks" a specified number of slave "threads" and a task is divided among them. The threads then run concurrently, with the runtime environment allocating threads to different processors. Hence, OpenMP is one of thread based parallel programming which will be used in this research. Figure.4 gives a better understanding about multithreading.

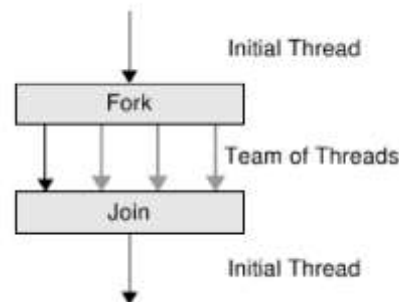


Figure 4. The fork-join programming model supported by OpenMP

OpenMP uses pragma directives to express parallelism in the code block. Parts of the program that are not enclosed by a parallel construct will be executed serially. When a thread encounters this construct, a team of threads is created to execute the associated parallel region, which is the code dynamically contained within the parallel construct. But although this construct ensures that computations are performed in parallel, it does not distribute the work of the region among the threads in a team. In fact, if the programmer

does not use the appropriate syntax to specify this action, the work will be replicated. At the end of a parallel region, there is an implied barrier that forces all threads to wait until the work inside the region has been completed. Only the initial thread continues execution after the end of the parallel region [8].

The thread that encounters the parallel construct becomes the master of the new team. Each thread in the team is assigned a unique thread number (also referred to as the "thread id") to identify it. They range from zero (for master thread) up to one less than the number of threads within the team, and they can be accessed by the programmer.

2) MPI

Message Passing Interface (MPI) is an API specification that allows computers to communicate with one another. It is used in computer clusters and supercomputers. MPI is a language-independent communications protocol used to program parallel computers. Both point-to-point and collective communication are supported. MPI is a message-passing application programmer interface, together with protocol and semantic specifications for how its features must behave in any implementation. MPI's goals are high performance, scalability, and portability [9]. MPI is not sanctioned by any major standards body; nevertheless, it has become a de facto standard for communication among process that model a parallel program running on a distributed memory system. Actual distributed memory supercomputers such as computer clusters often run such programs. The principal MPI-1 model has no shared memory concept, and MPI-2 has only a limited distributed shared memory concept. Nonetheless, MPI programs are regularly run on shared memory computers.

The MPI interface is meant to provide essential virtual topology, synchronization, and communication functionality between a set of processes (that have been mapped to nodes/servers/computer instances) in a language-independent way, with language-specific syntax (bindings), plus a few language-specific features. MPI programs always work with processes, but programmers commonly refer to the processes as processors. Typically, for maximum performance, each CPU (or core in a multi-core machine) will be assigned just a single process. This assignment happens at runtime through the agent that starts the MPI program (i.e. MPI daemon), normally called mpirun or mpiexec. Computer machine that initiates MPI ring daemon will have process manager in its core CPU. Process manager identified with ID 0 and all of his worker have ID greater than 0.

The initial implementation of the MPI 1.x standard was MPICH, from Argonne National Laboratory (ANL) and Mississippi State University. ANL has continued developing MPICH for over a decade, and now offers MPICH 2, implementing the MPI-2.1 standard.

III. WORKSHARE METHODOLOGY

A. Matrix Multiplication Workshare Algorithm

Matrix multiplication structure is as defined in Figure.5

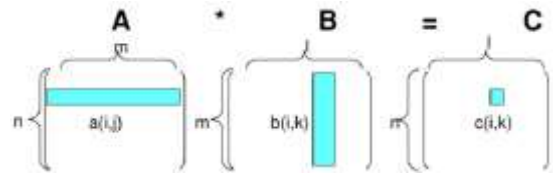


Figure 5. Matrix Multiplication Structure

Multiplying two $N \times N$ matrices in sequential algorithm takes obviously for each element N multiplications and $N-1$ additions. Since there are N^2 elements in the matrix this yields a total of $N^2 * (2N-1)$ floating-point operations, or about $2N^3$ for large N , that is, $O(N^3)$ [10].

Parallel algorithm workshare does not change matrices multiplication arithmetic operations. It only change the execution sequence for multiple processors. However, the complexity / operation count will change because of the workshare between core processors.

B. MPI Workshare Algorithm

MPI shares heir work among processing units by using message passing across network. Process identification between core CPU (both on the same computer and different computer) is similar with OpenMP (i.e. ID = 0 master process, ID >0 worker process).

Parallel programming model using message passing is similar with UNIX socket programming in which process manager can send a chunked task to all of his worker process and receive computation result from all of his worker [11].

Matrix Multiplication between two rectangular matrixes can be shared between processes using a certain rule. One of the rules is to make the master process as the process manager which divided and distribute matrix elements according to the number of CPU core workers. Thus, if there is 4 process used, 1 will be used as process manager and the other 3 will be used as worker process. Process ID 0 will become process manager and process ID 1 to 2 as workers. There are several MPI model to distribute matrix among the worker processes and one of them is row based distribution.

In row based distribution, For example there are two $N \times N$ matrixes, A_{ij} and B_{ij} , which will be multiplied. All of matrix B_{ij} elements (rows and columns) will be sent to all worker processes which are done by master process. For matrix A_{ij} , before it is sent, it will be first divided according to its amount of row. For example if matrix A_{ij} has 4 rows and there are 3 workers available, each process will has $4/3$ which is 1 row with another 1 residual row value generated from the arithmetic division. The residual row value will be added to the worker process which has ID lower or equal than amount of residual row value in a for repetition order (start from worker ID 1 to 2). Thus, 1 residual row value will be added to worker process ID 1.

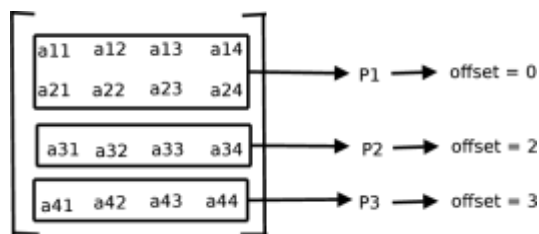


Figure 6. Matrix A Row Based Division

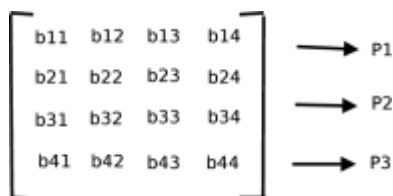


Figure 7. Matrix B Distribution

Figure. 6 gives row based distribution analogy. Worker process ID 1 work on 2 rows because there is a residual value from the arithmetic division operation. Another reason why worker ID 1 which receives extra row is because worker ID 1 is the first worker process found on the iteration.

Offset variable value will be added for each row sent to worker process. Note that offset variable has a crucial role for keeping track of matrix *A* row index so that each worker process knows which row index needs to be worked on. While Figure.7 shows how all of rows and columns of matrix *b* sent to all worker process.

Matrix $C_{i,j}$ with $N \times N$ dimensions will be used to hold the matrix result elements. The computation of a single *i* row element $C_{1,j}$ (for $j=1,2,..N$) requires an entire matrix element of B_{ij} and a subset row element of A_{qj} (where $q < i$), respectively. Because each worker process has those required element, For number *P* process used, each *P-1* worker process can compute row element of $C_{(i(P-1))+extra,j}$ (for $j=1,2,..N$) (where *extra* is an residual variable value and may has different value for different *P-1*). Matrix computation for each of worker process is shown in Figure. 8.

After the sub process multiplication is done in each process, they will send back their matrix result and offset variable value to the master process. For each value received from worker process, master process will generate the final matrix result according to the number offset variable.

The most important thing in this matrix operation division is that there is no dependent data between each sub process matrix multiplication. Thus, there is not any data synchronization needed between sub processes, which can reduce program complexity.

MPI Matrix Multiplications algorithms workshare is divided into two parts, one is for master process and the other is for work process.

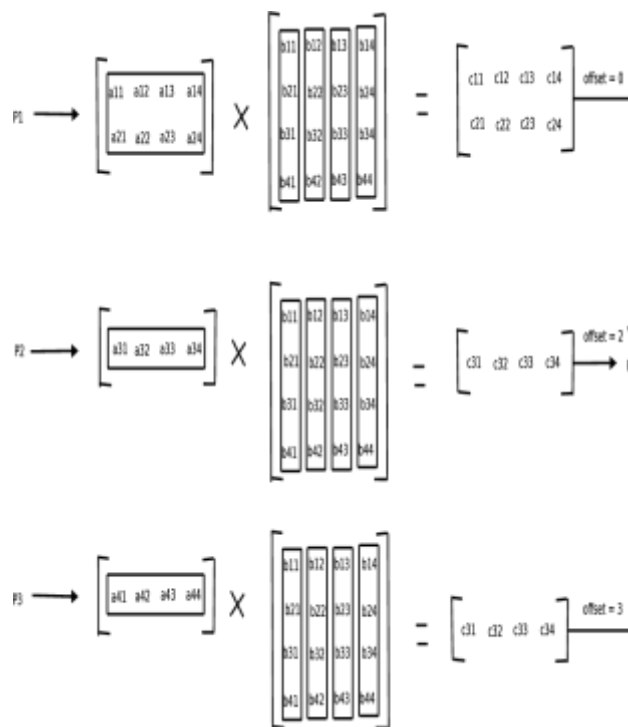


Figure 8. Matrix Multiplication For Each Worker Process

Master process algorithm steps are:

1. Value of matrixes is initialized using random function.
2. Wall time calculation process started using MPI_Wtime() function.
3. Row for each worker process is calculated including additional residual value.
4. Matrix *A* sub rows sent to all of worker process according to the row and offset variable. Offset variable will be iterated for each sent process.
5. All of Matrix *B* elements sent to all of worker process.
6. Master process wait to receive all of sub matrix results which will be sent from all worker processes.
7. Wall time calculation process stopped. Time interval between end and start time is calculated.
8. Total matrix operation is calculated using formula $N^2 * (2N - 1)$ in floating point type variable
9. Matrix operation per second in FLOPS is calculated by dividing the total matrix operations by the matrix runtime interval. For simplicity, FLOPS is converted into MFLOPS (i.e. Mega Floating Point Operation per Second) by dividing it again with (10^6) .

Worker process algorithm steps are:

1. Each worker process receive a subset rows of Matrix *A*, according to the offset variable sent from master process.

2. Each worker process receive all elements (rows * columns) of Matrix B which is sent from master process.
3. Matrix multiplication process is done for each worker process.
4. Each worker process send their sub rows of matrix C back to the master process.

In DSM machine architectures, communication cost is classified into two different types. First is communication cost between process which located on different machines, and second is communication cost between processes which located on same machines.

For communication cost between worker and master process which located on different machines over the network for matrix distributions, can be roughly calculated as:

- Cost distributing sub matrix A and matrix B to all worker process: $(P-1) * ((N^2) + (N^2/(P-1))) * t_c$, which is equal to $PN^2 * t_c$ (where t_c represents the time it takes to communicate one datum between processors over the network)
- Cost for receiving matrix result from all worker process: $(P-1) * (N^2/(P-1)) * t_c \rightarrow N^2 * t_c$.
- Total Communication cost:
 $(PN^2 + N^2) * t_c \rightarrow (P+1)N^2 * t_c$.

For communication cost between worker and master process which located on the same machines, its distribution process steps can be assumed to be same with the communication over the network with exception that time takes to communicate one datum between processors is not t_c but t_f , where t_f is represents the time it takes to communicate one datum between processors over the shared memory which is faster than t_c . Thus communication over the shared memory can be calculated as $(PN^2 + N^2) * t_f \rightarrow (P+1)N^2 * t_f$.

For distributed shared memory, the communication cost in shared memory side can be ignored because its fast and its assumed not influence the performance runtime.

Matrix multiplication complexity in this parallel program is divided into amount of worker process which is $P-1$ from the total amount of P process used. Thus, total matrix multiplication complexity in MPI for each worker process can be defined as $O(N^3/(P-1))$.

C. OpenMP Workshare Algorithm

Because OpenMP is an implementation of multithreading which uses multiple thread as it instruction carrier, OpenMP share their work among the amount of threads used in a parallel region. Thread classified into two types: master thread and worker thread [11].

By default, each thread executes the parallelized section of code independently. "Work-sharing constructs" can be used to divide a task among the threads so that each thread executes its allocated part of the code. Both Task parallelism and Data parallelism can be achieved using OpenMP in this way.

To determine how worksharing is done in OpenMP, OpenMP offer worksharing construct feature. Using worksharing construct, programmer can easily distribute work to each thread in parallel region in a well ordered manner. Currently OpenMP support four worksharing construct.

- omp for: used to split up loop iterations among the threads, also called loop constructs.
- sections: assigning consecutive but independent code blocks to different threads
- single: specifying a code block that is executed by only one thread, a barrier is implied in the end
- Master: similar to single, but the code block will be executed by the master thread only and no barrier implied in the end.

Since OpenMP is a shared memory programming model, most variables in OpenMP code are visible to all threads by default. But sometimes private variables are necessary to avoid race conditions and there is a need to pass values between the sequential part and the parallel region (the code block executed in parallel), so data environment management is introduced as data sharing attribute clauses by appending them to the OpenMP directive. The different types of clauses are:

- shared: the data within a parallel region is shared, which means visible and accessible by all threads simultaneously. By default, all variables in the work sharing region are shared except the loop iteration counter.
- private: the data within a parallel region is private to each thread, which means each thread will have a local copy and use it as a temporary variable. A private variable is not initialized and the value is not maintained for use outside the parallel region. By default, the loop iteration counters in the OpenMP loop constructs are private.
- default: allows the programmer to state that the default data scoping within a parallel region will be either shared, or none for C/C++, or shared, firstprivate, private, or none for Fortran. The none option forces the programmer to declare each variable in the parallel region using the data sharing attribute clauses.
- firstprivate: like private except initialized to original value.
- lastprivate: like private except original value is updated after construct.
- reduction: a safe way of joining work from all threads after construct.

Matrix multiplication workshare between threads in OpenMP, is done for each matrix row similar to MPI. The

difference is that MPI distribute its matrix element by sending it to all worker process, while OpenMP only need to declare the scope of matrix element variable as shared or private. Take an example, matrix multiplication between two $N \times N$ matrixes A_{ij} and B_{ij} which result will be contained in matrix C_{ij} . Each Matrix has 4 rows ($i=4$) and number threads used is 2 ($t=2$).

Rows distribution process done using workshare construct "pragma omp for" which is placed on the outer most of for loop repetitions. Thus, each thread (t) will responsible for calculating each matrix C_i row for all j column elements.

The amount of rows distributed to number of threads is determined by schedule clause. There are 3 types schedule clause (static, dynamic, and guided). Static schedule distribute iterations equally among all of threads (if there is a residual iterations, threads which has done its job first will be assigned to work on that iterations). Dynamic and guided allows iterations to be assigned to threads according their chunk size defined by programmer. In this program, iteration distribution among threads will be done using static schedule. To understand better how does matrix multiplication done in OpenMP look at Figure.9.

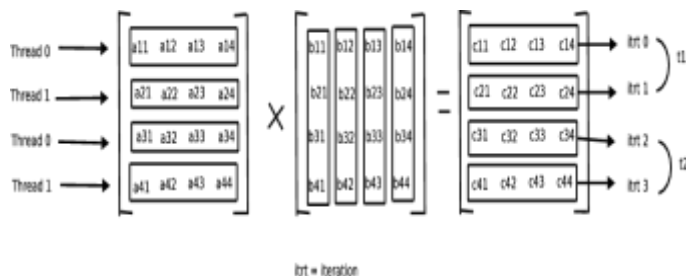


Figure 9. OpenMP Matrix Multiplication Algorithm Scheme

Figure.9 scheme gives us matrix multiplication process for two different time executions (t_1 and t_2). Because there are 4 rows in matrixes and only 2 thread used in programs, there will be 2 residual rows which will be assigned again to those two threads in different time. In t_1 , 2 threads (ID 0 and 1) will calculate first and second rows. After those two thread finished (assumed that time execution for each thread is same), in t_2 time, those 2 threads will calculate again for third and fourth rows.

Determining how many threads should be used in a parallel region is quite tricky. For the same operation performed by all threads (e.g. matrix multiplication) the most optimal number threads used is the same amount as the total number of cores available. But if in a parallel region consist a various operation (e.g. print, open file, read file, etc) using more than amount of CPU core might be a good idea. In this case, amount of thread can be determined by first, calculating operation cost for each different operation. Thus, number of threads used in matrix multiplication program must equal to the number of CPU cores.

The difference between MPI and OpenMP in process management is that MPI needs its master process to do only a specific job, which is distributing matrix elements, receiving the result calculation, and generating matrix result apart from calculating sub matrix like its workers. The reason behind this is to reduce parallel overhead when calculating a large of

matrix dimension over network transmission. Hence, master process can focus only on managing and distributing data.

Unlike MPI in OpenMP, process management and synchronization is done in the same memory (i.e shared memory) and not only master thread but all of thread also responsible of thread synchronization. Hence, master thread can also participate in the matrix multiplication process.

OpenMP matrix multiplication algorithm steps are:

1. Initializing matrixes value using random function
2. Wall time calculation process started using `omp_get_wtime()` function.
3. Matrix multiplication process for each thread is conducted using `pragma omp parallel` directives and `pragma omp for` workshare construct.
4. Wall time calculation process stopped. Time interval between end and start runtime calculation process is calculated.
5. Total matrix operation is calculated using formula $N^2 * (2N - 1)$ in floating point type variable
6. Matrix operation per second is calculated in FLOPS and then converted in MFLOPS which same with MPI.

Unlike MPI, which communication is done using message passing, communication cost in OpenMP is conducted between threads which is assumed to be fast and insignificant to the performance. Thus its time calculation can be ignored in this algorithm.

Matrix multiplication complexity in OpenMP parallel is divided into amount of threads which is t including master threads. Thus, total matrix multiplication complexity in OpenMPI for each thread can be defined as $O(N^3/t)$ (where number of threads is equal to number of CPU cores).

IV. RESULT AND DISCUSSION

A. Performance Test

Matrix multiplication algorithm tested ranging from dimension 100 up to 2000 on a three different scenario: sequential algorithm, MPI algorithm, and OpenMP algorithm. For OpenMP and sequential program, test was done on a single Intel core duo 1.7 Ghz T5300 laptop with 1GB RAM running on linux SUSE. For MPI program test was done on a two Intel core duo laptops one with frequency 1.7 GHz T5300 laptop with 1GB RAM running on Windows Xp SP3 and another one with frequency 1.83 GHz T5500 with 1GB RAM running on Windows-XP SP3.

Number of threads used in OpenMP is two (one master thread, and the other one is worker thread). Unlike OpenMP, number of process used is three (two worker process and one is master process). The reason is already discussed in the previous section. However, the number of worker process / threads which performed the matrix multiplication process is equal for both programming models (i.e. two workers).

Because there are three processes used in MPI which will be distributed on two multicore / SMP machines (i.e each machines will have two cores), one of the two machines will have its both of core CPUs occupied (i.e master process and worker process). Computer which initiates the MPI ring daemon has a master process in one of its core. Thus, computer machine with master process in it will also have a worker process, and the other machine will only has one worker process.

Statistical analysis conducted on one independent variable (i.e. Matrix Dimension) towards three dependent variable(e.g. runtime program, throughput program, and speedup). Using this statistical analysis, matrix dimension (i.e. as an independent variable) influence towards all of three dependent variable can be seen clearly.

B. Statistical Analysis Result

1) Parallel Runtime Towards Matrix Dimension

Table I. gives run time program obtained using wall time function for three different program (e.g. sequential, OpenMP, MPI). Wall time is the actual time taken by a computer to complete a task (i.e matrix multiplication). It is the sum of three terms: CPU time, I/O time, and the communication channel delay (e.g. if data are scattered on multiple machines (MPI)).

In OpenMP, wall time is calculated using `omp_get_wtime()` which starts from when the initial thread enter the parallel region until it exits the parallel region. Thus, process times calculated are thread creation, synchronization and multiplication tasks.

In MPI, wall time is calculated using `MPI_Wtime()` which starts from when the master process distribute the work among the worker processes until it receives matrix results sent from all worker processes. Process time calculated in MPI are communication between master - worker process and matrix multiplication for all worker process.

For $N=100$, runtime MPI is much slower up to 10 times compared to sequential and OpenMP. However For $N= 100$ to 2000 MPI runtime is gradually become faster compared to those two. MPI has the fastest runtime performance for $N > 500$.

TABLE I. RUNNING TIME COMPARISON WITH VARIOUS MATRIX DIMENSION

Matrix Dimension (N)	Sequential (s)	OpenMP (s)	MPI (s)
100	0.03	0.02	0.33
500	2.09	1.11	1.52
1000	22.52	14.36	8.19
2000	240.97	163.60	60.19

2) Parallel Throughput Towards Matrix Dimension

Table II. gives throughput result for three different program e.g. sequential, OpenMP, MPI). Throughput in MFLOPS is calculated by dividing number of matrix operations by wall time and 10^6 .

Both sequential and OpenMP has a throughput increase from $N= 100$ to 500, however, it starts to decrease from $N= 500$ to 2000. Nevertheless, MPI is different from the other two, It has a continuously increased throughput start from $N= 100$ to

2000. Eventhough, the throughput increase from $N= 1000$ to 2000 is not as significant as before.

TABLE II. THROUGHPUT COMPARISON WITH VARIOUS MATRIX DIMENSION

Matrix Dimension (N)	Sequential (MFLOPS)	OpenMP (MFLOPS)	MPI (MFLOPS)
100	59.08	86.82	6.07
500	119.54	224.35	164.85
1000	88.77	139.17	244.17
2000	8.91	13.17	265.77

3) Parallel Speedup Towards Matrix Dimension

Table III. gives speedup performance for two program(e.g. OpenMP, MPI) towards sequential program. Speedup performance in this research can be obtained by dividing wall-clock time of serial execution with wall-clock time of parallel execution OpenMP has a steady speedup for $N= 100$ to 2000 which has the average value at 1.5 s, while MPI gives a linear speed up growth for $N= 500$ to 2000 ranging from 1.38 s to 4 s. MPI gives no speedup for $N= 100$ because the matrix calculation is to small compared to the MPI running time and communication time.

TABLE III. SPEED COMPARISON WITH VARIOUS MATRIX DIMENSION

Matrix Dimension (N)	OpenMP (s)	MPI (s)
100	1.47	0.1
500	1.88	1.38
1000	1.57	2.75
2000	1.47	4

V. CONCLUDING REMARKS

A. Conclusion

OpenMP workshare between threads in matrix multiplication algorithm, done by using OpenMP FOR workshare construct. OpenMP FOR workshare in matrix multiplication algorithm is placed in the most outer loop of matrix multiplication operation. Using this placement, each OpenMP thread is assigned to work on each matrix C row for all columns.

MPI workshare in matrix multiplication algorithm done by using send and receive command. Matrix A row will be divided and sent together with all matrix B elements according to the number of worker process both on the different machines and the same machines. Each worker process will work on one row of matrix A multiplied by all row matrix B elements. If there are residual row, it will be added one each from the smallest worker process ID to the biggest worker ID.

The performance between OpenMP and MPI programming model is vary for matrix dimension N from 1 to 2000, although many standardizations made for both of parallel programming models (e.g. number of matrix workers, matrix algorithm steps, and machine specifications). Matrix multiplication complexity is divided for the same number of worker (i.e threads if its OpenMP with the complexity of $O(N^3/(P-1))$ and process if its MPI with the complexity of $O(N^3/t)$). Machine

specifications used in MPI also comparable with OpenMP which are: Intel Core Duo 1.7 GHz (for OpenMP) and Intel Core Duo 1.7 GHz together with Intel Core Duo 1.83 GHz both with 1 GB of RAM (for MPI).

Performance decline is common in every program testing performance especially when the data testing becomes large. This is due to the resources limitation (CPUs, memory, etc). However for different programming models which use the same resources and algorithm program, there are more reasons than just resources limitations.

For sequential because the worker process only one, its obvious that its overall performance is lower than the other two. For the MPI and OpenMPI, differences can be caused by how fast the workshare is done between worker processes / thread. MPI use message passing in sharing its work across processes which has network communication time over the network medium. In the other hand, OpenMP use thread in sharing its work inside shared memory machine which has no network communication time. Hence, OpenMP workshare should be faster than MPI. This can be seen at Table I, II, and III. OpenMP gains fast speedup and large throughput for $N=100$ to 500 while MPI gains slower but steady speedup and throughput. However, when as N grows larger (i.e $N=500$ to 2000) OpenMP performance is gradually become slower while MPI can still keep up with the growth of N .

Besides, the speed of the workshare, performance differences between OpenMP and MPI for large N computation can be caused by core CPUs access to memory. In parallel computing, memory is scalable with number of processors. Thus, increase in the number of processors and the size of memory will also increases the performance scalability.

MPI distribute its work by copying it on each worker process whether its located on the same memory or different memory machine. Thus, each processor which located on different machine can rapidly access its own memory without interference and without the overhead incurred with trying to maintain cache coherency (i.e MPI provides strong memory locality).

For this research, MPI is tested on distributed shared memory architectures using two SMP (Symmetric Multiprocessor) machines. MPI share two worker process between two different machines, thus MPI distribute the copy data located in different machines. Two worker processes can access its data on its own memory which will reduced the overhead half compared on single memory.

OpenMP in the other hand, use a single memory which is shared between core CPU in computer machine (UMA). Hence, the primary disadvantage is the lack of scalability between memory and CPUs. Adding more CPUs can geometrically increases traffic on the shared memory-CPU path, which leads to difficulty maintaining cache coherent systems between processors.

Therefore, the larger memory used in OpenMP, the more congested traffic on the shared memory-CPU path which result

in bottleneck. Increase in traffic associated with cache/memory management will produce more parallel overhead while maintaining cache coherency. OpenMP matrix program experienced this problem for $N=500$ to 2000 . The reason why the performance in OpenMP is decreasing starting from $N=500$ to 2000 is because traffic on the shared memory-CPU path is gradually become more congested for memory equal to 1GB. This can be seen at Table.III, where OpenMP does not give any more speedup than 1.5 s.

B. Future Work

Message Passing and Thread has been combined in a DSM (Distributed Shared Memory) parallel architecture to achieve a better performance results in nowadays. In this research MPI parallel expression used on shared memory architectures, has not exploited the thread safety programming explicitly. Using thread safety expression, MPI can explicitly control the threads which running multiple cores across SMP machines. This Message Passing - thread model also referred as Hybrid parallel programming model. In the next research, Hybrid parallel programming model will be used as evaluation material on DSM (Distributed Shared Memory) architecture.

ACKNOWLEDGMENT

The authors would like to thank to Gunadarma Foundation.

REFERENCES

- [1] Scalable High Performance Message Passing over InfiniBand for OpenMP, 2007
- [2] Performance Evaluation of MPI, UPC and OpenMP on Multicore Architectures, 2009
- [3] Answers, Message Passing Interface, 2010, <http://www.answers.com/topic/message-passing-interface>, accessed on August 2010
- [4] Answers, Shared memory, 2010, <http://www.answers.com/topic/shared-memory>, accessed on August 2010
- [5] Answers, Distributed memory, 2010, <http://www.answers.com/topic/distributed-memory>, accessed on August 2010
- [6] Answers, Parallel programming model, 2010, <http://www.answers.com/topic/parallel-programming-model>, access on August 2010
- [7] R. V. D. P. Barbara Chapman, Gabriele Jost, Using OpenMP. The MIT Press, 2007
- [8] B. Barney, OpenMP, 2010, <https://computing.llnl.gov/tutorials/openMP/>, accessed on August 2010
- [9] B. Barney, Message passing interface (mpi), 2010, <https://computing.llnl.gov/tutorials/mpi/>, accessed on August 2010
- [10] D. a. May, Matrix multiplication using mpi
- [11] hpccommunity, Multi-core Strategies: MPI and OpenMP, 2010, <http://www.hpccommunity.org/f55/multi-core-strategies-mpi-openmp-702/>, access on August 2010

AUTHORS PROFILE

- R. Refianti** is a Ph.D-Student at Faculty of Computer Science and Information Technology, Gunadarma University.
- A. B. Mutiara** is a Professor of Computer Science at Faculty of Computer Science and Information Technology, Gunadarma University
- D.T. Hasta**, Graduate from Master Program in Information System, Gunadarma University, 2010.

Hybrid Approaches to Image Coding: A Review

Rehna. V. J

Department of Electronics & Communication Engineering
Noorul Islam University
Kanyakumari District, India

Jeya Kumar. M. K

Department of Computer Application
Noorul Islam University
Kanyakumari District, India

Abstract— Now a days, the digital world is most focused on storage space and speed. With the growing demand for better bandwidth utilization, efficient image data compression techniques have emerged as an important factor for image data transmission and storage. To date, different approaches to image compression have been developed like the classical predictive coding, popular transform coding and vector quantization. Several second generation coding schemes or the segmentation based schemes are also gaining popularity. Practically efficient compression systems based on hybrid coding which combines the advantages of different traditional methods of image coding have also being developed over the years. In this paper, different hybrid approaches to image compression are discussed. Hybrid coding of images, in this context, deals with combining two or more traditional approaches to enhance the individual methods and achieve better quality reconstructed images with higher compression ratio. Literature on hybrid techniques of image coding over the past years is also reviewed. An attempt is made to highlight the neuro-wavelet approach for enhancing coding efficiency.

Keywords- Hybrid coding; Predictive coding; Segmentation; Vector Quantization; Compression ratio.

I. INTRODUCTION

Image Compression is an important area in the field of digital image processing. It deals with techniques for reducing the storage space required for saving an image or the bandwidth required for transmitting it. The main goal of image compression is to reduce irrelevance and redundancy of the image data thereby optimizing the storage space and increasing the transmission rate over WebPages. Image compression is performed in such a way that it enables image reconstruction. The amount of compression achieved depends on the contents of image data. A typical photographic image can be compressed to about 80% of its original size without experiencing noticeable degradation in the quality. The strong correlation between image data items enables reduction in data contents without significant quality degradation.

Image compression schemes [1] are generally classified as lossless compression schemes and lossy compression schemes. Lossless compression is an error free compression where the original data can be recovered after decompression. This scheme provides low compression ratio but has several applications, like in the compression of medical images where the loss of information are not acceptable. In lossy compression, some extend of the original data is lost during compression and so, after the decompression process, an approximation of original data is obtained.

Lossy schemes achieves higher compression ratio than lossless schemes and are used in applications, like compression of natural images where perfect reconstruction is not essential and we can afford the partial loss in the image data as long as it is within tolerance. During the design of a lossy compression scheme, two important issues are considered, the compression ratio and the tolerance in the visual quality degradation. Compression ratio [2] is the ratio of the size of the original image to that of the compressed image. It gives an indication of how much compression is achieved for a particular image. The compression ratio, starting at 1 with the first digital picture in the early 1960s, has reached a saturation level around 300:1 a couple of years ago. Image quality still remains as an important problem to be investigated. As the compression ratio increases, the quality of the resulting image degrades. So, a trade off between compression ratio and the tolerance in the visual quality degradation need to be considered during compression.

This paper focuses on hybrid image coding systems which combine the advantages of different classical methods to enhance the individual techniques and achieve better quality reconstructed image with higher compression ratio. Stress is given on the combined approach of image compression using neural networks and wavelet transforms, called the neuro-wavelet approach.

Rest of the paper is organized as follows: Section II deals with the error matrices, section III briefs about traditional techniques of image coding, section IV gives an overview of the early literature on image compression, section V is devoted to hybrid techniques to image compression followed by VQ-based hybrid techniques in section V.1, wavelet-based hybrid techniques in section V.2, ANN-based hybrid techniques in V.3 and the Neuro-Wavelet model in section V.4. Discussion & conclusion of the review is presented in section VI.

II. ERROR MATRICS

The different compression algorithms can be compared based on certain performance measures. Compression Ratio (CR) is the ratio of the number of bits required to represent the data before compression to the number of bits required after compression. Bit rate is the average number of bits per sample or pixel (bpp), in the case of image. The image quality can be evaluated objectively and subjectively. A standard objective measure of image quality is reconstruction error given by equation 1.

$$\text{Error, } E = \text{Original image} - \text{Reconstructed image} \quad (1)$$

Two of the error metrics used to compare the various image compression techniques are the mean square error (MSE) and the Peak Signal to Noise Ratio (PSNR). MSE refers to the average value of the square of the error between the original signal and the reconstruction as given by equation 2. The important parameter that indicates the quality of the reconstruction is the peak signal-to-noise ratio (PSNR). PSNR is defined as the ratio of square of the peak value of the signal to the mean square error, expressed in decibels.

$$MSE = E / (\text{SIZE OF IMAGE}) \quad (2)$$

The MSE is the cumulative squared error between the compressed and the original image, whereas PSNR is a measure of the peak error. The mathematical formulae for the computation of MSE & PSNR is :

$$MSE = 1/MN \left[\sum_{i=1}^M \sum_{j=1}^N (I_{ij} - I'_{ij})^2 \right] \quad (3)$$

$$PSNR = 20 * \log_{10} (255 / \text{sqrt}(MSE)) \quad (4)$$

where $I(x,y)$ is the original image, $I'(x,y)$ is the approximated version (which is actually the decompressed image) and M, N are the dimensions of the images, 255 is the peak signal value. A lower value for MSE means lesser error, and as seen from the inverse relation between the MSE and PSNR. Higher values of PSNR produce better image compression because it means that the ratio of Signal to Noise is higher. Here, the 'signal' is the original image, and the 'noise' is the error in reconstruction. So, a compression scheme having a lower MSE (and a high PSNR), can be recognized as a better one. Subjective quality is measured by psychophysical tests and questionnaires.

III. TRADITIONAL TECHNIQUES

To date, many compression algorithms have been developed for image coding such as the classical predictive coding [3], the popular transform coding [4], the commercially successful wavelet coding [5] and vector quantization [6]. Predictive coding refers to the de-correlation of similar neighbouring pixels within an image to remove redundancy. Transform coding, an efficient coding scheme is based on utilization of inter-pixel correlation which is a core technique recommended by JPEG. Wavelet coding is a popular form of data compression well suited for image and audio compression. The wavelet transform have become the most prevalent techniques among the image coding techniques as they are localized in both spatial and frequency domains. With wavelets, a compression rate of up to 1:300 can be achieved. Wavelet compression allows the integration of various compression techniques into one algorithm. Vector quantization, a technique often used in lossy data compression requires the development of an appropriate codebook to compress data.

Another recent lossy image compression method is the fractal compression [7, 32] which is best suited for textures and natural images, relying on the fact that parts of an image often resemble other parts of the same image. Fractal algorithms convert these parts into mathematical data called "fractal codes" which are used to recreate the encoded image. Recently, several segmentation based, or the second generation image

coding techniques [8] are also gaining popularity. Many image compression algorithms such as the Bandelets [9], the Prune tree [10], the Prune-Join tree [10], the GW image coding method [11] based on the sparse geometric representation etc have also been introduced. Image compression is also achieved with considerable efficiency using neural networks [12, 13] due to their parallel architectures and flexibility. Neural networks have the ability to preprocess input patterns to produce simpler patterns with fewer components. This compressed information (stored in a hidden layer) preserves the full information obtained from the external environment.

IV. EARLY LITERATURE

The concept of compressing 2 dimensional signals, especially images was introduced in the year 1961, by Wholey. J [14]. The first data compression approach was the predictive coding technique in which the statistical information of the input data is considered to reduce redundancy. Although the resulting compression was not great, there were reasons for believing that this procedure would be more successful with realistic pictorial data. A method of data compression by run length encoding was published in 1969, by Bradley, S.D [15]. In his paper, the optimal performance of the code was for a compression factor of 13.20. An adaptive variable length coding system was presented by Rice et al. in 1971 [16]. Using sample to sample prediction, the coding system produces output rates within 0.25 bits/picture element (pixel) of the one dimensional difference entropy, for entropy values ranging from 0 to 8 bits/pixel.

The transform coding approaches to image compression was introduced in the year 1971 with application of discrete Fourier transform for achieving image compression [17]. Pratt and Andrews [18] studied bandwidth compression using the Fourier transform of complete pictures. The most commonly used transform coding uses the Fourier related transforms such as the KL transform [19], HADAMARD transform [20] etc. Singular value decomposition [21] is the representation of data using smaller number of variables and had been widely used for face detection and object recognition. SVD has been applied for image compression in 1976 and was found successful. In the past decades, Discrete Cosine Transform or DCT has been the most popular for image coding because it provides optimal performance and can be implemented at a reasonable cost.

Recent advances in signal processing tools such as wavelets opened up a new horizon in sub and image coding. Wavelets were applied to image coding in the year 1989. The wavelet transform have proven to be very effective and has gained popularity over the DCT. Discrete Wavelet Transforms has the ability to solve the blocking effect introduced by the DCT. Different wavelets and its variants were used in later years to achieve better compression. These include the harmonic wavelets, the very efficient embedded zero tree wavelet (EZW) [22], the much popular SPIHT (Set Portioning in Hierarchical Trees) [23], EBCOT (Embedded Block Coding with Optimized Truncation) [24] etc to name a few. EZW coding for image compression presented by Shapiro in his paper "Smart compression using the EZW algorithm" in 1993

uses wavelet coefficients for coding. EZW coding exploits the multi resolution properties of the wavelet transforms to give a computationally simple algorithm with better performance compared to other existing wavelet transforms. The techniques of EZW, SPIHT, EBCOT etc are used as reference for comparison with the new techniques of image compression.

The second generation coding methods [8] or the segmentation based methods of image coding were introduced in the year 1985 and many variations have been introduced since then. Two groups can be formed in this class: methods using local operators and combining their output in a suitable way and methods using contour-texture descriptions. For low bit-rate compression applications, segmentation-based coding methods provide, in general, high compression ratios when compared with traditional (e.g. transform and subband) coding approaches. Among the many segmentation techniques that have been developed, the binary space partition scheme (BSP) [25] is a simple and effective method of image compression. The concept of BSP for hidden surface removal was published in the year 1996 by Hyder Radha et. al. Recently the BSP scheme is enhanced with the wavelet approach called as geometric wavelets [11] by Dekel et. al.

Over the last decade, numerous attempts have been made to apply artificial neural networks (ANNs) for image compression. Neural network approaches used for data compression seem to be very efficient due to their structures which offer parallel processing of data. Kohonen's self organizing maps were the first neural networks used to achieve vector quantization for image compression. This is discussed by Luttrell, S.P [26] in his paper. Direct applications of neural networks to image compression came with the Back Propagation Neural Network (BPN) [29] in 1989 proposed by Sonehara et al. Apart from Kohonen Selforganizing Maps (SOM) and BPNs, other neural networks that are used for image coding include Hierarchical SOMs (HSOMs)[27], Modular Neural networks (MNNs)[30], and Cellular Neural Networks[28]. Researches on neural networks for image compression are still making steady advances.

V. HYBRID TECHNIQUES

Hybrid approaches to image compression deals with combining two or more traditional approaches to enhance individual methods and achieve better quality reconstructed images with higher compression ratio. The concept of hybrid coding was introduced in the early 1980's itself by Clarke R.J [31] on transform coding combined with predictive coding. Since then, various hybrid techniques have evolved namely the vector quantization combined with DCT, Block Truncation Coding (BTC) with Hopfield neural networks, predictive coding with neural networks wavelet coding with neural networks, segmentation based techniques with predictive coding techniques, fractal coding with neural networks, subband coding with arithmetic coding, segmentation coding with wavelet coding, DCT with DWT, SPIHT with fractal coding, cellular neural networks with wavelets etc. Some of the different successful hybrid coding techniques are discussed in the next few sections.

V.1 VQ-Based Hybrid Techniques

Vector quantization (VQ) is a successful, effective, efficient, secure, and widely used compression technique over two decades. The strength of it lies in higher compression ratio and simplicity in implementation, especially of the decoder. The major drawback of VQ is that, decompressed image contains blockiness because of the loss of edges due to which the quality of image degrades. VQ has been combined with traditional techniques of image coding to achieve better performance compared to the conventional VQ scheme. Some works related to VQ based hybrid approaches to image coding over the past two decades are discussed here.

Vector Quantization of images based on a neural network clustering algorithm, namely the Kohenons Self Organising Maps proposed by Feng et. Al [33] were one of the early works in hybrid VQ techniques. P. Daubechies et. al introduced the coding of images using vector quantization in the wavelet transform domain [34]. Here, a wavelet transform is first used in order to obtain a set of orthonormal subclasses of images; the original image is decomposed at different scales using pyramidal algorithm architecture. The decomposition is along the vertical and horizontal directions and maintains the number of pixels required to describe the image at a constant. Then according to Shannon's rate-distortion theory, the wavelet coefficients are vector quantized using a multiresolution codebook. To encode the wavelet coefficients, a noise-shaping bit-allocation procedure which assumes that details at high resolution are less visible to the human eye is proposed in the work.

A hybrid BTC-VQ-DCT (Block Truncation Coding-Vector Quantization - Discrete Cosine Transform) [35] image coding algorithm was proposed by Wu et. al. The algorithm combines the simple computation and edge preservation properties of BTC and the high fidelity and high-compression ratio of adaptive DCT with the high-compression ratio and good subjective performance of VQ. This algorithm and can be implemented with significantly lower coding delays than either VQ or DCT alone. The bit-map generated by BTC is decomposed into a set of vectors which are vector quantized. Since the space of the BTC bit-map is much smaller than that of the original 8-bit image, a lookup-table-based VQ encoder has been designed to 'fast encode' the bit-map. Adaptive DCT coding using residual error feedback is implemented to encode the high-mean and low-mean subimages. The overall computational complexity of BTC-VQ-DCT coding is much less than either DCT or VQ, while the fidelity performance is competitive. The algorithm has strong edge-preserving ability because of the implementation of BTC as a precompress decimation. The total compression ratio achieved is about 10:1.

A hybrid coding system that uses a combination of set partition in hierarchical trees (SPIHT) and vector quantisation (VQ) for image compression was presented by Hsin. H. C et. Al [36]. Here, the wavelet coefficients of the input image are rearranged to form the wavelet trees that are composed of the corresponding wavelet coefficients from all the subbands of the same orientation. A simple tree classifier has been proposed to group wavelet trees into two classes based on the amplitude distribution. Each class of wavelet trees is encoded using an appropriate procedure, specifically either SPIHT or

VQ. Experimental results show that advantages obtained by combining the superior coding performance of VQ and efficient cross-subband prediction of SPIHT are appreciable for the compression task, especially for natural images with large portions of textures.

Arup Kumar Pal et. al have recently proposed a hybrid DCT-VQ based approach for efficient compression of color images [37]. Initially DCT is applied to generate a common codebook with larger codeword sizes. This reduces computation cost and minimizes blocking artifact effect. Then VQ is applied for final compression of the images that increases PSNR. Table 1 shows the simulation results for two test images using the conventional VQ method and the proposed hybrid method. Better PSNR values are obtained for the hybrid technique compared to the conventional VQ process. So the proposed hybrid scheme improves the visual quality of the reconstructed image compare to the conventional VQ process. The simulation result also shows that the proposed scheme reduces the computation cost (including codebook construction, VQ encoding process and VQ decoding process time) compared to the conventional VQ process.

TABLE I. SIMULATION RESULTS SHOWING THE COMPARISON BETWEEN CONVENTIONAL VQ & HYBRID VQ

Method	Code-book Size	Block Size	Test Images (512 x 512)			
			Sailboat		Pepper	
			PSNR in dB	Overall Computation Time in seconds	PSNR in dB	Overall Computation Time in seconds
Conventional VQ	1024	8 x 8	25.6392	485.91	27.6969	484.01
		16 x 16	23.5795	520.02	25.5791	518.69
Hybrid DCT-VQ	1024	8 x 8	26.7528	164.34	28.6675	159.75
		16 x 16	25.3996	43.35	26.3590	42.34

These works are some examples that prove the improvement in performance of VQ based hybrid techniques over the individual methods.

V.2 Wavelet Based Hybrid Techniques

The wavelet transform, which provides a multiresolution representation of images, has been widely used in image compression. Wavelet transforms have been combined with classical methods of image coding to obtain high quality compressed images with higher compression ratios. Some of the wavelet based hybrid techniques are discussed in this section. Durrani et. Al [38] combined the run length encoding with the wavelet transforms to achieve better compression. The main attraction of this coding scheme is its simplicity in which no training and storage of codebooks are required. Also its high visual quality at high compression ratio outperforms the standard JPEG codec for low bitrate applications. Jin Li Kuo et. al [39] proposed a hybrid wavelet-fractal coder (WFC) for image compression. The WFC uses the fractal contractive mapping to predict the wavelet coefficients of the higher resolution from those of the lower resolution and then encode the prediction residue with a bitplane wavelet coder. The fractal prediction is adaptively applied only to regions where the rate saving offered by fractal prediction justifies its overhead. A rate-distortion criterion is derived to evaluate the fractal rate saving and used to select the optimal fractal

parameter set for WFC. The superior performance of the WFC is demonstrated with extensive experimental results.

According to F. Madeiro et. al., [40] wavelet based VQ is the best way of quantizing and compressing images. This methodology takes multiple stage discrete wavelet transform of code words and uses them in both search and design processes for the image compression. Accordingly, the codebook consists of a table, which includes only the wavelet coefficients. The key idea in the mechanism of this algorithm is finding representative code vectors for each stage, They are found by first combining n code words in k groups, where kn gives the codebook size. This technique has a major drawback in the amount of computations during the search for optimum code vector in encoding. This complexity can be reduced by using an efficient codebook design and wavelet based tree structure.

Iano, Y et. Al [41] presents a new fast and efficient image coder that applies the speed of the wavelet transform to the image quality of the fractal compression. Fast fractal encoding using Fisher's domain classification is applied to the lowpass subband of wavelet transformed image and a modified set partitioning in hierarchical trees (SPIHT) coding, on the remaining coefficients. Furthermore, image details and wavelet progressive transmission characteristics are maintained, no blocking effects from fractal techniques are introduced, and the encoding fidelity problem common in fractal-wavelet hybrid coders is solved. The proposed scheme promotes an average of 94% reduction in encoding-decoding time comparing to the pure accelerated Fractal coding results. The simulations results show that, the new scheme improves the subjective quality of pictures for high-medium-low bitrates.

Alani et. al [11] proposes a well suited algorithm for low bit rate image coding called the Geometric Wavelets. Geometric wavelet is a recent development in the field of multivariate piecewise polynomial approximation. Here the binary space partition scheme which is a segmentation based technique of image coding is combined with the wavelet technique [51]. The discrete wavelet transforms have the ability to solve the blocking effect introduced by the DCT. They also reduce the correlation between neighboring pixels and gives multi scale sparse representation of the image. Wavelet based techniques provide excellent results in terms of rate distortion compression, but they do not take advantage of underlined geometry of the edge singularities in an image. The second generation coding techniques exploits the geometry of the edge singularities of the image. Among them the binary space partition scheme is a simple and efficient method of image coding, which is combined with geometric wavelet tree approximation so as to efficiently capture edge singularities and provide a sparse representation of the image. The geometric wavelet method successfully competes with the state-of-the-art wavelet methods such as EZW, SPIHT and EBCOT algorithms. A gain of 0.4 dB over SPIHT and EBCOT algorithms is reported. This method also outperforms other recent methods that are based on sparse geometric representation. For eg: this algorithm reports a gain of 0.27 dB over the bandelets algorithms at 0.1 bits per pixel.

A hybrid compression method for integral images using Discrete Wavelet Transform and Discrete Cosine Transform is proposed by Elharar et. Al [42]. A compression method is developed for the particular characteristics of the digitally recorded integral image. The compression algorithm is based on a hybrid technique implementing a four-dimensional transform combining the discrete wavelet transform and the discrete cosine transform. The proposed algorithm outperforms the baseline JPEG compression scheme.

V.3 ANN Based Hybrid Techniques

The existing conventional image compression technology can be developed into various learning algorithms to build up neural networks for image compression. This will be a significant development and a wide research area in the sense that various existing image compression algorithms can actually be implemented by one neural network architecture empowered with different learning algorithms.

Hence, the powerful parallel computing and learning capability of neural networks can be fully exploited to build up a universal test bed where various compression algorithms can be evaluated and assessed. Three conventional techniques are covered in this section, which include predictive coding, fractal coding, and wavelet transforms.

A. Predictive Coding Neural Networks

Predictive coding has been proved to be a powerful technique in de-correlating input data for speech and image compression where a high degree of correlation is embedded among neighboring data samples. The autoregressive (AR) model, a classification of predictive coding, has been successfully applied to image compression. Predictive coding in terms of applications in image compression can be further classified into linear and non-linear AR models. Conventional technology provides a mature environment and well developed theory for predictive coding which is represented by LPC (linear predictive coding), PCM (pulse code modulation), DPCM (delta PCM) or their modified variations. Non-linear predictive coding, however, is very limited due to the difficulties involved in optimizing the coefficients extraction to obtain the best possible predictive values. Under this circumstance, a neural network provides a very promising approach in optimizing non-linear predictive coding [43, 44]. Based on a linear AR model, a multilayer perceptron neural network can be constructed to achieve the design of its corresponding non-linear predictor as shown in Fig. 1. For the pixel X_n which is to be predicted, its N neighbouring pixels obtained from its predictive pattern are arranged into a one dimensional input vector $X = \{X_{n-1}, X_{n-2}, \dots, X_{n-N}\}$ for the neural network.

A hidden layer is designed to carry out back propagation learning for training the neural network. Predictive performance with neural networks is claimed to outperform the conventional optimum linear predictors by about 4.17 and 3.74 dB for two test images [44]. Further research, especially for non-linear networks, is encouraged by the reported results to optimize their learning rules for prediction of those images whose contents are subject to abrupt statistical changes.

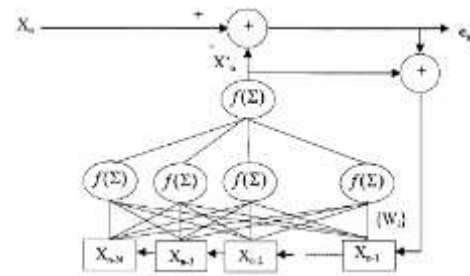


Figure 1 Predictive Neural Network

B. Fractal Neural Networks

Fractal configured neural networks [45,46], based on iterated function system (IFS) codes [47], represent another example along the direction of combining existing image compression technology with neural networks. Its conventional counterpart involves representing images by fractals and each fractal is then represented by so called IFS, which consists of a group of affined transformations. To generate images from IFS, random iteration algorithm is used which is the most typical technique associated with fractal based image decompression [47]. Hence, fractal based image compression features lower speed in compression and higher speed in decompression. By establishing one neuron per pixel, two traditional algorithms of generating images using IFSs are formulated into neural networks in which all the neurons are organized as a topology with two dimensions [46].

Fig. 2 illustrates the network structure in which $w_{ij,i'j'}$ is the coupling weight between (ij) th neuron to $(i'j')$ th one, and s_{ij} is the state output of the neuron at position (i,j) . The training algorithm is directly obtained from the random iteration algorithm in which the coupling weights are used to interpret the self similarity between pixels. In common with most neural networks, the majority of the work operated in the neural network is to compute and optimize the coupling weights, $w_{ij,i'j'}$. Once these have been calculated, the required image can typically be generated in a small number of iterations. Hence, the neural network implementation of the IFS based image coding system could lead to massively parallel implementation on a dedicated hardware for generating IFS fractals. Although the essential algorithm stays the same as its conventional algorithm, solutions could be provided by neural networks for the computing intensive problems, which are currently under intensive investigation in the conventional fractal based image compression research area.

C. Wavelet Neural Networks

Based on wavelet transforms, a number of neural networks are designed for image processing and representation [48, 49]. Wavelet networks are a combination of radial basis function (RBF) networks and wavelet decomposition, where radial basis functions were replaced by wavelets. When a signal $s(t)$ is approximated by daughters of a mother wavelet $h(t)$, for instance, a neural network structure can be established as shown in Fig. 3 [48, 49].

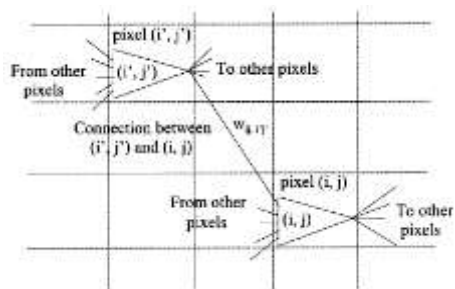


Figure 2 Fractal Neural network

Here, step1 computes a search direction $[s]$ at iteration i . Step2 computes the new weight vector using a variable step-size α . By simply choosing the stepsize α , as the learning rate, the above two steps can be constructed as a learning algorithm for the wavelet neural network in Fig.3. Experiments reported [19] on a number of image samples support the wavelet neural network by finding out that Daubechie's wavelet produces a satisfactory compression with the smallest errors. Haar's wavelet produces the best results on sharp edges and low-noise smooth areas.

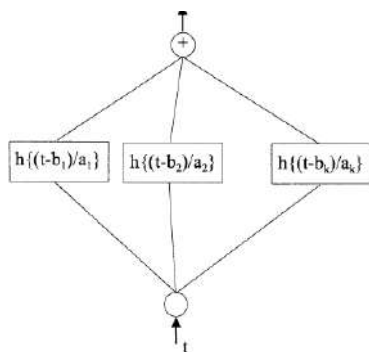


Figure 3 Structure of Wavelet Neural Network

D. The Neuro-Wavelet Model

A neuro-wavelet model [50] for compression of digital images which combines the advantage of wavelet transform and neural network was proposed by Vipula Singh et. al. Here images are decomposed using wavelet filters into a set of sub bands with different resolution corresponding to different frequency bands. Different quantization and coding schemes are used for different sub bands based on their statistical properties. The coefficients in low frequency band are compressed by differential pulse code modulation (DPCM) and the coefficients in higher frequency bands are compressed using neural network. Satisfactory reconstructed images with large compression ratio can be achieved by this method.

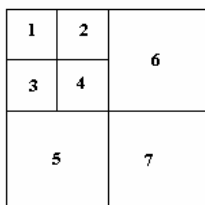


Figure 4 Decomposition on frequency plane by wavelet transform



Figure 5 Image compression system based on the neuro-wavelet model

The neuro-wavelet model is described in the fig. 5. First the image is decomposed into different sub bands using wavelet transforms as shown in the fig. 4. Since the human visual system has different sensitivity to different frequency components, the scheme shown here may be adapted. The low frequency band i.e band1 is encoded with DPCM (Differential Pulse Code Modulation). After that these coefficients are scalar quantized. The remaining frequency bands are coded using neural networks. Band2 and Band3 contain the same frequency contents for different orientation. Same neural network is used to compress the data in these bands and a different neural network is used for both band5 and band6. Band4 coefficient is coded using a separate neural network as frequency characteristics of this band does not match with other bands. Band7 is discarded as it contains little information to contribute to the image. This band has little effect on the quality of the reconstructed image. The output of the hidden layer of the neural network is then scalar quantized. Finally these quantized values are entropy coded. Huffmann coding is used here. This paper concludes that compared to the traditional neural network compression or the classical wavelet based compression applied directly on the original image, the neural network based approach improved the quality of the reconstructed image. It also enhances the overall processing time.

TABLE II. BIT RATE & PSNR FOR DIFFERENT WAVELET FILTERS FOR LENA IMAGE

Wavelet Filter	Bit Rate in bpp (bits per pixel)	PSNR in dB
db18	0.40	29.371
db6	0.39	29.25
db4	0.37	29.058

Experiments were conducted using the images 'lena', 'pepper', and 'house' of size 256 x 256, with $2^8 = 256$ gray levels. Image was decomposed using Daubechies' 4-coefficient filter (DAUB 4), 6-coefficient filter (DAUB 6) and 18 coefficient filter (DAUB 18). Band-1 is coded using DPCM, Band-2 and 3 is coded using a neural network with eight units in the input and the output and 6 hidden units i.e 8-6-8 neural network. Band-4 is coded using a 8-4-8 neural network, and band-5 and 6 using 16-1-16 network. Scalar quantization and Huffman coding was used on the coefficients of hidden layer. PSNR was evaluated for the resulting image and the comparison between bit rate and PSNR are shown in table 2.

VI. CONCLUSION

This paper takes a detailed survey on the existing and most significant hybrid methods of image coding. Every approach is found to have its own merits and demerits. VQ based hybrid approaches to compression of the images helps in improving the PSNR along with reducing the computational complexity. It is seen that good quality reconstructed images are obtained, even at low bit-rates when wavelet based hybrid methods are applied to image coding. The powerful parallel processing and learning capability of neural networks can be fully exploited in the ANN based hybrid approaches to image compression. Predictive coding neural networks are found very suitable for compression of text files. High encoding efficiency and good reproduction quality are realized with this type of compression. Fractal neural networks reduce the computation time of encoding/decoding since the compression/ decompression process can be executed in parallel. Simulated results show that the neural network approach can obtain a high compression-ratio and a clear decompressed image. Wavelet networks applied to image compression provide improved efficiency compared to the classical neural networks. By combining wavelet theory and neural networks capability, significant improvements in the performance of the compression algorithm can be realised. Results have shown that the wavelet networks approach succeeded in improving performance and efficiency, especially for rates of compression lower than 75%. The proposed scheme of neuro-wavelets in section C can achieve good compression at low bit rates with good quality reconstructed images. It can be considered that the integration of classical with soft computing based image compression methods enables a new way of achieving higher compression ratio.

The existing conventional image compression technology can be developed by combining high performance coding algorithms in appropriate ways, such that the advantages of both techniques are fully exploited. This will be a significant development and a wide research area in the sense that various traditional image compression algorithms can be empowered with different successful algorithms to achieve better performance. Future research work can be made in this direction to build up new advancements in the field of image compression.

ACKNOWLEDGMENT

The authors thank the reviewers for their valuable comments and suggestions that helped us to make the paper in its present form.

REFERENCES

- [1] Rafael C. Gonzalez and Richard E. Woods, "Digital Image Processing", Pearson Edition, 2005.
- [2] David Salomon, "Data Compression: The Complete Reference", Springer international Edition, 2005.
- [3] Bahl. L. R, Kobayashi H, "Image Data Compression by Predictive Coding I: Prediction Algorithms", IBM Journal of Research & Development, vol. 18, no. 2, 1974.
- [4] Wen-Jun Zhang Song-Yu Yu Hong-Bin Chen , "A new adaptive classified transform coding method [image coding]" International Conference on Acoustics, Speech & Signal Processing, 1989.
- [5] M. Antonini, M. Barlaud, P. Mathieu, and I. Daubchies, "Image coding using wavelet transform," *IEEE Trans. Image Process.*, vol. 1, no. 4, pp. 205–220, Apr. 1992.
- [6] Budge, S.; Baker, R, "Compression of color digital images using vector quantization in product codes", *IEEE Trans. Image Process.*, vol. 10, no. 4, pp. 129–132, Apr. 1985.
- [7] Hoces, C, "Fractal compression theory", *IEEE Trans. Multimedia.*, vol. 2, no. 3, pp. 76–94, Apr. 1995.
- [8] M. Kunt, A. Ikonomopoulos, and M. Koche, "Second generation image coding techniques," *Proc. IEEE*, vol. 73, no. 4, pp. 549–574, Apr. 1985.
- [9] E. L. Pennec and S. Mallat, "Sparse geometric image representation with bandelets," *IEEE Trans. Image Process.*, vol. 14, no. 4, pp. 423–438, Apr. 2005.
- [10] R. Shukla, P. L. Daragotti, M. N. Do, and M. Vetterli, "Rate-distortion optimized tree structured compression algorithms for piecewise polynomial images," *IEEE Trans. Image Process.*, vol. 14, no. 3, pp.343–359, Mar. 2005.
- [11] D. Alani, A. Averbuch, and S. Dekel, "Image coding with geometric wavelets," *IEEE Trans. Image Process.*, vol. 16, no. 1, pp. 69–77, Jan. 2007.
- [12] N. Sonhera, M. Kawato, S. Miyake and K. Nakane, "Image data compression using neural networks model", *Proceeding of IJCNN, Washington, DC*, 1989, pp. 1135–1141.
- [13] Manphol s. Chin and M. Arozullah, "Image compression with a hierarchical neural networks", *IEEE trans. Aerospace and Electronic Systems*, vol. 32, no 1. 1996.
- [14] Wholey, J. "The coding of pictorial data", *IRE Trans. Information Theory.*, vol. 7, no. 2, pp. 99–110, Apr. 1961.
- [15] Bradley, S.D, "Optimizing a scheme for run length encoding", *Proceedings of the IEEE.*, vol. 57, no. 1, pp. 108–120, Jan. 1969.
- [16] Rice. R. Plaunt, J, "Adaptive Variable-Length Coding for Efficient Compression of Spacecraft Television Data", *IEEE Trans. Communication Technology*, vol. 19, no. 6, pp. 889–905, Jan. 1971.
- [17] Anderson, G. Huang, T, "Piecewise Fourier Transformation for Picture Bandwidth Compression", *IEEE Trans. Communication Technology*, vol. 19, no. 2, pp. 133–140, Apr. 1971.
- [18] Pratt, W, Andrews, H, " Performance Measures for Transform Data Coding" *Trans. Communications* , vol. 20, no. 3, pp. 411–415, Jun. 1972.
- [19] Ready P, Wintz P, "Information Extraction, SNR Improvement, and Data Compression in Multispectral Imagery", *IEEE Trans. Communications*, vol. 21, no. 10, pp. 1123–1131, Oct. 1973.
- [20] Ferial, Erlan H. Barba, Joseph Scheinberg, Norman, "A Simple Predictive Transform Coder for Images" *IEEE Military Communications Conference - Communications - Computer*, 1986.
- [21] Andrews, H. Patterson, C, "Singular Value Decomposition (SVD) Image Coding ", *IEEE Trans. Communications*, vol. 24, no. 4, pp. 425–432, Apr. 1976.
- [22] J. M. Shapiro, "Embedded image coding using zerotrees of wavelet coefficients," *IEEE Trans. Signal Process.*, vol. 41, no. 12, pp. 3445–3462, Dec. 1993.
- [23] A. Said and W. A. Pearlman, "A new, fast and efficient image codec based on set partitioning in hierarchical trees," *IEEE Trans. Circuits Syst.Video Technol.*, vol. 6, no. 3, pp. 243–250, Jun. 1996.
- [24] D. Taubman, "High performance scalable image compression with EBCOT," *IEEE Trans. Image Process.*, vol. 9, no. 7, pp. 1158–1170, Jul. 2000.
- [25] H. Radha, M. Vetterli, and R. Leonardi, "Image compression using binary space partitioning trees," *IEEE Trans. Image Process.*, vol. 5, no. 12, pp. 1610–1624, Dec. 1996.
- [26] Luttrell, S.P, "Image compression Using A Neural Network", *Geoscience and Remote Sensing Symposium, 1988. IGARSS, 1988.*
- [27] Jose M, Barbalho et.al, "Hierarchical SOM applied to Image Compression", *Proc. IEEE*, 2001, pp 442-447.
- [28] L. O. Chua and L. Yang, "Cellular neural networks: Theory and applications," *IEEE Trans. Circuits Systems.*, vol. 35, pp. 1257–1290, Oct. 1988.

- [29] M. Mougeot, R. Azeneott, B. Angeniol, "Image compression with back propagation: improvement of the visual restoration using different cost functions" *IEEE Trans.neural networks* Vol 4, No 4 1991, pp 467-476.
- [30] Eiji Watanbe and Katsumi Mori, "Lossy Image compression using a modular structured neural network", *Proc. of IEEE Neural Network and Signal Processing Society*, XI, Sept 2001.
- [31] Clarke, R.J. "Hybrid intraframe transform coding of image data" *IEE Proceedings on Communications, Radar and Signal Processing*, 1984.
- [32] Michael, F Barnsley, "Fractal image compression", *Notices of the AMS*, Vol. 43, No. 6, June 1996, pp 657-662.
- [33] Nasrabadi, N.M. Feng, Y, "Vector quantization of images based upon the Kohonen self-organizing feature maps", *IEEE International Conference on Neural Networks*, 1988.
- [34] Antonini, M. Barlaud, M. Mathieu, P. Daubechies, I, "Image coding using vector quantization in the wavelet transform domain", *International Conference on Acoustics, Speech & Signal Processing*, 1990.
- [35] Wu, Y. Coll, D.C, "BTC-VQ-DCT hybrid coding of digital images", *IEEE Trans. Communications*, vol. 39, no. 9, pp. 1283-1287, Sept. 1991.
- [36] C.K. Hsin, H.C. Lin, S.F, "Wavelet tree classification and hybrid coding for image compression" *IEE Proceedings on Vision, Image and Signal Processing*, vol. 152, no. 6, pp. 752-756, Dec. 2005.
- [37] Pal, A.K.; Biswas, G.P.; Mukhopadhyay, S, "A Hybrid DCT-VQ Based Approach for Efficient Compression of Color Images" *International Conference on Computer and Communication Technology (ICCCCT)*, 2010.
- [38] Goh, K.H, Soraghan, J.J, Durrani, T.S, "Wavelet transform based adaptive bit-plane run-length coding for still images" *Electronics Letters*, vol. 30, no. 5, pp. 752-756, Mar. 1994.
- [39] Jin Li Kuo, C.-C.J, "Image compression with a hybrid wavelet-fractal coder", *IEEE Trans. Image Process.*, vol. 8, no. 6, pp. 868-874, Jun. 1999.
- [40] Madeiro, F.; Vajapeyam, M.S.; Morais, M.R.; Aguiar Neto, B.G.; de Alencar, M.S, "Multiresolution codebook design for wavelet/VQ image coding" *International Conference on Pattern Recognition*, 2000.
- [41] Iano, Y. da Silva, F.S. Cruz, A.L.M, "A fast and efficient hybrid fractal-wavelet image coder" *IEEE Trans. Image Process.*, vol. 15, no. 1, pp. 98-105, Jan. 2006.
- [42] Elharar, E. Stern, A. Hadar, O. Javidi, B, A Hybrid Compression Method for Integral Images Using Discrete Wavelet Transform and Discrete Cosine Transform, *Journal of Display Technology*, vol. 3, no. 3, pp. 321-325, Sept. 2007.
- [43] R.D. Dony, S. Haykin, "Neural network approaches to image compression", *Proc. IEEE*, Vol. 83, No. 2, pp 288-303, Feb. 1995.
- [44] C.N. Manikopoulos, "Neural network approach to DPCM system design for image coding", *IEE Proc.*, Vol. 5, pp 501-507, Oct. 1992.
- [45] A W H Lee, and L M Cheng, "Using Artificial Neural Network for the calculation of IFS Codes, *Proc. of IEEE*, pp 4038- 4043, 1994.
- [46] S J Lee et. al, "Fractal Image compression using Neural Networks", *Proc.. IEEE*, pp 613-618, 1998.
- [47] Yuval Fisher, "Fractal Image Compression-Theory and application", *Springer-Verlag*, New York, 1995.
- [48] T.K. Denk, V. Parhi, Cherkasky, "Combining neural networks and the wavelet transform for image compression", *IEEE Proc. ASSP*, vol. 1, pp. 637-640, 1993.
- [49] S.G. Mallat, "A theory for multiresolution signal decomposition: The wavelet representation", *IEEE Transactions on Pattern Analysis & Machine Intelligence*, vol. 11, no.7, pp 674-693, July 1989.
- [50] An Algorithmic Approach for Efficient Image Compression using Neuro-Wavelet Model and Fuzzy Vector Quantization Technique Vipula Singh1, Navin Rajpal2, K. Srikanta Murthy3, (*IJCSE*) *International Journal on Computer Science and Engineering*, vol. 02, no. 07, 2366-2374, 2010.
- [51] Chopra, G. Pal, A.K, "An Improved Image Compression Algorithm Using Binary Space Partition Scheme and Geometric Wavelets" *IEEE Trans. Image Process.*, vol. 20, no. 1, pp. 270-275, Jan. 2011.

AUTHORS PROFILE



Rehna. V. J was born in Trivandrum, Kerala State, India in 1980. She studied Electronics & Communication Engineering at the PET Engineering college, Vallioor, Tirunelveli District, Tamilnadu State, India fom 1999 to 2003. She received Bachelor's degree from Manonmanium Sundarnar University, Tirunelveli in 2003. She did post graduation in Microwave and TV Engineering at the College of Engineering, Trivandrum and received the Master's degree from Kerala University, Kerala, India in 2005.

Presently, she is a research scholar at the Department of Electronics and Communication Engineering, Noorul Islam Center for Higher Education, Noorul Islam University, Kumarakoil, Tamilnadu, India; working in the area of image processing under the supervision of Dr. M. K. Jeya Kumar.

She is currently working as Assistant Professor at the Department of Telecommunication Engineering, Atria Institute of Technology, Bangalore, India. She has served as faculty in various reputed Engineering colleges in South India over the past seven years. She has presented and published a number of papers in national/international journals/conferences. She is a member of the International Association of Computer Science & Information Technology (IACSIT) since 2009. Her research interests include numerical computation, soft computing, enhancement, coding and their applications in image processing.



M. K. Jeya Kumar received his PhD degree in Mobile Adhoc Networks from Dr. MGR University, Chennai, India, in 2010. He is Assistant Professor at the Department of Computer Application, Noorul Islam University, Kanyakumari District, Tamilnadu, India. His research interests include networks and network security, image processing and soft computing techniques.

Software Security Requirements Gathering Instrument

Smriti Jain

Reader, MCA Department
SRGPPI
Indore, India

Maya Ingle

Principal
Indore Institute of Computer Applications
Indore, India

Abstract — Security breaches are largely caused by the vulnerable software. Since individuals and organizations mostly depend on softwares, it is important to produce in secured manner. The first step towards producing secured software is through gathering security requirements. This paper describes Software Security Requirements Gathering Instrument (SSRGI) that helps gather security requirements from the various stakeholders. This will guide the developers to gather security requirements along with the functional requirements and further incorporate security during other phases of software development. We subsequently present case studies that describe the integration of the SSRGI instrument with Software Requirements Specification (SRS) document as specified in standard IEEE 830-1998. Proposed SSRGI will support the software developers in gathering security requirements in detail during requirements gathering phase.

Keywords – *Software Requirements Specification; Security Policy; Security Objectives; Security Requirements.*

I. INTRODUCTION

Requirements define necessary and desired capabilities of the proposed system. Hence, requirements' gathering is the first step towards the development of software. The requirements gathered are functional and non-functional. The functional requirements describe the functionality of the product whereas the non-functional requirements attribute to quality features of the software. Functional requirements define the business rules. The non-functional requirements focus on issues like maintainability, portability, usability, security etc. Requirements are concerned with what the system should do whereas the security requirements are concerned with what the system should not do. Security requirements gathering allow gather information about the malicious part of the environment and decides how security breaches can be nullified [1]. To develop secured software, the core security services (confidentiality, integrity, availability, authentication, authorization and auditing) should be incorporated in the requirements phase of a software development project. Good requirements must be complete, correct, feasible, necessary, prioritized, unambiguous, and verifiable [2]. Common requirements are business rules, budgets, interfaces, reports, security, hardware, software etc. These requirements are defined by the stakeholders. Studies have shown that 40% to 60% of all defects found in software projects are due to errors made while gathering requirements. The main reasons contribute to the lack of user inputs, incomplete user requirements and changing requirements [3]. With the help of

field study, the reasons for poorly specified requirements have been identified as inconsistency in the selection of requirements, inconsistency in level of detail, and almost no requirements on standard security solutions [4]. Including security specifications during the requirements phase will not only reduce defects but will also assist in reducing security breaches.

The software requirements can be identified using the guidelines specified in IEEE Std. 830-1998 Software Requirements Specification (SRS) document [5]. In the literature survey, a Software Security Checklist has been developed that builds the software security assessment instrument. It focuses on the software security checklist to ensure that all the security aspects have been included during the software development process [6]. A process has been developed that enables the developers to identify, analyze and finalize the security requirements by the means of software security components. The process identifies and analyzes the conflicts between different security requirements [7]. In the SQUARE methodology, the security requirements are treated as add-ons to the functional requirements and are carried out in early stages of software development in nine discreet steps [8]. It is also stated that Common Criteria (CC) allows for the development of security requirements, and is being used on the architectural level of the security requirements. This made the usage of CC more beneficial [9]. In a paper, the functional and security requirements are combined to develop Distributed Aircraft Maintenance Environment (DAME) system in order to meet both the objectives [10]. Thus, it is evident that most of the work deals with security requirements only, enhancing existing security requirements standards, or security as a non-functional requirement in SRS. It has also been revealed that security is considered during requirements gathering in brief. We propose a Software Security Requirements Gathering Instrument (SSRGI) which can be used to gather the security requirements. The functioning of the proposed instrument is anticipated by case studies from different domains.

In the rest of the paper, we first present a brief overview of IEEE Standard 830-1998 in section II. Section III introduces SSRGI and its integration with SRS, and we verify our instrument with the help of case studies in section IV. Finally, section V concludes with the results, conclusion and the scope of SSRGI.

II. IEEE STANDARD 830-1998

IEEE Standard 830-1998 explains the content and qualities of good SRS. It aims in specifying the requirements of software to be developed for in-house and commercial products. The standard is divided in three parts consisting of Introduction, Overall Description and Specific Requirements. Introduction includes Purpose, Scope, Definitions and Acronyms, References, and Overview. Overall description consists of six subsections viz. Product Perspectives, Product Functions, User Characteristics, Constraints, Assumptions and Dependencies, and Apportioning of Requirements. Product perspectives describe how software operates in various constraints. These constraints are System interfaces, User interfaces, Hardware interfaces, Software interfaces, Communication Interfaces, Memory, Operations, and Site Adaptation requirements. Constrains subsection provide description that limit the developer's options. It includes Regulatory Policies, Hardware Limitations, Audit Functions, Control Functions, Safety and Security Considerations etc. Specific requirements focus on External Interfaces, Functions, Performance Requirements, Logical Database Requirements, Design Constraints, Software System Quality Attributes, and Object Oriented Models. The external interfaces requirements compliment the interface requirements and detail the system inputs and outputs. Functional requirements define fundamental actions in accepting and processing the inputs and generating the outputs. Standards compliance specifies the requirements derived from existing standards or regulations. The software system attributes include Reliability, Availability, Security, Maintainability and Portability.

III. PROPOSED SOFTWARE SECURITY REQUIREMENTS GATHERING INSTRUMENT (SSRGI)

Fig. 1 illustrates the proposed SSRGI that demonstrate the course of action to gather security instruments. The various security requirements to be gathered are Secure Functional Requirements (SFR), Drivers, Functional Security Requirements (FSR), Non-Functional Security Requirements (NFSR), Security Development Requirements (SDR), and Security Testing Requirements (STR). The instrument specifies the security policy which helps in identifying security needs and objectives that decide the security requirements. These requirements can be gathered from the various roles such as customers, managers, designer, coders, and QA/ Testers.

A. Security Policy

Security policy allows an organization to set security practices and procedures to reduce the likelihood of attack. It defines rules that regulate an organization in accomplishing its security objectives. Policies describe the roles of users, managers, designers, coders and quality assurance team in achieving security. Security policies reduce the damage to the business by safeguarding the confidentiality, availability and

integrity of the data and information. Security policies identify security needs and objectives. The policies may include the regulatory acts like HIPAA, Sarbanes-Oxley etc.

B. Security Needs and Objectives

The needs and objectives facilitate to create and better understand the comprehensive security plan. Objectives are goals and constraints that affect confidentiality, integrity and availability of data and application. It also defines roles and responsibilities and privileges to be assigned to the roles. Various other security objectives include – resource protection, authentication, authorization, non-repudiation, auditing security objectives etc.

C. Security Requirements

The security requirements are to be gathered from the various roles viz. customer, manager, designers, coders, and Quality Assurance/ Tester. The various types of security requirements are discussed below:

Secure Functional Requirements (SFR) - SFR is a security related description that specifies the services to be integrated into each functional requirement. SFR specifies what shall not happen while executing the software. The customer helps in determining the SFRs. These requirements are normally gathered by means of misuse cases which capture requirements in negative space. The counter measures of misuse cases are design decisions [16].

Drivers – The security drivers determine the security needs as per the industry standards, thereby shaping security requirements for a software project. The drivers for security requirements include regulatory compliance like Sarbanes-Oxley, Health Insurance Portability and Accountability Act (HIPAA), Gramm-Leach-Bliley Act etc.; industry regulations and standards like ISO 17799, OASIS etc.; company policies like privacy policies, coding standards, patching policies, data classification policies etc.; and security features like authentication and authorization model, role-based access control, and administrative interfaces etc. [11]. The policies when transformed to detailed requirements demonstrate the security requirements. By using the drivers, managers can determine the security requirements necessary for the project.

Functional Security Requirements (FSR) - FSRs are the requirements that focus on the system under inspection. The requirements for the FSRs can be gathered from the managers using the security drivers. FSRs comprises of authentication, authorization, backup, server-clustering, access control, encryption, data integrity etc. Examples include verification of all the users and allow them to access information relevant for their use. The managerial level of the organization can help determine the FSRs.

Non-Functional Security Requirements (NFSR) - NFSR are security related architectural requirements, like

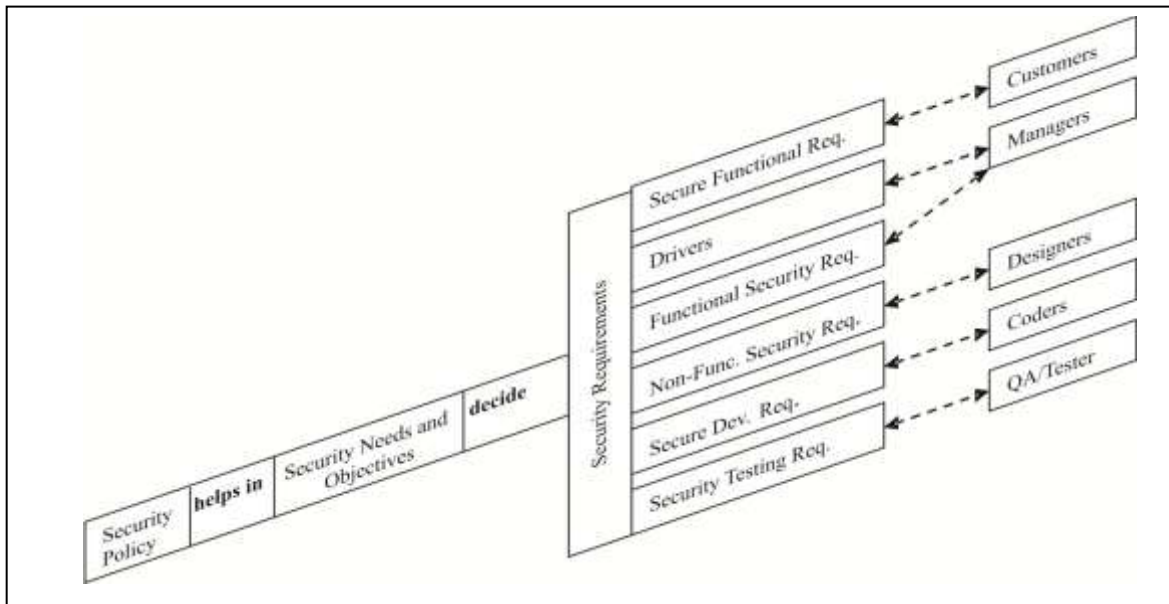


Figure 1: Software Security Requirements Gathering Instrument (SSRGI)

robustness, privacy, reliability, data authenticity, integrity etc. This requirement type is typically derived from architectural principles and good practice standards using Microsoft's SDL or Cigital's TouchPoints. NFSRs are security related quality attributes. Design patterns like creational, structural or behavioral can be used to generate NFSRs in object oriented programming. It also identifies system's resilience and level of immunity to attack [12]. NFSR requirements can detect and report all unauthorized access. The designers normally focus on NFSR.

Secure Development Requirements (SDR) - SDRs describe required activities during system development which assures that the outcome is not subject to vulnerabilities. Coding guidelines specifies the SDRs. Also, frameworks like Comprehensive, Lightweight Application Security Process (CLASP), Cigital TouchPoints, OWASP etc. may assist in implementing secure development practices. CLASP describes 104 coding problem types specified in 5 overlapping categories [15]. OWASP specifies top ten web vulnerabilities like Injection, Cross Site Scripting (XSS), broken authentication and session management, etc. these vulnerabilities are mainly due to lack of secure coding hence, the coders centers on SDRs.

Security Testing Requirements (STR) - STR includes testing the security requirements gathered using a parametric approach [13]. Security testing mainly focus on testing security functionality as gathered in the requirements document. The QA/ Testers needs to gather information about the hardware architecture, software architecture, and the user model to develop the security test cases. The testing team can test the valid and invalid access rights to check for authentication and authorization of the proposed software.

IV. CASE STUDY

Based on the integration of SSRGI into IEEE 830-1998 SRS, Fig. 2 shows the said merger. The SSRGI is incorporated in the software system's security attribute. The SSRGI elaborates on gathering SFR, Drivers, FSR, NFSR, SDR, and STR requirements from the various stakeholders. We describe three different cases viz. Web Based, LAN based Client/Server, and Single User system that illustrate the use of our SSRGI. An integrated approach of SSRGI with SRS has been presented for each of the three cases.

Case I: Web Based System - Journal Publishing System

Journal Publishing System (JPS) is a Web publishing system designed for a regional society. The system is designed to assist editors by automating the article review and publishing process thereby maximizing his efficiency. The software will facilitate communication between editors, authors and reviewers via E-mail. Preformatted reply forms are used for communication between editor, author and reviewer. The system also maintains a database of reviewers, authors and articles. The main objectives of the system include accepting articles online from contributors, email acceptance letter to them, send the articles to reviewers, receive the feedback from the reviewer and further communicate the feedback to the contributor using E-mail, accept the camera-ready copy of the article online from the contributor, publish the article and make the published articles available to the contributor for 1 year. The articles can be subscribed either for 6 months or 1 year. Considering it to be a moderately used system with approximately having 1000 users online in 5 minutes, minimum server configuration include 3.2 GHz Single Processor, Quad Core, 4 GB RAM and having at least 300GB HDD with Web server configuration as Apache 2.x

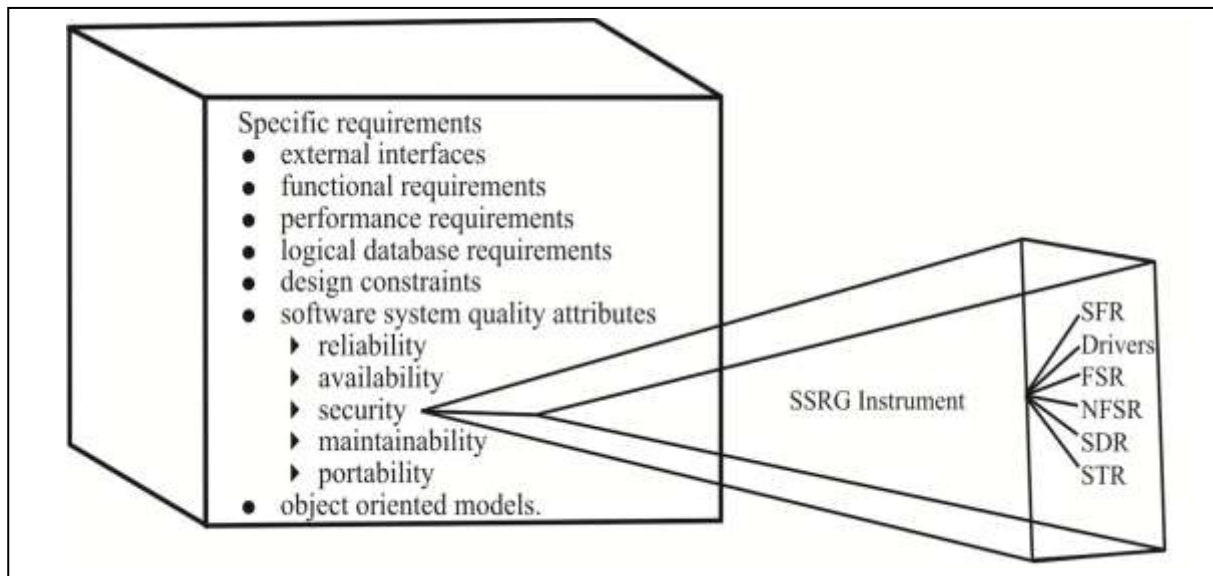


Figure 2: Integration of SSRGI into SRS

and above having Linux supporting Redhat Linux EL4 and above as operating system. The software is developed in PHP 5.x and above, having database as MySQL 5.x. The minimum requirement at client side must be Windows XP/ Windows 7 Professional, IE 7.0 and above/ Firefox 3.0/ Google Chrome, MS Office and Adobe Reader. The predefined messages can be sent using Outlook Express.

Here, SRS explains the purpose of the system along with the features, interfaces and outputs. At the same time, it will clarify the constraints under which it will operate and external environment it will react. The system allows editor to interact with the reviewers and the contributors, and to publish the articles on the website. The articles are published on some nominal charges and the contributors can access the website free of cost for 1 year. The subscribers are allowed to view the published articles on the basis of subscription fee.

The various security requirements of JPS are specified in security section of SRS. SFR includes logon page, password security for various users, password reset, account creation for new contributor and reviewer, contacting the editor, submitting information to web site, preventing spamming of website submission, and backup of the data. The managers can take the help of Open Web Application Security Project (OWASP) for requirements gathering. The managerial level of the organization decides on the need for secure data transmission, securing user identification for the contributors, reviewers and the editor using Secure Socket Layer (SSL) protocol. The company policy decides access requirements for read/ write/ delete to authorized users. Editors are given read/ write/ delete access, reviewers are provided read/ write access of the articles of their own subject area, and contributors and subscribers are given read access to all the articles. Editors need to identify the unauthorized users who can pose threats to the system; and the technical and business impacts like loss of revenues, loss of identity of the authors, loss of honorium of the reviewers etc. FSRs like backups, authentication, authorization, access control, and encryption should also be specified by the

managers. The SDR can be specified by the developers using OWASP and CLASP. In SDRs, the coders also need to state the formatting of the data, exceptional conditions etc. The software tester should detail the contents of test plan to evaluate security of software, software test procedures, software test reports, and acceptance criteria for the users in STR specification. The test plan may address issues on password cracking, URL manipulation, SQL injection, XSS and spoofing.

A study reveals that 47% of banks places secure login boxes on insecure pages, and 55% put contact information and security advice on insecure pages. As a result, an attacker could change the information and set up his own call center to gather private data from customers who need help from banks [14]. Since JPS asks for personal information from the subscribers, it allows to specify the need for SSL protocol. XSS is one of the flaws which affect the website most. To avoid such flaw, the system designer must include requirement of either filtering the input from the sender or by using frameworks that specify libraries for making user input safe from XSS like ASP.NET. To secure data from potential loss, a disaster recovery plan can be tailored to suit the requirements. Another such flaw lies in SQL injection in which databases are accessed by the hackers. To avoid SQL Injection attack, check and validate input to SQL statements and never use string concatenation to build SQL statements, instead use parameterized queries. The testing requirement includes manual code review and check for the keywords that validate the input.

Case II: LAN based Client/ Server System - Patient Management System

Patient Management System (PMS) is a LAN based client/ server system that allows the hospitals to keep record of the patient's data. This aids in the management of personalized patient lists, physicians etc. The system is intended to assist doctors, nurses, social workers, and dieticians. The system supports internal messaging among various users. The system

is designed to register patients, doctors, nurses and dieticians. It allows generating the list of patients with their ailments, medications and tests (if suggested), and the doctor and nurses in-charge of the same. The system also permits to view the case history of the patients and fix appointment with the doctor. The system generates birth and death records, test reports, diagnosis with medicines, and billing and payments. Considering 100 patients daily including old and new ones, the minimum server configuration include 2.8 GHz Single Processor, Quad Core, 4 GB RAM and having at least 300GB HDD. The software is developed on DotNet Framework and database used is SQL Sever 2008 Express. The client machine must be Intel Pentium Dual Core (E5800), 2 GB DDR3 SDRAM, 320 BG SATA Hard drive (7200 rpm) and Broadcom Integrated Gigabit Networking (BCM 57780) with Windows XP/ Window 7 Professional with DotNet Framework and; dot matrix and laser printers.

In PMS, SFR includes information regarding logon page, password security for the various types of users, password reset, account creation of new user etc. The company policy facilitates to decide the access rights of all the users as the security threats are mainly from the internal users. The managers decide upon the need for encryption and password strength depending upon the type of security required. The requirements gathering team gathers security requirements from the managers by help of misuse cases to identify the unauthorized users who can pose threats to the system. The designers may use security lifecycle to develop a secured design of the software. They must specify the vulnerable points of the software and must ensure that the unused features must be off by default. SFRs can be regarding the authentication, authorization, access control, backups, encryption etc. The designers must specify the audit mechanisms to identify intruders. These mechanisms are the counter measures for misuse cases. The designers, in addition, can take help of CLASP to gather security requirements during coding. In SDRs, the coders must specify the exceptional cases as well as input and output validation. The tester needs to state the test plans to evaluate security of the software, the test procedures, software test reports, and the acceptance criteria in STR specification. The test plans should address communication threats, password cracking etc.

Access control is one of the major design issues in a client/server based system. Access control list can be developed by threat modeling. It is gathered from the customers to achieve secured system. The designers must understand the design issues related to access control on the target platform.

Case III: Single-User System - Shop Management System

Shop Management System (SMS) permits a shopkeeper to keep track of the inventory, sales, and accounts (i.e. preparation of ledger and balance sheet). The system allows maintaining list of inventory available and required, daily/ weekly/ monthly sales, raises purchase indent, and maintains outstanding amount. It generates reports on daily/ weekly/ monthly sales, outstanding amounts, purchase details, list of suppliers, customers with addresses (for home delivery of goods) and their credit amount. The minimum requirements include 2 GHz processor, 2 GB RAM, MS-Access, Windows XP with

SP3 or Vista, Office 2003, 40 GB disk space and Broadband Internet connection with IE 7.0/ IE 8.0/ Firefox 3.0/ Google Chrome, bill and laser printers.

The shop-owner, the user of the system, is the administrator and has access to all the data. FSR includes logon and password facility for accessing the computer system, finger print recognition pocket device to access the software to make it safe from the helpers in the shop, and backup of the data at regular intervals.

V. RESULTS AND CONCLUSION

Requirements gathering is one of the most important steps towards the development of a software product. The traditional approaches of requirements gathering do not include security in detail. In this paper, we presented SSRGI that provides a general approach to incorporate security during the requirements gathering phase of the software development process. It focuses on different types of security requirement that can be gathered from different roles. Gathering security requirements with the help of the instrument ensure that the security aspects are considered systematically during development process itself and can thus help avoid serious flaws in the resultant software product.

SSRGI is then integrated in the SRS guidelines, as suggested in IEEE 830-1998 document, to provide a more detailed approach to incorporate security during the software development process. This instrument is then applied to a Journal Publishing System, Patient Management System and Shop Management System and is presented as case studies. The results of integrating SSRGI in the various softwares considered in case study is detailed below.

- Web enabled software involves the highest need for security. SSRGI when applied is able to gather the security requirements in more detail. The access rights are detailed for all the various types of users. It also assists in identifying the unauthorized users, coding guidelines and test requirements for security, thus serving to develop more secured software. The instrument allows setting up the password policy. It permits to gather need for SSL protocol.
- SSGRI allows gathering requirements from the stakeholders. Business requirements and security requirements are gathered via customer interaction, whereas the other requirements are gathered from the development team members.
- LAN based client/ server system is more prone to threats from internal users. The need for communications security as well as the security measures required for web applications is reduced. SSRGI allows capturing requirements for authentication and authorization, proper password strength, and secure internal communication.
- In a single user system, login, password, and the backup of the data are the security measures required. Hence in such conditions, the need for applying security gathering instrument is also reduced.

From the above cases, it is evident that SSRGI will ensure the systematic consideration of security aspects during development process itself and can thus avoiding serious flaws in the resultant software product. SSRGI will support the software developers to gather security requirements in detail during requirements gathering phase. It will also ensure that the security is not considered as an add-on after the implementation of the project. This will also assist in identifying the security flaws during the early stages of the software development.

REFERENCES

- [1] H. Schmidt, "Threat- and risk-analysis during early security requirements engineering," In the Proc. of Availability, Reliability, and Security, ARES'10 International Conference, IEEE Computer Society, 2010, pp. 188 – 195.
- [2] E. Whitney, "An introduction to gathering requirements, creating Use Cases and the UML," White Paper, EPS Software Corporation. http://www.eps-cs.com/pdf/whitepaper_the_development_process.pdf.
- [3] Al Neimat, "Why IT projects fail?" 2005. http://www.projectperfect.com.au/info_it_projects_fail.php.
- [4] J. Wilander and J. Gustavsson, "Security requirements – A field study of current practice," Presented at the Symposium on Requirement Engineering for Information Security (SREIS' 2005), Paris, France, 2005.
- [5] "IEEE recommended practice for software specifications requirements," *IEEE Std. 830-1998*, 1998.
- [6] D. Gilliam, T. Wolfe, J. Sherif, and M. Bishop, "Software security checklist for the software life cycle," In the Proc. of the 12th IEEE International Workshop on Enabling Technologies: Infrastructure for Collaborative Enterprise, June 2003, pp. 243–248.
- [7] D. Hatebur, M. Heisell, and H. Schmidt, "Analysis and component-based realization of security requirements," In the Proc. of the Third International Conference on Availability, Reliability and Security, IEEE Computer Society, 2008, pp. 195-203.
- [8] N.R. Mead, E.D. Hough, and T.R. Stehney II, "Security Quality Requirements Engineering (SQUARE) Methodology," CMU/SEI, Technical Report CMU/SEI-2005-TR-009, ESC-TR-2005-009, Nov. 2005.
- [9] J. R. Mariona , H. Ziv , D. J. Richardson, "CCARCH: Architecting Common Criteria security requirements," In the Proc. of Third International Symposium on Information Assurance and Security, IEEE Computer Society, 2007, pp. 349-354.
- [10] M. Fletcher, H. Chivers, and J. Austin, "Combining functional and security requirements' processes," In the Proc. of All Hand Meeting, 2005.
- [11] R. Araujo, "Security requirements engineering: A road map," Security Feature, July 2007. <http://www.softwagemag.com/1.cfm?doc=1067-7/2007>
- [12] W. J. Lloyd, "A Common Criteria based approach for COTS component selection," Journal of Object Technology, Vol. 4, No. 3, 2005, pp. 27–34.
- [13] A. K. Singh, A. J. Iyar, and V. Seshadri, "A parametric approach for security testing of Internet applications," QAI India Limited, In the Proc. of the 3rd Annual International Software Testing Conference, 2000.
- [14] "Potentially serious security flaws found in most bank websites, including large bank sites, study shows," Science Daily, July 23, 2008. <http://www.sciencedaily.com/releases/2008/07/080722175802.htm>.
- [15] "CLASP version 2.0," Secure Software Inc., 2006.
- [16] G. Sindre, and A. L. Opdahl, "Capturing security requirements through misuse cases," In the Proc. of the 14th annual Norwegian Informatics Conference, Norway, 2001.

AUTHORS PROFILE

Smriti Jain, Associate Professor at SRGP GPI, Indore, India. She has 14 years of teaching experience. She is pursuing Ph.D. in Computer Science and is MCA from School of Computer Science, Devi Ahilya Vishwavidhyalaya, Indore, India. She has 12 papers published to her name in various National and International journals and conferences.

Dr. Maya Ingle is Professor & Senior System Analyst at School of Computer Science and Information Technology, Devi Ahilya University, Indore since 25 years. Presently, she is Principal and Professor at Indore Institute of Computer Application, Indore on extra ordinary leave. She is also Chair Assessment & Research committee. She is Ph. D. in Computer Science and M. Tech in Computer Science from IIT, Kharagpur. Her research interest includes Software Engineering, NLP, Speech Recognition, Usability Engineering and Agile Computing. She has published more than 80 papers in national and international journals and conferences.

The Development Process of the Semantic Web and Web Ontology

K. Vanitha, K. Yasudha,
K.N.Soujanya
Asst. Prof, Dept of CS
GIS, GU
Visakhaptnam, India

M.Sri Venkatesh
Assoc. Prof, Dept of CS
GIS, GU
Visakhaptnam, India

K.Ravindra, S.Venkata Lakshmi
Dept. of IT,
GIS, GU
Visakhaptnam, India

Abstract—This paper deals with the semantic web and web ontology. The existing ontology development processes are not catered towards casual web ontology development, a notion analogous to standard web page development. Ontologies have become common on the World-Wide Web[2]. Key features of this process include easy and rapid creation of ontological skeletons, searching and linking to existing ontologies and a natural language-based technique to improve presentation of ontologies[6]. Ontologies, however, vary greatly in size, scope and semantics. They can range from generic upper-level ontologies to domain-specific schemas. The success of the Semantic Web is based on the existence of numerous distributed ontologies, using which users can annotate their data, thereby enabling shared machine readable content. This paper elaborates the stages in a casual ontology development process.

Key words- Toolkits; ontology; semantic web; language-based; web ontology.

I. INTRODUCTION

The notion of the Semantic Web has been gaining prominence, in which users can create precise, unambiguous encodings of information in a machine readable format. Central to this notion is the idea of an *Ontology*, which is a formal specification of a conceptualization. The success of the Semantic Web is based on the existence of numerous distributed ontologies, using which users can annotate their data, thereby enabling shared machine readable content. Ontologies, however, vary greatly in size, scope and semantics. They can range from generic upper-level ontologies to domain-specific schemas. They can be created by Knowledge Representation (KR) experts or novice web users, differing widely in authoring style and formal semantics.

They can be small ontologies containing a handful of concepts or large ontologies containing thousands of terms and relationships. In such a diverse and heterogeneous information space, *ontology engineering* assumes tremendous practical significance. Tools supporting it need to provide a seamless environment for browsing, searching, sharing and authoring ontological data. A number of ontology development tools currently exist. Most of the tools provide an integrated environment to build and edit ontologies, check for errors and inconsistencies, browse multiple ontologies, share and reuse existing data by establishing mappings among different ontological entities. However, these tools are influenced by traditional KR-based ontology engineering methodologies, with steep-learning curves, making it cumbersome to use for casual

web ontology development. In this paper, we outline the lifecycle of a casual web ontology development process. Key emphasis is given to the following aspects:

- 1) *Aiding authors (esp. domain experts) build ontologies from scratch rapidly, using a short hand notation instead of a Direct Manipulation (DM) interface [3].*
- 2) *Facilitating reuse of existing data by providing advanced search capabilities to help locate specific concepts that can be borrowed or linked while creating a new ontology.*
- 3) *Helping novice web users explicitly understand ontological terminologies.*

II. SEMANTIC WEB

The meaning of the word *semantic* is the study of meaning and changes of meaning, which provides information of a word. This information becomes knowledge on analyzing the semantics and the network information or knowledge is semantic web. The semantic web brings a set of new emerging technologies and models that need to be found and executed. Semantic web is a platform that integrates data sources using semantic rules, ontologies, web services and web processes[8]. Where semantic web is not an application but an infrastructure where applications can be developed. The various applications include B2B E-Commerce, Bio-informatics, Tourism, personal semantic assistants etc., The Semantic Web activity statement of the World Wide Web Consortium (W3C)[2] describes the Semantic web as an extension of the current web in which information is given in a well-defined meaning, better enabling computers and people to work in cooperation. It is the idea of having data on the web defined and linked in a way that it can be used for more effective discovery, automation, integration, and reuse across various applications. The Web can reach its full potential if it becomes a place where data can be shared and processed by automated tools as well as by people [2].

The semantic web development can be categorized broadly into four clusters. They are

- a) *Identification and localization*: Identification of web resources, considering the semantics of representation languages and localizing these resources for processing.
- b) *Relationships between semantic models* : There is a need to develop a layered and modular representation languages for the semantic web, considering the heterogeneity as an intrinsic feature as there is no language, no model and no ontology suitable for all purposes.

c) *Tolerant and safe reasoning:* As web metadata is considered it is necessary to provide tolerant computing techniques in order to implement safe computing. Also to provide, trust, proofs and rewards on the web new computational models are to be developed.

d) *Facilitating web adoption:* By considering the availability of resources and with the support of developing web ontology's, ontology libraries on meta data(text, audio, video, images), the semantic web can be made user friendly which is the most critical point.

The Semantic web is based on a set of language such as RDF and OWL that can be used to markup the content of web pages. These languages have a well –defined semantics in proof theory that alllows agents to draw inferences over the state of the language[1].Examples of applications that use Semantics and ontologies

- 1) *Semantic web services*
- 2) *Semantic integration of tourism information sources*
- 3) *Semantic digital libraries*
- 4) *Semantic electronic patient health record*
- 5) *Semantic E-learn Services*
- 6) *Semantic Intelligent Systems.*

III. ONTOLOGY DEVELOPMENT PROCESS

An ontology defines a common vocabulary for researchers. The knowledge which varies greatly in size, scope and semantics is conceptualized based on a concept ontology, which is the success of the semantic web thus the heart of the semantic web. Ontology can be large or small containing thousands of terms and relationships. These can be created by knowledge representation experts or novice web users. In this way, ontology gained its importance in research to share information in a particular domain in machine readable format. Modeling experts build simple ontology's and instances to enter information easily. Ontology together with a set of individual instances of classes constitutes a knowledge base. Classes are the focus of most anthologies. Classes describe concepts in the domain. A class can have subclasses that represent concepts that are more specific than the super class. Ontology is a single and main building block of semantic web. Ontology is divided into 3 categories

- a) *Natural Language Ontology*
- b) *Domain Ontology*
- c) *Ontology Instances*

There are seven activities involved in ontology development process which is an iterative process

1) *Determine the domain and scope of the ontology that will give the information and answer several basic questions: What is the domain that the ontology will cover? For what we are going to use the ontology? For what types of questions the information in the ontology should provide answers? Who will use and maintain the ontology? The answers to these questions may change during the ontology-design process. But it help limit the scope of the model.*

2) *Reusing existing ontologies considering what someone else has done and checking if we can refine and extend existing sources for our particular domain and task. If our system needs to interact with other applications that may requires reusing existing ontologies. Many ontologies are already available in electronic form and can be imported into an ontology-development environment that many knowledge-representation systems can import and export ontologies. Knowledge representation system cannot work directly with a particular formalism. The task of translating an ontology from one formalism to another is usually not a difficult task[4].*

3) *Enumerate terms in the ontology, it is a list of all terms to make the statements about or to explain to a user. What are the terms we would like to talk about? which type of properties ?*

4) *Define the classes and the class hierarchy, the developing the class hierarchy and defining properties of concepts are closely intertwined. There are several possible approaches in developing a class hierarchy.*

- a) *Top-down development process.*
- b) *Bottom-up development process.*
- c) *Combination development process.*

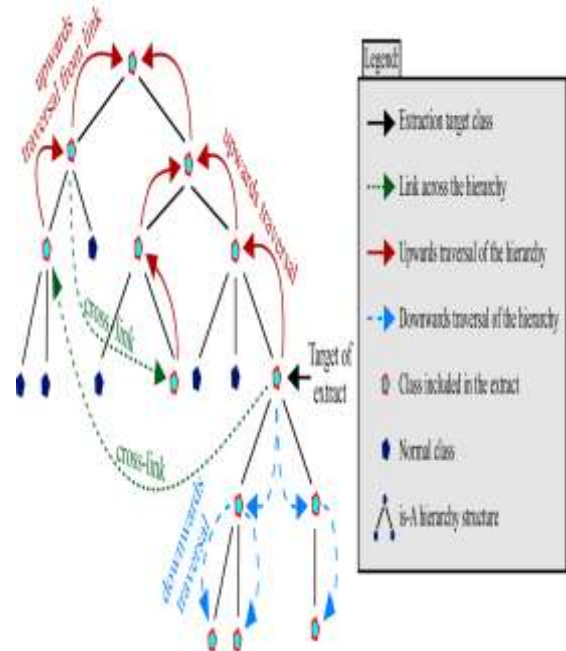


Fig 1. Different approaches of Ontology

If the developer has the top-down approach, the combination approach is often the easiest for many ontology developers, since the concepts in the middle tend to be the more descriptive concepts in the domain(in the year1978 by Rosch). Depending on the usage propriety to think and distinguish the most general classification. Then top-down approach may work better. If we use the specific propriety the information we get through the bottom-up approach may be appropriate. Either of the approaches usually starts with

defining classes. Then select describe objects which is dependent on the existence rather than describing these objects.

1) Define the properties of classes, sometimes the classes alone will not provide enough information so we have to define some of the classes and must describe the internal structure of the concepts.

2) Define the facets of the slots, slots can have different facets describing the value type, allowed values, the number of the values and other features of the values the slot can take.

3) Create instances creates individual instances of classes in the hierarchy. As a final word on defining a class hierarchy the following set of rules are always helpful in deciding when an ontology definition is complete.

Ontology should not contain all the possible information about the domain and similarly the ontology should not contain all the possible properties and distinctions among classes in the hierarchy. In practical terms, developing an ontology includes:

- a) defining classes in the ontology.
- b) arranging the classes in a taxonomic (subclass superclass) hierarchy.
- c) defining slots and describing allowed values for these slots.
- d) filling in the values for slots for instances.

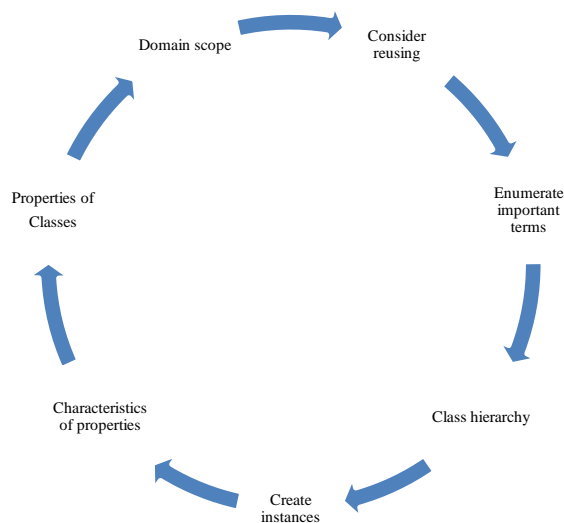


Fig 2. Ontology development activities

The Artificial-Intelligence literature contains many definitions of an ontology; many of these contradict one another[7]. For this purpose to guide, an **ontology** is a formal explicit description of concepts in a domain of discourse (**classes** (sometimes called **concepts**)), properties of each concept describing various features and attributes of the concept (**slots** (sometimes called **roles** or **properties**)), and restrictions on slots (**facets** (sometimes called **role**

restrictions))[6]. An Ontology together with a set of individual **instances** of classes constitutes a knowledge base. In reality, there is a fine line where the ontology ends and the knowledge base begins. Classes are the focus of most ontologies. Classes describe concepts in the domain.

IV. CASUAL WEB ONTOLOGY DEVELOPMENT

The casual web ontology development process is analogous to the standard web page development process, in which users have certain information to deploy on the web, and though the use of standard HTML editors such as MS Front page etc., they can quickly and easily arrange and layout the information as desired, while linking to existing relevant information. Casual ontology development process is to be aimed at average semantic. Web users who would rather have a fast and guided approach to web ontology building instead of manual approach. The process already said above is regarding the concepts and domain, arranging the hierarchy and specific properties, refine the terms and refinement stages. While browsing related ontological terms, natural language explanations of these terms are provided to help users easily understand their semantics.

V. NATURAL LANGUAGE EXPLANATIONS

The need to provide a natural language explanation of terms in an ontologies arises from the fact that the intended purpose of ontologies is information sharing which could involve external parties that have little or no background knowledge of the ontology domain[6]. In such cases, it becomes the responsibility of the domain experts crating the ontology to provide textual documentation for the terms within. When this is not available, understanding the explicit meaning behind the terms can be difficult. Readability can be greatly enhanced if a natural language representation of the DL-based terms is provided and the NL generation system should be flexible in that the parameters used to specify textual descriptions can be customized based on user preferences[4].

Most ontology editors assume that the user is well aware of the semantics of the ontology language, whereas in many cases this is not true. While the user may be familiar with the basics of the language, such as its underlying model, types of semantic constructs and its basic syntax/purpose, there are too many hidden semantic nuances in a DL-based language that even an experienced user might not know[5]. A rule based system seems an ideal choice to implement this functionality. A set of manually hard coded rules can be written beforehand, each of which gets fired on specific user-actions such as adding a class, specifying an intersection class definition. Accordingly displays the alternatives or implications of the action based on current state of the ontology and semantics of the language. Backend reasoning would be needed in order to make inferences based on the user action.

VI. CONCLUSION

This paper presented a detailed definition about semantic web and web ontology and some outlined information of a casual web ontology development process. Various key stages are involved in this process and its use of shorthand information of shorthand notation to draft ontology[1]. A powerful ontology search algorithm that combines keywords

with DL-based constructs to find related concepts and related ontology and, natural language based presentation [6]. This is described as an ontology-development methodology for frame based systems. Listed the steps in the ontology-development process and addressed the complex issues of defining class hierarchies and properties of classes and instances. One of the most important things to remember is there is no single correct ontology for any domain [7]. Ontology design is a creative process and no two ontologies designed by different people would be the same application of the ontology and the designer's understanding and view of the domain will undoubtedly affect ontology design choices. We can assess the quality of our ontology only by using in its applications for which we have designed it.

REFERENCES

- [1] DRTC Workshop on Semantic web December,2003, Bangalore. Resource Description Frame work: "ATutorial for Developing Web Ontology".
- [2] "W3C Semantic Web Activity Statement",
- [3] Chimaera (2000). Chimaera ontology Environment.
- [4] Duineveld, A.J.,Stoter, R., Weiden, M.R., Kenepa, B. and Benjamins, .R.(2000).WonderTools? "A Comarative study of ontological engineering tools". International Journal of Human-Computer Studies.
- [5] "Reusable ontologies, knowledge-acquisition tools, and performance systems; PROTÉGÉ-II solutions to Sisyphus-2". International journal of Human-Computer Studies44: 301-334. Rothenfluh, T.R Gennari, J.H.,Eriksson, H., puerta, A.R., Tu,S.W.and Musen, M.A. (1996).
- [6] McGuinness, D.L.,Abrahams, M.k.,Resnick, L.A., Patel-Schneider,P.F., Thomason, R.H., Cavalli-Sforza, V. and Conati, C.(1994). Classic Knowledge Representation system Tutorial.
- [7] Musen, M.A.(1992) "Dimensions of Knowledge sharing and reuse". Computers and Biomedical Research 25:435-467.
- [8] Jorge Cardoso, Universidade da madeira, portugal. "Developing Dynamic Packaging Applications using Semantic Web-based Integration".

Solving the Vehicle Routing Problem using Genetic Algorithm

Abdul Kadar Muhammad Masum¹

Dept. of Business Administration
International Islamic University Chittagong

Mohammad Shahjalal²

Dept. of Electrical & Electronic Engineering
International Islamic University Chittagong

Md. Faisal Faruque³

Dept. of Computer Science & Engineering
University of Information Technology & Sciences

Md. Iqbal Hasan Sarker⁴

Dept. of Computer Science & Engineering
Chittagong University of Engineering & Technology

Abstract— The main goal of this research is to find a solution of Vehicle Routing Problem using genetic algorithms. The Vehicle Routing Problem (VRP) is a complex combinatorial optimization problem that belongs to the NP-complete class. Due to the nature of the problem it is not possible to use exact methods for large instances of the VRP. Genetic algorithms provide a search technique used in computing to find true or approximate solution to optimization and search problems. However we used some heuristic in addition during crossover or mutation for tuning the system to obtain better result.

Keywords: Vehicle Routing Problem (VRP); Genetic Algorithm; NP-complete; Heuristic.

I. INTRODUCTION

The VRP can be described as follows: given a fleet of vehicles with uniform capacity, a common depot, and several customer demands, finds the set of routes with overall minimum route cost which service all the demands [1]. All the itineraries start and end at the depot and they must be designed in such a way that each customer is served only once and just by one vehicle. Genetic algorithms have been inspired by the natural selection mechanism introduced by Darwin [2]. They apply certain operators to a population of solutions of the problem at hand, in such a way that the new population is improved compared with the previous one according to a pre-specified criterion function. This procedure is applied for a pre-selected number of iterations and the output of the algorithm is the best solution found in the last population or, in some cases, the best solution found during the evolution of the algorithm. In general, the solutions of the problem at hand are coded and the operators are applied to the coded versions of the solutions. The way the solutions are coded plays an important role in the performance of a genetic algorithm. Inappropriate coding may lead to poor performance. The operators used by genetic algorithms simulate the way natural selection is carried out. The most well-known operators used are the reproduction, crossover, and mutation operators applied in that order to the current population. The reproduction operator ensures that, in probability, the better a solution in the current population is, the more (less) replicates it has in the next population. The crossover operator, which is applied to the temporary

population produced after the application of the reproduction operator, selects pairs of solutions randomly, splits them at a random position, and exchanges their second parts. Finally, the mutation operator, which is applied after the application of the reproduction and crossover operators, selects randomly an element of a solution and alters it with some probability. Hence genetic algorithms provide a search technique used in computing to find true or approximate solutions to optimization and search problems.

II. SOLUTION DETAILS

At the beginning an initial generation has to be defined. This can be done using a random initialization or can use some kind of seeding which allows the algorithm to work in a search space where solutions are more likely. From now until a valid solution is found or the maximal level of allowed generations is reached, the following steps are performed.

Selection: first we select a proportion of the existing population to breed a new generation. The selection is done on a fitness-based approach where fitter individuals are more likely to breed than others.

Reproduction: during the reproduction phase the next generation is created using the two basic methods, crossover and mutation. For every new child a pair of parents is selected from which the child inherits its properties. In the crossover process genotype is taken from both parents and combined to create a new child.

With a certain probability the child is further exposed to some mutation, which consists of modifying certain genes. This helps to further explore the solution space and ensure, or preserve, genetic diversity. The occurrence of mutation is generally associated with low probability. A proper balance between genetic quality and diversity is therefore required within the population in order to support efficient search.

Implementation: We have used C++ programming language to implement our system. The main advantages of C++ include a clean object oriented approach. The following figure describes the flowchart of the system.

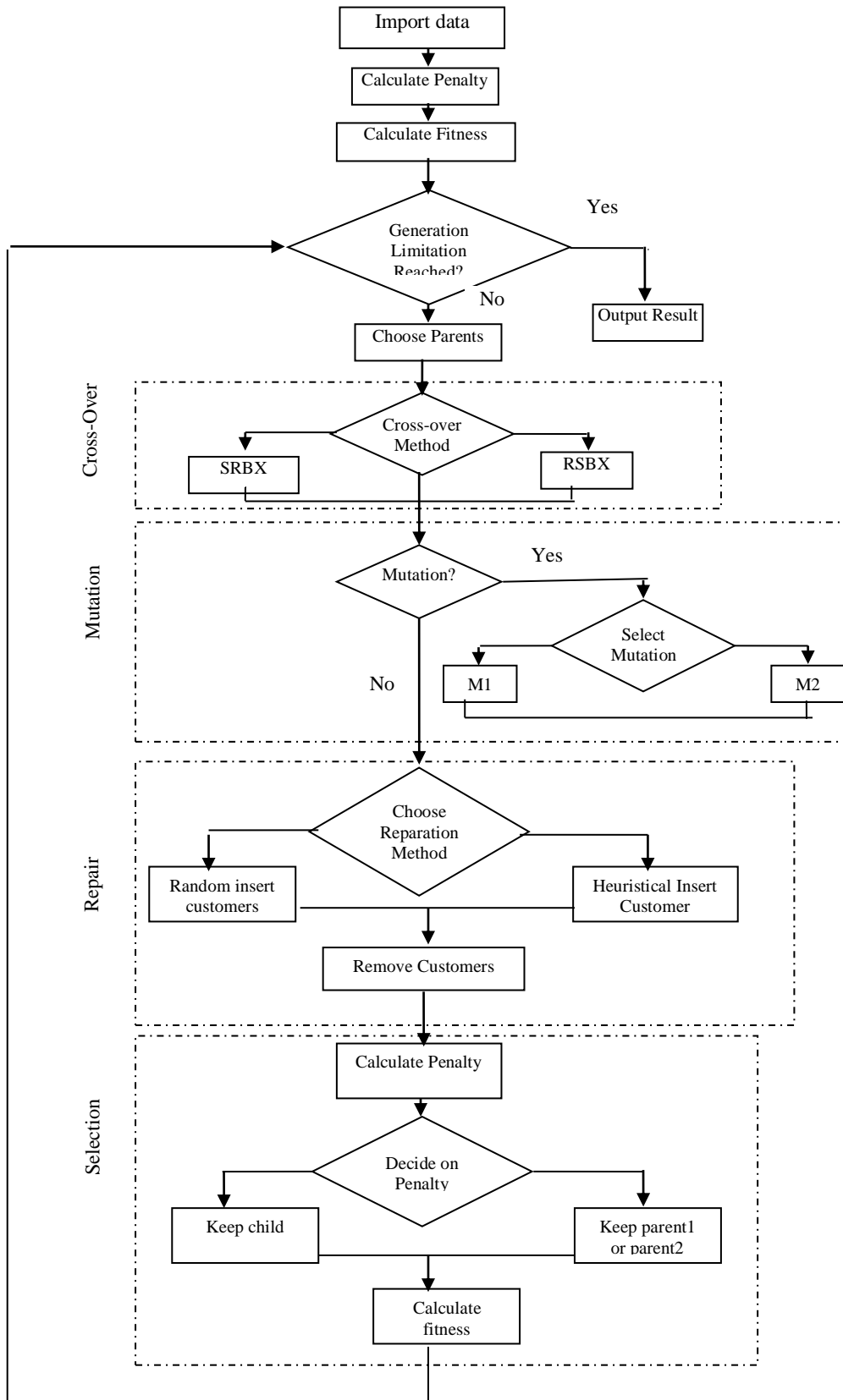


Figure1: Flow Chart of solution of VRP using Genetic Algorithm.

A. Chromosome representation

The individuals of a population in the GA can be seen as an ordered list of artificial chromosomes where every chromosome represents a route a truck is going to take. Each chromosome contains K integers, where K is the number of genes a chromosome holds. A gene itself is an integer as well and represents the number of customer. Example of a solution of 4 trucks with 10 customers.

route1: [2 4 9 10]

route2: [4 6]

route3: []

route4: [3 1 6 7 8]

Route1 is served by truck1 that visits the ordered list from left, starting with customer2, to the right ending at the customer 10 before it goes back to the depot. Trucks that aren't needed in the solution have an empty list.

B. Chromosome implementation

Each set of chromosomes represents one individual, which is one possible solution to the VRP (if all constraints are satisfied then it can be considered a valid solution). Each chromosome represents a Route and is implemented by a Route object. The Route Object stores all the genes (references to customer objects) in an array. The index of the array specifies the position of the customer in the route. All the routes of a solution are stored in an array in the VRP Object, where the index defines the route number. On the top level the VRPManager stores all the VRP objects which define the population. The implementation choice to use an array is optimal for the VRPManager (to hold the VRP objects) and the VRP objects (to hold the routes) as we have a non-changing population and set of routes. For the storage of the genes (customers) a simply linked list would be more suitable than an array as the insertion and removal process could be faster than its currently implemented.

C. Crossovers

In genetic algorithms, crossover is a genetic operator used to vary the programming of a chromosome or chromosomes from one generation to the next. It is an analogy to reproduction and biological crossover, upon which genetic algorithms are based. Both implemented crossovers don't do mutual exchange of genetic material between two parents. They take information from one individual and insert it in the other to create a new child. The probability which crossover method should be used can be configured.

D. Mutation

In genetic algorithms, mutation is a genetic operator used to maintain genetic diversity from one generation of a population of chromosomes to the next. It is analogous to biological mutation. The probability which mutations will take place and if mutation takes place at all can be configured.

E. Reparation

In the reparation process the child first gets checked if it contains some genetic information too much or is missing some. In other words, the process checks which customers are missing on the routes and which ones would be served several

times. Customers that are served more than once are removed from the chromosomes that one customer is only present one time. The location from where the duplicated genes are removed is chosen randomly. Customers that are missing need to be re-inserted. Here the heuristic comes into place, the customers are not just inserted in a random location but in a location where they are applicable. This location is found by trying to insert a customer to an existing route in a specific position and checking how much the penalty increases for this route. This process is now applied to all routes, until the route and the position in the route is found where the customer adds the least possible penalty. This step is very time consuming, therefore this method is just used depending on a defined probability. Else the customer is just inserted in a random route at a random position.

F. Penalties

To rate the fitness of a chromosome a special penalty system was integrated. This principle helps to distinguish good routes from bad routes. Different aspects are considered when applying the penalty calculation like the distance of the route or the delay if a customer is served too late. These different penalty operators can be individually adjusted.

G. Child or Parent(s)

After the penalties have been calculated for a new child, the system decides if the child is accepted or not. This process compares the penalties of its parents with the ones from the child. If the child does better, it will be accepted for the next generation. However if the child has a bigger penalty then there will be another selection process, which favors the parents depending on their penalties. In this process also the child has a chance to survive, as it is important for the genetic diversity. If the child wouldn't have a chance to survive in case it has a bigger penalty than its parents, the system would be strictly monotone decrease the overall penalty level of its whole population. This however could make the system stuck in local minimum penalty level from which it couldn't escape any more. Therefore it's important to give even a bad child a chance to survive.

H. Fitness

To choose which children from the newly created population will be favored to breed, the fitness of every individual has to be computed. This is done by summing up all the penalties of its chromosomes and using them in the following formula where the max_penalty is the biggest total penalty of one individual found in this generation.

$$\text{Fitness} = 100 * \frac{\text{max Penalty} - \text{penalty}}{\text{max Penalty}}$$

Therefore the fitness is not an absolute measure like the penalty (which can be compared over different generations) but a local measurement for this generation. The Fitness can take values between 0 (which is assigned to the individual with the maximal penalty) up to theoretically 100 (which in practice is not reached).

I. Selection process depending on the Fitness

The calculated fitness helps now to select members for the next generation. This is done using the Roulette Wheel Selection

method where individuals with a higher fitness are more likely to be selected than others.

III. RESULTS

First we checked our engine with different datafiles. For all datafiles tested, we found sooner or later a valid solution. Some solutions were quite good (compared to published values on the internet) while others were not really satisfying. Here is an example of a solution which is valid, however we can already visually tell that it's not optimal as there are some bigger detours which most likely are unnecessary.

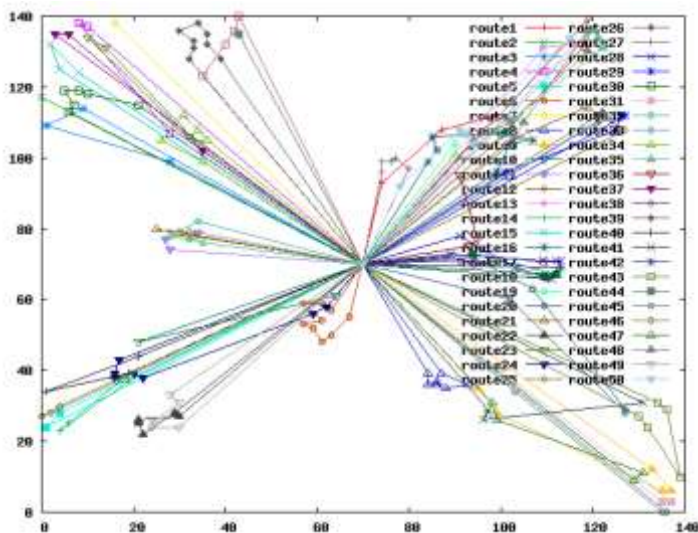


Figure2: Route with 50 trucks.

We used a couple of files [7] to measure how long it takes till the system finds the first valid solution. The following dump lists the filename of the testdata, the traveling distance of all trucks, the time all the trucks together spend on the road and the time it took to find the first valid solution.

- file: R101.txt ODist 962 OTime 1140 time: 4.68799996376038
- file: R102.txt ODist 770 OTime 1085 time: 5.59299993515015
- file: R103.txt ODist 768 OTime 942 time: 5.625
- file: R104.txt ODist 717 OTime 1021 time: 5.6100001335144
- file: R105.txt ODist 799 OTime 1009 time: 6.0939998626709
- file: R106.txt ODist 731 OTime 1048 time: 5.60900020599365
- file: R107.txt ODist 727 OTime 1076 time: 5.64099979400635

IV. SYSTEM TUNING

We used some heuristic to place missing customers back to the different routes after they disappeared during crossover or mutation. We tried different probabilities on how often the heuristic should be used and measured the different penalties we found as an end solution. We have to set a maximal generation limit which was higher for test runs with lower heuristic probability than with higher probability that every test

run took more or less the same time.

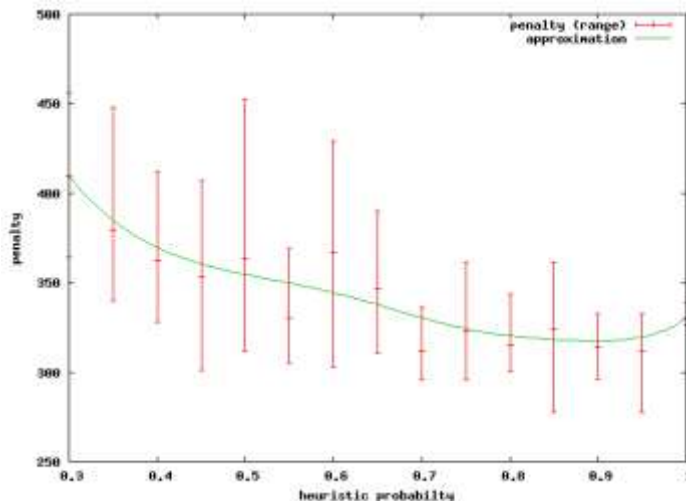


Figure3a: Heuristic probabilities

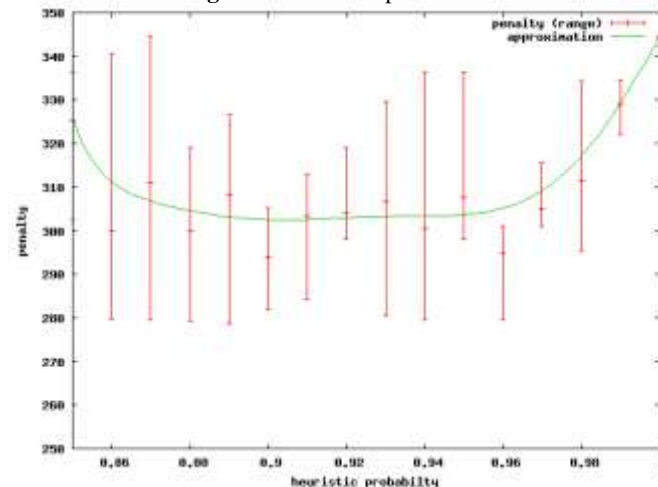


Figure3a: Heuristic probabilities

It can be seen, that with a higher heuristic probability, better results are archived. However if the probability of using heuristics get close to 1, the penalty increases. Therefore we used a finer granulation to see what is going on. It looks like if when the probability gets close to 1, the genetic diversity is not anymore sufficient and we get stuck in a local minimum. It is observed that the penalty range (indicated by the error bars) almost collapses where the deviance is much higher else.

Population size: The other important parameter is the generation size. The next figure shows different generations sizes combined with different heuristic probabilities. P30 refers to a population of 30 individuals where p10 represents 10 individuals. R0.3 means that the insertion heuristic was used in 30% of the time.

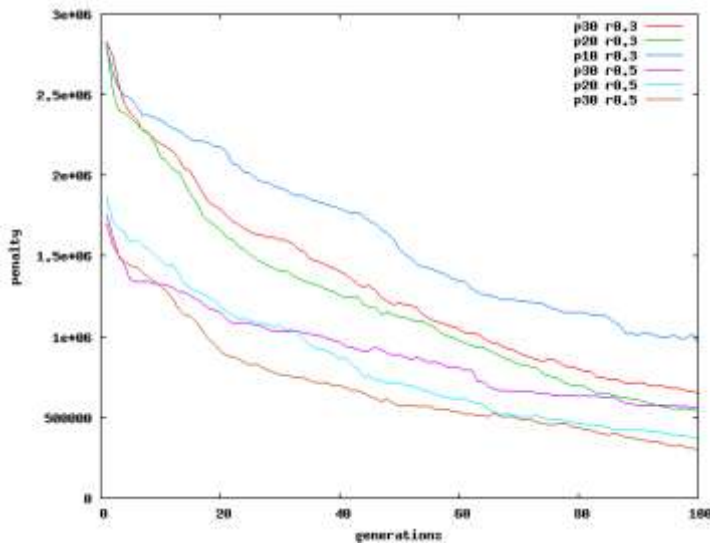


Figure4: population size 1/2

The first thing that sticks to the eye is, that a higher heuristic probability results in a lower initial penalty and also in a lower end penalty, however the difference is not that big any more. The second thing to note is, that the two graphs with a population size of 10 result in the worst end result. Both the population with 20 and 30 individuals are doing quite well. The next graph continues this picture and plots the generations 100 up to 200.

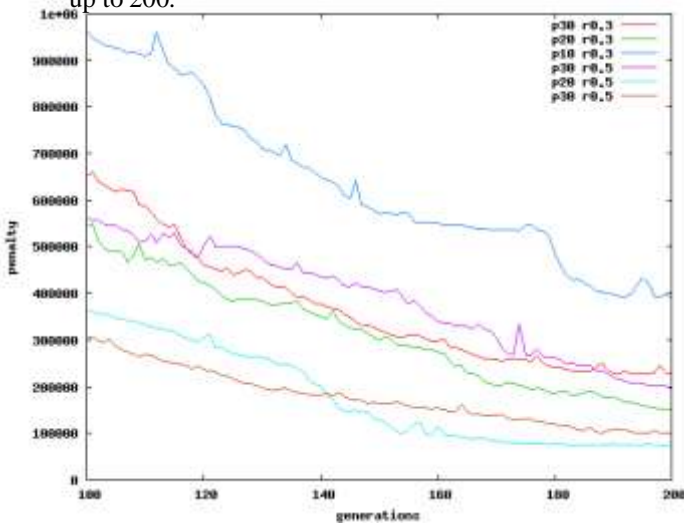


Figure5: population size 2/2

Here now something interesting happens. One would assume that the population size of 30 results in the best end result, however in both cases of the different heuristic probabilities the generation size of 20 finds the best solution. We ran this tests a couple of time and always got the same results.

V. BEST POSSIBLE SOLUTION

We checked for different datafiles if we can get close to the best known solutions and managed to archive the same best

result for the file RC208.txt as it is published on the internet. The solutions just uses 1 truck which drives the minimal distance of 328.2.

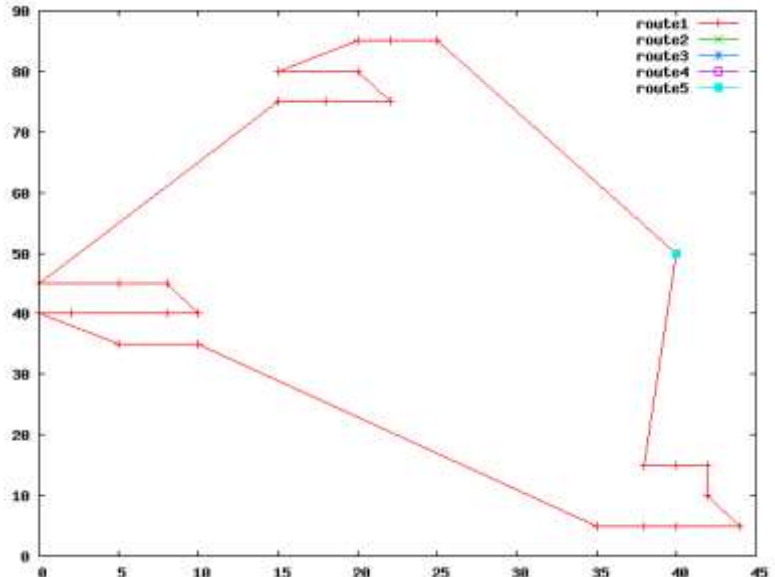


Figure6: Shortest Path.

VI. CONCLUSION

Genetic algorithms provide a very interesting approach to solve problems where an exact method can not be applied. We were a bid disappointed that it took many generations to find a solution, which was not even really good. Therefore we decided to implement some custom insertion heuristic which helps the system to faster approach a good solution. The choice of the crossover method was pretty intuitive and we can't assess if they are good or not. We implemented one that inserts new elements as a subroute using our heuristic method and another one, which does a simple sequence based crossover. We found out that if we put a too high heuristic level, we get on one hand quite fast good results, however in most cases we are unable to get to the best results. Therefore we tuned the system to have a balance between finding fast a solution and limiting the search space.

REFERENCES

- [1] M. Fisher. Vehicle routing. Handbooks of Operations Research and Management Science, Chapter 1, 8:1-31,1995
- [2] Sergios Theodoridis, Konstantinos Kourtoombas. Pattern Recognition Second Edition page 582
- [3] M.Gendreau, G. Laprte, and J-Y. Potvin. Metaheuristics for the vehicle routing problem. Management Science, 40:1276-1290,1994.
- [4] G. Laporte, M. Gendreau, J-Y. Potvin, and F. Semet. Classical and modern heuristics for the vehicle routing problem. International Transactions in Operational Research, 7:285-300,2000
- [5] G. Laporte and F. Semet. Classical heuristics for the vehicle routing problem. Technical Report G-98-54, GERAD, 1999.
- [6] The VRP Web. The vrp web, 2004. URL <http://neo.lcc.uma.es/radi-aeb/WebVRP/index.html?results/BestResults.h%tm>.
- [7] Vehicle Routing Data Sets. Vehicle routing data sets, 2003. URL <http://branchandcut.org/VRP/data/>
- [8] Fogel. D.: An evolutionary approach to the graveling salesman problem. Biological Cybernetics 60.

- [9] Rochat, Y., Taillard, E.: Probabilistic diversification and intensification in local search for vehicle routing. *J. of Heuristics* 1 (1995) 147-167
- [10] Croes, G.: A method for solving traveling salesman problems. *Operations Research* 6. 791-812
- [11] Berger, J., Barkaoui, M.: A hybrid genetic algorithm for the capacitated vehicle routing problem. In Cantu-Paz, E., ed.: GECCO03, LNCS 2723, Illinois, Chicago, USA, Springer-Verlag. 646-656
- [12] Dantzing, G., Ramster, R.: The truck dispatching problem. *Management Science* 6(1959) 80-91

AUTHORS PROFILE



Abdul Kadar Muhammad Masum is a graduate of B.Sc and MSc in Computer Science and Engineering from International Islamic University Chittagong, and United International University, Dhaka, Bangladesh, respectively. He has been serving as a faculty member in IIUC since 2005. Now he is an Assistant Professor of Department of Business Administration, International Islamic University Chittagong, Bangladesh. Moreover, he has mentionable research works on Data Mining, E-commerce and E-governance and has a great interest in MIS field. He has also experience in research paper presentation in many International and National Conferences.



Mohammad Shahjalal has received his B. Sc. degree in Electrical and Electronic Engineering from Chittagong University of Engineering and Technology in 2009. Now he is serving as a lecturer in the department of Electrical and Electronic Engineering of International Islamic University Chittagong since February 28, 2010. His research interests focus on Artificial Intelligence, image processing, wireless communication, wireless networking, digital signal processing.

Md. Iqbal Hasan Sarker has received his B.Sc degree in Computer Science & Engineering from Chittagong University of Engineering & Technology (CUET) in 2009. Now he is serving as a Lecturer in Chittagong University of Engineering & Technology (CUET) in the department of Computer Science & Engineering since September 19, 2010. His research interests focus on Artificial Intelligence, Digital Image Processing and Natural Language Processing, Wireless Communication.



Md. Faisal Faruque has received his B.Sc degree in Computer Science & Engineering from International Islamic University Chittagong (IIUC) in 2007. Now he is serving as a Lecturer in University of Information Technology & Sciences (UITS) in the department of Computer Science & Engineering since February 18, 2008. His research interests focus on Artificial Intelligence, Digital Image Processing and Natural Language Processing.

Reconfigurable Efficient Design of Viterbi Decoder for Wireless Communication Systems

Swati Gupta¹

Faculty Member, ECE Department
D.I.E.T
Karnal, India-132001
swatigupta13@gmail.com

Rajesh Mehra²

Faculty Member, ECE Department
NITTTR
Chandigarh, India-160019
rajeshmehra@yahoo.com

Abstract—Viterbi Decoders are employed in digital wireless communication systems to decode the convolution codes which are the forward correction codes. These decoders are quite complex and dissipate large amount of power. With the proliferation of battery powered devices such as cellular phones and laptop computers, power dissipation, along with speed and area, is a major concern in VLSI design. In this paper, a low power and high speed viterbi decoder has been designed. The proposed design has been designed using Matlab, synthesized using Xilinx Synthesis Tool and implemented on Xilinx Virtex-II Pro based XC2vpx30 FPGA device. The results show that the proposed design can operate at an estimated frequency of 62.6 MHz by consuming fewer resources on target device.

Keywords—Clock Gating; FPGA; VHDL; Trace Back; Viterbi Decoder.

I. INTRODUCTION

Viterbi Decoder has been recognized as an attractive solution to a variety of digital estimation problems, as the Kalman filter has been adapted to analog estimation problems. Viterbi algorithm is widely used in many wireless and mobile communication systems for optimal decoding of convolutional codes. Convolutional codes which are forward error correction codes offer a good alternative to block codes for transmission over a noisy channel. The purpose of forward error correction (FEC) is to improve the capacity of a channel by adding some carefully designed redundant information to the data being transmitted through the channel [1]. The Viterbi algorithm essentially performs maximum likelihood decoding to correct the errors in received data which are caused by the channel noise. However it reduces the computational load by taking advantage of special structure in the code trellis. Moreover viterbi decoding has a fixed decoding time which is well suited for hardware decoder implementation [2]. The requirements for the Viterbi decoder, which is a processor that implements the Viterbi algorithm, depend on the application in which it is used. This results in a very wide range of data throughput. The decoder structure is very simple for short constraint length, making the decoding feasible at rates of up to 100 Mbit/s. Viterbi decoder is effective in achieving noise tolerance, but the cost is an exponential growth in memory, computational resources and power consumption.

II. VITERBI DECODER AND ALGORITHM

The Viterbi algorithm is commonly used in a wide range of communication and data storage applications. It is also used for decoding convolutional codes, in base band detection for wireless systems, and for detection of recorded data in magnetic disk drives. The Viterbi detectors used in cellular telephones have low data rates (typically less than 1Mb/s) and should have very low energy consumption. On the opposite end of the scale, very high speed Viterbi detectors are used in magnetic disk drive read channels, with throughputs over 600Mb/s but power consumption is not as critical

Viterbi Maximum Likelihood Algorithm is one of the best techniques for communications, especially wireless where energy efficiency is the most important factor. It works on the principle of selecting a code word closest to the received word. The Viterbi decoder examines an entire sequence of received signal of a given length. The decoder computes a metric for each path and makes a decision based on this metric. The metric is hamming distance between the received branch word and expected branch word [4]. This is just the dot product between the received codeword and the allowable codeword. All paths are followed until two paths converge on one node. Then the path with the lower metric is kept and the one with higher metric is discarded. The paths selected are called the survivors. For an N bit sequence, total numbers of possible received sequences are 2^N . The Viterbi algorithm applies the maximum-likelihood principles to limit the comparison to 2 to the power of kL surviving paths instead of checking all the paths. The selection of survivors lies at the heart of the Viterbi algorithm and ensures that the algorithm terminates with the maximum likelihood path. The algorithm terminates when all of the nodes in the trellis have been labeled and their entering survivors are determined. We then go to the last node in the trellis and trace-back through the trellis. At any given node, we can only continue backward on a path that survived upon entry into that node. Since each node has only one entering survivor, our trace-back operation always yields a unique path. This path is the maximum likelihood estimate that predicts the most likely transmitted sequence. The maximum likelihood is given by:

$$P(Z/U(m')) = \max P(Z/U(m)) \text{ over all } U(m) \quad (1)$$

where Z is the received sequence, and $U(m)$ is one of the possible transmitted sequences, and chooses the maximum (closest possible received sequence).

III. ARCHITECTURE OF THE VITERBI DECODER

The input to the communication systems is a stream of analog, modulated signals. The primary task of the receiver is the recovery of the carrier signal and also synchronization of bit timing so that the individual received data bits can be removed from the carrier and also separated from one another in an efficient manner. Both tasks are generally performed through the use of phase locked loops [5]. The analog base band signal is applied to the analog-to-digital converter with b-bit quantizer to get a received bit stream. The bit stream is then applied as the input to the Viterbi decoder. In order to compute the branch metrics at any given point in time, the Viterbi decoder must be able to segment the received bit stream into n -bit blocks, each block corresponding to a stage in the trellis.

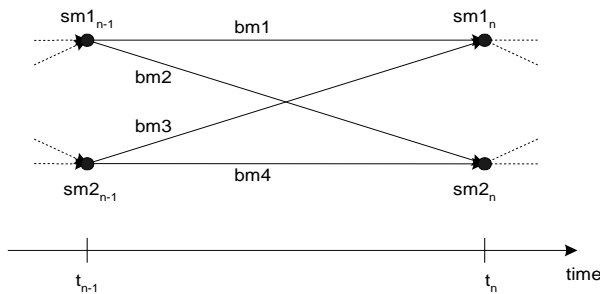


Fig.1 Two State Trellis

A trellis diagram is a time-indexed version of a state machine, and the simplest 2-state trellis is shown in Fig.1. Each state in the trellis corresponds to a possible pattern of recently received data bits and each branch corresponds to a receipt of the next (noisy) input. The goal is to find the path through the trellis of maximum likelihood because that path corresponds to the most likely pattern that the transmitter actually sent [8]. In this paper, we assume that the input to our proposed design is an identified code symbols and frames.

The basic building blocks of viterbi decoder are:-

A. Branch Metric Unit

The branch metric unit (BMU) takes the fuzzy bit and calculates the cost for each branch of the trellis. A simple branch metric unit may use hamming or Euclidean distance as the metric for calculating the cost of the branch [7]. It is based on a look-up table containing the various bit metrics. The computer looks up the n -bit metrics associated with each branch and sums them to obtain the branch metric.

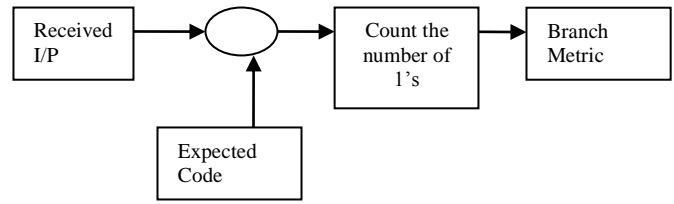


Fig.2 Branch Metric Computer

B. Add-Compare-Select Unit

The add-compare-select unit (ACSU) is the heart of the Viterbi algorithm and calculates the state metrics. It recursively accumulates the branch metrics as the path metrics (PM), compares the incoming path metrics, and makes a decision to select the most likely state transitions for each state of the trellis and generates the corresponding decision bits. The path metrics are added to state metrics from the previous time instant and the smaller sum is selected as the new state metric:

$$sm1_n = \min(sm1_{n-1} + bm_1, sm2_{n-1} + bm_3) \quad (2)$$

$$sm2_n = \min(sm1_{n-1} + bm_2, sm2_{n-1} + bm_4) \quad (3)$$

bm_k is the hamming distance between received and expected sequence.

For a given code with rate $1/n$ and total memory M , the number of ACSU required to decode a received sequence of length L is $L \times 2^M$.

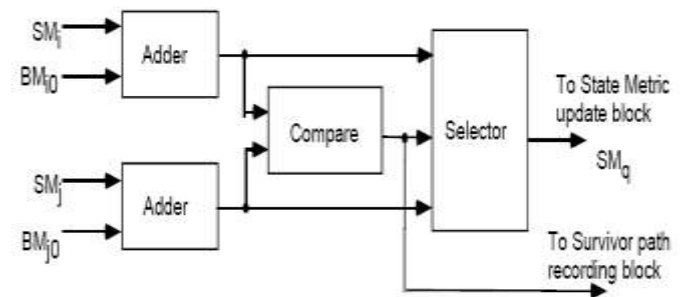


Fig.3 ACS Module

C. Survivor Memory Unit

The survivor memory unit (SMU) is responsible for keeping track of the information bits associated with the surviving paths designated by the path metric updating and storage unit. There are two basic design approaches for SMU:

Register Exchange and Trace Back. In both techniques, a shift register is associated with every trellis node throughout the decoding operation. This register has a length equal to the frame length. The register exchange method works well for small constraint lengths. The traceback method works well for longer constraint length codes. The traceback method stores the decisions from the ACS into a RAM and also the path information in the form of an array of recursive pointers [9]. The best path is determined by reading backwards through the RAM. The general approach to traceback is to accumulate path metrics for up to five times the constraint length ($5 * (K - 1)$), find the node with the largest accumulated cost, and begin traceback from this node [15]. The trace-back unit can then output the sequence of branches used to get to that state. In practice, the survivor paths merge after some number of iterations. The trellis depth at which all the survivor paths merge with high probability is referred to as the survivor path length.

IV. PROPOSED LOW POWER DESIGN

The ACSU and SMU consume most of the power of the decoder. In this paper we will be focusing on Survivor Memory Unit of viterbi decoder to develop a low power model. Among the two memory organization technique in the SMU, i.e. register exchange and trace back, the trace back approach is being used for low power applications. In the traceback approach, each register storing the survivor path information updates its content only once during the entire period of a code word. In contrast, all the registers in the register-exchange approach update their contents for each code symbol. Hence, the switching activity of the registers in a traceback approach is much lower than that for the registers in a register-exchange approach. So low power design techniques can be applied readily to the traceback module. In our work we will be utilizing the benefit of clock gating to develop a low power design [2]. The key issue is that the content of each register does not change as soon as it is updated. This is very useful in our low power design, as we don't have to activate the registers after each updation which reduces the switching activity leading to a reduction in power dissipation. Some blocks of a circuit are used only during a certain period of time. The clock of these blocks can be disabled to eliminate unnecessary switching not in use. Fig. 4 shows clock gating to disable

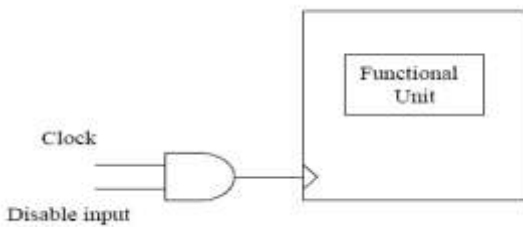


Fig.4 Clock Gating

The survivor path storage block holds the information on survivor paths. When the i^{th} code symbol is received, the survivor path information is obtained and stored in the i^{th} register. At this moment all other registers hold their contents,

and hence their clocks can be gated to save power as shown in Fig. 5. The clock is gated by the information coming from a ring counter that tells what the current state is so far.

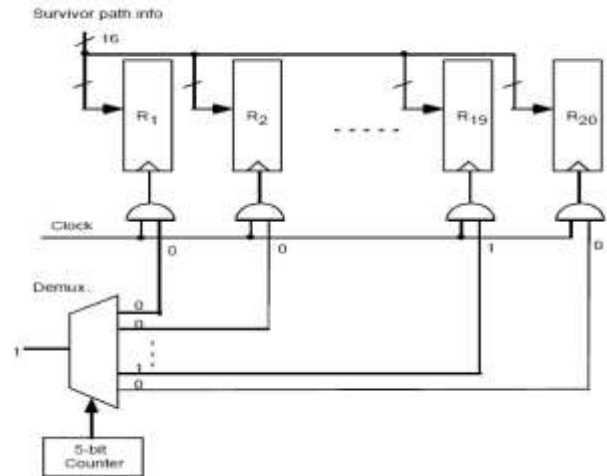


Fig.5 Implementation of Clock Gating

V. HARDWARE IMPLEMENTATION

A Matlab code is initially written for the convolutional encoder with constraint length, $K= 7$ and rate $\frac{1}{2}$ and the two generator polynomials $G1G2$ as $\{171,133\}$ and our proposed viterbi decoder design using trace back with clock gating to evaluate the performance of the proposed design. Fig.6 shows the BER curve vs. E_b/N_0 using the AWGN channel for both the uncoded data and the coded data using convolutional coding with viterbi decoding. The data is decoded every clock cycle but delayed 20 clocks. Since the traceback module is not activated until the end of the frame and only for one clock cycle, this feature helps in saving the power.

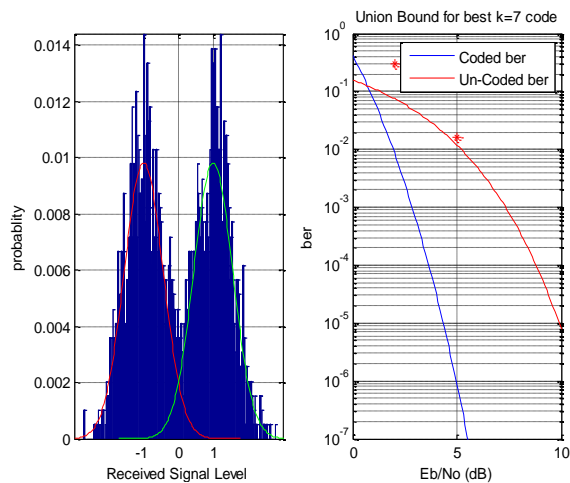


Fig.6 Matlab Simulation for Viterbi Decoder

Next step was the development of VHDL code. The test bench is written for both the convolutional encoder and viterbi decoder using ModelSim SE 6.4b simulator to test the functionality of the implemented decoder. Fig shows the

simulated results after applying an error pattern to show the efficiency of the decoder in correcting those errors.

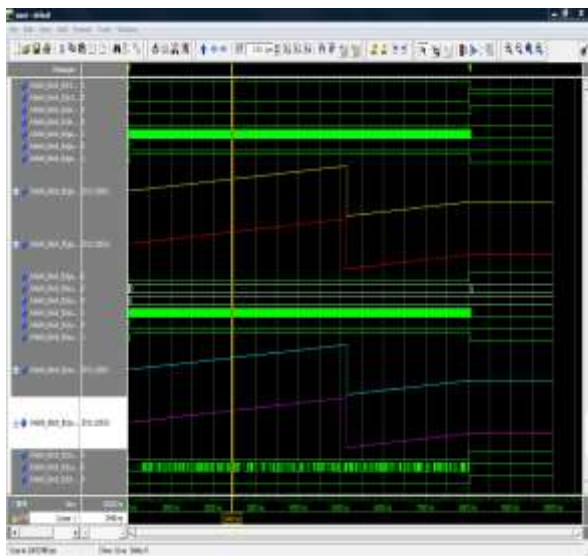


Fig7. ModelSim Simulation for Decoder

Xilinx ISE 10.1 tool has been used to map the design to FPGA Xilinx Virtex-II Pro xc2vpx70 with speed grade -5. The proposed design using the clock gating is then applied to Xilinx Xpower analyzer tool. Table 1 shows the device utilization summary

TABLE 1: DEVICE UTILIZATION SUMMARY

Device Utilization Summary		
Logic Utilization	Used/Available	Utilization
Number of Slices	5687/33088	17%
Number of Slice Flip-flops	2433/66176	3%
Number of 4 input LUTs	10686/66176	16%
Number of IOBs	17/996	1%
Number of MULT 18x18s	4/328	1%

TABLE 2: COMPARISON OF POWER DISSIPATION AND SPEED

	Trace back with Shift Register	Trace back with Shift Update and clock gating [6]	Proposed Design
Speed (In MHz.)	-----	47	62.52
Power Consumed (In Watt)	0.246	0.068	0.103

The results in Table 2 shows how the speed is being enhanced and the power is being reduced for the proposed design using traceback with clock gating as compared to other conventional designs.

VI. CONCLUSION

Features like flexibility, re-configurability and shorter time to market provides for a wide range of applications for FPGA. In this paper, a high speed and low power viterbi decoder has been designed which benefits from the concept of clock gating, switching off the blocks when not in use and hence helping in power saving. The design has been described using VHDL and implemented on VirtexII Pro based xc2vpx70 FPGA using ISE10.1. The power analysis has been done using Xilinx Xpower analyzer tool. The overall design shows that the effective speed of operation increases by 24.8% and a reduction in power dissipation to about 45% as compared to the design which was not benefiting clock gating and was using the conventional design using shift registers.

REFERENCES

- [1] Yeu-Hong Shiau, Pei-Yin Chen, Hung-Yu Yang, Yi-Ming Lin, Shi-Gi Huang, "An efficient VLSI architecture for convolutional code decoding", International Symposium on Next Generation Electronics, 2010, pp. 223-226
- [2] Sherif Welsen Shaker, Salwa Hussien Elramly and Khaled Ali Shehata, "FPGA Implementation of a Configurable Viterbi Decoder for Software Radio Receiver", Autotestcon, IEEE, July 2009, pp. 140 – 144.
- [3] Jinjin He, Huaping Liu, Zhongfeng Wang, "A fast ACSU architecture for Viterbi decoder using T-algorithm", Forty-Third Asilomar Conference on signals, Systems and Computers, 2009, pp. 231-235.
- [4] Abdallah R.A., Seok-Jun Leey, Goel M., Shanbhag N.R., "Low-power pre-decoding based viterbi decoder for tail-biting convolutional codes", IEEE Workshop on Signal Processing Systems, 2009, pp. 185-190
- [5] Abdallah R.A., Shanbhag N.R., "Error-Resilient Low-Power Viterbi Decoder Architectures", IEEE Transactions on Signal Processing, Vol. 57, 2009, pp. 4906-4917
- [6] Sherif Welsen Shaker, Salwa Hussien Elramly, and Khaled Ali Shehata, "Design and Implementation of Low-Power Viterbi Decoder for Software-Defined WiMAX Receiver", International Conference on Microelectronics, pp. 264 – 267, 2009.
- [7] Adam O., Shengli Fu, Varanasi M, "Hardware Efficient Encryption Encoder and Decoder Unit", Military Communication Conference, IEEE, 16-19 Nov. 2008, pp. 1 – 6
- [8] Wei Shao, Brackenburg L., "Pre-processing of convolutional codes for reducing decoding power consumption", IEEE International Conference on Acoustics, Speech and Signal Processing, 2008, pp. 2957 - 2960
- [9] Ajay D. Jadhav, Anil. R. Yardi, "Folding ADC Design for Software Defined GSM Radio-Mobile Station Receiver", IJCSNS International Journal of Computer Science and Network Security, vol. 8 No.9, September 2008.
- [10] Ying Li, Weijun Lu, Dunshan Yu, Xing Zhang, "Design Technique of Viterbi Decoder in Satellite Communication", IET Conference on Wireless, Mobile and Sensor Networks, 2007, pp. 162-165.
- [11] Sun F., Zhang T, "Low-Power State-Parallel Relaxed Adaptive Viterbi Decoder", IEEE Transactions on Circuits and Systems, Vol. 54, Issue. 5, 2007, pp. 1060-1068
- [12] Noguera J, Kennedy I.O, "Power Reduction in Network Equipment through Adaptive Partial Reconfiguration", International Conference on Field Programmable Logic and Applications, 2007, pp. 240 - 245
- [13] Guichang Zhong, Willson, A.N., "An Energy-efficient Reconfigurable Viterbi Decoder on a Programmable Multiprocessor", International Symposium on Circuits and Systems, IEEE, May 2007, pp. 1565-1568.
- [14] Dong-Sun Kim D.S., Seung-Yerl Lee, S.Y., Kyu-Yeul Wang, K.Y., Jong-Hee Hwang, J.H., Duck-Jin Chung, D.J., "Power Efficient Viterbi Decoder based on Pre-computation Technique for Portable Digital Multimedia Broadcasting Receiver", IEEE Transactions on Consumer Electronics, Vol. 53, Issue. 2, 2007, pp. 350-356
- [15] Russell Tessier, Sriram Swaminathan, Ramaswamy Ramaswamy, Dennis Goeckel, and Wayne Burlison, "A Reconfigurable, Power- Efficient

Adaptive Viterbi Decoder”, IEEE Transactions on VLSI Systems, Vol.13, No.4, April 2005.

- [16] Yao Gang, Ahmet T.Erdogan and Tughrul Arslan, “An effective Pre-trace back architecture for the viterbi decoder Targeting Wireless Communication Applications”, IEEE Transactions on Circuits and Systems, Vol.53, No.9, pp. 725-729, Sep 2006.

AUTHORS PROFILE



Ms. **Swati Gupta** is currently Assistant Professor at Doon Valley Institute of Engineering and Technology, Karnal, India. She is pursuing M.E. from NITTTR, Panjab University, Chandigarh, India. Ms. Swati has completed her B.E. (Hons.) from Vaish College of Engineering, Rohtak, India. She has 9 years of academic experience. Ms. Swati has authored 3 review papers and 2 research papers in reputed National Conferences. Her areas of interest include Communication Systems, Wireless and Mobile Communication and Digital Signal Processing.



Mr. Rajesh Mehra is currently Assistant Professor at National Institute of Technical Teachers’ Training & Research, Chandigarh, India. He is pursuing his PhD from Panjab University, Chandigarh, India. He has completed his M.E. from NITTTR, Chandigarh, India and B.Tech. from NIT, Jalandhar, India. Mr. Mehra has 15 years of academic experience. He has authored more than 25 research papers in reputed International Journals and 35 research papers in National and International conferences. Mr. Mehra’s interest areas include VLSI Design, Embedded System Design, Advanced Digital Signal Processing, Wireless & Mobile Communication and Digital System Design. Mr. Mehra is life member of ISTE.

Survey of Contrast Enhancement Techniques based on Histogram Equalization

Manpreet Kaur, Jasdeep Kaur, Jappreet Kaur
M.tech Computer Science,
Department of CSE,
Guru Nanak Dev Engineering College,
Ludhiana (Punjab), India.

Abstract—This Contrast enhancement is frequently referred to as one of the most important issues in image processing. Histogram equalization (HE) is one of the common methods used for improving contrast in digital images. Histogram equalization (HE) has proved to be a simple and effective image contrast enhancement technique. However, the conventional histogram equalization methods usually result in excessive contrast enhancement, which causes the unnatural look and visual artifacts of the processed image. This paper presents a review of new forms of histogram for image contrast enhancement. The major difference among the methods in this family is the criteria used to divide the input histogram. Brightness preserving Bi-Histogram Equalization (BBHE) and Quantized Bi-Histogram Equalization (QBHE) use the average intensity value as their separating point. Dual Sub-Image Histogram Equalization (DSIHE) uses the median intensity value as the separating point. Minimum Mean Brightness Error Bi-HE (MMBEBHE) uses the separating point that produces the smallest Absolute Mean Brightness Error (AMBE). Recursive Mean-Separate Histogram Equalization (RMSHE) is another improvement of BBHE. The Brightness preserving dynamic histogram equalization (BPDHE) method is actually an extension to both MPHEBP and DHE. Weighting mean-separated sub-histogram equalization (WMSHE) method is to perform the effective contrast enhancement of the digital image.

Keywords-component image processing; contrast enhancement; histogram equalization; minimum mean brightness error; brightness preserving enhancement, histogram partition.

I. INTRODUCTION

Image enhancement is a process involving changing the pixels' intensity of the input image, so that the output image should subjectively look better [1]. The purpose of image enhancement is to improve the interpretability or perception of information contained in the image for human viewers, or to provide a "better" input for other automated image processing systems. There are many image enhancement methods that have been proposed. A very popular technique for image enhancement is histogram equalization (HE). This technique is commonly employed for image enhancement because of its simplicity and comparatively better performance on almost all types of images. The operation of HE is performed by remapping the gray levels of the image based on the probability distribution of the input gray levels. It flattens and stretches the dynamic range of the image's histogram and resulting in overall contrast enhancement [2].

However, histogram equalization suffers from major drawbacks especially when implemented to process digital

images. Firstly, histogram equalization transforms the histogram of the original image into a flat uniform histogram with a mean value that is in the middle of gray level range. Accordingly, the mean brightness of the output image is always at the middle – or close to it in the case of discrete implementation – regardless of the mean of the input image. For images with high and low mean brightness values, this means a significant change in the image outlook for the price of enhancing the contrast. Secondly, histogram equalization performs the enhancement based on the global content of the image and in its discrete version large bins cannot be broken and redistributed to produce the desired uniform histogram. In other words, histogram equalization is powerful in highlighting the borders and edges between different objects, but may reduce the local details within these objects, especially smooth and small ones. Another consequence for this merge between large and small bins is the production of over enhancement and saturation artifacts [25].

Some researchers have also focused on improvement of histogram equalization based contrast enhancement such as mean preserving bi-histogram equalization (BBHE) [9], equal area dualistic sub-image histogram equalization (DSIHE) [15] and minimum mean brightness error bi-histogram equalization (MMBEBHE) [5], [16]. BBHE separates the input image histogram into two parts based on input mean. After separation, each part is equalized independently. This method tries to overcome the brightness preservation problem. DSIHE method uses entropy value for histogram separation. MMBEBHE is the extension of BBHE method that provides maximal brightness preservation. Though these methods can perform good contrast enhancement, they also cause more annoying side effects depending on the variation of gray level distribution in the histogram [17]. Recursive Mean-Separate Histogram Equalization (RMSHE) [5] is another improvement of BBHE. However, it also is not free from side effects [21].

The mean brightness preserving histogram equalization (MBPHE) methods basically can be divided into two main groups, which are bisections MBPHE, and multi-sections MBPHE. Bisections MBPHE group is the simplest group of MBPHE. Fundamentally, these methods separate the input histogram into two sections. These two histogram sections are then equalized independently. The major difference among the methods in this family is the criteria used to divide the input histogram [9]. Next, Dynamic Histogram Equalization (DHE) technique takes control over the effect of traditional HE so that it performs the enhancement of an image without making any loss of details in it. DHE partitions the image histogram based

on local minima and assigns specific gray level ranges for each partition before equalizing them separately. These partitions further go through a repartitioning test to ensure the absence of any dominating portions. This method outperforms other present approaches by enhancing the contrast well without introducing severe side effects, such as washed out appearance, checkerboard effects etc., or undesirable artifacts [21]. The brightness preserving dynamic histogram equalization (BPDHE), which is an extension to HE that can produce the output image with the mean intensity almost equal to the mean intensity of the input, thus fulfil the requirement of maintaining the mean brightness of the image [22].

Multilevel Component-Based Histogram Equalization (MCBHE) where we combine the global histogram equalization, BPBHE, multiple graylevel thresholding, and connected component analysis to produce an image with improved global and local contrast and with minimal distortion [22]. Weighting mean-separated sub-histogram equalization (WMSHE) method is to perform the effective contrast enhancement of the digital image [26].

The paper is organised as follows: HE for digital input image is reviewed together with their mathematical formulation and BBHE, DSIHE, MMBEBHE, and generalization of BBHE, namely - Recursive Mean Separate Histogram Equalization (RMSHE) in section II. Mean Brightness Preserving Histogram Equalization (MBPHE) will be presented in section III and Dynamic Histogram Equalization (DHE) in section IV. Section V includes the Brightness Preserving Dynamic Histogram Equalization (BPDHE) and Multilevel Component-Based Histogram Equalization (MCBHE) in section VI respectively. In section VII, Weighting Mean-Separated Sub-Histogram Equalization (WMSHE) is discussed. Paper concludes with Section VIII containing discussion of various Histogram Equalization techniques.

II. HISTOGRAM EQUALIZATION (HE)

For a given image \mathbf{X} , the probability density function $p(X_k)$ is defined as

$$p(X_k) = \frac{n^k}{n} \quad (1)$$

For $k = 0, 1, \dots, L - 1$, where n^k represents the number of times that the level (X_k) appears in the input image \mathbf{X} and n is the total number of samples in the input image. Note that $p(X_k)$ is associated with the histogram of the input image which represents the number of pixels that have a specific intensity X_k . In fact, a plot of n^k vs. X_k is known histogram of \mathbf{X} . Based on the probability density function, the cumulative density function is defined as

$$c(X) = \sum_{j=0}^k p(X_j) \quad (2)$$

Where $X_k = x$, for $k = 0, 1, \dots, L - 1$. Note that $c(X_{L-1}) = 1$ by definition. HE is a scheme that maps the input image into the entire dynamic range, (X_0, X_{L-1}) , by using the cumulative density function as a transform function. Let's define a transform function $f(x)$ based on the cumulative density function as

$$f(x) = X_0 + (X_{L-1} - X_0)c(x) \quad (3)$$

Then the output image of the HE, $\mathbf{Y} = \{Y(i, j)\}$, can be expressed as

$$\mathbf{Y} = f(\mathbf{X}) \quad (4)$$

$$= \{f(X(i, j)) \mid \forall X(i, j) \in \mathbf{X}\} \quad (5)$$

The high performance of the HE in enhancing the contrast of an image as a consequence of the dynamic range expansion, Besides, HE also flattens a histogram. Base on information theory, entropy of message source will get the maximum value when the message has uniform distribution property [4]. As addressed previously, HE can introduce a significant change in brightness of an image, which hesitates the direct application of HE scheme in consumer electronics.

A. Brightness Preserving Bi-Histogram Equalization (BBHE)

This method divides the image histogram into two parts as shown in Fig.1. In this method, the separation intensity X_T is presented by the input mean brightness value, which is the average intensity of all pixels that construct the input image. After this separation process, these two histograms are independently equalized. By doing this, the mean brightness of the resultant image will lie between the input mean and the middle gray level [2].

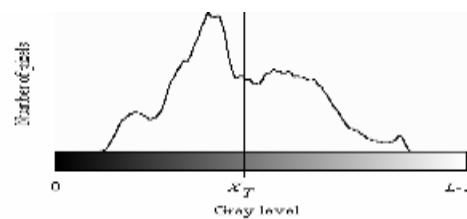


Figure 1. Bi-histogram equalization. The histogram with range from 0 to $L-1$ is divided into two parts, with separating intensity X_T . This separation produces two histograms. The first histogram has the range of 0 to X_T , while the second histogram has the range of X_{T+1} to $L-1$.

B. Dualistic Sub-Image Histogram Equalization (DSIHE)

Following the same basic ideas used by the BBHE method of decomposing the original image into two sub-images and then equalize the histograms of the sub-images separately, [4] proposed the so called equal area dualistic sub-image HE (DSIHE) method. Instead of decomposing the image based on its mean gray level, the DSIHE method decomposes the images aiming at the maximization of the Shannon's entropy [5] of the output image. For such aim, the input image is decomposed into two sub-images, being one dark and one bright, respecting the equal area property (i.e., the sub-images has the same amount of pixels). In [4], it is shown that the brightness of the output image O produced by the DSIHE method is the average of the equal area level of the image I and the middle gray level of the image, i.e., $L/2$. The authors of [4] claim that the brightness of the output image generated by the DSIHE method does not present a significant shift in relation to the brightness of the input image, especially for the large area of the image with the same gray-levels (represented by small areas in histograms with great concentration of gray-levels), e.g., images with small objects regarding to great darker or brighter backgrounds.

C. Minimum Mean Brightness Error Bi-HE Method (MMBEBHE)

Still following the basic principle of the BBHE and DSIHE methods of decomposing an image and then applying the HE method to equalize the resulting sub-images independently, [6] proposed the minimum mean brightness error Bi-HE (MMBEBHE) method. The main difference between the BBHE and DSIHE methods and the MMBEBHE one is that the latter searches for a threshold level l_t that decomposes the image I into two sub-images $I[0, l_t]$ and $I[l_t + 1, L - 1]$, such that the minimum brightness difference between the input image and the output image is achieved, whereas the former methods consider only the input image to perform the decomposition.

Once the input image is decomposed by the threshold level l_t , each of the two sub-images $I[0, l_t]$ and $I[l_t + 1, L - 1]$ has its histogram equalized by the classical HE process, generating the output image. Assumptions and manipulations for finding the threshold level l_t in $O(L)$ time complexity was made in [6]. Such strategy allows us to obtain the brightness l_m ($O[0, l_t] \cup O[l_t + 1, L - 1]$) of the output image without generating the output image for each candidate threshold level l , and its aim is to produce a method suitable for real-time applications.

D. Recursive Mean-Separate HE Method (RMSHE)

Recall that the extensions of the HE method described so far in this section were characterized by decomposing the original image into two new sub-images. However, an extended version of the BBHE method named recursive mean-separate HE (RMSHE), proposes the following. Instead of decomposing the image only once, the RMSHE method proposes to perform image decomposition recursively, up to a scale r , generating 2^r sub-images. After, each one of these sub-images $I^r[l_s, l_r]$ is independently enhanced using the CHE method. Note that when $r = 0$ (no sub-images are generated) and $r = 1$, the RMSHE method is equivalent to the CHE and BBHE methods, respectively. In [7], they mathematically showed that the brightness of the output image is better preserved as r increases. Note that, computationally speaking, this method presents a drawback: the number of decomposed sub-histograms is a power of two.

III. MEAN BRIGHTNESS PRESERVING HISTOGRAM EQUALIZATION (MBPHE)

The mean brightness preserving histogram equalization (MBPHE) methods basically can be divided into two main groups, which are bisections MBPHE, and multi-sections MBPHE. Bisections MBPHE group is the simplest group of MBPHE. Fundamentally, these methods separate the input histogram into two sections. These two histogram sections are then equalized independently.

However, bisections MBPHE can preserve the mean brightness only to a certain extent. However, some cases do require higher degree of preservation to avoid unpleasant artifacts [7]. Furthermore, bisections MBPHE can only preserve the original mean brightness if and only if the input histogram has a quasi-symmetrical distribution around its separating point [8]. But, most of the input histograms do not

have this property. This condition leads to the failure of bisections MBPHE in preserving the mean intensity in real life applications.

Works in [7], [8]-[19] are a few of multi-sections MBPHE. Multi-sections MBPHE group has a better mean brightness preservation as compared with the group of bisections MBPHE. In multi-sections MBPHE, the input histogram is divided into R sub-histograms, where R is any positive integer value. Each sub-histogram is then equalized independently. The creation of the sub-histograms can be carried out recursively (e.g. by using the mean or median intensity value), or based on the shape of the input histogram itself (e.g. using the locations of local maximum or local minimum). Yet, in these methods, the detection of the separating points' process normally requires complicated algorithms, which then associated with relatively high computational time. Furthermore, these methods usually increase the hardware requirement in the implementations for consumer electronic products. In addition, most of these methods put too much constrain on keeping the mean intensity value. As a consequence, not much enhancement could be obtained from most of these methods [20].

IV. DYNAMIC HISTOGRAM EQUALIZATION (DHE)

This Dynamic Histogram Equalization (DHE) technique takes control over the effect of traditional HE so that it performs the enhancement of an image without making any loss of details in it. DHE divides the input histogram into number of sub-histograms until it ensures that no dominating portion is present in any of the newly created sub-histograms. Then a dynamic gray level (GL) range is allocated for each sub-histogram to which its gray levels can be mapped by HE. This is done by distributing total available dynamic range of gray levels among the sub-histograms based on their dynamic range in input image and cumulative distribution (CDF) of histogram values. This allotment of stretching range of contrast prevents small features of the input image from being dominated and washed out, and ensures a moderate contrast enhancement of each portion of the whole image. At last, for each sub-histogram a separate transformation function is calculated based on the traditional HE method and gray levels of input image are mapped to the output image accordingly. The whole technique can be divided in three parts – partitioning the histogram, allocating GL ranges for each sub-histogram and applying HE on each of them [21].

V. BRIGHTNESS PRESERVING DYNAMIC HISTOGRAM EQUALIZATION (BPDHE)

The brightness preserving dynamic histogram equalization (BPDHE), which is an extension to HE that can produce the output image with the mean intensity almost equal to the mean intensity of the input, thus fulfils the requirement of maintaining the mean brightness of the image [22]. This method is actually an extension to both MPHEBP and DHE. Similar to MPHEBP, the method partitions the histogram based on the local maximums of the smoothed histogram. However, before the histogram equalization taking place, the method will map each partition to a new dynamic range, similar to DHE. As the change in the dynamic range will cause the change in mean brightness, the final step of this method

involves the normalization of the output intensity. So, the average intensity of the resultant image will be same as the input. With this criterion, BPDHE will produce better enhancement compared with MPHEBP, and better in preserving the mean brightness compared with DHE [22].

VI. MULTILEVEL COMPONENT BASED HISTOGRAM EQUALIZATION (MCBHE)

The MCBHE algorithm starts just like the BPBHE algorithm by decomposing the input image I into two

Sub images using the original mean brightness μ_I . We refer to these two sub images as the background I_b and foreground I_f sub images, where

$$I = I_b \cup I_f$$

$$I_b(m, n) = \{I(m, n) | I(m, n) < \mu_I, \forall I(m, n) \in I\} \quad (6)$$

$$I_f(m, n) = \{I(m, n) | I(m, n) \geq \mu_I, \forall I(m, n) \in I\} \quad (6)$$

Unlike BPBHE that equalizes each sub image using the conventional histogram equalization, the gray levels of each sub image in MCBHE are processed using multiple gray level thresholding and connected component analysis. This type of analysis is one of the techniques used in image segmentation applications such as tumor detection [23] and handwriting recognition [24]. In this approach the image under consideration is threshold at multiple predetermined gray levels. At each of these threshold levels, sequential labeling is used to identify those connected components that are below or above the current threshold. Depending on the application and the segmentation objective, some features of these components are extracted and saved to be analyzed later along with values obtained for other components at other levels. The benefit of this approach is that it allows for capturing the change and variation of gray levels within the object as the threshold value is changed. Actually, this is the reason for incorporating this approach in MCBHE, as it will help enhancing the local details [25].

VII. WEIGHTING MEAN-SEPARATED SUB-HISTOGRAM EQUALIZATION (WMSHE)

Weighting mean-separated sub-histogram equalization (WMSHE) method is to perform the effective contrast enhancement of the digital image. This method consist the following steps:

- A. *A. Separation of histogram based on our proposed weighting mean function.*
- B. *B. Achieving contrast enhancement by equalizing sub-histogram respectively in small-scale detail.*

1) Histogram Separation

Suppose that an input image W is composed of V discrete gray levels and is denoted by $\{G_0, G_1, \dots, G_n, \dots, G_{V-1}\}$, the Probability Density Function (PDF) and Cumulative Distribution Function (CDF) for an input image W is expressed as:

$$PDF(G_n) = \frac{n^h}{n} \quad (7)$$

where $h = 0, 1, \dots, V - 1$,

Where n^h denotes the number of pixels that correspond to the value h , and n is the total number of the pixels in the input image W . Then the weighting mean value X_t can be calculated by using our proposed weighting mean function, which can be expressed as follows:

$$X_t = \frac{\sum_{l=a}^b l \times CDF(l)}{\sum_{l=a}^b CDF(l)} \quad (8)$$

Where $[a, b]$ represents the sub-interval of histogram, l represents the corresponding gray-level, and t represents the recursion level. Notice that the sub-interval $[a, b]$ is initialized as $[0, 255]$ and t is initialized as 1. Here we consider that the existing sub-histograms defined over a gray-level range $[X_r, X_{r+1}]$ at the recursion level $t-1$ ($0 \leq r \leq t-1$). In this paper, the recursion level t is experimentally set at 6.

2) Piecewise Transformed Function

After the ideal weighting mean values are determined, we can directly decide the optimum number of sub-images based on the histogram separation, which can be expressed as follows:

$$W_k = \{W(x, y) | X_k \leq W(x, y) < X_{k+1}, \forall W(x, y) \in W\} \quad (9)$$

Where W_k represents each sub-image, and $k = 0, 1, 2, \dots, t-1$. Then the relationship between gray-level G and each sub image W_k is defined as the respective PDF $_k$:

$$PDF_k(G_h) = \frac{n^k}{n_k} \quad (10)$$

Where $k = 0, 1, \dots, t-1$, and $h = X_k + 1, X_k + 2, \dots, X_{k+1}$.

Notice that n_h denotes the number of pixels that correspond to the value h , and n_k is the total number of the pixels in k -th sub image, $PDF_k(G_h)$ is associated with the histogram of k -th sub image, which represents the frequency of a specific input gray level G_h . In the next step, the respective CDF_k is defined for each sub-image based on the respective PDF_k .

$$CDF_k(G_j) = \sum_{i=X_k+1}^j PDF_k(G_i) \quad (11)$$

Where $k = 0, 1, \dots, t-1$, and $h = X_k + 1, X_k + 2, \dots, X_{k+1}$.

Finally, the piecewise transformed function is used to map the equalized image. This is characterized by utilizing CDF_k of sub-image W_k for k segments [26].

VIII. DISCUSSION

The comparative study of Histogram Equalization based methods shows that the cases which require higher brightness preservation and not handled well by HE, BBHE and DSIHE, have been properly enhanced by RMSHE. MMBEBHE is the extension of BBHE method that provides maximal brightness preservation. Though these methods can perform good contrast enhancement, they also cause more annoying side

effects depending on the variation of gray level distribution in the histogram [6].

DHE ensures consistency in preserving image details and is free from any severe side effects. BPDHE can preserve the mean brightness better than BBHE, DSIHE, MMBEHE, RMSHE, MBPHE, and DHE. MCBHE is simple and heuristic method for contrast enhancement in grayscale images and able to enhance the quality of images such that both global and local contrast is enhanced with minimum distortion in the image appearance [25]. WMSHE achieves the best quality through qualitative visual inspection and quantitative accuracies of Peak Signal-to- Noise Ratio (PSNR) and Absolute Mean Brightness Error (AMBE) compared to other state-of-the-art methods [26].

ACKNOWLEDGMENT

The authors would like to thank Associate Professor Akshay Gridhar for their insightful and valuable suggestions.

REFERENCES

- [1] Rafael C. Gonzalez, and Richard E. Woods, "Digital Image Processing", 2nd edition, Prentice Hall, 2002.
- [2] Yeong-Taeg Kim, "Contrast enhancement using brightness preserving Bi-Histogram equalization", *IEEE Trans. Consumer Electronics*, vol. 43, no. 1, pp. 1-8, Feb. 1997.
- [3] J.-Y. Kim, L.-S. Kim, and S.-H. Hwang, "An advanced contrast enhancement using partially overlapped sub-block histogram equalization," *IEEE Trans. Circuits Syst. Video Technol.*, vol. 11, no. 4, pp. 475-484, Apr. 2001.
- [4] Y. Wang, Q. Chen, and B. Zhang, "Image enhancement based on equal area dualistic sub-image histogram equalization method," *IEEE Trans. on Consumer Electronics*, vol. 45, no. 1, pp. 68-75, Feb. 1999.
- [5] C. Shannon, "A mathematical theory of communication," *Bell Syst. Tech. J.*, vol. 27, pp. 379-423, 1948.
- [6] S.-D. Chen and A. Ramli, "Minimum mean brightness error Bi-Histogram equalization in contrast enhancement," *IEEE Trans. on Consumer Electronics*, vol. 49, no. 4, pp. 1310-1319, Nov. 2003.
- [7] S.-D. Chen and A. Ramli, "Contrast enhancement using recursive Mean-Separate histogram equalization for scalable brightness preservation," *IEEE Trans. on Consumer Electronics*, vol. 49, no. 4, pp. 1301-1309, Nov. 2003.
- [8] Chao Wang and Zhongfu Ye, "Brightness preserving histogram equalization with maximum entropy: a variational perspective", *IEEE Trans. Consumer Electronics*, vol. 51, no. 4, pp. 1326-1334, November 2005.
- [9] K. Wongsritong, K. Kittayarusiriwat, F. Cheevasuvit, K. Dejhan, and A. Somboonkaew, "Contrast enhancement using multi-peak histogram equalization with brightness preserving", *The 1998 IEEE Asia-Pacific Conference on Circuit and Systems*, pp. 24-27, November 1998. [10] M. Abdullah-Al-Wadud, M. H. Kabir, M. A. A. Dewan, and Oksam Chae, "A dynamic histogram equalization for image contrast enhancement", *IEEE Trans. Consumer Electronics*, vol. 53, no. 2, pp. 593 - 600, May 2007.
- [11] K. S. Sim, C. P. Tso, and Y. Y. Tan. "Recursive sub-image histogram equalization applied to gray scale images", *Pattern Recognition Letters*, vol. 28, no. 10, pp. 1209-1221, July 2007.
- [12] David Menotti, Laurent Najman, Jacques Facon, and Araujo de A. Araujo, "Multi histogram equalization methods for contrast enhancement and brightness preserving", *IEEE Trans. Consumer Electronics*, vol. 53, no. 3, pp. 1186 - 1194, August 2007.
- [13] Chun-Ming Tsai, and Zong-Mu Yeh, "Contrast enhancement by automatic and parameter-free piecewise linear transformation for color images", *IEEE Trans. Consumer Electronics*, vol. 54, no. 2, pp. 213-219, May 2008.
- [14] Haidi Ibrahim, and Nicholas Sia Pik Kong, "Brightness preserving dynamic histogram equalization for image contrast enhancement", *IEEE Trans. Consumer Electronics*, vol. 53, no. 4, pp. 1752 - 1758, November 2007.
- [15] Nicholas Sia Pik Kong, and Haidi Ibrahim, "Improving the visual quality of abdominal magnetic resonance images using histogram equalization", In *Technology and Applications in Biomedicine, 2008. ITAB 2008. International Conference on*, pp. 138-139, Shenzhen, China, May 2008.
- [16] Nicholas Sia Pik Kong, and Haidi Ibrahim, "Color image enhancement using brightness preserving dynamic histogram equalization", *IEEE Trans. Consumer Electronics*, vol. 54, no. 4, pp. 1962 - 1968, November 2008.
- [17] Nymkhaigva Sengee, and Heung Kook Choi, "Brightness preserving weight clustering histogram equalization", *IEEE Trans. Consumer Electronics*, vol. 54, no. 3, pp. 1329 - 1337, August 2008.
- [18] Gyu-Hee Park, Hwa-Hyun Cho, and Myung-Ryul Choi, "A contrast enhancement method using dynamic range separate histogram equalization", *IEEE Trans. Consumer Electronics*, vol. 54, no. 4, pp. 1981 - 1987, November 2008.
- [19] Mary Kim and Min Gyo Chung, "Recursively separated and weighted histogram equalization for brightness preservation and contrast enhancement", *IEEE Trans. Consumer Electronics*, vol. 54, no. 3, pp. 1389 - 1397, August 2008.
- [20] Chen Hee Ooi, Nicholas Sia Pik Kong, and Haidi Ibrahim, "Bi-Histogram Equalization with a Plateau Limit for Digital Image Enhancement", *IEEE Trans. Consumer Electronics*, Vol. 55, No. 4, NOVEMBER 2009.
- [21] M. Abdullah-Al-Wadud, Md. Hasanul Kabir, M. Ali Akber Dewan, and Oksam Chae, "A dynamic histogram equalization for image contrast enhancement", *IEEE Trans. Consumer Electron.*, vol. 53, no. 2, pp. 593-600, May 2007.
- [22] Haidi Ibrahim, and Nicholas Sia Pik Kong, "Brightness preserving dynamic histogram equalization for image contrast enhancement", *IEEE Trans. Consumer Electronics*, vol. 53, no. 4, pp. 1752 - 1758, November 2007.
- [23] S. Armato, M. Giegr, C. Moran, J. Blackburn, K. Doi, H. Macmahon, "Computerized detection of pulmonary nodules in CT Scans," *RadioGraphics* 1999; 19:1303-1311.
- [24] S. Wu, A. Amin, "Automatic thresholding of gray-level using multi-stage approach." In the proceedings of the *Seventh International Conference on Document Analysis and Recognition (ICDAR'03)*, Vol. 1, p.493, 2003.
- [25] *Iyad Jafar ,and Hao Ying,* "Multilevel Component-Based Histogram Equalization for Enhancing the Quality of Grayscale Images", *IEEE EIT*, pp. 563-568, 2007.
- [26] Pei-Chen Wu, Fan-Chieh Cheng, and Yu-Kung Chen, "A Weighting Mean-Separated Sub-Histogram Equalization for Contrast Enhancement", *IEEE Trans. Biomedical Engineering and Computer Science*, 2010.

AUTHORS PROFILE

Manpreet Kaur was born in July, 26, 1987 in Ludhiana, Punjab (India) and she received the B.Tech degree (with distinction) in Computer Science & Engineering from Guru Nanak Dev Engineering College Ludhiana, Punjab, India, in 2009. She is currently pursuing the Master degree in Computer Science & Engineering from Guru Nanak Dev Engineering College Ludhiana, Punjab, India. Her research interests include image processing.

Jasdeep Kaur received the B.Tech degree (with distinction) in Computer Science & Engineering from Ludhiana Group of Colleges of Engineering and technology Ludhiana, Punjab, India, in 2009. She is currently pursuing the Master degree in Computer Science & Engineering from Guru Nanak Dev Engineering College Ludhiana, Punjab, India. Her research interests gray scale image enhancement.

Jappreet Kaur was born in Ludhiana, Punjab (India). In 2009, she received the B.Tech degree (with distinction) in Computer Science & Engineering from Guru Nanak Dev Engineering College Ludhiana, Punjab, India. She is currently pursuing the Master degree in Computer Science & Engineering from Guru Nanak Dev Engineering College Ludhiana, Punjab, India. Her research interests include image enhancement and noise reduction.

Status of Wireless Technologies Used For Designing Home Automation System - A Review

Ashish J. Ingle, Bharti W. Gawali

Department of Computer Science and Information Technology
Dr. Babasaheb Ambedkar Marathwada University,
Aurangabad, India.

Abstract-The concept of “Automation” have just started flourishing, companies have developed automated systems of their own to control alarms, sensors, actuators and video cameras and moving further the concept of automated buildings is being recognized. This Paper attempts to study standards / technologies which are used for Home Automation. In brief, concern of this Paper is to cover the detail Technical aspects of the Home Automation Standard/ Technology.

Keywords: - Automation; Technology; Reliable.

I. INTRODUCTION

Building automation systems nowadays are common place in office, commercial and industrial constructions. Airports, commercial centers, hospitals and factories are all built with automated controlling systems to create the best possible indoor conditions. Yet, homes where people spend most of their time are built nearly without any automation. Still the automation systems could improve health, energy-conservation and comfort [1].

There are several competing home automation systems in the market but none of them has gained competitive advantage over others. Technologies are available but there are no standard practices among designers, contractors and installers to realize the systems. Lack of regulation of electrical design has lowered the quality of electrical documentation and electrical contractors often receive inadequate designs based on which they are expected to realize the home automation systems. The electrical designers are not responsible over their documentation leaving the contractors liable for the realization of the system.

Home automation has not been actively studied from the point of view of electrical designers and contractors before. The past research has concentrated mostly on the end users, especially on the elderly and disabled users who benefit from automation the most. It is important to study the actual process of developing the home automation systems so that the operations can be improved and updated where needed. Electrical industry is very conservative and thus the changes within the field are slow. However, small changes in procedures can make significant improvements in the workflow and accuracy of the product. The paper is organized as follows. Section 2 briefly introduces the wireless protocols which includes Bluetooth, Wi-Fi, USB and ZigBee and explains their independent parameters like Hardware Dimensions, Memory Requirements, Bandwidth and Range, Power Consumption, Network Features, Security and

Reliability and Costs and finally Section 3 concludes the paper.

II. HOME AUTOMATION TECHNOLOGIES - AN OVERVIEW

Home automation, or the idea of smart homes, is the controlling and monitoring of home appliances in a unified system. These include lighting, heating, and even home electronics. Home automation is closely related to (industrial) building automation where lighting, climate control (HVAC: Heating, Ventilation, and Air Conditioning), and security systems are integrated for central and/or automated control. Building automation often focuses on the automation of large commercial buildings. In contrast, home automation focuses more on comfort and entertainment, but both HVAC and security can be (and often are) part of a smart home.

There are many different types of home automation systems available. These systems are typically designed and purchased for different purposes. In fact, one of the major problems in the area is that these different systems are neither interoperable nor interconnected [2]. These systems range from simple remote controlled light switches to fully integrated and networked devices controlling all appliances in an entire building. From a technical point of view these systems can be divided into two main groups differing in complexity. Infrared remote controls, commonly used in home entertainment systems, can also be a part of a home automation system [3].

To be precise, for measuring in small devices the data rate demand is an insignificant parameter compared to e.g. the reliability or power consumption, we have decided to Study Four of the technologies for study they are [4].

- 1) *Bluetooth*
- 2) *Wi-Fi*
- 3) *Certified Wireless USB*
- 4) *ZigBee*

A. Bluetooth

Bluetooth is a wireless standard that belongs to the PAN (respectively WPAN) protocol family. It operates in the 2.4GHz band divided into 79 sub channels with 1MHz spacing, employing FHSS [5] [6]. GFSK and/or PSK modulations are used, depending on the Bluetooth version used. Full duplex transfers are realized via TDD. It is defined by the IEEE 802.15.1 standard and extended by the Bluetooth Special Interest Group [7].

- a) *Hardware Dimensions*

The smallest Bluetooth devices currently available on the market are utilizing the v2.1 EDR chips manufactured by CSR in the Blue Core series [8]. The dimensions of these chips in the WLCSP are no larger than 4x4mm (0.17x0.17in), thus they can be easily integrated e.g. into USB-A type connectors [9].

b) Memory Requirements

A disadvantage of Bluetooth usage in small medical devices is the fact that a full Bluetooth stack is too large for embedded applications [10]. Because of that, most simple applications only include a fraction of the stack in their firmware [11]. Full stack is then implemented in a device with more computational power (and usually acts as a host),

As for hardware in numbers, the latest BlueCore series chips (BlueCore6) are equipped with 6MB of ROM and 48kB of RAM (parts of the ROM are used not only for Bluetooth stack, but for audio and other libraries as well).

c) Bandwidth and Range

Both bandwidth and ranges have been extended along with the popularization of Bluetooth [12]. The latest IEEE 802.15.1-2005 specification defines Bluetooth 1.2. Bluetooth 2.0/2.1 is developed under Bluetooth SIG only. The EDR technology allows higher speeds by using PSK modulation for parts of the transmission instead of GFSK and also uses different packet structure.

d) Power Consumption

Power consumption has become an important concern of end device manufacturers recently. Bluetooth SIG responded by enhancing the feature set of new Bluetooth versions. The power consumption can be primarily lowered by adjusting network scanning and transmission parameters, which, however, sacrifices bandwidth and prolongs the link initialization [11]. An average Bluetooth chip usually drains about 50mW for both receive and transmit modes. In sleep mode (or equivalent mode, e.g. Parked state), some of the chips (e.g. CSR's BlueCore) can lower the consumption below 1mW.

e) Network Features

In basic mode, Bluetooth creates a temporary device link in a process called 'pairing' – a process of establishing point-to-point ad-hoc connection between two devices. So called 'piconet' is a network created on a temporary basis (although usually the intention is to create a permanent network) and is an extension to the point-to-point topology. Fig.1 shows the piconet and scatternet of Bluetooth. It forms a 'star' master-slave topology. To create a piconet, in the process of device pairing one device has to be elected as the network master, while other devices join the network as slaves. Master defines the physical layer parameters of the network. The maximum number of active devices in piconet is limited by the structure of Bluetooth's MAC layer to 7 slaves and one master.

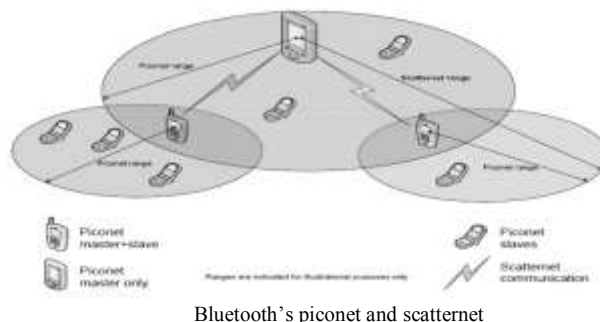


Fig.1.

Bluetooth's piconet and scatternet

f) Security and Reliability

Bluetooth offers an authentication method using 128bit key [13]. Bluetooth is more resistant to eavesdropping than other technologies, because in difference to e.g. Wi-Fi or ZigBee, the modulation it uses on the physical layer is FHSS and not DSSS, which means we need to follow the frequency hopping in order to continue receiving data [14]. Reliability is a rarely discussed attribute of Bluetooth. The technology used on physical layer makes Bluetooth slightly more likely to suffer from interferences and intentional jamming. The scatternet is also not a topology that can guarantee reliable multi-hop data transfers. Moreover, the spontaneous nature of all connections is not an attribute that benefits the reliability.

g) Costs

There are several manufacturers of Bluetooth chips available on the market. Broadcom offers the BCM2046 SoC, however, at unknown price and probably only for wholesale. Texas Instruments' portfolio contains a number of Bluetooth chips (e.g. the BlueLink series). All of them are available to 'high-volume wireless OEMs and ODMs only. The same situation repeats with Infineon. They also offer more information about their solutions than other manufacturers. Their BlueCore4 SoC and BlueCore5 SoC (Bluetooth transceivers without ROM/Flash) cost from \$3 to about \$10 / unit, depending on the range of included multimedia.

B. Wi-Fi

Wi-Fi is probably the most exploited wireless technology nowadays. It belongs to the family of (W) LAN networks, but with latest amendments it could also be belonging to the (W) MAN family. It is built on the IEEE 802.11 standard, which first version was announced in 1997 and first successful commercial standard (the 802.11b and 802.11a) was adopted in 1999.

The physical layer defines the operation frequency to 2.4GHz (802.11b/g/n) and 5GHz (802.11a/n) employing DSSS (802.11b) or OFDM (for higher speeds in 802.11a/g). In difference to Bluetooth, the Wi-Fi spectrum is divided into only 13 partly overlaying sub channels (14th available in Japan only), each occupying the band of 22MHz. At an instant moment, the 802.11a/b/g versions are always occupying only a single channel [15].

a) Hardware Dimensions

The average size of a Wi-Fi RoC (usually means Wi-Fi + Radio-MCU + Caches) is about 8x8mm. Most of the modern chips that are being introduced now are even smaller,

some of them, mostly coming in the TFBGA packaging, have the size of 5x3 mm (0.2x0x12 in). The disadvantage of Wi-Fi is its requirement of external memories and processors, which in the end means that general Wi-Fi device is much larger (scope of centimeters) than all of the other devices mentioned in this Research paper.

b) Memory Requirements

Wi-Fi is, compared to Bluetooth, WUSB and ZigBee, the most memory and computing-power demanding. Modern chips contain 400MHz RISC processors with 64KB-128KB caches, and are using external RAM and ROM in the sizes of MB. Common Wi-Fi USB dongles do not contain the Wi-Fi stack in their firmware.

c) Bandwidth and Range

The theoretical maximum for Wi-Fi range is in the units of kilometers (miles). There are working installations on the distance of above 2 km (1.2 mile) in the 5GHz band and above 1 km (0,6 miles) using a standard hardware.

Standard ranges achieved by stock antennas and standard output power are 100 m (300 feet) for outdoor (line-of-sight) range, and about 10 m (30 feet) for indoor use.

d) Power Consumption

The main purpose of Wi-Fi is to deliver enhanced data rate. The power consumption issue is in this technology not significant, and there is no main intention in the development to try to lower it. There were some attempts to create low power Wi-Fi devices, but the results are not as persuasive as e.g. Bluetooth or Zigbee can be. Broadcom has developed a chip that drains 270 mW in full speed, and calls it low power. Gainspan has developed another chip, GS1010, which is truly SoC, with radio, MCU, RAM and Flash integrated in single chip, thus lowering the final power needed. They claim that single AA battery will last years in their product [17]. In numbers, an average full speed power consumption of an 802.11g device ranges from 400mW up to 1W.

e) Network Features

Wi-Fi defines two types of networks – ad-hoc and infrastructure. In ad-hoc network, there is no master device, all devices have equal roles and all of the connections made are peer-to-peer. These are mostly used for temporary purposes. Infrastructure is a network with one (or more) master devices. These devices define the parameters of the network. Devices that join the masters and are not providing connection to the network to other devices are called slaves.

The topologies possible to form using Wi-Fi are star or tree (using multiple AP). There are also proprietary mesh network applications being developed, with the aim on metropolitan networks.

f) Security and Reliability

Wi-Fi is well known for its former weak WEP encryption. In last few years, as its popularity grew up, new security algorithms were applied in Wi-Fi. Nowadays, the security standard is defined by 802.11i. WPA2 supplies most features defined by that standard (using AES for enciphering) and

together with authentication protocols (various forms of Extensible Authentication Protocol (EAP)) it is at least for now considered secure.

g) Costs

It is difficult to obtain prices for single chips for Wi-Fi, as most of the SoCs / RoCs are currently under development, and the others are not for sale separately and wholesale prices are kept as confidential. The total price of the wireless card is far below 100\$. So, for a single chip, the price could be approximately ten of dollars.

C. Certified Wireless USB

This is the only technology that, at the moment, is not based on an actively maintained IEEE standard. Thus, there is a lot more competition in this field – various companies are using the name ‘Wireless USB’ for their products, which are, however, not compatible with other company’s ‘Wireless USB’ [16]. Due to this confusion in terminology, the largest group of industries concerned in Wireless USB development decided to call their solution ‘Certified Wireless USB’. It is officially supported by the authors of USB – the USB Implementers Forum, and names such as Microsoft, Samsung, HP, Intel, NEC, Nokia, LSI and NXP figure among companies supporting and contributing to its development.

a) Hardware Dimensions

Alereon is the main manufacturer of UWB chipsets. The company maintains a 3rd generation of Certified Wireless USB compliant chips; one of the current chips (the AL5300) can be used worldwide (bands 1, 3, 4 and 6), others only in USA (band 1 only). There is no official information on the dimensions of the chips, but according to original scale images, they come in both TFBGA and WLCSP package in the sizes of about 5x5 mm (0.2x0.2 in). Artimi delivers another SoC to the market, which, however, needs an external WiMedia compliant chip to function. It comes in 10x10 mm (0.4x0.4 in) LFBGA package [18].

b) Memory Requirements

For the host adaptors, it is assumed that a computer or other powerful computational device is present that will manage all the required calculations. For the device adaptors, the computational power correlates with the required speed of the device. Most of the manufacturers use RISC processors with tens of MHz and under 100kB of RAM and ROM [19].

c) Bandwidth and Range

As was already mentioned in the introduction, Wireless USB is supposed to replace the current wired USB, thus it offers the 480 Mbit/s maximum data. But, due to the design of physical layer, this speed can be achieved only at short (3 m (10 feet)), line-of-sight distances. For longer distances it drops rapidly, to about 110 Mbit/s at 10 m (33 feet) and even less at longer distances. The maximum range for reliable transfers is not far behind 10 m [20].

d) Power Consumption

The general power consumption of Wireless USB can be defined as lower than Wi-Fi but higher than Bluetooth. All the chip manufacturers I found were boasting with low power.

Wireless USB solutions, but only one gives exact numbers: Artimi's draining 100mW under certain circumstances when online. A-150 can run The Wireless USB devices are also able to sleep, lowering the consumption to under 5mW.

e) Network Features

Only a simple peer-to-peer star topology network is offered by Certified Wireless USB. The central device is the 'host adapter' which provides connection for 'device adapters'. The maximum number of device adapters for single host adapter is 127. They are sharing the common bandwidth through a TDMA.

f) Security and Reliability

There are several uses of encryption / authentication methods in WUSB. The standard method is AES-128 Counter with CBC-MAC. It also specifies a public key encryption, but for authentication purposes only. It has to be as strong as the CBC-MAC, so it uses RSA cipher with 3072 bit keys for encryption and SHA-256 for hashing [16]. The security architecture is also capable of wired connection detection as a form of encryption, allowing leaving out additional cryptography. Wired connections can be also used for secure initial CCM Connection Key distribution. Most of the reliability considerations were already mentioned, in general transfers within the 10 m (33 feet) range can be considered reliable, although, there is a large influence on the reliability with the presence of other wireless technologies.

g) Costs

The cost of single chip is not publicly available from any of the above-mentioned manufacturers. Nevertheless, it should not be much higher than 10\$, as the technology claims to be low-cost and also because it is trying to compete Bluetooth, which chips cost about 10\$.

D. ZigBee

ZigBee is an extension to the IEEE 802.15.4 (low-rate (W) PAN1) standard. It is focused on embedded platforms - low power consumption and very low complexity are the main concerns, as well as security and jamming resistivity. The ZigBee Alliance is an association of companies working on a standard, which would enable low-power, cost-effective, reliable, wireless communication. Its members are for example Free scale, Motorola, Texas Instruments, Honeywell, Samsung, Philips, Siemens and over hundred others. First release of the ZigBee specification was in the beginning of 2005 and the latest was released in the end of 2007.

a) Hardware dimension

The dimensions of both ZigBee SoCs and ZigBee transceivers are approximately the same, ranging from 4x4 mm (0.15x0.15 in) to about 7x7 mm (0.27x0.27 in), mostly in QFN packages. Additionally, because of a low number of external components, the final product can reach similar sizes to Bluetooth, as the only larger external part required is an antenna.

b) Memory Requirements

When compared to other technologies, memory requirements of ZigBee are the least demanding. The total required memory is based on the particular ZigBee stack you

want to use [21]. But, in global terms, 100kB of ROM and units of kilobytes of RAM should be sufficient for most of the stacks. Also the computational power is reasonable – usually RISC MCUs at frequency below 30 MHz are used.

c) Bandwidth and Range

ZigBee belongs to the low-speed WPAN network family, thus its bandwidth is limited. The maximum data rate is 250kb/s at every physical layers defined in the latest 802.15.4 standard [17]. The standard range for indoor application is about 30 m (100 feet) for indoor applications and about 100 m (300 feet) for outdoor use. The range can be also extended by using higher power, whip / external antennas, and clearing the Fresnel zone. In numbers, typical ZigBee radio uses from 30 to 50 mW for receive and about one quarter more for transmit. The sleep power is about (but mostly lower than) 0,001 mW.

d) Power down and wake up cycles

As most of the devices in the network are sleeping endpoints, the duration of a power down and wake up cycle is important factor that influences the length of battery life. Speaking about the SoCs or modules, the time required for them to wake up is mostly dependent on the software (firmware) used. E.g. a radio running only the 802.15.4 compliant software does not need to undergo the initialization process of a ZigBee stack, which can in case of very low duty cycle save valuable milliseconds [22]. This fact should be considered when deciding between ZigBee and proprietary 802.15.4 application [23]. The power down is not a computationally difficult task. Generally, the end devices can be turned down instantly at any time. Nevertheless, a timeout is usually implemented for applications that use duplex transfers [24].

e) Network Features

ZigBee networks can be established by a coordinator only [25]. Upon correct PAN parameters settings, other devices may join the network, forming one of the following topologies [26].

III. CONCLUSION AND FUTURE SCOPE

This paper covers the review of four Technologies which strongly support the Home Automation systems in Reliable way. Future scope can be defined as the comparative study of the above referred technology, this comparative study may include

- 1) *Illustrate different ways to control of a home network using standardized technologies.*
- 2) *Demonstrate the possibility of an ubiquitous access to the home network using different technologies*
- 3) *What are the possible functions and designs for home automation systems?*
- 4) *How can the Technological Method of Problem Solving be used to find solutions to everyday problems?*

REFERENCE

- [1] <http://www.automatedbuildings.com/news/aug05/articles/ibtpe/ibtpe.htm>
- [2] Stevens, Tim. "The Smart Office". ISBN 0965708101 (1994)
- [3] <http://www.answers.com/topic/office-automation>

- [4] Neng-Shiang Liang, Li-Chen Fu, Chao-Lin Wu: "An integrated, flexible, and Internet-based control architecture for home automation system in the Internet Era". IEEE 0 7803 7272 7. (2002) 1-6
- [5] Bluetooth Profile Specifications
<http://www.bluetooth.com/Bluetooth/Technology/Building/Specifications/Default.htm>
- [6] Texas Instruments Bluetooth chips BlueLink
<http://focus.ti.com/general/docs/wtbu/wtbugencontent.tsp?templateId=6123&navigationId=12019&contentId=4635>
- [7] CSR BlueCore
<http://www.csr.com/products/bcrange.htm>
- [8] Broadcom Bluetooth SoC
<http://www.broadcom.com/products/Bluetooth/Bluetooth-RF-Silicon>
- [9] CzFree Network Map <http://mapa.czfree.net/>
- [10] CSR BlueCore price list
<http://www.csr.com/products/bcrange.htm>
- [11] Infineon Bluetooth chips
<http://www.infineon.com/cms/en/product/channel.html?channel=ff80808112ab681d0112ab6aab1905bd>
- [12] lwBT – Lightweight Bluetooth Stack
<http://www.sm.luth.se/~conny/lwbt/>
- [13] Setrag Khoshafian; A. Brad Baker; Razmik Abnous, and Kevin Shepherd. "Intelligent Buildings". ISBN: 8428321043 (1994)
- [14] IEEE Task Group 802.15.3 802.15.3-2003 Draft
<http://standards.ieee.org/getieee802/download/802.15.3-2003.pdf>
- [15] Gainspan's low power Wi-Fi solution product brief
http://www.gainspan.com/Docs/GS1010_SoC_Product_Brief.pdf
- [16] Alereon – Wireless USB Chipsets manufacturer
<http://www.alereon.com>
- [17] ZigBee Specification 2007 by ZigBee Alliance
http://www.zigbee.org/en/spec_download/download_request.asp
- [18] NXP – another Wireless USB Chip manufacturer
<http://www.nxp.com/>
- [19] Artimi – another Wireless USB Chips manufacturer <http://artimi.com>
- [20] Wisair – another Wireless USB Chip manufacturer
<http://www.wisair.com>
- [21] ZigBee Alliance, ZigBee Specification, December 1, 2006, [online]. Available: www.zigbee.org
- [22] IEEE: IEEE Std 802.15.4™-2003, [online]. Available: <http://standards.ieee.org>
- [23] ZigBee Alliance Official Site, [online]. Available: www.zigbee.org
- [24] Clendenin, M. ZigBee's improved spec incompatible with v1.0, EE Times Europe, [online].
- [25] IEEE 802.15.1-2005 - Standard for Information technology
- [26] Brent Ivie, Lovell; Gilstrap, Daniel. "Automated appliance control system". USP 5815086. (Sep 1998)

AUTHORS PROFILE



Ashish J. Ingle has earned his M.sc Degree in Information Technology and M.B.A Degree in Human Resource and Development both from Dr B.A.M University Aurangabad, India. Recently he is pursuing his M.Tech (By Research) Degree in Computer Science and Engineering specialized in embedded system designing from Department of Computer Science and Information

Technology, Dr B.A.M University Aurangabad, India under the guidance of Bharti W. Gawali. His Areas of Interest are Embedded System, Wireless Communication, Satellite Technology and VLSI Designing. Complying with his Interest Areas He has contributed Fifteen Research Papers/Articles in International/National Conference Proceedings.



Bharti W. Gawali has received her M.sc, PhD in Computer Science from Dr B.A.M University Aurangabad, India. Presently she is affiliated with Department of Computer Science and Information Technology, Dr B.A.M University Aurangabad, India as Associate Professor she has around Thirteen Years of Teaching and Research Experience. Her Areas of Interest are (Not Limited to) Image Processing, Speech

Recognition, Computer networks, Microprocessor and interfacing, Software Testing. She has contributed number of Research Paper /Articles in Refereed Journals and Conference Proceedings. She is Recognised Guide of Dr B.A.M University Aurangabad, India for M.sc (Information Technology), M.sc (Computer Science), M.Phil (Computer Science) and M.Tech (By Research) in Computer Science and Engineering.

A Comparative Study Of Wireless Technologies Used For Designing Home Automations System

Ashish J. Ingle, Bharti W. Gawali

Department of Computer Science and Information Technology
Dr. Babasaheb Ambedkar Marathwada University,
Aurangabad, India.

Abstract- Bluetooth (over IEEE 802.15.1), ultra-wideband (UWB, over IEEE 802.15.3), ZigBee (over IEEE 802.15.4), and Wi-Fi (over IEEE 802.11) are four protocol standards for short-range wireless communications with low power consumption. From an application point of view, Bluetooth is intended for a cordless mouse, keyboard, and hands-free headset, UWB is oriented to high-bandwidth multimedia links. ZigBee is designed for reliable wirelessly networked monitoring and control networks, while Wi-Fi is directed at computer-to-computer connections as an extension or substitution of cabled networks. In this paper, we provide a study of these popular wireless communication standards, evaluating their main features and behaviors in terms of various metrics, including the transmission time, data coding efficiency, complexity, and power consumption. It is believed that the comparison presented in this paper would benefit application engineers in selecting an appropriate protocol.

Keywords – Automation; Technology; Reliable.

I. INTRODUCTION

In the past decades, factory automation has been developed worldwide into a very attractive research area. It incorporates different modern disciplines including communication, information, computer, control, sensor, and actuator engineering in an integrated way, leading to new solutions, better performance and complete systems. One of the increasingly important components in factory automation is the industrial communication [1]. For interconnection purposes, a factory automation system can be combined with various sensors, controllers, and heterogeneous machines using a common message specification. Many different network types have been promoted for use on a shop floor, including control area network (CAN), Process fieldbus (Profibus), Modbus, and so on. However, how to select a suitable network standard for a particular application is a critical issue to the industrial engineers. Lain et al. [2] evaluated the Ethernet (carrier sense multiple access with collision detection, CSMA/CD bus), Control Net (token-passing bus), and Device Net (CSMA with arbitration on message priority, CSMA/AMP bus) for networked control applications. After a detailed discussion of the medium access control (MAC) sub layer protocol for each network, they studied the key parameters of the corresponding network when used in a control situation, including network utilization and time delays.

On the other hand, for accessing networks and services without cables, wireless communications is a fast-growing technology to provide the flexibility and mobility [3]. Obviously, reducing the cable restriction is one of the benefits of wireless with respect to cabled devices. Other benefits include the dynamic network formation, low cost, and easy deployment. General speaking, the short-range wireless scene is currently held by four protocols: the Bluetooth, and UWB, ZigBee, and Wi-Fi, which are corresponding to the IEEE 802.15.1, 802.15.3, 802.15.4, and 802.11a/b/g standards, respectively. IEEE defines the physical (PHY) and MAC layers for wireless communications over an action range around 10-100 meters. For Bluetooth and Wi-Fi, Ferro and Potorti [4] compared their main features and behaviors in terms of various metrics, including capacity, network topology, security, quality of service support, and power consumption. In [5], Wang et al. compared the MAC of IEEE 802.11e and IEEE 802.15.3. Their results showed that the throughput difference between them is quite small. In addition, the power management of 802.15.3 is easier than that of 802.11e. For ZigBee and Bluetooth, Baker [6] studied their strengths and weaknesses for industrial applications, and claimed that ZigBee over 802.15.4 protocol can meet a wider variety of real industrial needs than Bluetooth due to its long-term battery operation, greater useful range, flexibility in a number of dimensions, and reliability of the mesh networking architecture. In this paper, after an overview of the mentioned four short-range wireless protocols, we attempt to make a preliminary comparison of them and then specifically study their transmission time, data coding efficiency, protocol complexity, and power consumption. The rest of this paper is organized as follows. Section 2 briefly introduces the wireless protocols including Bluetooth, UWB, ZigBee, and Wi-Fi. Next, a comprehensive evaluation of them is described in Section 3. Then, in Section 4, the complexity and power consumption are compared based on IEEE standards and commercial off-the-shelf wireless products, respectively. Finally, Section 5 concludes this paper.

II. WIRELESS PROTOCOLS

This section introduces the Bluetooth, UWB, ZigBee, and Wi-Fi protocols, which corresponds to the IEEE 802.15.1, 802.15.3, 802.15.4, and 802.11a/b/g standards, respectively. The IEEE defines only the PHY and MAC layers in its standards. For each protocol, separate alliances of companies worked to develop specifications covering the network, security and application profile layers so that the commercial potential of the standards could be realized.

The material presented in this section is widely available in the literature. Hence, the major goal of this paper is not to contribute to research in the area of wireless standards, but to present a comparison of the four main short-range wireless networks.

A. Bluetooth over IEEE 802.15.1

Bluetooth, also known as the IEEE 802.15.1 standard is based on a wireless radio system designed for short-range and cheap devices to replace cables for computer peripherals, such as mice, keyboards, joysticks, and printers. This range of applications is known as wireless personal area network (WPAN). Two connectivity topologies are defined in Bluetooth: the piconet and scatternet. A piconet is a WPAN formed by a Bluetooth device serving as a master in the piconet and one or more Bluetooth devices serving as slaves. A frequency-hopping channel based on the address of the master defines search piconet. All devices participating in communications in a given piconet are synchronized using the clock of the master. Slaves communicate only with their master in a point-to-point fashion under the control of the master. The master's transmissions may be either point-to-point or point-to-multipoint. Also, besides in an active mode, a slave device can be in the parked or standby modes so as to reduce power consumptions. A scatternet is a collection of operational Bluetooth piconets overlapping in time and space. Two piconets can be connected to form a scatternet. A Bluetooth device may participate in several piconets at the same time, thus allowing for the possibility that information could flow beyond the coverage area of the single piconet. A device in a scatternet could be a slave in several piconets, but master in only one of them.

B. UWB over IEEE 802.15.3

UWB has recently attracted much attention as an indoor short-range high-speed wireless communication. [7]. One of the most exciting characteristics of UWB is that its bandwidth is over 110 Mbps (up to 480 Mbps) which can satisfy most of the multimedia applications such as audio and video delivery in home networking and it can also act as a wireless cable replacement of high speed serial bus such as USB 2.0 and IEEE 1394. Following the United States and the Federal Communications Commission (FCC) frequency allocation for UWB in February 2002, the Electronic Communications Committee (ECC TG3) is progressing in the elaboration of a regulation for the UWB technology in Europe. From an implementation point of view, several solutions have been developed in order to use the UWB technology in compliance with the FCC's regulatory requirements. Among the existing PHY solutions, in IEEE 802.15 Task Group 3a (TG3a), multi-band orthogonal frequency-division multiplexing (MB-OFDM), a carrier-based system dividing UWB bandwidth to sub-bands, and direct-sequence UWB (DS-UWB), an impulse-based system that multiplies an input bit with the spreading code and transmits the data by modulating the element of the symbol with a short pulse have been proposed by the WiMedia Alliance and the UWB Forum, respectively. The TG3a was established in January 2003 to define an alternative PHY layer of 802.15.3. However, after three years of a jammed process in IEEE 802.15.3a, supporters of both proposals, MB-OFDM and DS-UWB, supported the

shutdown of the IEEE 802.15.3a task group without conclusion in January 2006. On the other hand, IEEE 802.15.3b, the amendment to the 802.15.3 MAC sub layer has been approved and released in March 2006.

C. ZigBee over IEEE 802.15.4

ZigBee over IEEE 802.15.4 defines specifications for low-rate WPAN (LR-WPAN) for supporting simple devices that consume minimal power and typically operate in the personal operating space (POS) of 10m. ZigBee provides self-organized, multi-hop, and reliable mesh networking with long battery lifetime [8] [9]. Two different device types can participate in an LR-WPAN network: a full-function device (FFD) and a reduced-function device (RFD). The FFD can operate in three modes serving as a PAN coordinator, a coordinator, or a device. An FFD can talk to RFDs or other FFDs, while an RFD can talk only to an FFD. An RFD is intended for applications that are extremely simple, such as a light switch or a passive infrared sensor. They do not have the need to send large amounts of data and may only associate with a single FFD at a time. Consequently, the RFD can be implemented using minimal resources and memory capacity. After an FFD is activated for the first time, it may establish its own network and become the PAN coordinator. All star networks operate independently from all other star networks currently in operation. This is achieved by choosing a PAN identifier, which is not currently used by any other network within the radio sphere of influence. Once the PAN identifier is chosen, the PAN coordinator can allow other devices to join its network. An RFD may connect to a cluster tree network as a leave node at the end of a branch, because it may only associate with one FFD at a time. Any of the FFDs may act as a coordinator and provide synchronization services to other devices or other coordinators. Only one of these coordinators can be the overall PAN coordinator, which may have greater computational resources than any other device in the PAN.

D. Wi-Fi over IEEE 802.11a/b/g

Wireless fidelity (Wi-Fi) includes IEEE 802.11a/b/g standards for wireless local area networks (WLAN). It allows users to surf the Internet at broadband speeds when connected to an access point (AP) or in ad hoc mode. The IEEE 802.11 architecture consists of several components that interact to provide a wireless LAN that supports station mobility transparently to upper layers. The basic cell of an IEEE 802.11 LAN is called a basic service set (BSS), which is a set of mobile or fixed stations. If a station moves out of its BSS, it can no longer directly communicate with other members of the BSS. Based on the BSS, IEEE 802.11 employs the independent basic service set (IBSS) and extended service set (ESS) network configurations. As shown in Fig. 1, the IBSS operation is possible when IEEE 802.11 stations are able to communicate directly without any AP. Because this type of IEEE 802.11 LAN is often formed without pre-planning, for only as long as the LAN is needed, this type of operation is often referred to as an ad hoc network. Instead of existing independently, a BSS may also form a component of an extended form of network that is built with multiple BSSs. The architectural component used to interconnect BSSs is the

distribution system (DS). The DS with APs allow IEEE 802.11 to create an ESS network of arbitrary size and complexity. This type of operation is often referred to as an infrastructure network

III. COMPARATIVE STUDY

Each protocol is based on an IEEE standard obviously UWB and Wi-Fi provide a higher data rate, while Bluetooth and ZigBee give a lower one. In general, the Bluetooth, UWB, and ZigBee are intended for WPAN communication (about 10m), while Wi-Fi is oriented to WLAN (about 100m). However, ZigBee can also reach 100m in some applications. FCC power spectral density emission limit for UWB emitters operating in the UWB band is -41.3 dBm/Mhz. This is the same limit that applies to unintentional emitters in the UWB band, the so called Part 15 limit. The nominal transmission power is 0 dBm for both Bluetooth and ZigBee, and 20 dBm for Wi-Fi.

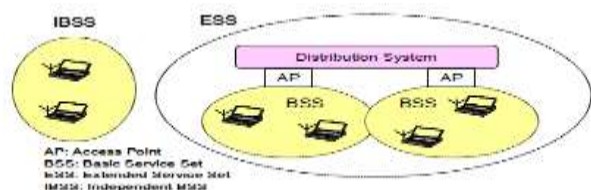


Fig. 1. IBSS and ESS configurations of Wi-Fi networks.

A. Radio Channels

Bluetooth, ZigBee and Wi-Fi protocols have spread spectrum techniques in the 2.4 GHz band, which is unlicensed in most countries and known as the industrial, scientific, and medical (ISM) band. Bluetooth uses frequency hopping (FHSS) with 79 channels and 1 MHz bandwidth, while ZigBee uses direct sequence spread spectrum (DSSS) with 16 channels and 2 MHz bandwidth. Wi-Fi uses DSSS (802.11), complementary code keying (CCK, 802.11b), or OFDM modulation (802.11a/g) with 14 RF channels (11 available in US, 13 in Europe, and just 1 in Japan) and 22 MHz bandwidth. UWB uses the 3.1-10.6 GHz, with an unapproved and jammed 802.15.3a standard, of which two spreading techniques, DS-UWB and MB-OFDM, are available.

B. Coexistence Mechanism

Since Bluetooth, ZigBee and Wi-Fi use the 2.4 GHz band, the coexistence issue must be dealt with. Basically, Bluetooth and UWB provide adaptive frequency hopping to avoid channel collision, while ZigBee and Wi-Fi use dynamic frequency selection and transmission power control. IEEE 802.15.2 discussed the interference problem of Bluetooth and Wi-Fi. Also, Sikora and Groza [10] provided quantitative measurements of the coexistence issue for ZigBee, Bluetooth, Wi-Fi, and microwave ovens. Shuaib et al. [11] focused on quantifying potential interferences between Zigbee and IEEE 802.11g by examining the impact on the throughput performance of IEEE 802.11g and Zigbee devices when coexisting within a particular environment. Moreover, Neelakanta and Dighe [12] presented a performance evaluation of Bluetooth and ZigBee collocated on an industrial floor for robust factory wireless communications.

C. Network Size

The maximum number of devices belonging to the network's building cell is 8 (7 slaves plus one master) for a Bluetooth and UWB piconet, over 65000 for a ZigBee star network, and 2007 for a structured Wi-Fi BSS. All the protocols have a provision for more complex network structures built from the respective basic cells: the scatternet for Bluetooth, peer-to-peer for UWB, cluster tree or mesh networks for ZigBee, and the ESS for Wi-Fi.

D. Security

All the four protocols have the encryption and authentication mechanisms. Bluetooth uses the E0 stream cipher and shared secret with 16-bit cyclic redundancy check (CRC), while UWB and ZigBee adopt the advanced encryption standard (AES) block cipher with counter mode (CTR) and cipher block chaining message authentication code (CBC-MAC), also known as CTR with CBC-MAC (CCM), with 32-bit and 16-bit CRC, respectively.

In 802.11, Wi-Fi uses the RC4 stream cipher for encryption and the CRC-32 checksum for integrity. However, several serious weaknesses were identified by cryptanalysts, any wired equivalent privacy (WEP) key can be cracked with readily available software in two minutes or less, and thus WEP was superseded by Wi-Fi protected access 2 (WPA2), i.e. IEEE 802.11i standard, of which the AES block cipher and CCM are also employed.

E. Transmission Time

The transmission time depends on the data rate, the message size, and the distance between two nodes. The formula for transmission time (μ s) can be described as:

$$T_{tx} = (N_{data} + (N_{data} / N_{maxPld} \times N_{ovhd})) \times T_{bit} + T_{prop} \quad (1)$$

Where N_{data} is the data size, N_{maxPld} is the maximum payload size, N_{ovhd} is the overhead size, T_{bit} is the bit time, and T_{prop} is the propagation time between any two devices. For simplicity, the propagation time is negligible in this paper. The typical parameters of the four wireless protocols used for transmission time evaluation are listed in Table II. Note that the maximum data rate 110 Mbit/s of UWB is adopted from an unapproved 802.15.3a standard. As shown in Fig. 2, the transmission time for the ZigBee is longer than the others because of the lower data rate (250 Kbit/s), while UWB requires less transmission time compared with the others. Obviously, the result also shows the required transmission time is proportional to the data payload size and disproportional to the maximum data rate.

TABLE I. TYPICAL SYSTEM PARAMETERS OF THE WIRELESS PROTOCOLS

Standard	Bluetooth	UWB	ZigBee	Wi-Fi
IEEE Spec.	802.15.1	802.15.3	802.15.4	802.11a/b/g
Max data rate (Mbit/s)	0.72	110*	0.25	54
Bit time (μ s)	1.39	0.009	4	0.0185
Max data payload (bytes)	339 (DH5)	2044	102	2312

Max overhead (bytes)	158/8	42	31	58
Coding efficiency (%)	94.41	97.94	76.52	97.18
* Unapproved 802.15.3a.	+ Where the data is 10K bytes			

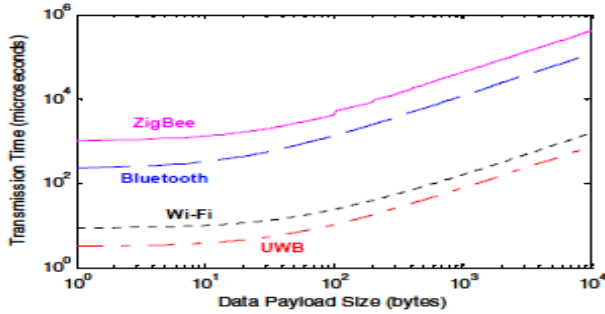


Fig. 2. Comparison of the transmission time versus the data size.

F. Data Coding Efficiency

In this paper, the data coding efficiency is defined by the ratio of the data size and the message size (i.e. the total number of bytes used to transmit the data). The formula for data coding efficiency (%) can be described as:

$$P_{\text{codEff}} = N_{\text{data}} / (N_{\text{data}} + (N_{\text{data}} / N_{\text{maxPld}} \times N_{\text{ovhd}})) \quad (2)$$

The parameters listed in Table I are also used for the coding efficiency comparison. Fig. 3 shows the data coding efficiency of the four wireless networks versus the data size. For small data sizes (around smaller than 339 bytes), Bluetooth is the best solution. Also, ZigBee have a good efficiency for data size smaller than 102 bytes. For large data sizes, Bluetooth, UWB, and Wi-Fi have much better efficiency of over 94%, as compared to the 76.52% of ZigBee (where the data is 10K bytes as listed in Table II). The discontinuities in Fig. 2 and 3 are caused by data fragmentation, i.e. the maximum data payload, which is 339, 2044, 102, and 2312 bytes for Bluetooth, Bee, and Wi-Fi, respectively. In a Wi-Fi infrastructure mode, note that most APs connect to existing networks with Ethernet, and therefore limit the payload size to the maximum Ethernet payload size as 1500 bytes. However, for a general comparison, an ad-hoc mode is assumed and the 2312 bytes is adopted in this paper.

For a wireless sensor network in factory automation systems, since most data size of industrial monitoring and control are generally small, (e.g. the temperature data in an environmental monitoring may required less than 4 bytes only), Bluetooth and ZigBee protocols may be a good selection (from a data coding efficiency point of view) in spite of their slow data rate.

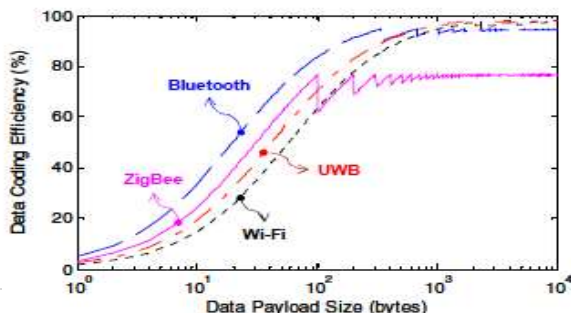


Fig. 3. Comparison of the data coding efficiency versus the data size.

In this section, an evaluation of the Bluetooth, UWB, ZigBee, and Wi-Fi on different aspects is provided. It is important to notice that several slight differences exist in the available sources. For example, in the IEEE 802.15.4 standard, the action range is about 10m, while it is 70-300m in the released documents from ZigBee Alliance. Thus, this paper intends to provide information only, since other factors, such as receiver sensitivity and interference, play a major role in affecting the performance in realistic implementations.

IV. PROTOCOL COMPLEXITY AND POWER CONSUMPTION

A. Protocol Complexity

In this paper, the complexity of each protocol is compared based on the numbers of primitives and events. Table II shows the number of primitives and host controller interface (HCI) events for Bluetooth, and the numbers of MAC/PHY primitives for UWB, ZigBee, and Wi-Fi protocols. In the MAC/PHY layers, the Bluetooth primitives include client service access point (SAP), HCI SAP, synchronous connection-oriented (SCO) SAP, and logical link control and adaptation protocol (L2CAP) primitives.

As shown in Fig. 4, the Bluetooth is the most complicated protocol with 188 primitives and events in total. On the other hand, ZigBee is the simplest one with only 48 primitives defined in 802.15.4. This total number of primitives is only about one fourth the number of primitives and events defined in Bluetooth. As compared with the Bluetooth, UWB, and Wi-Fi, the simplicity makes ZigBee very suitable for sensor networking applications due to their limited memory and computational capacity.

TABLE II. NUMBER OF PRIMITIVES AND EVENTS FOR EACH PROTOCOL

Standard	Bluetooth	UWB	ZigBee	Wi-Fi	Standard
IEEE Spec.	802.15.1	802.15.3	802.15.4	802.11a/b/g	IEEE Spec.
Primitives	151	77*	35	32	MAC primitives
HCI events	37	29	13	43	PHY primitives
					* Approved 802.15.3b.

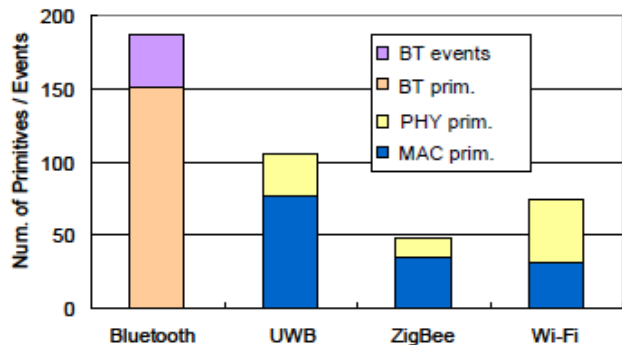


Fig. 4. Comparison of the complexity for each protocol.

B. Power Consumption

Bluetooth and ZigBee are intended for portable products, short ranges, and limited battery power. Consequently, it offers very low power consumption and, in some cases, will not measurably affect battery life. UWB is proposed for short-range and high data rate applications. On the other hand, Wi-Fi is designed for a longer connection and supports devices with a substantial power supply. In order to practically compare the power consumption, four wireless products for which detailed characteristics are publicly available are briefly presented as an example, including BlueCore2 [13] from Cambridge Silicon Radio (CSR), XS110 [14] from Freescale, CC2430 [15] from Chipcon of Texas Instruments (TI), and CX53111 [16] from Conexant (previous Intersil's Prism). The current consumptions of the transmit (TX) and receive (RX) conditions for each protocol are shown in Table IV. The data shown are for particular products, although are broadly representative for examples of the same type. Fig. 5 indicates the power consumption in mW unit for each protocol. Obviously, the Bluetooth and ZigBee protocols consume less power as compared with UWB and Wi-Fi. Based on the bit rate, a comparison of normalized energy consumption is provided in Fig. 6. From the mJ/Mb unit point of view, the UWB and Wi-Fi have better efficiency in energy consumption.

In summary, Bluetooth and ZigBee are suitable for low data rate applications with limited battery power (such as mobile devices and battery-operated sensor networks), due to their low power consumption leading to a long lifetime. On the other hand, for high data rate implementations (such as audio/video surveillance systems), UWB and Wi-Fi would be better solutions because of their low normalized energy consumption.

TABLE III. CURRENT CONSUMPTION OF CHIPSETS FOR EACH PROTOCOL

Standard	Bluetooth	UWB	ZigBee	Wi-Fi
Chipset	BlueCore2	XS110	CC2430	CX53111
VDD (volt)	1.8	3.3	3.0	3.3
TX (mA)	57	~227.3	24.7	219
RX (mA)	47	~227.3	27	215
Bit rate (Mb/s)	0.72	114	0.25	54

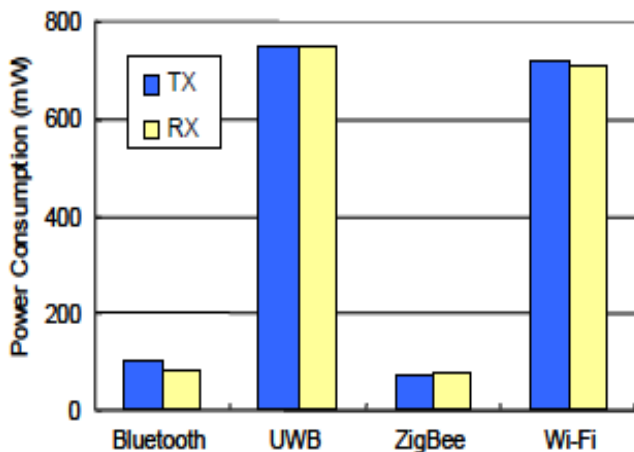


Fig. 5. Comparison of the power consumption for each protocol.

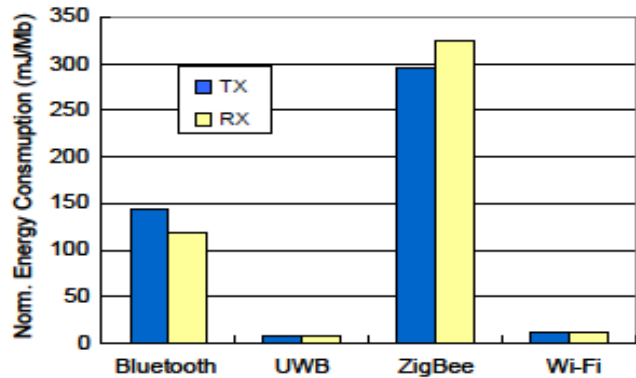


Fig. 6. Comparison of the normalized energy consumption for each protocol.

V. CONCLUSION

This paper has presented a broad overview of the four most popular wireless standards, Bluetooth, UWB, ZigBee, and Wi-Fi with a quantitative evaluation in terms of the transmission time, data coding efficiency, protocol complexity, and power consumption. Furthermore, the radio channels, coexistence mechanism, network size, and security are also preliminary compared. This paper is not to draw any conclusion regarding which one is superior since the suitability of network protocols is greatly influenced by practical applications, of which many other factors such as the network reliability, roaming capability, recovery mechanism, chipset price, and installation cost need to be considered in the future.

REFERENCE

- [1] R. Zurawski, "Guest editorial of special section on factory communication systems," IEEE Trans. Ind. Electron., vol. 49, no. 6, pp. 1186-1188, Dec. 2002.
- [2] F. L. Lian, J. R. Moyne, and D. M. Tilbury, "Performance evaluation of control networks: Ethernet, ControlNet, and DeviceNet," IEEE Contr. Syst. Mag. vol. 22, no. 1, pp. 66-83, Feb. 2001.
- [3] A. Willig, "An architecture for wireless extension of Profibus," in Proc. IEEE Int. Conf. Ind. Electron. (IECON'03), Roanoke, VA, Nov. 2003, pp. 2369-2375.
- [4] E. Ferro and F. Potorti, "Bluetooth and Wi-Fi wireless protocols: A survey and a comparison," IEEE Wireless Commun., vol. 12, no. 1, pp. 12-16, Feb. 2005.
- [5] X. Wang, Y. Ren, J. Zhao, Z. Guo, and R. Yao, "Comparison of IEEE 802.11e and IEEE 802.15.3 MAC," in Proc. IEEE CAS Symp. Emerging Technologies: Mobile & Wireless Commun, Shanghai, China, May, 2004, pp. 675-680.
- [6] Baker, N. "ZigBee and Bluetooth: Strengths and weaknesses for industrial applications," IEE Computing & Control Engineering, vol. 16, no. 2, pp 20-25, April/May 2005.
- [7] D. Porcino and W. Hirt, "Ultra-wideband radio technology: Potential and challenges ahead," IEEE Commun. Mag., vol. 41, no. 7, pp. 66-74, July 2003.

- [8] J. S. Lee, "Performance evaluation of IEEE 802.15.4 for low-rate wireless personal area networks," IEEE Trans. Consumer Electron., vol.52, no. 3, pp. 742-749, Aug. 2006.
- [9] J. S. Lee and Y. C. Huang, "ITRI ZBnode: A ZigBee/IEEE 802.15.4 platform for wireless sensor networks," in Proc. IEEE Int. Conf. Systems, Man & Cybernetics, Taipei, Taiwan, Oct. 2006, pp. 1462-1467.
- [10] A. Sikora and V. F. Groza, "Coexistence of IEEE802.15.4 with other systems in the 2.4 GHz-ISM-Band," in Proc. IEEE Instrumentation & Measurement Technology Conference, Ottawa, May 2005, pp.1786-1791.
- [11] K. Shuaib, M. Boulmalf, F. Sallabi, and A. Lakas, "Co-existence of Zigbee and WLAN: A performance study," in Proc. IEEE/IFIP Int. Conf. Wireless & Optical Communications Networks, Bangalore, India, April 2006.
- [12] P. S. Neelakanta and H. Dighe, "Robust factory wireless communications: A performance appraisal of the Bluetooth and the ZigBee collocated on an industrial floor," in Proc. IEEE Int. Conf. Ind. Electron. (IECON'03), Roanoke, VA, Nov. 2003, pp. 2381-2386.
- [13] Cambridge Silicon Radio, BlueCore2-External Product Data Sheet. Cambridge, UK, Aug. 2006.
- [14] Freescale, XS110 UWB Solution for Media-Rich Wireless Applications. San Diego, CA, Dec. 2004.
- [15] Chipcon, CC2430 Preliminary Data Sheet (rev. 1.03). Oslo, Norway, 2006.
- [16] Conexant, Single-Chip WLAN Radio CX53111. Newport Beach, CA, 2006.

AUTHORS PROFILE



Ashish J. Ingle has earned his M.sc Degree in Information Technology and M.B.A Degree in Human Resource and Development both from Dr B.A.M University Aurangabad, India. Recently he is pursuing his M.Tech (By Research) Degree in Computer Science and Engineering specialized in Embedded system designing from Department of Computer Science and Information Technology, Dr B.A.M University Aurangabad, India under the guidance of Bharti W. Gawali. His Areas of Interest are Embedded System, Wireless Communication, Satellite Technology and VLSI Designing. Complying with his Interest Areas He has contributed Fifteen Research Papers/Articles in International /National Conference Proceedings.



Bharti W. Gawali has received her M.sc, PhD in Computer Science from Dr B.A.M University Aurangabad, India. Presently she is affiliated with Department of Computer Science and Information Technology, Dr B.A.M University Aurangabad, India as Associate Professor she has around Thirteen Years of Teaching and Research Experience. Her Areas of Interest are (Not Limited to) Image Processing, Speech Recognition, Computer networks, Microprocessor and interfacing, Software Testing. She has contributed number of Research Paper /Articles in Refereed Journals and Conference Proceedings. She is Recognised Guide of Dr B.A.M University Aurangabad, India for M.sc (Information Technology), M.sc (Computer Science), M.Phil (Computer Science) and M.Tech (By Research) in Computer Science and Engineering.

Image Compression Techniques Using Modified high quality Multi wavelets

M.Ashok
Assoc.Professor,
S.S.J.EC

Dr.T.BhaskaraReddy
Assoc.Professor,
S.K.University-ATP

Abstract— over the past decade, the success of wavelets in solving many different problems has contributed to its unprecedented popularity. For best performance in image compression, wavelet transforms require filters that combine a number of desirable properties, such as orthogonality and symmetry. Advances in wavelet transforms and quantization methods have produced algorithms capable of surpassing the existing image compression standards like the Joint Photographic Experts Group (JPEG) algorithm. For best performance in image compression, wavelet transforms require filters that combine a number of desirable properties, such as orthogonality and symmetry. This paper presents new multi wavelet transform and quantization methods and introduces multi wavelet packets. Extensive experimental results demonstrate that our techniques exhibit performance equal to, or in several cases superior to, the current wavelet filters.

Keywords- Multi wavelets; DWT; Image coding; Quantizers; ANN.

I. INTRODUCTION

Digital Image Processing is defined as analyzing and manipulating images. Image Compression has become the most recent emerging trend throughout the world. Some of the common advantages image compressions over the internet are reduction in time of webpage uploading and downloading and lesser storage space in terms of bandwidth. Compressed images also make it possible to view more images in a shorter period of time [7]. Image compression is essential where images need to be stored, transmitted or viewed quickly and efficiently. The benefits can be classified under two ways as follows: First, even uncompressed raw images can be stored and transmitted easily. Secondly, compression provides better resources for transmission and storage. Image compression is the representation of image in a digitized form with a few bits maintenance only allowing acceptable level of image quality. Compression addresses the problem of reducing the amount of data required to represent a digital image. A good compression scheme is always composed of many compression methods namely wavelet transformation, predicative coding, and vector quantization and so on.

Wavelet transformation is an essential coding technique for both spatial and frequency domains, where it is used to divide the information of an image into approximation and detail sub signals [8]. Artificial Neural Networks (ANN) is also used for image compression. It is a system where many algorithms are used. The ANN is viewed as a graph with various nodes namely source, sink and internal [9]. The input

node exists in the input layer and output node exists in the output layer whereas hidden nodes exist in one or more hidden layers.

In ANN various learning method are used namely Unsupervised, Reinforcement learning and Back propagation. Counter Propagation Neural Network (CPN) has become popular since it converges faster. A level of advancement in CPN is forward only Counter Propagation (FOCPN), where correlation based technique is used [10], [11],[12]. Modified forward only Counter Propagation (MFOCPN) is proposed where distance metrics are used to find the winner among the hidden layers neurons [13].

II. DISCRETE WAVELET TRANSFORM

Wavelet analysis is based on a decomposition of a signal using an orthonormal family of basic functions [2]. Wavelets are well suited for the analysis of transient and time-varying signals [3]. The wavelet transform has been developed as an alternate approach to Short Time Fourier transform to overcome the resolution problem. The wavelets transform is computed separately for different segments of the time-domain signal at different frequencies. This approach is called Multi resolution analysis (MRA) [4], as it analyzes the signal at different frequencies giving different resolutions. The basic set of wavelets is generated from the mother or basic wavelet is defined as

$$\psi_{a,b}(t) = \frac{1}{\sqrt{|a|}} \psi\left(\frac{t-b}{a}\right)$$

Where $a, b \in \mathbb{R}^1$ and $a > 0$ The variable ‘ a ’ (inverse of frequency) reflects the scale (width) of a particular basis function such that its large value gives low frequencies and small value gives high frequencies. The variable ‘ b ’ specifies its translation along x-axis in time. The term $1/a$ is used for normalization [5]. The discrete wavelet transform utilizes two main functions which are scaling and wavelet functions for the multi resolution analysis. The coefficients obtained from scaling and wavelet functions are known as approximate and detail coefficients respectively. The approximate coefficients are low frequency components which are having more significant values than detail coefficients [6]. The scaling and

wavelet functions are given as follows

$$W_\phi(j_0, k) = \frac{1}{\sqrt{M}} \sum_x f(x) \phi_{j_0, k}(x)$$

$$W_\psi(j, k) = \frac{1}{\sqrt{M}} \sum_x f(x) \psi_{j, k}(x)$$

A. Multi wavelet Transform

Dyadic wavelet decomposition is achieved by iterative two-channel perfect reconstruction filter bank operations over the low frequency band at each level. This leads to a full tree decomposition as depicted in Figure 1. The final decomposition structure will be a subset of that full tree, chosen by the best basis selection algorithm. Multi wavelets provide one alternative to the wavelet transform. Despite its general success, the wavelet transform often fails to accurately capture high frequency information, especially at low bit rates where such information is lost in quantization noise.

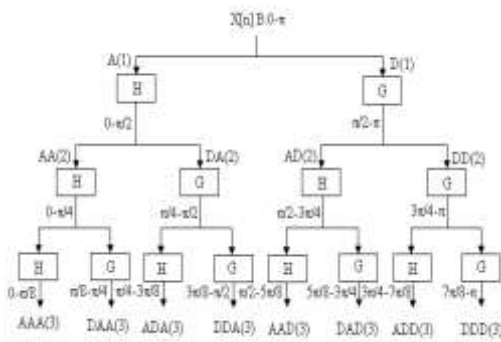


Fig 1: Full tree decomposition for Multi wavelet Transform

A multilevel wavelet filter bank involves iterating the low pass–high pass filtering and down sampling procedure only on the output of the low pass branch of the previous stage. formulated an extension of the octave-band wavelet decomposition to full tree decomposition by allowing the low pass–high pass filtering and down sampling procedure to be iterated also on high pass (band pass) branches in the tree [6].

B. Motivation for Multi wavelets

Algorithms based on scalar wavelets have been shown to work quite well in image compression. Consequently, there must be some justification to use multi wavelets in place of scalar wavelets. Some reasons for potentially choosing multi wavelets are summarized below [1]: The extra degrees of freedom inherent in multi wavelets can be used to reduce the restrictions on the filter properties.

For example, it is well known that a scalar wavelet cannot simultaneously have both orthogonality and symmetric property. Symmetric filters are necessary for symmetric signal extension, while orthogonality makes the transform easier to design and implement. Also, the support length and vanishing moments are directly linked to the filter length for scalar wavelets. This means longer filter lengths are required to achieve higher order of approximation at the expense of increasing the wavelet’s interval of support.

A higher order of approximation is desired for better coding gain, but shorter support is generally preferred to achieve a better localized approximation of the input function. In contrast to the limitations of scalar wavelets, multi wavelets are able to possess the best of all these properties simultaneously. One desirable feature of any transform used in image compression is the amount of energy compaction achieved.

A filter with good energy compaction properties can decorrelate a fairly uniform input signal into a small number of scaling coefficients containing most of the energy and a large number of sparse wavelet coefficients [13]. This becomes important during the quantization since the wavelet coefficients are represented with significantly fewer bits on average than the scaling coefficients. Therefore better performance is obtained when the wavelet coefficients have values clustered about zero with little variance, to avoid as much quantization noise as possible.

III. ITERATION OF DECOMPOSITION IN MULTI WAVELET TRANSFORM

Since multi wavelet decompositions produce two low pass sub bands and two high pass sub bands in each dimension, the organization and statistics of multi wavelet sub bands differ from the scalar wavelet case. During a single level of decomposition using scalar wavelet transform, the 2-D image data is replaced with four blocks corresponding to the sub bands representing either low pass or high pass in both dimensions. These sub bands are illustrated in Figure 3-a.

The data in sub band ‘LH’ was obtained from high pass filtering of the rows and then by low pass filtering of the columns. The multi wavelets used here have two channels, so there will be two sets of scaling coefficients and two sets of wavelet coefficients. The multi wavelet decomposition sub bands are shown in Figure 3-b.

For multi wavelets, the L and H labels have subscripts denoting the channel to which the data corresponds. For example, the sub band labeled L1H2 corresponds to data from the second channel high pass filter in the horizontal direction and the first channel low pass in the vertical direction.

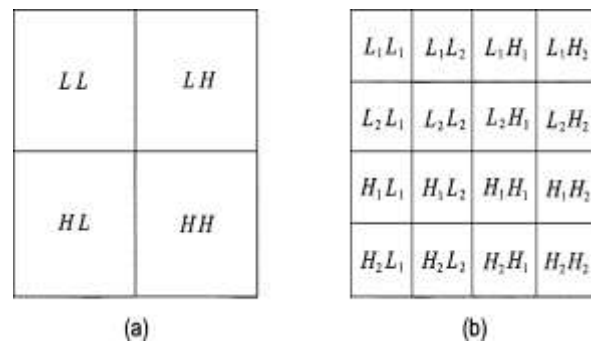


Fig2. Image sub bands after single-level decomposition for (a) scalar wavelets and (b) multi wavelets.

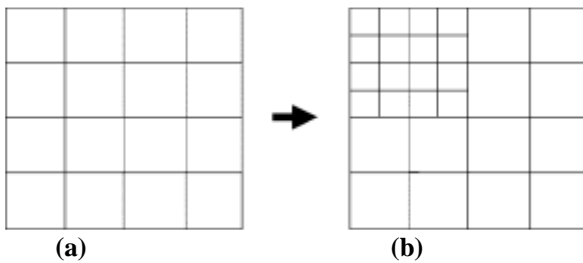


Fig3. Conventional iteration of multi wavelet decomposition.

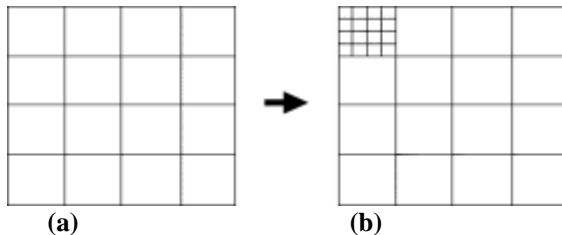


Fig4. Proposed iteration method for multiwavelet decomposition. Compare to Fig 3.

The multi wavelet decomposition sub bands are shown in Fig. 2(b). For multi wavelets, the labels have subscripts denoting the channel to which the data corresponds. For example, the sub band labeled corresponds to data from the second channel high pass filter in the horizontal direction and the first channel low pass filter in the vertical direction. Scalar wavelet transforms give a single quarter-sized low pass sub band from the original larger sub band, as seen in sub band in Fig. 2(a). In previous multiwavelet literature, multi-level decompositions are performed in the same way. The multiwavelet decompositions iterate on the low pass coefficients from the previous decomposition, [the sub bands in Fig. 2(b)], as shown in Fig. 3. In the case of scalar wavelets, the low pass quarter image is a single sub band. But when the multiwavelet transform is used, the quarter image of “low pass” coefficients is actually a block of sub bands—one low pass and three band pass. This is due to the use of SA multi filters. The scaling function associated with the second channel is band pass since its anti symmetric form gives a zero. Two conclusions may be drawn from these observations. First, since these four sub bands possess different statistical characteristics, mixing them together using the standard multiwavelet decomposition results in subsequent sub bands with mixed data characteristics. This implies that typical quantization schemes that assume the statistics in each sub band are either low pass or high pass will not give the best possible results. Second, since only the sub band is entirely comprised of low pass characteristics, we only need to perform further iterations on that one sub band.

Let $\theta(t)$ and $\varphi(t)$ be the scaling and wavelet functions, respectively, which obey the two-scale equations

$$\phi(t) = \sqrt{2} \sum_{k=-\infty}^{\infty} h_k \phi(2t - k),$$

$$\psi(t) = \sqrt{2} \sum_{k=-\infty}^{\infty} g_k \phi(2t - k).$$

Experimental results demonstrate that iterating only on the sub band at each stage in the decomposition does indeed yield better compression than iterating on the four sub bands. Some of these results are depicted in Table I. The 1–2 dB performance improvement indicated in Table I is typical of this new decomposition scheme. It is also worth noting the computational savings realized on all iterations subsequent to the first: iterating on only the sub band requires one-fourth the numbers of computations as iterating over the four sub bands. The structure of this new improved multi wavelet decomposition method is illustrated in Fig. 4.

A. Quantization: Shuffling

The quantization method used to generate the results in this paper is the SPIHT zero tree quantizer developed by Said and Pearlman [13]. SPIHT and other zero tree quantizers achieve good performance by exploiting the spatial dependencies of pixels in different sub bands of a scalar wavelet transform. It has been noted [14] that there exists a spatial dependence between pixels in different sub bands in the form of a child–parent relationship. In particular, each pixel in a smaller sub band has four children in the next larger sub band in the form of a block of adjacent pixels. This relationship is illustrated in Fig. 5, which shows three-level scalar wavelet decomposition and some sample pixel relations.

In this figure, each small square represents a pixel and each arrow points from a particular parent pixel to its group of children. The importance of the parent–child relation in quantization is this: if the parent coefficient has a small value, then the children will most likely also have small values; conversely, if the parent has a large value, one or more of the children might also. Figure 5 shows the comparison between many multi wavelets when applied for ‘Peppers’ image at $b_{pp}=1$. From the figure, it is clear that out of all available multi wavelets, Sa₄ multi filter performs well. Figure 6 shows a comparison when SPECK compression is applied to wavelet and multi wavelets.

From the figure, it is clear that multiwavelet compression gives 3 dB improvements against wavelet compression. Figure 7 shows the comparison graph between the algorithms using ‘Dabauchies’ wavelet. SPECK shows 8 dB improvements over SPIHT [14].

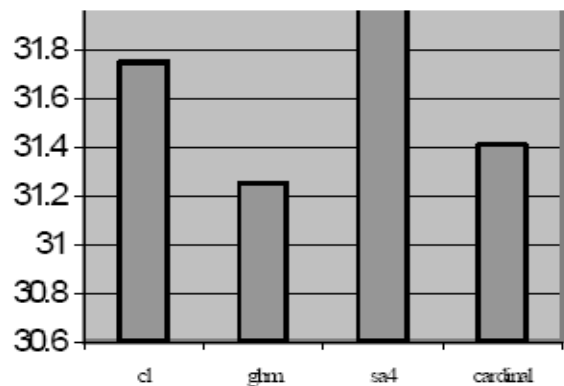


Fig5. PSNR values for various multi wavelets at CR=13.33.

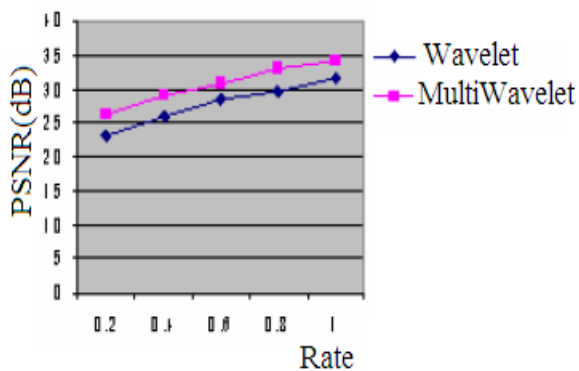


Fig6. Comparison of wavelets vs. multi wavelets

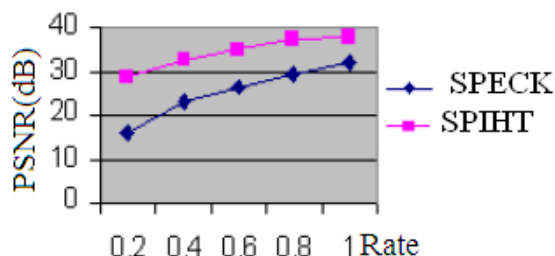


Fig7. Comparison between SPECK and SPIHT

IV. WAVELET BASED FRACTAL IMAGE CODING ALGORITHM

A. Encoding Process

1. Take an image as input of size 512 x 512.
2. Calculate (DWT) wavelet up to $i = 1, 2, 3, \dots, N$ levels.
3. For all N levels, divide the H, V, D components of the i^{th} level in to domain blocks of size $2B \times 2B$ and that of $(i+1)^{th}$ level in to range blocks of size $B \times B$.
4. For domain block, find the best matching range block.
5. Save the mapping information i.e. scaling factor and position of the best matched block into a text file.
6. Also save the n th level approximation component in to the same text file.
7. Transmit this text file as encoded as message.

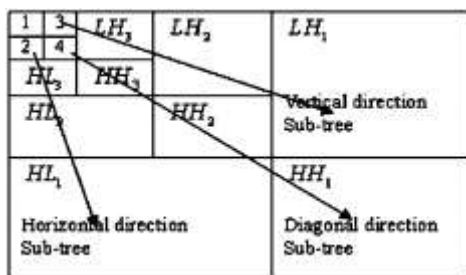


Fig8. Wavelet Sub tree

Fractal Image Compression Technique in Wavelet Domain using Threshold

Encoding Process can be speeded up if a suitable threshold value for MSE is chosen. This speeds up the encoding process because after getting the suitable value it will stop finding the matches for range blocks and domain blocks.

B. Encoding Algorithm

1. Take an image as input of size 512x512.
2. Calculate (DWT) wavelet up to $i=1, 2, 3, \dots, N$ levels.
3. For all N levels, divide the H, V, D components of the i^{th} level in to domain blocks of size $2B \times 2B$ and that of $(i+1)^{th}$ level in to range blocks of size $B \times B$.
4. Choose suitable value for threshold.
5. For every domain block find the matching of range block (depending on threshold value)
6. When the error value is less than the defined threshold value then save the mapping information i.e. scaling factor and position of the best matched block in to a text file.
7. Also save the N^{th} level approximation component in to the same text file.
8. Transmit this text file encoded as message.

C. Decoding Process

1. Read the encoded message file.
2. Take a bitmap image of size 512x512.
3. For all N levels compute (DWT) wavelet of the image and process the H, V, D components with the help of the data in the encoded message file.
4. Take Inverse Discrete Wavelet Transform for all N levels and get the reconstructed image. Repeat the process for k iterations.

D. Decoding Algorithm

The process for decoding the image is the same as that used for wavelet based Fractal Image Compression.



Fig.9: Original Image of baby.tif

Using fractal image compression technique in wavelet domain without threshold. Fig. 5 shows an image lenna.tif of size 512x512. This image is compressed and decompressed using Fractal Image compression Technique in Wavelet Domain. The encoding time is 124 seconds and the size of the encoded text file is 351KB. Fig. 6 shows the reconstructed image.



Fig10. Reconstructed image

The same original image Lenna.tif (Fig.6) is compressed and decompressed using Fractal Image

Compression Technique in Wavelet domain with Threshold. The encoding time is 15 seconds and the size of the encoded text file is 344KB. Fig.8 shows the reconstructed images. The given tables shows comparison between Fractal Image Compression in Wavelet Domain without Threshold and with Threshold

TABLE 1: SHOWS THE PSNR, DECODING TIME FOR DIFFERENT ITERATION USING FRACTAL IMAGE IN WAVELET DOMAIN WITHOUT THRESHOLD

Iteration No	PSNR	Decoding Time in sec
1	20.8637	1.9230
2	23.9965	2.1236
3	25.5867	2.4580
4	29.5050	2.7600
5	29.3475	2.9830
6	29.3475	3.6490
7	29.3475	3.7110
8	29.3475	4.4480

TABLE 2: PSNR AND DECODING TIME FOR ITERATIONS USING FRACTAL IMAGE COMPRESSION IN WAVELET DOMAIN WITH THRESHOLD

Iteration No	PSNR	Decoding Time in sec
1	20.1923	1.3240
2	22.6774	1.9090
3	23.0321	2.1800
4	23.0348	2.8700
5	23.0392	3.1050
6	23.0398	3.6960
7	23.0398	3.8570
8	23.0398	4.5040

Fig.9 shows comparison of PSNR obtained, using Fractal Image Compression technique in wavelet domain, and wavelet

domain with threshold, for an image Lenna.tif of 512x512 sizes.

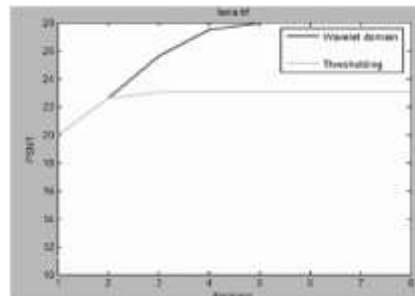


Fig11: Graph Showing Comparison

V. CONCLUSIONS

The performance of multi wavelets in general depends on the image characteristics. For the images with mostly low frequency content, (ordinary still images) scalar wavelets generally give better performance. However multi wavelets appear to excel at preserving high frequency content. In particular, multi wavelets better capture the sharp edges and geometric patterns that occur in images. Two new methods for improving the multi wavelet transform have been proposed in this paper: a new multi wavelet decomposition that iterates only on the sub band, and a coefficient shuffling method to improve performance with zero tree-based quantizers. Both methods have been shown to improve the performance of multi wavelet image compression in many cases.

As a result of the collective benefits that JPEG has to offer, despite its computational complexity, it is the lossless compression of choice for mammogram images. JPEG gives way to a mechanism that can provide maximum exchange of mammogram images to healthcare facilitators in an effective, rapid manor, efficient database access and remote access to digital libraries, all aiding to reduce the waiting times for diagnosis.

REFERENCES

- [1] Martin M., "Applications of Multi wavelets to Image Compression," PhD Thesis, Department of Electrical Engineering, Virginia Polytechnic Institute & State University, June 1999.
- [2] Amara Graps. An introduction to wavelets, *IEEE computational science and engineering*, summer 1995, Vol 2, No.2.
- [3] Ingrid Daubechies, Ten Lectures on Wavelets, SIAM, Philadelphia PA, 1st Edition, 1992.
- [4] Amir Averbuch, Danny Lazar, and MoshelIsraeli, Image Compression Using Wavelet Transform and Multi resolution Decomposition, *IEEE transactions on Image processing*, Vol.5, No.1, Jan 1996.
- [5] Raghuvver M.Rao, Ajit S. Bopadikar., "Wavelet Transforms", Addison Wesley Longman, Singapore.
- [6] Rafel C. Gonzalez, Richard E. Woods., Digital Image Processing, 2nd Edition, Pearson Education.
- [7] David Salomon, Data Compression, Springer- Verlag NewYork 3rdEdition, 2005.
- [8] Sonja Grgic, Kresimir Kers, and Mislav Grgic, "Image compression using wavelets," ISIE'99- Bled, Slovenia, pp. 99-104.
- [9] Hornik K., "Multilayer feed forward networks are universal approximators," *Neural Networks*, vol. pp. 359- 366, 1989.
- [10] Hecht-Nielsen, "Counterpropagation Networks," *Applied Optics*, vol.26, pp. 4979- 4984, 1987.

- [11] J.A. Freeman, and D.M. Skapura, Neural Networks, Addison WesleyLongman, 1999.
- [12] Donald Woods, "Back and counter propagation aberrations," Proc. IEEE, Neural Networks, vol.1, Pp 473-479,1988.
- [13] S.Malarvizhi,U.S.Ragupathy, A.Tamilarasi, "Mammogram Image Compression Using Multiwavelet Transform", Conference Proceedings RTCSP'09
- [14] Sudhakar Radhakrishnan and Jayaraman Subramaniam, "Novel Image Compression Using Multi wavelets with SPECK Algorithm" IAJIT, Vol.5, No.1, January 2008, pp45-51.

AUTHORS PROFILE

¹**M.Ashok**, Associate Professor, Dept. of Computer Science & Engg in S. S. J. Engg College, V.N. Palli, Gandipet, A.P, India. His B.Tech from



S.K.University and M.Tech from JNTU-Ananthapur. He has over 13 years teaching experience and he has published many papers in National, International conferences and journals. His area of interest is in Image Processing and Embedded Systems.
E-Mail: maram_ashokssjec@yahoo.com



²**Dr.T.Bhaskara Reddy**, Associate Professor Dept. of Computer Science & Tech in S. K. University, Anantapur, A.P. India.His M.Sc from S.K.University and M.Tech from ANU-Guntur, A.P . He has over 20 years teaching experience and he has published many papers in National, International conferences and journals. His area of interest is in Image Processing and EmbeddedSystems.
E-Mail:bhaskarreddy_sku@yahoo.co.in

On Algebraic Spectrum of Ontology Evaluation

Adekoya Adebayo Felix¹, Akinwale Adio Taofiki²

Department of Computer Science,
University of Agriculture,
Abeokuta, Nigeria

Sofoluwe Adetokunbo³

Department of Computer Science,
University of Lagos,
Lagos, Nigeria

Abstract— Ontology evaluation remains an important open problem in the area of its application. The ontology structure evaluation framework for benchmarking the internal graph structures was proposed. The framework was used in transport and biochemical ontology. The corresponding adjacency, incidence matrices and other structural properties due to the class hierarchical structure of the transport and biochemical ontology were computed using MATLAB. The results showed that the choice of suitable choice must depend on the purpose of ontology structure evaluation.

Keywords- Ontology evaluation; adjacency matrix; graph; algebraic spectrum.

I. INTRODUCTION

Class relationships are represented by three special kinds of graphs; namely lattice, tree and acyclic, which supports partial ordering Sowa (2004). An ontology describes class relationships using acyclic graphs and provides a convenient means of using appropriate tools to analyze and solve a given concepts. Ontology uses two graph components: nodes and edges to represents concepts (classes, objects, and entities), and the relations between these concepts respectively. In practice, ontologies are acyclic graph models which describe the semantic relationships between the inherent concepts and relations, between concepts and concepts, and between relations and relations. The internal structure and the structural dimension reveal their computational complexity and memory utilization, and also aid fast concept-relation retrievals.

A subset of the nodes and edges in a graph possesses certain characteristics or relate to each other in particular ways which are quite useful for describing the structural relationships existing among concepts, relations and between concepts and relations in ontology. A vast amount of ontologies for diverse domain of discourse have been designed and are available across many ontology libraries. Thus many applications in such areas as knowledge engineering, artificial intelligence, natural language processing, e-commerce, database design and integration, bioinformatics, semantic web, education have been developed using these ontologies. However, many of these ontologies are not well documented and evaluated, therefore hindering their effective re-use and inter-operability in many applications (Staab, 2009 and Lu and Haarslev, 2006).

The lack of tools to analyze these ontologies has not helped the effective utilization of the inherent knowledge that is contained in these ontologies. In this paper, an algebraic framework for benchmarking the internal graph structures of ontologies was proposed.

II. LITERATURE REVIEWS

There is a need to evaluate the ontology and also the results from the ontology. Many researchers have tried various ways of evaluation of ontologies. Maedche and Staab (2002) proposed the evaluation of ontology using lexical or vocabulary level. The process compared two strings based on the Levenshtein edit distance and it was normalized to produce scores in the range of 0 and 1. In 2005, Velardi et al used a body of natural language text to generate natural language glosses for multiple word terms. Part of their techniques employed is-a relation. Brewster et al (2004) suggested using a data-driven approach to evaluate the degree of structural fit between an ontology and a corpus of documents. The ideas was based on clustering algorithm using unsupervised way. Spyns (2005) used relational model to evaluate ontology by extracting a set of lexons from natural language text. Ding et al (2004) used cross-reference between semantic web documents to define a graph and then compute a score for each ontology. Porzel and Malaka (2004) described a scenario where the ontology with its relations was used primarily to determine how closely related the meaning of two concepts was by using the final output of speech recognition problem as a case study.

Patel et al (2005) showed how to determine if the ontology was referred to a particular topic and classified the ontology into a directory topics using standard machine learning algorithms. Brewster et al (2004) extracted a set of relevant domain specific terms from the corpus of documents using latent semantic analysis. Bruton-Jones et al (2004) proposed ten simple criteria of lawfulness, richness, interpretability, consistency, clarity, comprehensiveness, accuracy, relevant, authority and history to evaluate the ontology which were based on scores. Fox et al (1998) proposed another set of criteria which were geared more towards manual assessment and evaluation of ontologies. Luzano-Tello and Gomez-Perez (2004) defined an even more detailed sets of 117 criteria, organized in a three- level framework for evaluation of ontology. Willen Rober et al (2005) proposed two alternative techniques for the evaluation of ontology-matching systems. In this work structural dimensions of ontology by Gangen et al (2006) were used to evaluate the ontology and characteristic polynomial equation of eigenspace with their corresponding adjacency matrix.

III. SPECTRAL ANALYSIS OF GRAPHS

Graph spectrum is the set of its eigenvalues in addition with their multiplicities. There are two standards computational representations of graphs; namely as a collection of adjacency lists or as an adjacency matrix. The adjacency-list representation provides compact way to represent sparse graphs

where $(|E| < |V|^2)$. The adjacency-matrix of a graph $G = (V, E)$ consists of a $|V| \times |V|$ matrix $A = (a_{ij})$

such that
$$a_{ij} = \begin{cases} 1 & \text{if } (i, j) \in E \\ 0 & \text{otherwise} \end{cases}$$

where the vertices are numbered $1, 2, 3, \dots, |V|$ in some arbitrary order. The adjacency-matrix A of an undirected graph is its own transpose

i.e $A = A^T$, If $A = (a_{ij})$ then $A^T = (a_{ij}^T)$ and $a_{ij}^T = a_{ji}$.

In undirected graph, $(u, v) = (v, u)$ means the same edge. In some applications, it pays to store only the entries on and above the diagonal of the adjacency matrix, therefore cutting the memory needed to store the graph almost in half.

The simplicity of an adjacency-matrix makes it preferable to compute the algebraic spectrum especially with small graphs. For weighted graph, there is an additional advantage in the sense that the adjacency matrix uses only one bit per entry instead of one word of computer memory for each matrix entry. Adjacency-matrix makes it easier to search for sub-graphs of particular pattern or identities.

The incidence matrix for an undirected graph $G = (V, E)$ is a $|V| \times |E|$ matrix M

such that

$$M_{ve} = \begin{cases} 1 & \text{if edge } e \text{ is incident on vertex } v \\ 0 & \text{otherwise} \end{cases}$$

A set of columns of M is linearly independent if and only if the corresponding set of edges is acyclic.

The incidence matrix for a digraph $G = (V, E)$ is a $|V| \times |E|$ matrix M such that

$$M_{ve} = \begin{cases} -1 & \text{if edge } e \text{ leaves vertex } v \\ 1 & \text{if edge } e \text{ enters vertex } v \\ 0 & \text{otherwise} \end{cases}$$

If a set of edges in G is linearly independent, then the corresponding set of edges does not contain a directed cycle.

Whereas the adjacency-matrix encapsulate vertex-to-vertex relationships, the incidence matrix encapsulate vertex-to-edge relationships and its Eigen values reveals the relationship between two classes of objects. The advantage of the incidence matrix is that it enables data to be rapidly indexed either for vertices or for edges.

IV. AN ILLUSTRATION OF SPECTRAL ANALYSIS OF ONTOLOGICAL STRUCTURE

Ontologies are directed acyclic graphs and since an inverse of a relation can be obtained from that relation, it follows that information flows in both direction. Consider the transport ontology in figure 1, we computed the adjacency and incidence matrices as depicted tables 1 – 4.

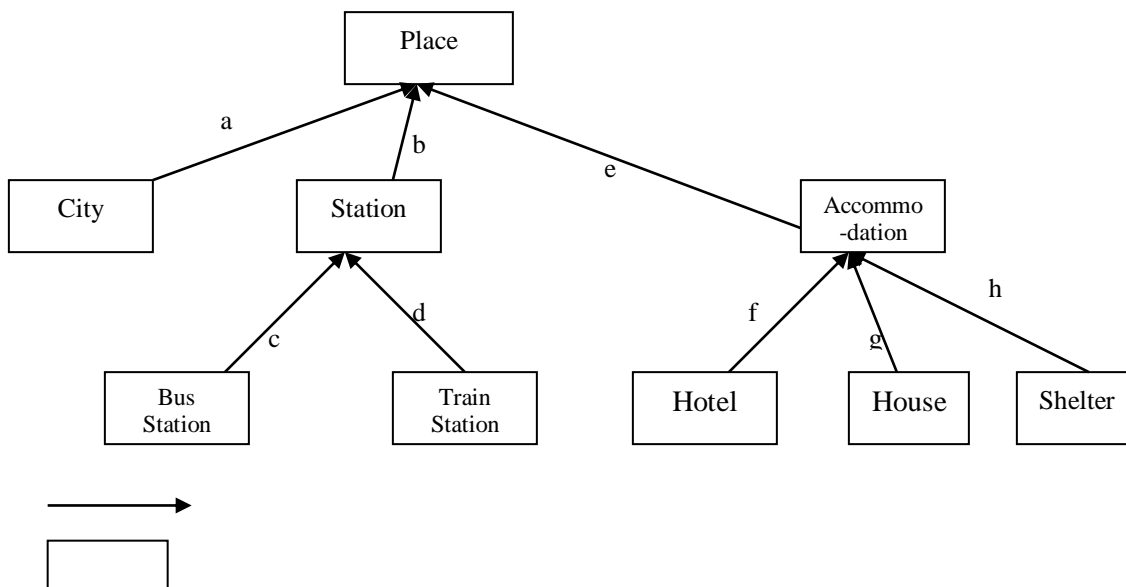


Figure 1: Transport ontology with $V = \{Place, City, Station, Bus Station, Train Station, Accommodation, Hotel, House, Shelter\}$ and $E = \{a, b, c, d, e, f, g, h\}$

TABLE 1: Incidence matrix of DAG ontological Structure in Figure 1

	a	B	C	d	E	f	g	h
Place	1	1	0	0	1	0	0	0
City	-1	0	0	0	0	0	0	0
Station	0	-1	1	1	0	0	0	0
Bus Station	0	0	-1	0	0	0	0	0
Train Station	0	0	0	-1	0	0	0	0
Accommodation	0	0	0	0	-1	1	1	1

Hotel	0	0	0	0	0	-1	0	0
House	0	0	0	0	0	0	-1	0
Shelter	0	0	0	0	0	0	0	-1

TABLE 2: Incidence matrix of undirected ontological structure of Figure 1 (Inverse relation)

	A	b	c	d	E	f	g	H
Place	1	1	0	0	1	0	0	0
City	1	0	0	0	0	0	0	0
Station	0	1	1	1	0	0	0	0
Bus Station	0	0	1	0	0	0	0	0
Train Station	0	0	0	1	0	0	0	0
Accommodation	0	0	0	0	1	1	1	1
Hotel	0	0	0	0	0	1	0	0
House	0	0	0	0	0	0	1	0
Shelter	0	0	0	0	0	0	0	1

TABLE 3: Adjacency matrix of DAG ontological Structure

	Place	City	Station	Bus Station	Train Station	Accommodation	Hotel	House	Shelter
Place	0	0	0	0	0	0	0	0	0
City	1	0	0	0	0	0	0	0	0
Station	1	0	0	0	0	0	0	0	0
Bus Station	0	0	1	0	0	0	0	0	0
Train Station	0	0	1	0	0	0	0	0	0
Accommodation	1	0	0	0	0	0	0	0	0
Hotel	0	0	0	0	0	1	0	0	0
House	0	0	0	0	0	1	0	0	0
Shelter	0	0	0	0	0	1	0	0	0

TABLE 4: Adjacency-matrix of the undirected ontological structure

	Place	City	Station	Bus Station	Train Station	Accommodation	Hotel	House	Shelter
Place	0	1	1	0	0	1	0	0	0
City	1	0	0	0	0	0	0	0	0
Station	1	0	0	1	1	0	0	0	0
Bus Station	0	0	1	0	0	0	0	0	0
Train Station	0	0	1	0	0	0	0	0	0
Accommodation	1	0	0	0	0	0	1	1	1
Hotel	0	0	0	0	0	1	0	0	1
House	0	0	0	0	0	1	1	0	0
Shelter	0	0	0	0	0	1	0	0	0

V. COMPUTING EIGEN VALUES AND EIGEN VECTORS

In this work, we used the characteristic polynomial equation to compute the eigenspace of the example ontology given in figure 1 and the corresponding adjacency matrix in Table 4.

If A is an $n \times n$ matrix, then its corresponding eigenvalues (λ) are the roots of the characteristics polynomial

$\det(A - \lambda I)$ and the eigenvectors would be $v_1, v_2, v_3, \dots, v_n$ respectively. An eigenvalue λ mapped to an eigenvector and the set of all eigenvectors which satisfy $Av = \lambda v$ are referred to as the eigenspace of A . v must be a non-zero and the characteristics polynomial must be set to zero.

$$\text{i.e } \det(A - \lambda I) = 0$$

The number of eigenvalues for a $n \times n$ matrix is n , though some of the eigenvalues might be equal to one another.

Consider the ontology figure 1 and the adjacency matrix in table 4, the eigenvalues are

$$\text{Transont (9 x 9)} = \begin{bmatrix} 0 & 1 & 1 & 0 & 0 & 1 & 0 & 0 & 0 \\ 1 & 0 & 0 & 0 & 0 & 0 & 0 & 0 & 0 \\ 1 & 0 & 0 & 1 & 1 & 0 & 0 & 0 & 0 \\ 0 & 0 & 1 & 0 & 0 & 0 & 0 & 0 & 0 \\ 0 & 0 & 1 & 0 & 0 & 0 & 0 & 0 & 0 \\ 1 & 0 & 0 & 0 & 0 & 0 & 1 & 1 & 1 \\ 0 & 0 & 0 & 0 & 0 & 1 & 0 & 0 & 1 \\ 0 & 0 & 0 & 0 & 0 & 1 & 1 & 0 & 0 \\ 0 & 0 & 0 & 0 & 0 & 1 & 0 & 0 & 0 \end{bmatrix}$$

$$\text{The eigenvalues } \det(A - \lambda I) = \begin{bmatrix} -\lambda & 1 & 1 & 0 & 0 & 1 & 0 & 0 & 0 \\ 1 & -\lambda & 0 & 0 & 0 & 0 & 0 & 0 & 0 \\ 1 & 0 & -\lambda & 1 & 1 & 0 & 0 & 0 & 0 \\ 0 & 0 & 1 & -\lambda & 0 & 0 & 0 & 0 & 0 \\ 0 & 0 & 1 & 0 & -\lambda & 0 & 0 & 0 & 0 \\ 1 & 0 & 0 & 0 & 0 & -\lambda & 1 & 1 & 1 \\ 0 & 0 & 0 & 0 & 0 & 1 & -\lambda & 0 & 1 \\ 0 & 0 & 0 & 0 & 0 & 1 & 1 & -\lambda & 0 \\ 0 & 0 & 0 & 0 & 0 & 1 & 0 & 0 & -\lambda \end{bmatrix}$$

We use MATLAB to compute the $\det(A - \lambda I)$ since n is large.

$$\text{Therefore, } \det(A - \lambda I) = \lambda^9 - 8\lambda^7 - 2\lambda^6 + 15\lambda^5 + 8\lambda^4 - 2\lambda^3 - 4\lambda^2 - 2\lambda$$

The eigenvalues are 2.4046, 1.6785, -2.1667, 0.7390, -1.4299
-0.6731, -0.2762 + 0.4952i, -0.2762 - 0.4952i and 0.0000.

$$\text{The eigenvectors (V)} = \begin{bmatrix} -0.4345 & 0.5532 & 0.2891 & -0.0162 & -0.4694 & -0.4190 \\ -0.1807 & -0.2553 & 0.1722 & 0.0113 & -0.6351 & 0.6225 \\ -0.2762 & -0.4448 & 0.5936 & 0.5174 & 0.2386 & -0.1823 \\ -0.1149 & 0.2053 & 0.3537 & -0.3619 & 0.3229 & 0.2708 \\ -0.1149 & 0.2053 & 0.3537 & -0.3619 & 0.3229 & 0.2708 \\ -0.5878 & -0.4985 & -0.2806 & -0.5056 & 0.0496 & -0.1582 \\ -0.3461 & 0.1239 & -0.2668 & 0.1063 & 0.1580 & -0.1141 \\ -0.3884 & 0.1729 & -0.3261 & 0.2793 & 0.2809 & 0.4046 \\ -0.2444 & 0.2301 & -0.1672 & 0.3536 & 0.0671 & 0.2350 \end{bmatrix}$$

$$D = \begin{bmatrix} 2.4046 & 0 & 0 & 0 & 0 & 0 \\ 0 & -2.1667 & 0 & 0 & 0 & 0 \\ 0 & 0 & 1.6785 & 0 & 0 & 0 \\ 0 & 0 & 0 & -1.4299 & 0 & 0 \\ 0 & 0 & 0 & 0 & 0.7390 & 0 \\ 0 & 0 & 0 & 0 & 0 & -0.6731 \end{bmatrix}$$

flag = 0

where V represents the set of eigenvectors and D the set of eigenvalues. The flag = 0 implies that the eigenvalues converged.

VI. STRUCTURAL DIMENSION METRICS OF GRAPHS

The structural dimension of ontologies focuses on analysis of digraph structures and formal semantics. Gangemi, Catenacci, Ciaramita and Lehmann (2006) proposed the following formula which were used in the proposed ONTOSTEVAL for measuring the structural dimensions of ontologies among others. We compute the structural dimension of the sample ontology in figure 1.

A. Measures for depth

This measure is related to the cardinality of paths in a digraph where the arcs are only *is-a* relations. Three types of depth measures namely; absolute depth, average depth and maximal depth were used in the proposed ONTOSTEVAL.

1) Absolute Depth

$$D_{abs} = \sum_j^P N_{j \in P}$$

where $N_{j \in P}$ is the cardinality of each path j from the set of paths P in a graph G .

From figure 1,

$$P = \{a, bc, bd, ef, eg, eh\} = 6 \text{ paths}$$

$$N_{j \in P} = \left\{ \begin{array}{l} \{a\} \\ \{\{b\}, \{c\}\} \\ \{\{b\}, \{d\}\} \\ \{\{e\}, \{f\}\} \\ \{\{e\}, \{g\}\} \\ \{\{e\}, \{h\}\} \end{array} \right\} = \left\{ \begin{array}{l} 1 \\ 2 \\ 2 \\ 2 \\ 2 \\ 2 \end{array} \right\},$$

therefore $D_{abs} = 11$.

2) Average Depth

$$D_{ave} = \frac{1}{n_{p \subseteq G}} \sum_j^P N_{j \in P}$$

where $N_{j \in P}$ is the cardinality of each path j from the set of paths P in a graph G , and $n_{p \subseteq G}$ is the cardinality of P .

$$D_{ave} = \frac{1}{6}(11) = 1.83$$

3) Maximal Depth

$$D_m = N_{j \in P}$$

$$\forall i \exists j (N_{j \in P} \geq N_{i \in P})$$

where $N_{j \in P}$ and $N_{i \in P}$ are the cardinalities of any path i or j from the set of paths P in a graph G .

$$D_m = 2.$$

B. Measures for breadth

This measure is related to the cardinality of generations in a graph where the edges are only the *is-a* relations. Three types of depth measures namely; absolute depth, average depth and maximal depth were used in the proposed ONTOSTEVAL.

1) Absolute Breadth

$$B_{abs} = \sum_j^{G_L} N_{j \in G_L}$$

where $N_{j \in G_L}$ is the cardinality of each generation j from the set of generations G_L in the digraph G .

There are three levels (G_L) in the example ontology in figure 1 namely

Level 1 = { 1 } contain 1 vertex

Level 2 = { 2, 3, 4 } contain 3 vertexes

Level 3 = {5, 6, 7, 8, 9} contain 5 vertexes

Therefore, $B_{abs} = 9$

2) Average Breadth

$$B_{ave} = \frac{1}{n_{G_L \subseteq G}} \sum_j^{G_L} N_{j \in G_L}$$

where $N_{j \in G_L}$ is the cardinality of each generation j from the set of generations G_L in a digraph G , and $n_{G_L \subseteq G}$ is the cardinality of G_L .

$$B_{ave} = \frac{1}{3}(9) = 3$$

3) Maximal breadth

$$B_m = N_{j \in G_L}$$

$$\forall i \exists j (N_{j \in G_L} \geq N_{i \in G_L})$$

where $N_{j \in G_L}$ and $N_{i \in G_L}$ are the cardinalities of any generation i or j from the set of generations G_L in a graph G .

$$B_m = 5 \text{ (the highest number of vertexes)}$$

C. Measures for density

Gangemi (2005) defined density as the presence of clusters of classes with many non-taxonomical relations holding among them. We defined density based Coleman & Moré (1983) on as follows

$$D = \frac{2|E|}{|V|(|V|-1)}$$

where $|E|$ is total number of edges and $|V|$ is the total number of vertexes. The maximum number of edges is $\frac{1}{2} |V|(|V|-1)$, so the maximal density is 1 (for complete graphs) and the minimal density is 0.

$$|E| = \{ a, b, c, d, e, f, g, h \} = 8$$

$$|V| = \{ 1, 2, 3, 4, 5, 6, 7, 8, 9 \} = 9$$

$$D = \frac{2 \times 8}{9(9-1)} = 0.22$$

VII. ONTOLOGY STRUCTURE EVALUATION (ONTOSTEVAL) FRAMEWORK

The proposed Ontology Structure Evaluation (ONTOSTEVAL) Framework for benchmarking the internal graph structures of ontologies is described in this section. The ONTOSTEVAL architecture is presented in figure 2 and comprises of three sections, namely the input, processing and the output units. The input unit accepts an ontology written in OWL such as the domain ontology while the processing unit parses the OWL file, analyses and computes its internal structures such as the spectral properties.

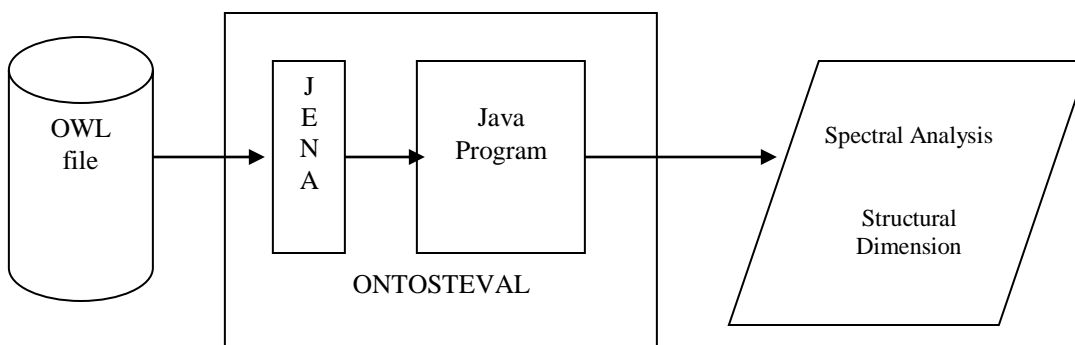


Figure 2: The ONTOSTEVAL Architecture

The Java program is embedded into Jena Framework and uses the well-known depth-first and breadth-first algorithms to determine the adjacent vertexes and the edges incident on a vertex as illustrated in figure 3. A Java program was written to compute the spectral analysis (adjacency and incidence matrices, eigenvalues and eigenvectors) and the structural dimension (depth, breadth and density) for ontologies written in OWL. The Java program was embedded in Jena Semantic Web Framework in order to enable the Java program read, parse and analyze any ontology file, and computes the inherent spectral and structural dimension metrics. In this section we

present the spectral and structural analyses of some ontologies which were used with the proposed Ontology Structural Evaluation Framework (ONTOSTEVAL).

Biochemical Ontology

Biochemical ontology aim to capture and represent biochemical entities and the relations that exist between them in an accurate and precise manner. Figures 3 described the class hierarchical structure of the biochemical ontology while figure 4 shows its graph in the protégé implementation.



Figure 3. Asserted Class Hierarchy of Biochemical Ontology

flag = 0 ; indicate that the eigenvalues converged.

The incidence matrix of the Biochemical ontology =

1	1	1	0	0	0	0	0	0	0	0	0
0	0	0	0	0	0	0	0	0	0	0	0
0	0	0	0	0	0	0	0	0	0	0	0
0	0	0	1	1	1	1	0	1	1	1	1
0	0	0	0	0	0	0	0	0	0	0	0
0	0	0	0	0	0	0	0	0	0	0	0
0	0	0	0	0	0	0	0	0	0	0	0
0	0	0	0	0	0	0	0	1	0	0	0
0	0	0	0	0	0	0	0	0	0	0	0
0	0	0	0	0	0	0	0	0	0	0	0
0	0	0	0	0	0	0	0	0	0	0	0
0	0	0	0	0	0	0	0	0	0	0	0
0	0	0	0	0	0	0	0	0	0	0	0
0	0	0	0	0	0	0	0	0	0	0	0

Structural Dimension

Absolute Depth = 34

Absolute Breadth = 18

Density = 0.11

Average Depth = 2.43

Average Breadth = 3.6

Maximal Depth = 4

Maximal Breadth = 8

The Transport Ontology

Transport ontologies aim to capture and represent different entities and the relations that exist between them in an accurate

and precise manner. Figures 5 described the class hierarchical structure of the transport ontology while figure 6 shows its corresponding graph in the protégé implementation.

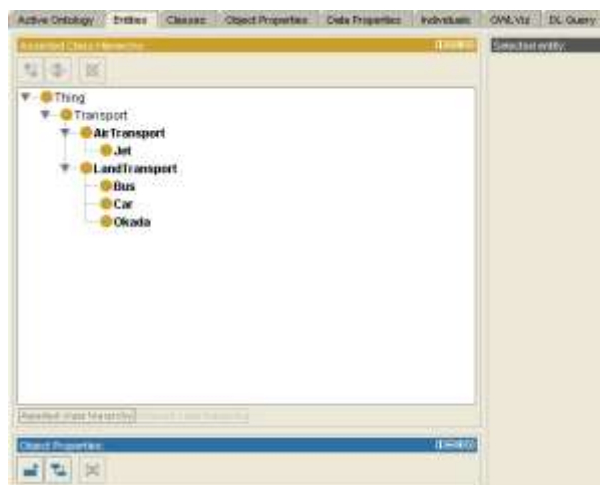


Figure 5. Asserted Class Hierarchy of Transport Ontology

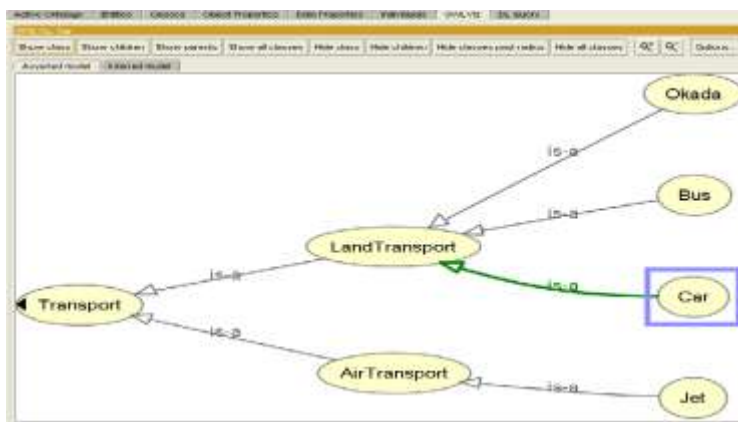


Figure 6. Transport OWL graph

$$\text{Adjacency matrix (Transport)} = \begin{bmatrix} 0 & 1 & 0 & 1 & 0 & 0 & 0 \\ 1 & 0 & 1 & 0 & 0 & 0 & 0 \\ 0 & 1 & 0 & 0 & 0 & 0 & 0 \\ 1 & 0 & 0 & 0 & 1 & 1 & 1 \\ 0 & 0 & 0 & 1 & 0 & 0 & 0 \\ 0 & 0 & 0 & 1 & 0 & 0 & 0 \\ 0 & 0 & 0 & 1 & 0 & 0 & 0 \end{bmatrix}$$

The characteristics polynomial $\det (A - \lambda I) = \lambda^7 - 6\lambda^5 + 7\lambda^3$
The Eigenvalues = -2.1010, -1.2593, 0, 0, 0.0000, 1.2593, 2.1010

$$\text{The Eigenvectors (V)} = \begin{bmatrix} -0.4397 & 0.3039 & -0.4377 & 0.4047 & 0.3039 & -0.4397 \\ -0.2706 & 0.6533 & 0.0000 & 0.0000 & -0.6533 & 0.2706 \\ -0.1288 & 0.5188 & 0.4377 & -0.4047 & 0.5188 & -0.1288 \\ -0.6533 & -0.2706 & 0.0000 & 0.0000 & 0.2706 & 0.6533 \\ -0.3109 & -0.2149 & 0.7437 & 0.2323 & -0.2149 & -0.3109 \\ -0.3109 & -0.2149 & -0.2452 & -0.7743 & -0.2149 & -0.3109 \\ -0.3109 & -0.2149 & -0.0608 & 0.1372 & -0.2149 & -0.3109 \end{bmatrix}$$

flag = 0

$$\text{The incidence matrix} = \begin{bmatrix} 1 & 0 & 1 & 0 & 0 & 0 \\ 0 & 1 & 0 & 0 & 0 & 0 \\ 0 & 0 & 0 & 0 & 0 & 0 \\ 0 & 0 & 0 & 1 & 1 & 1 \\ 0 & 0 & 0 & 0 & 0 & 0 \\ 0 & 0 & 0 & 0 & 0 & 0 \\ 0 & 0 & 0 & 0 & 0 & 0 \end{bmatrix}$$

Structural Dimension

Absolute Depth = 8

Average Depth = 4

Maximal Depth = 2

Absolute Breadth = 7

Average Breadth = 2.33

Maximal Breadth = 4

Density = 0.29

VIII. CONCLUSION

The work used the simplicity of an adjacency matrix of a graph to compute the algebraic spectrum and structural dimensions of ontology. It presented an application of the state of the art on ontology evaluation. The applications showed that the choice of suitable method must depend on the theme of ontology evaluation.

REFERENCES

- [1] N. Alon and V. D. Isoperimetric Inequalities for Graphs and Super Concentrators, *Journal of Combinatorial Theory, Series B* 38, pp 73-88 0095-8956/85, Academic Press Inc., (1985)
- [2] T. F. Coleman and J. J. More, Estimation of Sparse Jacobian Matrices and Graph Coloring Problems, *SIAM journal on Numerical Analysis*, vol 20(1), pp 187-209, (1983) Aussenac-Gilles and D. Sorgel, Supervised Text Analysis for Ontology and Terminology Engineering, *Applied Ontology: An*
- [3] A. Gangemi, Ontology Design Patterns for Semantic Web Content, *Proceedings of the fourth International Semantic Web Conference*, Berlin Springer, (2005)
- [4] Gangemi A., C. Catenacci, M. Ciaramita, J. Lehman, Modelling Ontology Evaluation, In *Proceedings of the Third European Semantic Web Conference Berlin Springer*, (2006)
- [5] L. Lovasz, On the Shannon Capacity of a Graph, *IEEE Trans. Inform. Theory*, IT 25, pp 1-7, (1979)
- [6] Q. Lu and V. Haarslev, OntoKBEval, DL-Based Evaluation of OWL Ontologies, In *Proceedings of OWLED*, (2006)
- [7] B. Mohar, Some Applications of Laplace Eigenvalues of Graphs, *Algebraic Methods and Applications*, Eds G. Hahn serie C 497, pp 225-250, Kluwer, (1997)
- [8] J. F. Sowa, *Ontology*, <http://www.jfsowa.com/ontology>
- [9] S. Staab, *Handbook on Ontologies*, Springer (2009)
- [10] A. Maedche and S. Staab, Measuring Similarity between Ontology, *Proceedings CIKM LNAI vol. 2473*, (2002)
- [11] P. Spyn, Assessing Triples Mined from Texts, Technical Report 09, STAR Lab, Brussel Belgium, (2005)
- [12] R. Porzel and R. Malaka, A Task Based Approach for Ontology Evaluation, *ECA/2004, Workshop on Ontology Learning and population* (2004)
- [13] P. Avesani, F. Giunchiglia, and M. Yatskevish, A large Scale Taxonomy Mapping Evaluation, In *Proceedings of the International Semantic Web Conference ISUC*, (2005)
- [14] D. Hull, Evaluating Evaluation Measures Stability, In *Proceedings of SIGIR* (2000)
- [15] A. Lozano-Tello and A. Gomez-Perez, Ontometric: A Method to Choose the Appropriate Ontology, *Journal of Database Management Vol 15(2)*, pp 1-18,(2004)
- [16] A. Gomez-Perez, A Toward a Framework to verify Knowledge Sharing Technology: Expert Systems with Applications Vol. 11(4), pp 519-529, (1996)
- [17] K. Superkar, A Peer-Review Approach for Ontology Evaluation, *Proceedings 8th International Protégé Conference* , Madrid, Spain (2005)

Evaluation of SIGMA and SCTPmx for High Handover Rate Vehicle

Hala Eldaw Idris Jubara
Faculty of Electrical Engineering
Universiti teknologi Malaysia
Skudai 81310 Johor Malaysia

Sharifah Hafizah Syed Ariffin
Faculty of Electrical Engineering
Universiti teknologi Malaysia
Skudai 81310 Johor Malaysia

Abstract— Rapid technological advance in wireless mobile communication offered Internet accessibility at anytime and anywhere including high speed wireless environment such as in high speed trains, fast moving cars etc. However, wireless Quality of Service (QoS) provisioning in such high speed movement is more difficult and challenging to be tackled than in a fixed-wired environment. This paper discussed transport layer protocol, SCTP to support seamless handover that can guarantees and maintain high QoS in high speed vehicle. The comparison of the selected protocol have been identified and analysed in two handover techniques SIGMA and SCTPmx to optimize its performance in high speed vehicular environment.

Keywords—handover latency; speed; SCTP; mobility management; vehicle.

I. INTRODUCTION

The need for host mobility support in the Internet is increasing with the explosion of wireless and mobile communication devices. Therefore, network layer solutions (such as Mobile IP) are common to support host mobility in the Internet. Network layer solutions however have their own drawbacks, such as the need of support from the network (Home/Foreign Agents), triangular routing, long handoff latency, etc. Moreover, network layer solutions hide the mobility from the transport protocols, where the flow and congestion control tasks are performed, which Impedes performance optimization. Transport layer solutions on the other hand allow the transport protocol to be aware of mobility and hence adjust changes in the path characteristics when required. Therefore, transport layer could be a better place to tackle the host mobility problem in the Internet [1][2][4][17][18][21]. However, transport layer mobility solution needs to have the following functionalities: Movement Detection, Handoff Management, and Location Management [3].

High-speed transportations; e.g., vehicle along highway are more usable around rapid growth of technologies and needs to maintain service continuity (e.g. real-time and delay-sensitive applications). In fact [2][18][22], making mobility seamless as the movement speed of vehicle increases is more challenging. Mobile users are expecting to receive similar services as fixed users at home or office. This work suppose a scenario of vehicle moving along highway with high speed up to 120km/hr, and perform horizontal handover between WiMAX

base stations (BS) because it is more frequent type of handover in daily usage, and using single interface is less power consumption and hardware.

The rest of the paper is organized as follows. Section II shows the related works. An overview of Mobility management in highly mobile vehicle communicate to infrastructure (V2I) in terms of five requirements is mentioned in section III. The selected two techniques to be compared related to the problem statement are well-defined in section VI respectively. Section V describes simulation topology and parameters. Section IV presents Handover latency comparison results of the selected techniques mentioned, and section IIV conclude the paper.

II. RELATED WORK

In high speed vehicles scenarios the needs for network communication for interactive and real-time applications is becoming gradually more important. Therefore many seamless mobility approaches have been developed. The intent is to avoid service disruption and minimize the awareness of service degradation while mobile device is moving fast and changing the point of attachment from one access point to another. References [2][14] and [15] described various approaches that can support seamless and lossless handover in high speed transportation system. Work in [2] exploit prediction technique is proposed to improve and optimize its performance in high speed environment. Thus, there would be no problem regarding insufficient time in connection establishment as the movement speed increase. A study shows in [15] also suggest 802.21 centric approaches to exploit a prior knowledge method where network information is gathered from both mobile terminal and network infrastructure to establish an earlier connection with new subnet. in order to reduce the effect of service interruption in high movement speed environment. Another research presented in [14] propose a packet forwarding control (PFC) scheme to select a common ahead point (CAP) as the tunnel source to forward packets. So that packets can be sent through a shorter delivery path during handover. Author in [19] proposed Network Mobility Protocol for Vehicular Ad Hoc Networks. They proposed NEMO protocol for VANET in highway, since every car is moving in a fixed direction with high moving speed, the car adopting our protocol can acquire IP address from the VANET through vehicle to vehicle communications. In [19]they presents a cross-layer fast handover scheme, called vehicular fast handover scheme

(VFHS), where the physical layer information is shared with the MAC layer, to reduce the handover delay. All of above mention works focus for the handover in lower layer (L2, L3) and the transportation layer will not be aware of handover and may cause packet loss.

III. MOBILITY MANAGEMENT FOR HIGHLY MOBILE VEHICULAR NETWORKS

Mobility management in vehicular networks should guarantee the reachability to correspondent nodes (CN) in the Internet as well as the global reachability to mobile nodes in a vehicular network. Therefore, the mobility management has to meet the following requirements [4].

A. Seamless mobility

Mobility of vehicles should be seamless regardless of vehicle's location and wireless technology. Also, accessibility and service continuity should be guaranteed.

B. Fast Handover

Fast handover is needed for delay sensitive ITS applications (e.g., safety, internet access, etc.). Fast handover is also a crucial requirement for wireless networks with small coverage area (e.g., WiFi network), since the vehicle with high speed spends short period of time at each point of attachment (e.g., Base station), consequently high handover rate.

C. IPv6 support

The global reachability requires a globally reliable routable IP address for each mobile node. IPv6 with large address space can support a unique address for each mobile device in the vehicles. In addition, IPv6 also has better support of security and quality of service (QoS) which are the necessary requirements of ITS applications.

D. High mobility speed

The Internet access is expected to be constantly connected regardless of the movement speed. It is highly desirable to make these contents available and reliable regardless of time, place, fixed or mobile. As the speed of vehicle increases, the successful probability of handover decreases. Moreover, successful probability of handover is reduced by the same reason as the handover execution time is increased.

E. Movement detection

The vehicle needs to detect the availability of different types of access networks (e.g., WiMAX base station) known as data link layer handover (L2), and obtain addresses in these networks for communication.

IV. COMPARISON OF SIGMA & SCTPMX IN HIGH HANDOVER RATE VEHICLE

A. SIGMA

SIGMA proposed to design a new scheme for supporting low latency and low packet loss mobility called Seamless IP diversity based Generalized Mobility Architecture (SIGMA). SIGMA uses SCTP; however it can be used with other protocols that support IP diversity. It can also cooperate with normal IPv4 or IPv6 infrastructure without the support of Mobile IP [5][6][7][8][9]. Figure.1 shows the timing diagram

of SIGMA. General analysis of factors that affect handover latency of SIGMA described as follows.

1) Seamless mobility

SIGMA needs to setup a location manager which is not restricted to the same subnet as MN's home network. Using location manager make vehicle movement seamless from upper layers (e.g., no need of home agent). This will make the deployment of SIGMA much more flexible than other protocols as MIP.

2) Handover latency

SIGMA experienced a seamless handover because it could prepare the new path in parallel with data forwarding over the old path. Therefore, SIGMA can achieve a low handover latency, low packet loss rate and high throughput.

3) IPv6 support

SIGMA can be used with other protocols that support IP diversity. It can also cooperate with normal IPv4 or IPv6 infrastructure without the support of Mobile IP. The reason is that MH can use any unique information as its identity such as home

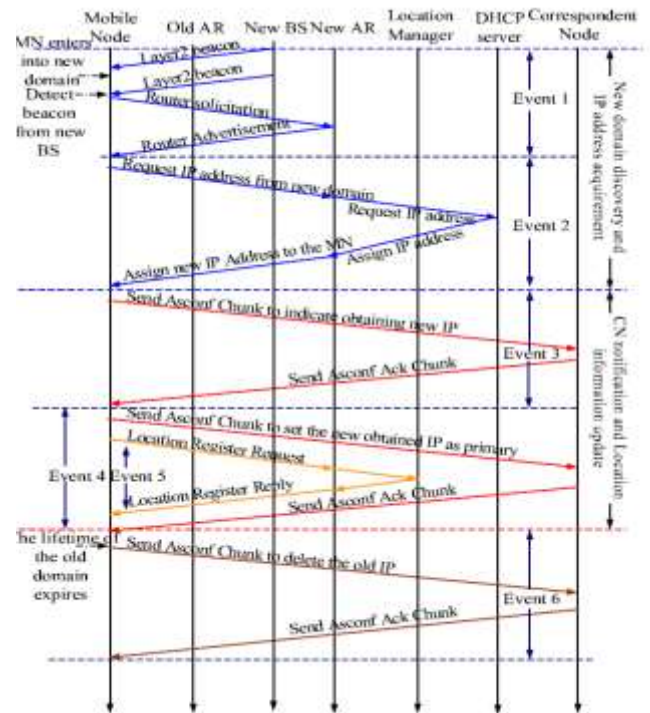


Fig.1 SIGMA handover procedure

address like MIP, or domain name, or a public key defined in Public Key Infrastructure (PKI).

4) High mobility speed

Because SIGMA do not rely on the assumption that detection of the new agent is well in advance of higher handover latency due to shorter time to prepare for the handover. Also, there is higher possibility that packets are forwarded to the outdated path and get lost; therefore the time instant that MN can receive packets from the new path will be postponed, and the handover latency increases accordingly.

5) Movement detection

SIGMA always requires updating CN before packets can be received from the new path. Therefore, the increase of this link delay will increase the handover latency (up to 109ms in the case of 200ms delay between CN and PAR).

6) Drawbacks of SIGMA

- In mobile systems such as IEEE 802.11, GPRS, UMTS, etc. there exists layer 2 handover/ setup latency, which is due to the physical and/or link layer limitations. The SIGMA signaling messages will experience an extra delay, which may break the parallelism that supposed to achieve with IP diversity.

- When MN moves into a new IP domain, it requires some time for MN to obtain a new IP address through DHCP, DHCPv6, or IPv6 Stateless Address Auto-configuration (SAA) [8]. Until this process is finished, MN cannot perform any SIGMA signaling.

- If MN's moving speed is too high, there is no time for MN to prepare for the new path; the parallelism that can be achieved by IP diversity will be broken. Therefore, the handover performance of SIGMA may be affected by these factors mentioned above, even though SIGMA does not require any change on the layer 2 or layer 3 implementation.

B. SCTPmx

SCTPmx employs a cross-layer control information exchange system between L2, L3 and L4 primitives called LIES to predict handover figure.2. Prior to handover SCTPmx can generate a new address that will be used after handover and can execute duplicate address detection of IPv6 [1].

1) Handover latency

In SCTPmx, completion of Link layer (L2) handover is immediately reported to the network layer (L2) and the transport layer (L4) by cross layer approach. In addition, duplicate address detection DAD is completed prior to the handover by fast DAD. Thus, the handover latency of SCTPmx is lower than SIGMA in predicting handover.

2) Seamless mobility

The multihoming mechanism of SCTP can support mobility. Therefore, SCTPmx employs a cross-layer architecture called CEAL to predict handover. This cross-layer allows information exchange between arbitrary layer (L2, L3, and L4) to achieve efficient SCTP communication.

3) IPv6 support

It observed that SCTPmx can support IPv6, the reason that it has many network layer primitives to achieve efficient TCP communication in a mobile environment through different infrastructure.

4) High vehicle speed

In SCTPmx handover latency is approximately 100ms. Thus, for high speed vehicle accordingly high handover rate it cannot receive packets for 100ms handover delay and then communication continue for 5999.9ms (WiMAX BS Dwell time*). Therefore, the throughput of SCTPmx is much better of an environment where consecutive handover occurs resulting of high MN speed.

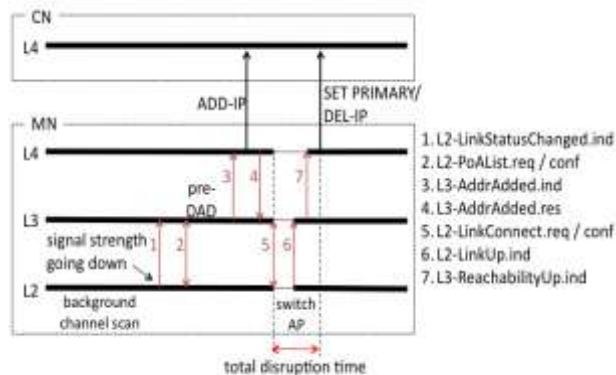


Fig.2 Handover procedure of SCTPmx

5) Movement detection

To reduce L2 handover of the vehicle to search for the best base station (BS) to switch when the communication quality is getting worse, SCTPmx introduces the selective background scan procedure. Also, by extending router advertisement (RA) to include options of channel number and send to network layer to learn about the channel number in adjacent cell. Thus, the network layer of the MN can decide the best access point to handover without channel scan the signal quality to the current access point is going down.

V. SIMULATION TOPOLOGY AND PARAMETERS

Using SCTP as an illustration is shown in Fig.3, where the vehicle is multi-homed node connected through four wireless access networks (WiMAX BS). Each 2 BSs connected to AR. The WiMAX BS has a radio coverage area of approximately 2000 meters in radius. The overlapping region between two ARs is 200 meters. The correspondent node (CN) is a single-homed node sending traffic to vehicle, which corresponds to the services like file downloading or web browsing by mobile users and Location Manager (LM) uses by SIGMA.

VI. HANDOVER LATENCY COMPARISON RESULTS

Handover latency as the time interval between the last data segment received through the old path and the first data segment received through the new path from CN to MH. In this section, we will examine the impact of different parameters on the overall handover latency of SIGMA and SCTPmx. For handover analysis, we consider the single-homing vehicle that can only use a single network interface at a time. This scenario could be applied to the horizontal handover of an MN that is moving within homogenous networks. In this case, the link-up of a new link and link-down of the old link will occur at the same time in the underlying link and network layers. That is, the SCTP handover will occur together with the link layer handover at the same time.

For the single-homing MN, the handover latency $T_{HO-latency}$ can be calculated by summing up the time T_{DHCP} (for the configuration of a new IP address from a DHCP server), the time T_{ASCONF} (for the configuration of a new IP address from a DHCP server), the time T_{ASCONF} (for the Add-IP and Primary-Change and Delete-IP operations in the SCTP handover), and the time T_{L2} (for the handover at the link layer). Accordingly, the total handover latency of SCTP will be:

$$T_{HO} = T_{ASCONF} + T_{L2} + T_{DHCP} \quad (1)$$

A. Impact of L2 handover

Handover latency of SIGMA is very low at 10ms L2 delay, however, in high speeds vehicle SIGMA experience more handover delay (section IV.a.4) as appear in figure 4. In contrast, SCTPmx employs the selective background scan during data communication and L3 can decide next BS without waiting L2 channel scan.

B. Impact of L3 handover

SCTPmx uses fast DAD procedure to complete DAD prior to handover. According to RA L3 knows the IPv6 prefix of the next BS and generate the new IPv6 address before handover. Then L3 send fast DAD request to NAR. Therefore, L3 handover latency of SCTPmx is much lower than mSCTP that uses in SIGMA, figure 4[1][6][7][8][9].

On other hand, triangle routing means the packets between CN and MH must be routed along a triangular path longer than the optimal one especially in higher speed vehicle [14], which definitely introduces higher latency and high network load in MIP.

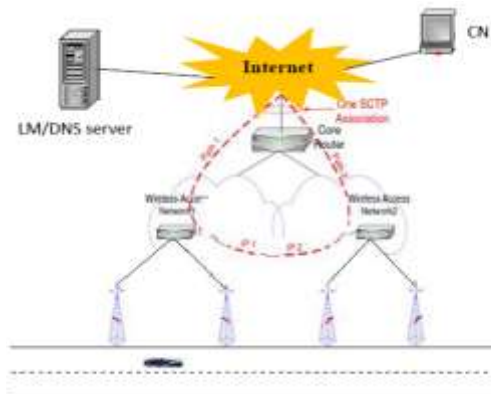


Fig.3 network scenario

In SIGMA, there is no triangle routing because the CN always sends the packets directly to the MH's current IP address.

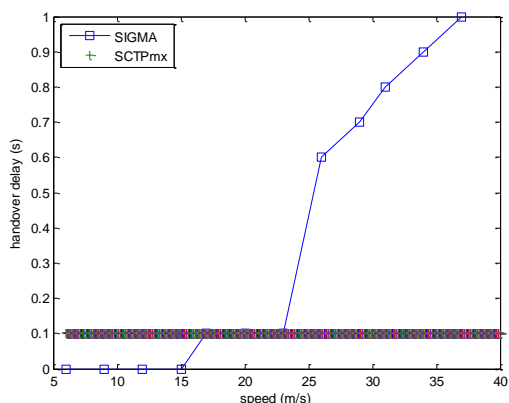


Fig.4 SIGMA & SCTPmx handover latency for. L2 & L3

c. Impact of moving speed

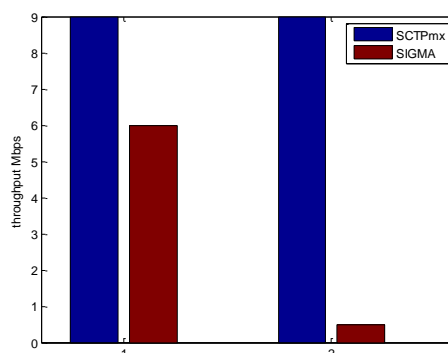
For SCTPmx high moving speed doesn't affect handover and throughput, because handover delay is very low compare to SIGMA protocol that affect by high speed vehicle as shown in figure 4&5.

Fig.5 comparison of SCTPmx and SIGMA handover for different speeds

VII. CONCLUSIONS

In this paper we have compared two approaches, SIGMA and SCTPmx, that using SCTP to support mobility in transportation layer in order to realize seamless handover in high speed environment. We have also discussed some of the method used in several approaches that promises seamless handoff and maintain the network quality in such rapidly moving environment.

The evaluation and analysis of these approaches shows the outstanding and drawbacks of each other in case of high



mobility vehicles.

Fig.5 comparison SCTPmx and SIGMA throughputs for different speeds (15-40m/s).

ACKNOELEDGEMENT

The support of my supervisor and others is gratefully acknowledged. This work was supported by mosti grant.

REFERENCES

- [1] Y. Han, F. Teraoka, "SCTPmx: An SCTP Fast Handover Mechanism Using a Single Interface Based on a Cross-Layer Architecture". IEICE Transactions, 2009: 2864-2873.
- [2] N.Yaakob,F.Anwar, "Seamless Handover Mobility Schemes over High Speed Wireless Environment", International Conference on Electrical Engineering and Informatics , Indonesia, June 17-19, 2007.
- [3] I. Aydin, C.C. Shen, "Evaluating Cellular SCTP over One-Hop Wireless Networks", Mar 2007.
- [4] K.Zhu et al, "Mobility and Handoff Management in Vehicular Networks: A Survey", Wiley InterScience, Communication and Mobile Computing, , pp.1-20, 2009.
- [5] S.K.Sivagurunathan et al, "Experimental Comparision of Handoff Performance of SIGMA and Mobile IP", Workshop on High Performance Switching and Routing, HPSR. 2005.
- [6] S. Fu, M.Atiqzaman, "Survivability evaluation of SIGMA and mobile IP", Springer, Wireless Communicatio,2007.
- [7] S. Fu, M.Atiqzaman, "Architecture and Performance of SIGMA: A Seamless Mobility Architecture for Data Networks", IEEE International Conference on Communications, vol.5, pp. 3249 – 3253, May 2005.
- [8] S. Fu, M.Atiqzaman, "Handover latency comparison of SIGMA, FMIPv6, HMIPv6, and FHMIPv6", IEEE GLOBECOM proceeding, Vol. 6, pp. 3809 – 3813, January 2006.

*Dwell time is the time to cross base station coverage area

- [9] P.Chowdhury, S.Reaz, T.Chun Lin, M.Atiqzaman “Design Issues for SIGMA: Seamless IP diversity based Generalized Mobility Architecture”, Technical Report, Feb 2006.
- [10] D-Phil Kim and S. Koh, “Analysis of Handover Latency for Mobile IPv6 and mSCTP”, Journal of Information Processing Systems, Vol.4, No.3, pp.87-96, September 2008.
- [11] D.Phil, S.Joo K, and S.W, “Analysis of SCTP Handover by Movement Patterns”, Springer-Verlag Berlin Heidelberg , pp. 521 – 529, 2005.
- [12] Y.HAN and F. TERAOKA, “SCTPfx: A Fast Failover Mechanism Based on Cross-Layer Architecture in SCTP Multihoming”, *AINTEC'08*, pp.113-122, Nov 2008, Bangkok, Thailand.
- [13] M.Ratola, “Which Layer for Mobility? - Comparing Mobile IPv6, HIP and SCTP”, Seminar on Internetworking, April 2004.
- [14] C.Ming ,M.Shu and Tz-Heng, “PFC: A packet forwarding control scheme for vehicle handover over the ITS networks”, Computer Communications, pp.2815–2826, 2008.
- [15] Q.Bouland, W.Yao, Z.Niu and X.Fu,“Optimized FMIPv6 Using IEEE 802.21 MIH Services in Vehicular Networks”, Members, IEEE transactions on vehicular technology, nov 2007.
- [16] F.TERAOKA, Y.HAN, “Fast handover and fast failover mechanisms based on cross-layer collaboration among the link layer, the network layer and the transport layer”, Infocommunications journal, volume LXV, pp10-14, 2010/I.
- [17] M. Chang, M.Lee, H.Lee, Y. Hong, and J. Park, “An Enhancement of Transport Layer Approach to Mobility Support”, Information Networking. Convergence in Broadband and Mobile Networking, Volume 3391/2005, pp864-873, 2005.
- [18] J.Fitzpatrick, S.Murphy, M. Atiqzaman, J.Murphy, “Using cross-layer metrics to improve the performance of end-to-end handover mechanisms”, Computer Communications, Vol.32 pp1600–1612, 2009.
- [19] Y.S. Chen and C.H. Cheng, “Network Mobility Protocol for Vehicular Ad Hoc Networks”, Wireless Communications and Networking Conference, WCNC, IEEE pp 1 – 6, April 2009.
- [20] K. Chiu, R. Hwang and Y. Chen, “Cross-Layer Design Vehicle-Aided Handover Scheme in VANETs”, wireless communications and mobile computing, pp.1–13, 2009.
- [21] M.Chang, M.Lee, H. Lee, Y. Hong and J. Park, “An Enhancement of Transport Layer Approach to Mobility Support”, Springer-Verlag Berlin, pp.864–873, 2005.
- [22] Abd. Ezzouhairi, Al. Quintero and S. Pierre, “adaptive end-to-end mobility scheme for seamless horizontal and vertical handoffs”, Ubiquitous Computing and Communication Journal, pp.1-14, 2009.